Role of Heparan Sulphate in Inflammation and Allograft Rejection

Julia Spielhofer

A thesis submitted in partial fulfilment of the requirements for the degree Doctor of Philosophy

Institute of Cellular Medicine

Newcastle University

August 2010

Abstract

Transplantation is often the only therapy for end-stage organ failure. Blood-borne leukocytes are guided into the grafts by proinflammatory chemokines. To achieve full functionality, chemokines interact with heparan sulphate (HS) proteoglycans, which are expressed on the majority of all animal cell surfaces, predominantly on the endothelium. Due to the modification, especially sulphation status of HS, chemokine function can be controlled. This study was designed to examine the expression of different HS epitopes during allograft rejection, dynamic changes of HS following experimental inflammation and investigate the regulation of HS biosynthesis, providing new targets for therapeutic intervention.

Human renal and hepatic allografts expressed distinct HS epitopes which were indicative for the stage of rejection. In both organs, N-sulphated HS domains were elevated during acute phases of rejection whereas 2-O- and 6-O-sulphation increased significantly during chronic stages. The HS motif investigated could be matched to selective HS ligands based on essential target modifications. Data from transplant tissues was largely confirmed by *in vitro* studies simulating an inflammatory response employing relevant cell lines and N-deacetylase/N-sulphotransferase (NDST1) transfectants.

Investigations of the regulation of HS biosynthesis at the protein level were carried out using tandem affinity purification. It revealed an interaction of NDST1, the key enzyme in HS biosynthesis, and beta tubulin. This interaction could provide an insight into general Golgi localisation and retention of glycosylation enzymes.

This study substantiates the strategy of targeting heparan sulphate proteoglycans in inflammation and organ rejection, as distinct changes in HS epitope expression dependent of the stage of rejection were identified. During renal rejection, these specific HS species could be used as a biomarker giving evidence about the progression of the disease. Overall, this could lead to a

novel anti-inflammatory therapy targeting an array of proinflammatory cytokines with less side affects compared to current treatment options.

AD	Activating Domain
AMR	Antibody mediated Rejection
APS	Ammonium Persulphate
AT III	Antithrombin III
BCA	Bicinchoninic Acid
BSA	Bovine Serum Albumin
CBP	Calmodulin Binding Peptide
DAPI	4', 6-Diamidino-2-Phenylindole
DBD	DNA Binding Domain
DMEM	Dulbecco's Modified Eagle Medium
DMSO	Dimethyl Sulphoxide
DNA	Deoxyribonucleic Acid
DPX	Dibutylphtalate Xylene
DST	Disuccinimidyl Tartrate
DTT	Dithiothreitol
ECM	Extracellular Matrix
EDTA	Ethylenediaminetetraacetic Acid
ESRD	End Stage Renal Disease
EXT	Exostosin
FBS	Fetal Bovine Serum
FCS	Fetal Calf Serum
FGF	Fibroblast Growth Factor
FGFR	Fibroblast Growth Factor Receptor
FPLC	Fast Protein Liquid Chromatography
GAG	Glycosaminoglycan
GPCR	G-protein Coupled Receptor
HA	Hyaluronan
HCC	Hepatocellular Carcinoma
HCL	Hydrochloric Acid
HCV	Hepatitis C Virus
HGF	Hepatocyte Growth Factor
HIV	Human Immunodeficiency Virus
HLA	Human Leukocyte Antigen
HS	Heparan Sulphate
HSPG	Heparan Sulphate Proteoglycans
HSV	Herpes Simplex Virus
ICAM	Intracellular Adhesion Molecule

IFN	Interferon
IL	Interleukin
IP	Immunoprecipitation
IRES	Internal Ribosome Entry Sites
LDL	Low Density Lipoproteins
LPS	Lipopolysaccaride
MCS	Multiple Cloning Site
MS	Mass Spectometry
NaCl	Sodium Chloride
Na_3VO_4	Sodium Vanadate
NDST	N-deacetylase/N-sulphotransferase
OST	O-Sulphotansferase
PAGE	Polyacrylamide Gel Electrophoresis
PAPS	3'Phospoadenosine 5'-Phosphosulphate
PBMC	Peripheral Blood Mononuclear Cells
PBS	Phosphate buffered Saline
PCR	Polymerase Chain Reaction
PFA	Parafomaldehyde
RNA	Ribonucleic Acid
SBP	Streptavidin Binding Peptide
SDS	Sodium Dodecyl Sulphate
sHRNA	Short Hairpin RNA
siRNA	Short Interfering RNA
SULF	Endosulphatase
SV40	Simian Virus 40
TAP	Tandem Affinity Purification
TBS	Tris Buffered Saline
TBST	Tris Buffered Saline Tween 20
TCA	Trichloroacetic Acid
TEMED	N'N'N'N'-Tetramethylethylenediamine
TGFß	Transforming Growth Factor beta
TNF	Tumour Necrosis Factor
UDP	Uridine Diphosphate
UTR	Untranslated Region
VEGF	Vascular Endothelial Growth Factor
X-Gal	5-Bromo-4-chloro-3-indolyl-ß-D-Galactopyranoside

Acknowledgments

The work presented in this thesis was generously funded by the EU and the Northern Counties Kidney Research Fund, without whose support my studies would not have been possible.

I would like to thank my supervisors Dr Simi Ali and Prof John A Kirby for the opportunity to join the Applied Immunobiology group as a Marie Curie fellow. They always had an open ear and door for all of their students. Their great deal of optimism sometimes had to compensate for the lack of mine and I am especially thankful for their patience, particulary towards the end of this project. Special thanks go to Graeme, for all his help with FACS and everything to do with computers, and Mo, for being such a lovely, helpful person with a wicked sense of humour (and of course for all her support in the lab). Thank also goes to Dr Jem Palmer, Dr Helen Robertson and Dr Trevor Booth. Further I want to thank Prof. van Kuppevelt for providing us with HS antibodies.
Thanks to all members of the group, past (some of you left too early) and present, my office ‘buddies’ and especially Marta and Ghada for being great friends.

Last but not least I want to thank my family and friends for their support in times when things were not going to plan. THANK YOU!

1 Introduction

1.1 Background to this study

This thesis addresses the role of Heparan Sulphate in inflammation and organ transplant rejection. The immune response is a complex, multistep process which can be characterized by a localised response to infection, tissue damage or inflammation. During this response, immune cells are required to migrate from the blood vessels into subendothelial tissues, a process which has to be tightly regulated as not to result in immune pathologies. Molecules directing immune cells into the tissue are expressed both on the endothelium as well as on leukocytes. Heparan Sulphate, which is expressed abundantly on the endothelium, is said to play a crucial role in this process. Heparan sulphate is capable of immobilizing a plethora of soluble factors such as cytokines and chemokines which then can direct vectorial migration of immune cells into the tissue.

As proinflammatory chemokines expressed during allograft rejection exert their function in conjunction with Heparan Sulphate, it appears feasible to target the interplay of these two key molecules for therapeutic intervention.

1.2 Inflammation and leukocyte migration

Inflammation is a complex immune response to local injury or damage. It is tightly regulated and imbalances can cause major harm. It was originally described by the following parameters: rubor/redness, calor/heat, tumor/swelling and dolor/pain by the Roman encyclopaedist Celsus in the first century A.D. (Lucignani, 2007). These signs can be explained by increased blood flow to sites of injury (redness and heat), accumulation of fluid and migration of leukocytes into the tissue (swelling) and stimulation of nerve endings by released factors such as bradykinins (pain).

Directed migration of leukocytes into the tissue also occurs during organ rejection whereby immune cells have to cross the endothelial cell barrier in order to infiltrate the transplanted organ.

1.2.1 The vascular endothelium

The vascular endothelium is a layer of cells lining blood vessel walls and therefore a critical barrier between blood and tissues. It plays a crucial role in inflammation. Under non pathological circumstances the endothelial monolayer and the basement membrane are not permeable for immune cells, such as leukocytes. During inflammation this barrier gets degraded and leukocytes can be recruited into the tissue in a multistep process (Butcher and Picker, 1996, Wong et al., 2010). This leukocyte infiltration can only occur when the endothelium actively promotes this process. This crucial step in the inflammatory cascade is partly regulated by pro-inflammatory chemokines and cytokines (Barreiro et al., 2010).

As blood flow would prevent the formation of a stable gradient, chemokines and cytokines are immobilized by cell surface glycosaminoglycans (GAGs) (Tanaka et al., 1998, Proudfoot, 2006), of which heparan sulphate is expressed most abundantly on the endothelium (Ihrcke et al., 1993). Thus, heparan sulphate plays an important role during inflammation.

1.2.2 Transendothelial migration

A significant feature of an inflammatory response is the transendothelial migration of inflammatory cells. Leukocytes are recruited from the blood vessel across the endothelium and the basement membrane into the inflamed tissue. This is a multi-step process involving different adhesion molecules.

The vectorial migration occurs in response to chemokine gradients, where chemokines are bound and immobilized by glycosaminoglycans present on the endothelium and the extracellular matrix (Middleton et al., 2002, Proudfoot, 2006). Selectins play an important role in the initial attachment and rolling of leukocytes. Selectins are a family of cell adhesion molecules which are expressed on the endothelium and the leukocyte (Vestweber and Blanks, 1999, Langer and Chavakis, 2009). L-selectin is constitutively expressed on leukocytes, whereas P- and E-selectin are upregulated following stimulation (Zarbock and Ley, 2008) of the endothelium. As L-selectin is expressed constitutively on circulating leukocytes regulation of adhesion takes place by controlling the expression of its glycoprotein ligands, such as GlyCAM-1

(glycosylated cell adhesion molecule), MAdCAM -1 (mucosal addressing cell adhesion molecule), CD34 and Spg200 (Vestweber and Blanks, 1999).These molecules can be found both on high endothelial venules as well as activated endothelium, thus confirming a role in both homing and inflammation (Rosen, 1999). After activation L-selectin is rapidly shed. This is thought to be a mechanism for limiting further leukocyte activation (Hafezi-Moghadam et al., 2001).

During selectin-mediated rolling, the G-protein-coupled chemokine receptors present on leukocytes can interact with chemokines, presented by GAGs on the endothelium (Dowsland et al., 2003).This leads to the activation of integrins on the cell surface (Shimaoka et al., 2002) and further to a more stable adhesion. Integrins are heterodimeric proteins consisting of α and ß chains and are expressed by all nucleated cells. In humans, 25 different forms of heterodimers can be built and the combination of the chains determines the ligand specificity. In order to mediate firm adhesion integrins have to be activated. This can occur by either clustering on the cell surface or conformational changes of the integrin itself (Humphries, 2000).

One of the most common integrins is LFA-1 (lymphocyte function associated antigen-1) or αLß2. It is present on lymphocytes, neutrophils and monocytes and binds to ICAM-1 (intercellular adhesion molecule-1) (Schenkel et al., 2004). Another member of the integrin family is VLA-4 (very late after activation protein-4) or α4ß1. VLA-4 is found on monocytes and lymphocytes and it binds to VCAM-1 (vascular cell adhesion molecule-1). Both ICAM-1 and VCAM-1 are upregulated on the endothelium during inflammatory processes (Johnson et al., 2006). After the passage of the immune cells from the blood vessel into the tissue, leukocytes follow a sub-endothelial chemokine-gradient and can perform multiple immune activities in the target tissue (Figure 1-1).

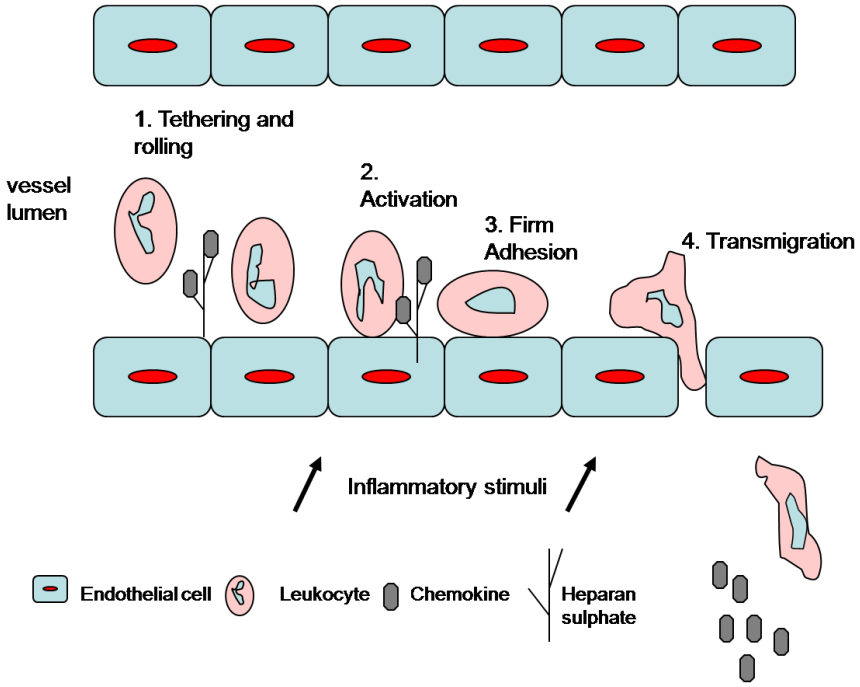

Figure 1-1 Stages of leukocyte extravastion.

Initially leukocytes bind weakly to the endothelium, resulting in leukocytes rolling. The chemokine receptor present on the leukocyte is able to interact with GAG bound chemokines, leading to integrin mediated firm adhesion. The cells then migrate towards a subendothelial chemokine gradient.

1.3 Chemokines

Chemokines are small (7-12kDa) chemo-attractant cytokines which can be divided into inflammatory (inducible) and homeostatic (constitutive) chemokines (Rot, 1996, Rot and von Andrian, 2004).

Constitutive chemokines play a role in lymphocyte homing under non-pathological circumstances, whereas inducible chemokines are upregulated during inflammation. They can act in a paracrine (on adjacent cells) or in an autocrine (self stimulatory) manner.

A broad range of cells are known to secrete chemokines and they are involved in different processes such as homeostasis, cell proliferation, haematopoesis and angiogenesis (D'Ambrosio et al., 2003). But most importantly chemokines are considered to be crucial in leukocyte extravasation during inflammation (Thelen, 2001, Barreiro et al., 2010).

Although there is a large degree of sequence diversity between members of the chemokines family, they show a similar three-dimensional structure consisting of three antiparallel β-strands overlaid by a α-helical region forming the C-terminus (Pease and Williams, 2006) stabilized by disulphide bonds between four conserved cysteines residues. These bonds are built between the first and the third and the second and the fourth cysteines.

Chemokines are synthesised as pro-peptides in an inactive form and it is only after cleavage of the signal peptide during the secretion process that the mature proteins are released.

So far, 47 human chemokines and 18 chemokine receptors have been identified (Murphy et al., 2000, Ransohoff, 2009). Some chemokines can bind to more than one receptor and some receptors can bind different chemokines (Nelson and Krensky, 2001b). Members of the chemokine family are categorized into four groups, dependent on the position of their first two cysteine residues. The two major groups are CC and CXC chemokines. In CC chemokines the two cysteine residues can be found next to each other whereas in CXC chemokines the cysteines are separated by a single amino acid. The two minor groups with one member each are CX3C (three amino acids are between the first two cysteines) and C (only one cysteine) chemokines.

In order to function as chemoattractant cytokines, chemokines must bind to their receptors. These are 7-transmembrane G-protein coupled receptors, where the N-terminus is extracellular and the C-terminus is intracellular (Gether et al., 2002). Binding of chemokines to their receptors usually takes place via the N-terminal domain and the first exposed loop (Monteclaro and Charo, 1996, Murdoch and Finn, 2000). Binding of the chemokine leads to the activation of the receptor resulting in migratory responses.

1.3.1 Glycosaminoglycans and chemokine interactions

All known chemokines interact with GAGs. Even acidic chemokines, such as CCL3 and CCL4, are known to bind GAGs; therefore ruling out the possibility that binding is solely charge dependent (Kuschert et al., 1999). Chemokines bind to GAGs via their GAG-binding domains which have been identified by sequence alignments and site directed mutagenesis studies. These domains

generally consist of the basic amino acids arginine and lysine (or more rarely histidine), which can be separated by other amino acids, resulting in the two consensus GAG-binding motifs XBBXBX and XBBBXXBX, also found in many other proteins. Within these motifs B represents the basic amino acid residue and X any other (Hileman et al., 1998). CCL5 is an example of the XBBXBX family (Proudfoot et al., 2001) whereas CCL7 conforms to the XBBBXXBX motif (Ali et al., 2005b).
Little is known about the corresponding regions of GAGs, albeit N- and O-sulphation have been reported to be involved (Schenauer et al., 2007).

1.3.2 Functional role of HS-chemokine interaction

Binding of chemokines to GAGs occurs both *in vitro* and *in vivo*. Studies of chemokine binding to HS have highlighted various essential roles for HS-dependent chemokine function.

Firstly, binding of chemokines to HS protects them from degradation via proteolysis (Sadir et al., 2004) and can facilitate their oligomerisation (Hoogewerf et al., 1997). Even though chemokines can form oligomers *in vitro*, to form active oligomers *in vivo* GAG binding is required. Mutant forms of CCL4 and CCL5, which were unable to form oligomers, could still stimulate the recruitment of cells *in vitro*, but no longer *in vivo* (Proudfoot et al., 2003). However, oligomerisation seems not to be essential for the function of all chemokines. A CCL2 mutant which was unable to form oligomers showed normal biological activity, indicating that multimerisation was not necessary for its function (Ali et al., 2001).

Secondly, GAGs are required for the presentation of chemokines on the surface of the vascular endothelium. Through the binding of chemokines to HS, chemokines are immobilized and a stable gradient can be formed. This is responsible for the recruitment of leukocytes to sites of inflammation (Middleton et al., 2002). A study with non-GAG binding CCL7 in a murine air pouch model of inflammation in our group demonstrated that the biologically active CCL7

mutant was unable to stimulate the recruitment of leukocytes into the air pouch *in vivo* (Ali et al., 2005b).

Finally, HS is required for the transport of chemokines across the endothelium before their presentation on the apical surface. In a model of transendothelial migration co-localasiaton of HS domains with CCL2 on the apical surface of EA.hy 296 cells after basally administered chemokine was demonstrated. Competition assays further confirmed CCL2-HS binding as addition of soluble heparin to the culture medium inhibited chemokine-HS binding (Hardy et al., 2004). Endothelial cells lacking HS were unable to transport chemokines to the apical surface of the endothelium and thus unable to stimulate leukocyte recruitment (Wang et al., 2005).

1.3.3 Glycosaminoglycans in inflammation

As already discussed, HSPGs plays multiple roles during inflammation. They are involved in almost every stage of leukocyte transmigration; the initial adhesion of leukocytes to the inflamed endothelium, the chemokine-mediated transmigration and the establishment of a chronic inflammatory response. A detailed listing of HSPGs involved in inflammation can be seen in Table 1-1 (adapted from (Parish, 2006).

Table 1-1 HSPGs in inflammation

HSPG	Location	Cellular expression	Function of HS chains in inflammation
Syndecan 1-4	Cell surface, integral membrane proteins Shed syndecan at inflammatory sites	• Endothelial cells, • Macrophages and monocytes • activated T cells	• Ligand for L-selectin and chemokines • Modulator of angiogenic growth factor activity
Glypican 1-6	Cell surface, GPi-anchored proteins	• Vascular endothelial cells • Macrophages in inflammatory sites • Activated CD4 T cells	• Functions similar to syndecans
Perlecan	Basement membrane and ECM	• Subendothelial basement membrane	• Barrier to leukocyte migration • Stabilizes chemokine gradients • Reservoir for HS binding growth factors and cytokines
Type XVIII collagen	Basement membrane and ECM	• Subendothelial basement membrane	• Functions similar to perlecan • Ligand for L-selectin
Agrin	Basement membrane and ECM	• Subendothelial basement membrane	• Functions similar to perlecan

In addition to HS, the GAG hyaluronan (HA) is well known for its influence on inflammation. As no chain modifications of GAG chains in HA occur, its function seems to be dependent on its size. After injury or during inflammation, HA is degraded either enzymatically by HA degrading enzymes or non-enzymatically by i.e. free radicals. Low molecular weight HA is able to induce proinflammatory cytokines and chemokines (Noble, 2002).

HA itself is expressed by endothelial cells upon activation with proinflammatory cytokines and is involved in leukocyte recruitment to sites of inflammation by its interaction with a CD44 isoform present on leukocytes. This interaction seems to be tightly controlled, as CD44 molecules on other cell types are not always capable of binding HA (Johnson et al., 2000). Another molecule that influences the effect of HA in inflammation is TSG-6 (tumour necrosis factor alpha induced protein 6), which is only found during inflammatory conditions, by stabilizing the HA-CD44 interaction (Lesley et al., 2004). In addition to HA, TSG-6 also binds to a range of differentially modified HS species and distinct binding sites for HA and HS have been identified. The interaction of TSG-6 with HS on the cell

surface or ECM could inhibit HA binding and modulate HA-CD44 interaction during inflammation (Mahoney et al., 2005).

1.4 Glycobiology

Glycobiology describes the study of structure and function of glycans (sugar chains) as well as their conjugates, such as glycoproteins, glycolipids and proteoglycans. Glycans can be found widespread on cell surfaces, extracellular matrix (ECM) or secreted in fluids. Like proteins, they are omnipresent and participate in a vast range of biological functions.

The glycan chains consist of individual monosaccharides, which are polymerized into oligosaccharides (up to 20 residues) or polysaccharides. Individual monosaccharides are joined by glycosidic linkage, which can be in either α or ß form. Glycosylation is the process whereby glycan chains are enzymatically attached to core molecules and it represents the most common post-translational modification of eukaryotic proteins. In this glycosylation reaction the glycan can be linked to either an asparagine residue of the protein (N-glycans) or a hydroxyl group of a serine or threonine residue (O-glycans). N-glycosylation occurs during protein biosynthesis in the ER whereas O-glycosylation is a post-translational modification occurring in the Golgi compartment.

Due to variable saccharide composition, differential linkage, chain length and branching as well as modification, glycoproteins are highly complex, information rich molecules. The field of glycobiology is a rapidly growing research area; publications have more than doubled over the last 10 years (based on publications containing the word glycobiology in PubMed).

1.4.1 Proteoglycans and Glycosaminoglycans

Proteoglycans (PG) are glycoproteins, where glycosaminoglycan (GAG) chains are covalently attached to serine residues of a core protein. The protein core determines where the proteoglycans are localized. Proteoglycans are found on cell surfaces, in extracellular matrix (ECM) or intracellularly, as in granules of mast cells (Kjellen and Lindahl, 1991). There is no mammalian cell known

without proteoglycans. GAGs are highly negatively charged linear heteropolysaccharides consisting of up to 150 characteristic disaccharide repeats. GAGs forming proteoglycans can be divided into four different families: keratan sulphate (disaccharide unit: N-acetylglucosamine and galactose), heparan sulphate and heparin (disaccharide unit: N-acetylglucosamine and glucuronic acid), chondroitin sulphate and dermatan sulphate (disaccharide unit: N-acetylgalactosamine and glucuronic acid). Another member of the GAG family is hyaluronic acid (disaccharide unit: N-acetylglucosamine and glucuronic acid), which is secreted into the ECM (Taylor and Gallo, 2006). The GAG chains can be sulphated to different extents on specific positions on the chain and the glucuronic acid in heparan sulphate and heparin can be converted into iduronic acid via C-5-epimerization (Sugahara and Kitagawa, 2000).

1.4.2 Heparan sulphate proteoglycans (HSPGs)

Proteoglycans carrying heparan sulphate chains can be divided into different groups, depending on their occurrence. They can be located in the ECM, on the cell surface and intracellularly (Parish, 2006).

1.4.2.1 Extracellular Matrix HSPGs

HSPGs in the ECM comprise a variety of molecules including perlecan, collagen XVIII and agrin.

Perlecan (~470kDa molecular weigth) can be found in basal membranes as well as the interstitial matrix and carries attachment site for 3 HS chains close to the N-terminus with one additional GAG attachment site near the C-terminus (Iozzo, 2005). It is involved in embryogenesis, tissue morphogenesis and cartilage development (Melrose et al., 2003, Farach-Carson and Carson, 2007).

Collagen XVIII (~180kDa molecular weight) can be found in almost all basement membranes and offers 3 HS attachment sites (Iozzo and San Antonio, 2001). Proteolytic cleavage leads to the release of endostatin, a fragment shown to have anti-angiogenic properties (O'Reilly et al., 1997, Marneros and Olsen, 2005).

Agrin, another large HSPG (214kDa molecular weight) aggregates acetylcholine receptors in neuromuscular junctions during synaptogenesis (Cole and Halfter, 1996) and plays an important role in glomerular filtration of the kidney (Groffen et al., 1999, Raats et al., 2000).

1.4.2.2 Cell surface HSPGs

Cell surface bound HSPGs are syndecans (4 members), which have a transmembrane domain and glypicans (6 members), which are bound via a glycosylphosphatidylinositol (GPI) anchor. Despite these 'full time' HSPGs, which always carry HS chains, so called 'part time' HSPG have been described, which only carry HS chains under specific conditions, including betaglycan, splice variants of CD44 and testican (Parish, 2006).

1.4.2.2.1 Syndecans

Syndecans comprise a family of 4 core proteins (~33kDa molecular weight). They are type I transmembrane proteins with a small cytoplasmic region, a transmembrane domain and an extracellular domain with 3-5 of GAG attachment sites (Bernfield et al., 1992). Syndecans 1 and 3 can be substituted with CS chains whereas syndecans 2 and 4 only carry HS chains (Carey, 1997). Syndecans are expressed in a tissue specific manner and upon interaction with an extracellular ligand they can transfer the signal via the membrane spanning domain into the cell (Woods, 2001).

The extracellular domain of syndecans can also be shed by proteolytic cleavage, possible playing a role in tissue repair. Increased levels of syndecan-1 ectodomain were found in dermal wound fluid (Fitzgerald et al., 2000) and shed syndecan-1 did indeed enhance cell migration and wound closure in a model of lung injury (Chen et al., 2009).

1.4.2.2.2 Glypicans

Glypicans, which are attached to the cell membrane via a GPI anchor at the C-terminus, can be found associated with lipid rafts (Filmus et al., 2008). There are 6 mammalian glypicans (~60kDa molecular weight) which each having 2 to

3 GAG chains (HS exclusively) attached to the extracellular region. Most importantly they play a role in regulating morphogens, thus controlling development and growth (Filmus and Selleck, 2001, Filmus et al., 2008). As shown for syndecans, glypicans can also be shed via the action of an extracellular lipase which cleaves the GPI anchor and glypican fragments have been demonstrated to play a role in the transport of morphogens (Belenkaya et al., 2004, Traister et al., 2007).

1.4.2.3 Intracellular PGs

Intracellularly, heparin is stored in secretory granules of connective-tissue-type mast cells linked to the core protein serglycin (~18kDa molecular weight). Heparin can be seen as a highly sulphated, highly epimerized form of HS (Kolset and Tveit, 2008).

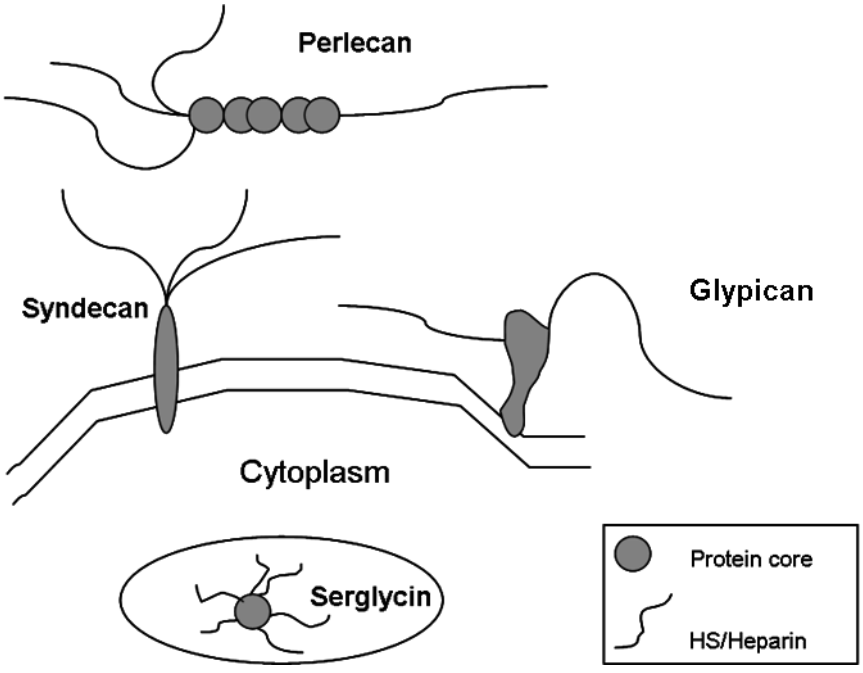

Figure 1-2 Schemativ representation of four types of common HSPGs

Overall, HSPGs are involved in the regulation of various cellular processes, including cell-matrix interaction, coagulation, binding of growth-factors, angiogenesis and inflammation depending on the interaction with a GAG-binding protein (Bernfield et al., 1999, Bishop et al., 2007).

1.5 Glycosaminoglycans and protein interactions

A vast number of proteins that bind to GAGs have been described in the literature (Table 1-2). Initially, it was thought that HS-protein interactions are non-specific. However, there is increasing evidence that these interactions require a certain level of specificity (Turnbull et al., 2001, Whitelock and Iozzo, 2005). In addition to ionic forces between basic amino acids of the proteins (lysine and arginine) and carboxyl and sulphate groups of the GAGs, van der Waals forces, hydrogen bonds and hydrophobic interactions with the carbohydrate backbone also seem to be involved (Mulloy and Rider, 2006). Most likely the interaction of HS and its ligands depends on the modification status of the chain and the spatial distribution of the groups involved.

Table 1-2 Examples of GAG binding proteins

Protein function	**Examples**	**References**
Cell adhesion molecules	L-selectin, P-selectin	(Celie et al., 2005, Koenig et al., 1998, Parish, 2006)
Extracellular matrix proteins	fibronectin, laminin, collagens	(Battaglia et al., 1992, Bernfield et al., 1999, Isemura et al., 1987, LeBaron et al., 1989)
Growth factors	FGFs, HGF, VEGF	(Bashkin et al., 1989, Iozzo and San Antonio, 2001, Lyon et al., 1994b)
Morphogens	TGFß superfamly	(Lyon et al., 1997, Rider, 2006)
Cytokines	IL-2,-3,-4,-5,-7,IFNγ, TNFα, chemokines	(Bernfield et al., 1999, Lortat-Jacob, 2006, Lortat-Jacob et al., 1990, Proudfoot, 2006, Webb et al., 1993)
Viral envelope proteins	Herpes simplex virus, human immundeficiancy virus, hepatitis C virus	(Chen et al, 2008)
Plaque proteins	Prion proteins, amyloid proteins	(Scholefield et al., 2003, Warner et al., 2002)
Lipid binding proteins	Apolipoprotein E and B	(Mac Arthur et al, 2007)

So far, the only example of a specific GAG-protein interaction is the binding between antithrombin III and heparin (Petitou et al., 2003). This interaction is of

great medical interest as heparin is widely used as an anticoagulant. This binding causes conformational changes in the protein, which enhances the neutralization of thrombin leading to anticoagulant effects. As not only antithrombin but also thrombin has heparin binding sites, heparin does not only activate the protease but also helps to hold both molecules in close proximity. Structural analysis revealed a unique pentasaccharide sequence containing a very rare 3-O-sulphation required for high affinity binding.

Well known interaction partners of HS are fibroblast growth factors (FGFs) and their receptors (FGFRs). Two FGF molecules and two FGFR must bind to HS forming a ternary complex in order to signal properly (Kan et al, 1993, Rapraeger et al, 1994). Although there is an oligosaccharide which is recognised preferentially, no unique or specific binding site has been described. The most favourable sequence is composed of N-sulphation on the non-reducing end glucosamine, 2-O-sulphation on iduronic acid and 6-O-sulphation on the reducing end glucosamine (Kreuger et al., 2001). The minimal FGF binding domain has been described as terasaccharide recently (Guglieri et al., 2008).

IFNγ has also been identified as a GAG ligand on the basement membrane. The structural domain of HS that is responsible for IFNγ binding has been investigated and is composed of a predominantly N-acetylated and GlcA-rich (NA-domain) fragment flanked by two small N-sulphated oligosaccharides (Lortat-Jacob et al., 1995, Lortat-Jacob et al., 1996). It is thought that this interaction limits the extent of its C-terminal domain degradation, thus increasing its activity. In addition, IFNγ can also bind to soluble heparin, thus preventing sequestration onto the cell surface HS and inhibiting its function (Fritchley et al., 2000).

As seen from these few examples, protein-GAG interaction has great physiological significance, as binding of proteins to GAGs can result in immobilisation and/or activation (antithrombin III), building of ligand-receptor complexes (FGF-FGFR) and protection against degradation (IFNγ).

1.6 Heparan sulphate biosynthesis

HS is produced by almost any cell type and in contrast to other biomolecules, such as proteins, no code or template for the polysaccharide structure exists. The biosynthesis of HS takes place in two compartments: in the endoplasmic reticulum and the Golgi compartment. It is a complex reaction which can be divided into the stages of chain initiation, polymerisation and modification, with each involving a set of enzymes (Figure 1-3).

1.6.1 Protein linkage

The attachment site for GAGs consists of a central serine-glycine dipeptide flanked by one or more acidic amino acids (Esko and Zhang, 1996).This first step occurs in the ER. A tetrasaccharide consisiting of glucuronic acid-galactose-galactose-xylose is linked to a hydroxyl group of the selected serine residue in the core protein (Sugahara and Kitagawa, 2000). The first monosaccharide, xylose, is transferred from its nucleotide sugar carrier UDP (uridine diphosphate)-xylose to the serine residue of the core protein in a reaction catalyzed by the enzyme UDP-xylotransferase (Esko and Zhang, 1996). Two human xylosyltransferase isoforms have been identified, XT-I and XT-II, but only XT-I has been shown to be active (Gotting et al., 2000). After the transport of the molecule to the Golgi compartment, the first galactose is transferred to the molecule by galactosyltransferase I, the second galactose by the galactosyltransferase II. Both galactose residues can be sulphated (Silbert and Sugumaran, 2002), which does not happen for HS/heparin but may for CS/DS (Ueno et al., 2001). Then the fourth monosaccharide, glucuronic acid, is added by glucuronyltransferase (Kitagawa et al., 1998).

1.6.2 Polymerization

After the addition of an N-acetylglucosamine residue to the tetrasaccharide by N-acetylglucosaminyltransferase I (Lidholt and Lindahl, 1992) the fate of the chain as HS is sealed and chain elongation occurs on the non-reducing end by addition of alternating glucuronic acid and N-acetylglucosamine residues from UDP-sugar donors by EXT1 and EXT2 (Esko and Zhang, 1996).

1.6.2.1 EXTs

Although EXT1 is capable of elongating the chain *in vitro* on its own, the chain elongation enzymes EXT1 and EXT2 have been shown to form a hetero-oligomeric complex in the Golgi compartment, which is the biologically active form of the chain elongation machinery (Nilsson et al., 1994, Munro, 1998, Busse and Kusche-Gullberg, 2003). In addition, there are three EXT-like proteins (EXTL1-3) which also have glycosyltransferase activities, but their contribution to chain polymerisation is not clear (Kim et al., 2001).

1.6.3 Modification

Chain modification targets the glucuronic acid part as well as the glucosamine and can occur during chain elongation (Esko and Lindahl, 2001). The initial modification step is catalyzed by the N-deacetylase/N-sulphotransferase (NDST) enzyme. This bifunctional enzyme is responsible first for the removal of acetyl groups from N-acetylglucosamine. The created free amine group than generally gets sulphated through the sulphotransferase activity of the enzyme. Further modification includes the epimerization of glucuronic acid to iduronic acid by C-5-epimerase (Li et al., 1997). Iduronic acid (to a lesser extent glucuronic acid) can be further O-sulphated at the C2 position by uronosyl-2-O-sulphotransferase (Rong et al., 2001).
6-O-sulphation of both uronic acid and glucosamine can occur on the C6 position by various glucosaminyl 6-O-sulphotransferases (6-OST) and the glucosamine can be further sulphated by glucosaminyl 3-O-sulphotransferase (3-OST) (Habuchi et al., 2004) (Figure 1-4).

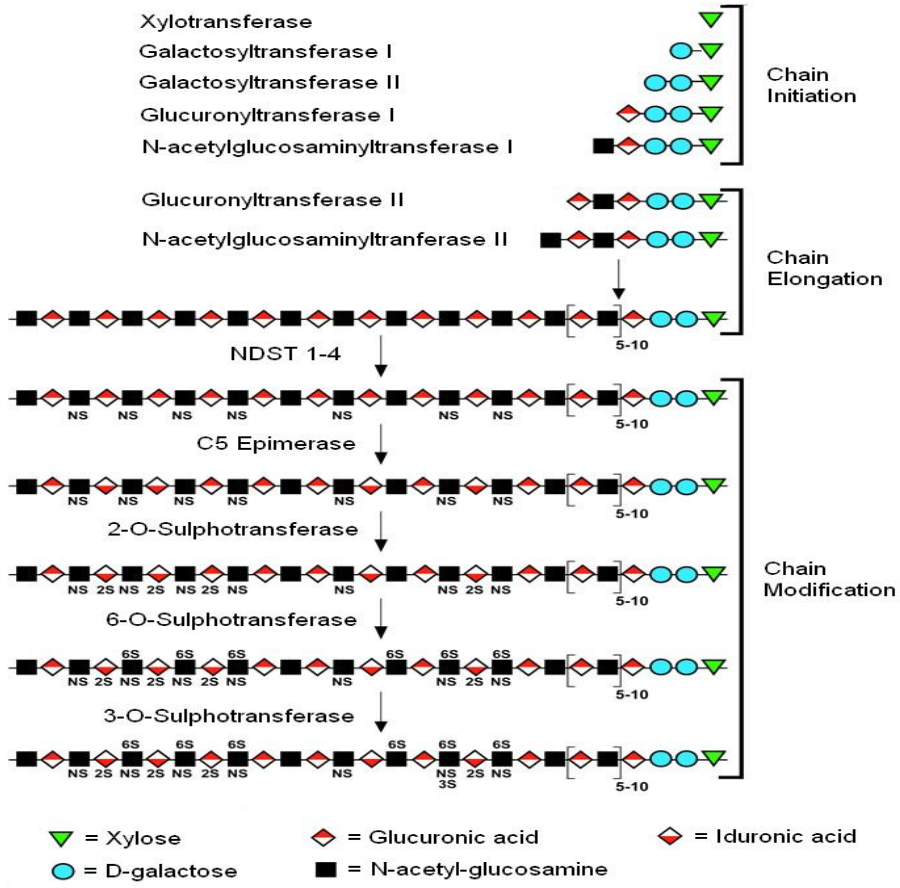

Figure 1-3 Schematic representation of HS biosynthesis

The synthesis of heparan sulphate is initiated by the attachment of xylose to a core protein, catalysed by xylotransferase. Two D-galactose residues and a glucuronic acid are then added sequentially by the enzymes galactosyltransferases I and II, and glucuronyltransferase I, respectively. Chain elongation then continues with addition of a single N-acetyl-glucosamine to the linkage tetrasaccharide, catalysed by N-acetylglucosaminyltransferase I followed by the addition of alternating D-glucuronic acid and N-acetyl-glucosamine residues, catalysed by glucuronyltransferase II (EXT1) and N-acetylglucosaminyltransferase II (EXT2). The chain is then modified through N-acetylglucosamine N-deacetylation/N-sulphation, epimerisation, and O-sulphation. Adapted from Esko et al, 2001.

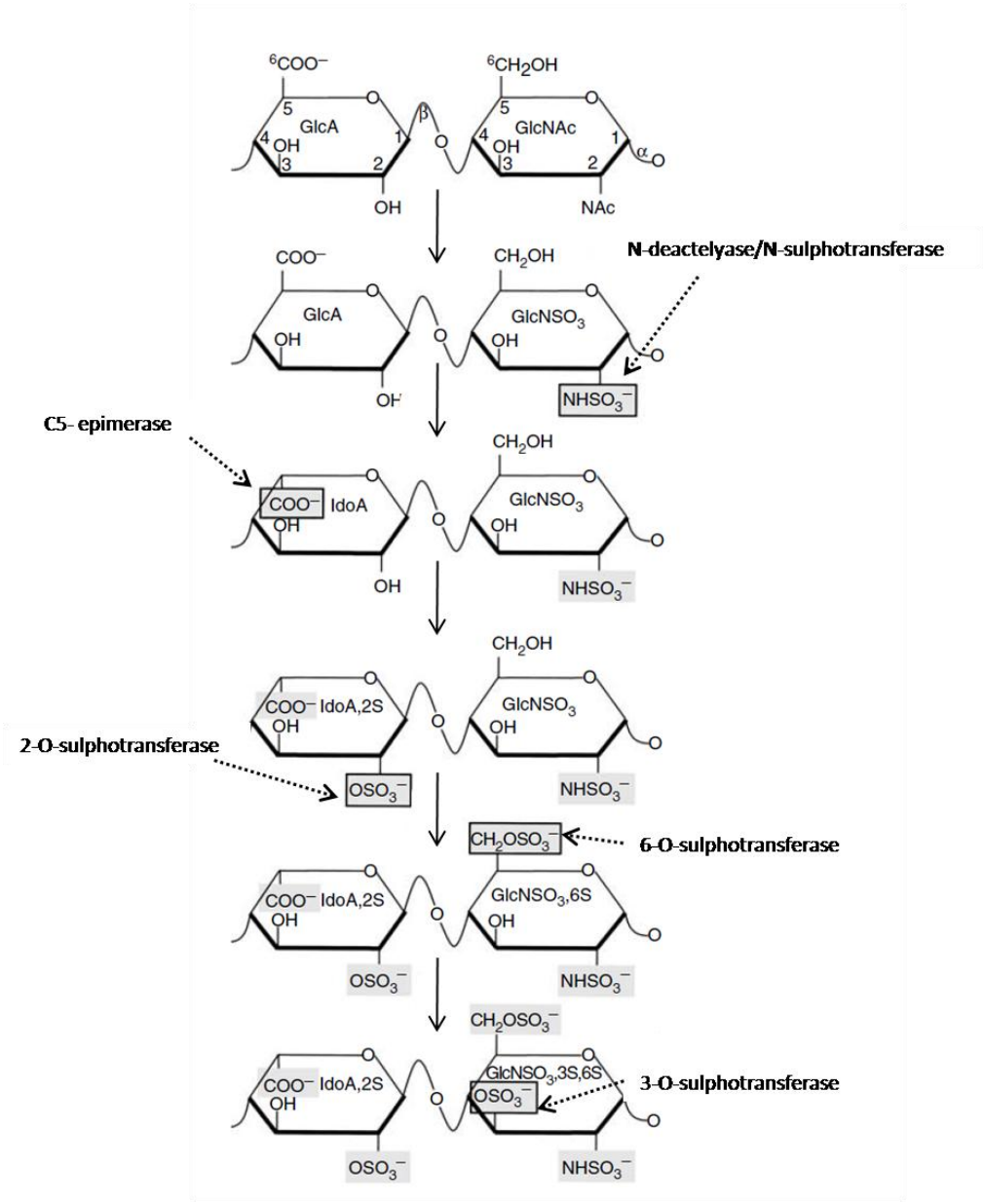

Figure 1-4 Schematic represenaton of HS chain modifications

It was shown that epimerization and O-sulphation are all dependent on prior N-sulphation. N-sulphation therefore predicts the overall struture of HS and without N-sulphation further modification will not occur (Unger et al., 1991). Due to this finding NDSTs are regarded as key regulators of HS biosynthesis.

1.6.3.1 N-deacetylase/N-sulphotransferase enzymes

NDSTs perform the first modification of the chain. The NDST enzyme family consists of 4 mammalian isoforms (Table 1-3), which show 65-80% sequence identity (Grobe et al., 2002, Esko and Selleck, 2002). In 1991 it was shown for

the first time that both the N-deacetylase and the N-sulphotransferase activity were combined in one enzyme (Pettersson et al., 1991). However, they do not always work together as free amine groups can occur.

Human NDST1 was first described by Dixon and colleagues (Dixon et al., 1995) and human NDST2 was cloned three years later (Humphries et al., 1998). NDST1 and 2 are expressed ubiquitously and abundantly at a transcriptional level, whereas NDST3 and NDST4, which have been identified later, are expressed in a more restricted manner in adult brain, kidney, liver and lung and during embryogenesis (Aikawa and Esko, 1999, Aikawa et al., 2001, Pallerla et al., 2008).

All 4 isoforms show different ratios in N-deacetylase/N-sulphotransefrase activity, where in NDST1 and NDST2 the N-deactylase activity is higher than the N-sulphotransferase activity (Aikawa et al., 2001).

Table 1-3 Comparision of human NDST isoforms

Isoform	**Size (aa)**	**Chromosomal location**	**Potential glycosylation sites**	**Site of expression**
1	882	5q33.1	4	ubiquitous
2	883	10q22	6	ubiquitous
3	873	4q26	6	tissue specific
4	872	4q25-26	5	tissue specific

As human NDST3 and 4 are located very close on chromosome 4 it can be speculated that they arise from the same ancestral origin and have diverged through duplication during evolution. This could also be true for NDST1 and 2 because of their similar expression pattern though their chromosomal location is not too close.

All 4 isoforms are found in the Golgi compartment and also analysis based on the hydrophobicity values (Yuan and Teasdale, 2002) confirmed Golgi localisation for all 4 NDSTs (Golgi localisation prediction tool: http://ccb.imb.uq.edu.au/golgi/documents/).

The N-deacetylase activity is located at the N-terminus of the enzyme and requires Mn^{2+} ions *in vitro* for its function (Riesenfeld et al., 1980).

The N-deacetylase activity predicts the degree of N-sulphation and is therefore rate limiting. This was shown by mutant studies in HEK 293 cells, where either a deacetylase or a sulphotransferase mutant was overexpressed. The sulphotransferase mutant still acted as a deacetylase and an endogenous N-sulphotransferase seemed to be responsible for the transfer of sulphate groups resulting in oversulphation of HS. Cells overexpressing the deacetylase mutant did not show any increase in N-sulphation, despite large amounts of N-sulphotransferase, pointing out that the deactelyse activity is a prerequisite for sulphation (Bengtsson et al., 2003).

These findings were further confirmed by a yeast system expressing rat NDST1. As yeast does not express GAGs, NDST1 could be analysed in a “clean room”, as no GAG synthesising or modifying enzymes could interfere with the enzymes activity (Saribas et al., 2004).

Both NDST1 and NDST2 act on a low sulphated HS better than on a non-sulphated one. Further it was shown that N-sulphated HS can inhibit NDST activity (van den Born et al., 2003).

The N-sulphotransferase activity is located in the C-terminus of the enzyme. The sulphotransferase domain of human NDST1 was crystallized and lysine614 was identified as catalytic residue. This lysine residue can interact with PAPS 5’phosphate (Sueyoshi et al., 1998).

3’-phosphoadenosine 5’-phosphosulphate (PAPS) is the universal sulphate donor for various sulphotransferases, where the 5’-sulphuronyl group is the sulphate donor. PAPS is synthesized by the bifunctional PAPS synthetase, which combines ATP sulphurylase and adenosinphosphosulphate kinase activity (Venkatachalam et al., 1998). As PAPS synthesis takes place in the cytoplasm, it is physically separated from the area where sulphation of GAGs takes place, which is the Golgi compartment. Therefore, the transport of PAPS from the cytoplasm to the Golgi is of importance. So far, two transporters have been identified, which are both located in the Golgi (Kamiyama et al., 2003, Kamiyama et al., 2006).

NDSTs remove acetyl groups from N-acetylglucosamine and then transfer sulphate groups to the substrate. But not every N-acteylglucosamine group is a

substrate for NDSTs. N-sulphated GlcNAcs can be found in areas with N-acetylated domains in between. A pattern consisting of NS (N-sulphated) domains, separated from NA (N-acetylated) domains by NA/NS transition zones can be observed (Grobe et al., 2002).

1.6.3.1.1 Regulation of NDST1

Not much is known about the regulation of NDSTs. In 2002 it was demonstrated that all 4 murine isoforms of NDST have unusually long and complex 5' untranslated regions (Grobe and Esko, 2002). These 5' UTR have a high degree of secondary structures and contain several upstream AUG codons which interfere with normal cap-dependent ribosome scanning and translation initiation. These Internal Ribosome Entry Sites (IRES) offer regulation on the translational level (Grobe and Esko, 2002).

Another model of NDST regulation was suggested recently. Studies in embryonic mouse liver led to the assumption that no regulation at transcriptional, translational, or posttranslational level takes place at all. Regulation is rather due to the assembly of the enzyme complex and the selection of enzymes into the complex, called the GAGosome (Ledin et al., 2006). This model offers a more flexible way of modification where enzymes involved in HS modification can act at the same time or before or after each other. The GAGosome is thought to offer restricted numbers of binding sites for NDSTs and that the affinity to the GAGosome will predict which isoform is incorporated. There have been studies supporting this new hypothesis. In 2004, it was demonstrated that HS synthesised by embryonic stem cells deficient in NDST1 and NDST2 lack N-sulphation, still contains 6-O-sulphate groups, indicating modification of HS without prior N-sulphation (Holmborn et al., 2004).

Recently, it was shown that N-sulphated domains were created in apparent processive mode. Extended N-sulphated domains were generated by a coupled N-deacetylase/N-sulphotransferase activity *in vitro*, which was dependent on the availability of the sulphate donor PAPS (Carlsson et al., 2008). It seems however unlikely that a process as complex as HS biosynthesis is not regulated at the transcriptional, translational or post-translational level at all and should be solely regulated by the assembly of the enzyme complex.

1.6.3.2 C-5-Epimerase

The uronyl C-5-epimerase is responsible for the conversion of D-glucuronic acid into L-iduronic acid by switching the COO^- group from above the ring to below the ring. So far this is the only epimerase known which acts on HS and heparin chains. Epimerisation seems to play an important role for protein binding to GAGs as almost all binding sites identified so far contain L-iduronic acid. Epimerisation itself is a reversible process. However, following 2-O-sulphation of the uronic acid and 6-O-sulphation of glucosamine the epimerisation state seems to be locked (Lindahl et al., 1989, Hagner-Mcwhirter et al., 2000).

1.6.3.3 O-Sulphotransferases

2-O-sulphotransferase is responsible for sulphate substitution on the C2 position of both iduronic and glucuronic acid, although iduronic acid seems to be the preferred target (Rong et al., 2001). O-sulphation can be found in NS and NS/NA domains, with a tendency to act more in N-sulphated regions (Maccarana et al., 1996).

3-O-sulphotransferases transfer sulphate to the C3 position of the glucosamine and seven different isoforms have been identified so far with distinct preferences for modification depending on disaccharide composition. All isoforms have restricted expression pattern in various tissues and not all of them are capable of creating anticoagulant HS (Shworak et al., 1999, Xia et al., 2002, Girardin et al., 2005). Three 6-O-sulphotransferases have been identified until now and they are responsible for the sulphation of the N-sulphoglucosamine residues. Similar to 3-O-sulphotransferases, their expression appears to be tissue specific (Habuchi et al., 2000, Habuchi et al., 2003, Habuchi et al., 2006).

1.6.3.4 Sulphatases

Recently, another class of enzymes which modify the HS chain have been discovered. They are a family of 6-O-endosulphatases whose action is distinct from the exosulphatases, which are responsible for HS breakdown. The two human endosulphates SULF1 and SULF2 remove specific 6-O-sulphate groups

and were discovered first in quail (Dhoot et al., 2001). Even though both SULF enzymes have redundant function, the loss of either form leads to a specific 6-O-sulphation pattern, possibly due to different preferred disaccharide composition (Ai et al., 2006). Despite the direct removal of the 6-O-sulphate groups, SULFs are also capable of influencing other modifications, such as 2-O-sulphation and N-sulphation. This observation would support the GAGosome model, where a balanced cross talk between individual biosynthetic enzymes occurs rather than action independent of other (Lamanna et al., 2007).

1.6.3.5 Heparanase

Mammalian heparanase is another enzyme important in HS biology. It is not involved in HS biosynthesis, but is a HS degrading endoglycosidase (Bame, 2001). It is highly expressed in placental tissue, but its role in normal development is not well understood (Haimov-Kochman et al., 2002). It seems to be important in pathological situations such as inflammation, whereby disruption of the ECM by heparanase helps immune cells to migrate into inflamed tissue, and cancer metastasis. HS breakdown by heparanase is required for angiogenesis and tumour growth and HS fragments can enhance FGF2 binding and signalling (Nasser, 2008). Expression of heparanase also correlates with the metastatic potential of tumours (Vlodavsky and Friedmann, 2001). High levels of heparanase were found to increase levels of overall sulphation, maybe compensating the loss of full chain length by ‘over’sulphating shorter fragments (Escobar Galvis et al., 2007).

1.7 HS in normal physiology

HSPGs are expressed universally and ubiquitously and regulate many physiological and pathophysiological processes by facilitating interaction between ligands and their receptors on the cell surface and the ECM (Figure 1-5). Both core proteins and the modified HS chains influence ligand binding in a cell/tissue and development specific manner.

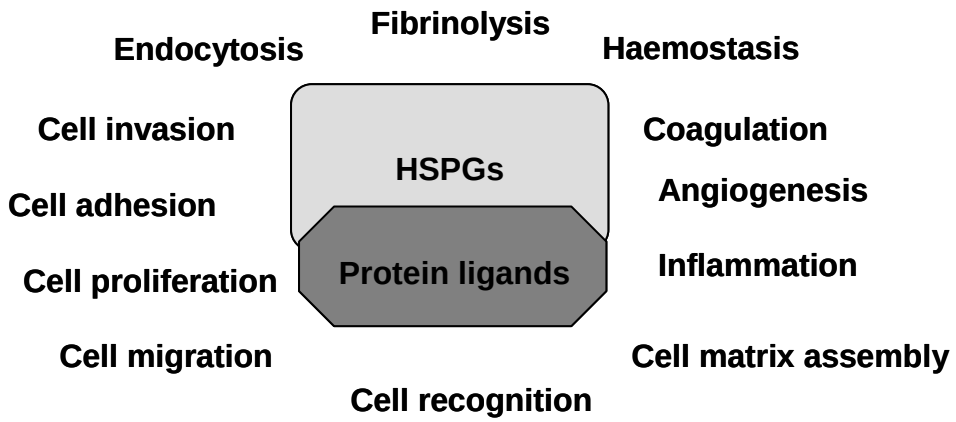

Figure 1-5 Physiological processes modulated by HS-protein interaction

The various functions of HS have been explored using mouse mutant models by either targeting the HS biosynthetic enzymes or the core proteins and a range of phenotypes have been described, as below.

1.7.1 Mice deficient in HS biosynthetic enzymes

1.7.1.1 EXT deficient mice

In humans, EXTs are linked to autosomal dominant hereditary multiple exostosis, a particular benign bone tumour type. EXT1 and EXT2 null mutants in mice are not viable and die during gastrulation most likely due to HS dependent morphogen signalling (Forsberg and Kjellen, 2001, Stickens et al., 2005). This is not surprising, as the EXTs are responsible for HS chain elongation and without EXT activity only short stubs will be attached to the core protein. A conditional inactivation of EXT1 in the brain revealed disturbed brain morphogenesis and axon formation in mice and zebrafish (Inatani et al., 2003, Lee and Chien, 2004).

1.7.1.2 NDST deficient mice

1.7.1.2.1 NDST1

Mice lacking NDST1 die perinatally due to respiratory failure. HS deficient epithelial cells are incapable of producing surfactant, thus resulting in lung failure (Ringvall et al., 2000, Fan et al., 2000). Additionally, defects of skull and

brain development have been observed due to disturbed growth factor signalling (Grobe et al., 2005).

1.7.1.2.2 NDST2

NDST2 deficient mice display hardly any structural alterations of HS. Defective connective tissue-type-mast cells lacking correctly sulphated heparin, reduced amounts of histamines and mast cell proteases are the only consequence of NDST2 loss. This relatively mild effect can be explained since NDST2 is the predominant form of NDSTs in mast cells whereas NDST1 appears to be the predominant isoform in other cells and tissues (Humphries et al., 1999, Forsberg et al., 1999).

1.7.1.2.3 2-O-sulphotransferase deficient mice

A gene trap mutation in mouse 2-O-sulphotransferase resulted in perinatal death and displayed severe renal, skeletal and neuronal defects (Bullock et al., 1998, Wilson et al., 2002).

1.7.1.2.4 C-5-epimerase deficient mice

Mice deficient in C-5-epimerase die perinatally possibly due to respiratory failure. These mice also lacked kidneys while other abdominal organs were unaffected (Li et al., 1997, Jia et al., 2009).

1.7.1.2.5 3-O-sulphotransferase deficient mice

Isoform 1 of the 3-O-sulphotransferase family has been inactivated in a mouse model with only mild effects such as intrauterine growth retardation (Shworak et al., 2002).

1.7.2 Mice deficient in HS core proteins

1.7.2.1 Syndecans

Mice lacking syndecans 1, 3 and 4 have been described in the literature and have only subtle effects, all being viable and healthy (Ishiguro et al., 2002, Ledin et al., 2004). Syndecan 1 deficient mice develop normally and

crossbreeding studies have revealed a genetic interaction between syndecan 1 and Wnt-1, indicating a role in tumorigenesis (Alexander et al., 2000).
Syndecan 3 regulates feeding behaviour in the hypothalamus as mice lacking syndecan 3 eat less and are partially resistant to obesity (Reizes et al., 2001, Strader et al., 2004).
Syndecan 4 deficient mice are healthy despite a delayed wound repair and impaired coagulation in fetal vessels in the placenta (Ishiguro et al., 2000, Echtermeyer et al., 2001).

1.7.2.2 Glypicans

The only glypican isoform inactivated in mice is glypican 3 and loss of function has major consequences. These mice exhibit developmental overgrowth and cystic and displastic kidneys (Pilia et al., 1996, Cano-Gauci et al., 1999). A similar phenotype is displayed by humans with the Simpsom-Golabi-Behmel syndrome, an X-linked disorder with mild phenotypes in females to lethal forms in some males (Filmus and Selleck, 2001).

1.7.2.3 Perlecan

Loss of perlecan is lethal in mice. Some mice die during embryonic development due to the rupture of the basement membrane of the heart whereas others die perinatally as a result of brain defects and skeletal abnormalities (Arikawa-Hirasawa et al., 1999). The Schwartz-Jampel syndrome in humans, which is also characterised by skeletal and developmental defects mutations, has been recently linked to mutations in the perlecan gene (Nicole et al., 2000).

1.7.2.4 Collagen XVIII

Loss of collagen XVIII affects the eye development in mice, similar to the reported Knobloch Syndrome in humans which harbour a mutation in the collagen XVIII gene (Sertie et al., 2000, Fukai et al., 2002).

1.7.2.5 Agrin

Agrin is present in neuromuscular junctions and the central nervous system. Mice devoid of agrin show defective synaptogenesis (Gautam et al., 1996).
These are the mutants of HS biosynthetic enzymes and core proteins investigated so far and phenotype analysis confirms the cell/tissue and time/developmental specific existence of HS species. This idea is strengthened by the observation that lack of one enzyme affects mainly one organ, whereas others are unaltered and vice versa, as it can be seen for C5-epimerase with loss of kidneys and NDST1 with impaired lungs. Also not surprising are the subtle effects of 3-O-sulphotransferase mutants as only one isoform is targeted and others may be capable of compensating the loss depending on their expression throughout the tissue. Common for all phenotypes investigated is that the individual defects are very distinct and specific and human and mouse data are coherent.

1.7.3 Tissue specific inactivation of NDST1

Inactivation of NDST1 affects a multitude of organ systems and thus confirms the vital role of this enzyme. A few examples can be seen listed below (adapted from (Bishop et al., 2007).

Digestive system: Inactivation of NDST1 in mouse liver revealed that HS acts a co-receptor for lipoprotein uptake (MacArthur et al., 2007).

Nervous system: NDST1 inactivation in mice leads to cerebral hypoplasia, neural tube closure defects and eye and lens defects (Grobe et al., 2005, Pan et al., 2006).

Skeletal system: craniofacial defects and delayed or even missing ossification (Grobe et al., 2005, Hu et al., 2007).

Immune system: endothelial and leukocyte specific NDST1 inactivation resulted in decreased chemokine transcytosis and presentation and neutrophil infiltration (Wang et al., 2005).

Respiratory system: Lung hypoplasia and surfactant insufficiency in mice resulting from NDST1 inactivation (Ringvall et al., 2000, Fan et al., 2000).

1.8 Transplant Biology

Transplantation is often the only therapy for end-stage organ failure. In 1954, the first successful renal transplantation was performed between identical twins in Boston, USA, by Dr. Murray (Murray, 2002). More than a decade later in 1967, the first liver transplant followed in Denver, USA, by Dr. Starzl (Penko and Tirbaso, 1999). Due to sophisticated surgical procedures nowadays organ transplantation is carried out routinely, but as most organs arise from genetically different donors (with the exception of identical twins), the immunological response against the graft can lead to rejection (Sayegh and Carpenter, 2004). Rejection is mostly due to the different major histocompatibility complex antigens (HLA, which exist in many different allelic forms), and AB0 blood groups of the donor and the recipient. Based on the onset and aetiology, the rejection process can be divided into three different types (Terasaki, 2003).

1.8.1 Hyperacute rejection

This type of rejection occurs within minutes of transplantation in patients with pre-existing host antibodies (such as blood type antibodies) that recognize antigens presented by the graft, which in turn activate the complement system (Fodor et al., 1994). Due to standard cross-matching and MHC tissue typing this process poses only limited risk in clinical settings.

1.8.2 Acute rejection

Acute rejection usually develops within weeks of transplantation and is caused by mismatched HLA antigens. It can take place on both the cellular (lymphocyte mediated) and the humoral (antibody mediated) level (Le Moine et al., 2002, Colvin, 2007). Donor dendritic cells migrate to the lymphoid tissue of the recipient (Nelson and Krensky, 2001a) and activate allo-reactive lymphocytes, which in turn react with the vascular endothelium of the graft,

guided by chemotactic cytokines (el-Sawy et al., 2002). Apart from the cytotoxic effect of graft infiltrating lymphocytes, other inflammatory cells can be involved leading to necrotic cell death in the allograft.

1.8.3 Chronic rejection

Chronic rejection occurs within months up to several years after transplantation. It is often thought of to be the consequence of a multitude of acute rejections. Generally it is characterised by vasculopathy and fibrosis (Cornell et al., 2008).

1.9 Heparan sulphate and chemokines in transplantation

Chemokines presented by HS of the activated endothelium initiate the first step of leukocyte extravasation. This process is based on the interaction of chemokines presented on the endothelium and their corresponding receptors on leukocytes. Once leukocytes have invaded the graft, the pattern of chemokines secreted and displayed by HS within the tissue determines the positioning of the infiltrating cells. The structural heterogeneity of the HS chains allows HS to interact with a multitude of biomolecules. Apart from rather unspecific charge dependent interactions, one structurally unique HS motifs has been reported for antithrombin III. The existence of specific HS-protein interaction implies that cells and tissues can change and adopt their HS structure in order to interact with different HS-binding partners. Indeed, it was shown recently that stimulation of endothelial cells with proinflammatory cytokines leads to an increase of N-sulphated HS on the cell surface and matrix, possibly offering new binding sites (Carter et al., 2003, Ali et al., 2005a).

1.10 Renal transplantation

The kidney is a paired organ which serves the excretion of waste products and toxins from the blood. The main components of the urine are urea and uric acid (break down products of proteins and nucleic acids). The kidney is further involved in homeostasis by regulating electrolytes, acid-base balance and blood

pressure. In addition, it acts as an endocrine organ producing several hormones and processing vitamin D.

Each kidney is a bean shaped organ with a concave and a convex side. Functionally, it can be divided into 3 anatomically distinct parts: the cortex, the medulla and the pelvis (which extends into the ureter). Blood is collected and filtered into the cortex, whereas the medulla concentrates the urine which in the end is excreted by the pelvis. The smallest structural and functional unit of the kidney is the nephron. The nephron consists of the renal corpuscle and the renal tubular structure. In the renal corpuscle the glomerulus, which is responsible for the blood filtration from capillaries, is embedded in a membranous structure, the Bowmen's capsule. The tubular structure has its origin in the cortex at the Bowmen's capsule and is divided into proximal tubule, loop of Henle and distal tubule. The proximal tubule has microvilli, the so called brush border, which increases the surface area for the absorption of nutrients (amino acids or glucose) and electrolytes (salts). The tissue surrounding the loop of Henle concentrates the urine by increasing the osmolarity, before the distal tubule reabsorbs salts for the maintenance of the appropriate pH. Finally, the fluid passes via the collecting ducts to the ureter and the bladder.

1.10.1 Kidney rejection

Renal transplantation has become the method of choice for end stage renal disease (ESRD) patients. There are many different causes for ESRDs, including diabetes, hypertension, glomerulonephritis or polycystic kidney disease. In general, patients in need for a renal transplant have a good prognosis with one year survival rates lying above 90% (Nguan and Du, 2009). Before transplantation, ABO blood antigens and partial HLA matching is carried out. Due to the shortage of donors a perfect match can rarely be found, which can lead to hyperacute rejection. It mainly targets the endothelium and complement activation results in vascular thrombosis and necrotic death of the renal tissue (Trpkov et al., 1996). Once this type of rejection is in full swing, which can happen within the first few minutes to hours after transplantation, it can be resistant to immunosuppressive therapy and therefore better cross matching

and panel reactive antibody titre tests (describing the level of sensitisation to donor antigens) should be carried out (Jordan and Pescovitz, 2006).

Acute rejection occurs within weeks up to months following transplantation and can be reoccurring throughout the entire lifespan of the graft, thereby increasing the chances of developing chronic rejection. It can be antibody mediated as well as T-cell mediated. Acute antibody mediated rejection (AMR) makes up for 25% of acute rejection episodes (Cornell et al., 2008) and resembles the histological changes described for hyperacute rejection. As compared to hyperacute rejection, its onset is days up to weeks after transplantation of the graft, which has been working before (Halloran et al., 1990). It is defined by injury to the endothelium and the existence of C4d, a cleavage product of the complement system that becomes bound to peritubular arteries at the site of activation (Racusen and Haas, 2006). Today, high dosage of intravenous Ig, plasmapheresis and immunoadsorption allow a reversal rate of up to 90% of AMR (Bohmig et al., 2001, Crespo et al., 2001, Racusen and Haas, 2006).

T-cell mediated rejection (acute cellular rejection) can occur alone or in conjunction with AMR. It is characterised by the infiltration of the allograft interstitium with mononuclear cells. This leukocyte recruitment is controlled by chemokines, which are present on endothelial cells and corresponding chemokine receptors, present on the leukocytes. After chemokine-mediated penetration of the graft tissue, the leukocytes can secrete cytokines which activate graft resident tubular epithelial cells which in turn can produce chemokines directing leukocyte subpopulations to tubular epithelial compartments within the graft. A number of chemokines have been shown to be expressed during acute cellular rejection, such as CCL2, CCL3, CCL4 and CCL5 (Robertson et al., 1998, Nguan and Du, 2009). The infiltration of CD4 and CD8 lymphocytes as well as monocytes to the tubules is called tubulitis. The number of T cells infiltrating the tubules correlates with long term survival of the graft and identification of the leukocyte subsets infiltrating the tubules could strengthen the diagnosis of acute rejection and could help to predict further outcome (Racusen et al., 1999, Robertson and Kirby, 2003). In most severe cases the arterial endothelium becomes a target and can undergo necrosis.

Acute rejection can be divided into different stages of disease according to the Banff Schema, a universal classification of renal allograft pathology (Table 1-4,

adapted from (Solez et al., 2007). This schema was introduced in 1995 (Racusen et al., 1995) and has been updated ever since (Racusen et al., 1999, Solez et al., 2007, Solez et al., 2008, Sis et al., 2010).

Table 1-4 Grading of acute renal allografts

Type (grade)	Histopathological findings
IA	Cases with significant interstitial infiltration (>25% of parenchyma affected) and foci of moderate tubulitis
IB	Cases with significant interstitial infiltration (>25% of parenchyma affected) and foci of severe tubulitis
IIA	Cases with mild to moderate intimal arteritis
IIB	Cases with severe intimal arteritis comprising >25% of the luminal area
III	Cases with transmural arthritis and/or fibrinoid changes and necrosis of medial smooth muscle cells with accompanying lymphcytic inflammation

Adapted from Banff 97 (Solez et al, 2007)

Chronic rejection is often thought of as the result of cumulative individual acute rejection episodes. It is still poorly understood, but there is evidence that chronic rejection correlates with the severity of the acute rejection (Robertson et al., 2004). It can be caused by both antibody or T-cell mediated rejection and is not curable at the time. Histological features of chronic rejection are transplant glomerulopathy (duplication or multilamination of the glomerular basement membrane; if accompanied by C4d deposits referred to as chronic humoral rejection), peritubular capillaropathy (duplication or multilamination of basement membrane), transplant arteriopathy (neointimal thickening with scattered mononuclear cells), interstitial fibrosis and tubular atrophy (Colvin, 2006, Cornell et al., 2008). Tubular epithelial cells undergo epithelial to mesenchymal transition (EMT) in response to TGFß and migrate to the interstitium where they transform into myofibroblasts (Liu, 2004). Myofibroblasts together with fibroblasts in the interstitium produce excessive amounts of ECM. Excessive production with reduced degradation of ECM can result in massive ECM

deposition and fibrosis (Qi et al., 2006). Chronic rejection can be graded semiquantitatively as mild, moderate or severe according to interstitial fibrosis and tubular atrophy.

1.11 Liver transplantation

The liver is the largest solid organ of the body and is highly metabolically active. It is involved in the production, the break down and the storage of glucose; the synthesis of various proteins including blood clotting factors and acts as a store for a range of molecules, including vitamins and minerals. It is also responsible for regulating lipid metabolism.

Another important feature of the liver is its capacity to remove impurities from the blood and the detoxification of undigested or harmful substances. Bile, a substance essential for the absorption of fat and fat soluble vitamins, is also produced and secreted by the liver. It is produced by hepatocytes and then transported to the gallbladder and small intestine, where it exerts its function.

The smallest functional unit of the liver are the lobules. A single lobule has a roughly hexagonal shape with the hepatic vein in the centre. At the corners of the lobule the portal tract (or portal triad) is located, consisting of the hepatic artery, the portal vein and the bile duct, which are covered by connective tissue and hepatocytes. The hepatic artery and portal vein bring blood, carrying oxygen and nutrients, to the sinusoids. Sinusoids are very thin blood vessels with a discontinuous endothelial cell layer, allowing an easy exchange of proteins, also closely associated with Kupffer cells.

1.11.1 Liver rejection

Transplantation has been proven to be very efficient treatment for endstage liver disease with excellent survival rates (90% one year after transplant and 75% long term survival (Desai and Neuberger, 2009). In the UK, the most common reasons for a liver transplant are alcoholic cirrhosis, chronic hepatitis and primary biliary cirrhosis (www.uktransplant.org.uk). Before transplantation, ABO blood group matching between donor and recipient is performed. Of minor importance is HLA cross-matching, as the liver is not very immunogenic.

In contrast to renal transplantation, hyperacute rejection, which is dependent on preformed antibodies and activation of the complement system, does rarely occur in hepatic rejection. It is not completely understood why livers hardly develop hyperacute rejection (also referred to as humoral rejection) but it could be due to the binding and inactivation of damaging antibodies to Kupffer cells or soluble histocompatibility antigens (Demetris and Markus, 1989).

The basis of the cellular rejection is lymphocyte infiltration into the allograft. These activated lymphocytes are guided into the graft by chemokines, which are expressed and presented by the endothelium of both sinusoids and portal vessels. After entering the graft, the pattern of chemokine secretion and retention determines the positioning of the infiltrating T-cells. Biliary epithelial cells have been shown to secrete a number of chemokines, such as CCL2 and CCL5, which direct lymphocytes in the proximity of bile ducts (Goddard et al., 2001).

Acute cellular rejection is characterized by mainly three pathological features. Firstly, a massive infiltrate of inflammatory cells. Cells infiltrating the portal tract usually comprise a mixture of inflammatory cells, but mononuclear cells are the most prominent. Secondly, bile duct inflammation and injury (Vierling and Fennell, 1985) and finally, inflammation of the portal or terminal hepatic veins, caused primarily by lymphocytes (Ludwig, 1989, Batts, 1999). At least two of the three above described features have to be displayed to establish the diagnosis of an acute rejection (together with other evidence, such as biochemical markers). Once this diagnosis has been established, the rejection can be graded according to severity based on the Banff Schema developed for liver rejection based on the Banff schema for renal rejection. It is based on the severity of inflammation plus morphological changes due to rejection related ischemia (Table 1-5).

Table 1-5 Grading of acute liver allogarfts

Global Assessment	Criteria
indeterminate	Portal inflammatory infiltrate fails to meet criteria for the diagnosis of acute rejection
mild	Rejection infiltrate in a minority of triads, generally mild and confined within the portal spaces
moderate	Rejection infiltrate, expanding most or all of the triads
severe	As moderate, with spillover into periportal areas and moderate to severe pervenular inflammation that extends into the hepatic parenchyma and is associated with pervenular hepatocyte necrosis

Adapted from Banff Schema for Grading Liver Allograft rejection, 1995

After the descriptive global assessment, a semi-quantitative scoring of the three specific features: portal-, bile duct- and venular inflammation, can be conducted if necessary. Acute hepatic rejection affects almost two thirds of the patient population (Tippner et al., 2001) and typically develops within the first 30 days (Neuberger and Adams, 1998) after transplantation. The early onset generally corresponds with a good prognosis and is susceptible to additional immunosuppression (Anand et al., 1995). Late acute rejection (onset after 6 months) affects up to 20% of transplant patients (Uemura et al., 2008) has a poorer prognosis and has been associated with reduced survival of the liver (D'Antiga et al., 2002).

Chronic hepatic rejection is a rare event, most likely due to the specific immunological characteristics of the organ and its regenerative capacity (Tiegs and Lohse, 2010) and the good recognition and treatment options of acute rejection. If acute rejecting liver is resistant to immunosuppression, chronic rejection, often linked to chronic graft failure, can develop. It is characterized by persistent inflammation of the portal tract and a severe damage and loss of intrahepatic bile ducts and hepatic arteriolar thickening (Demetris et al., 2000).

1.12 Heparan sulphate in tissue remodelling

Whilst tissue remodelling is an important physiological process which is crucial and beneficial during development or wound healing after injury, sustained tissue remodelling caused by persistent injury or chronic inflammation after transplantation can lead to fibrosis and ultimately results in graft failure. Fibrosis is characterized by excessive accumulation and reduced degradation of ECM (Qi et al., 2006). As HS facilitates cell-cell and cell-matrix interaction by binding many factors involved in this process it is not surprising that HS is thought to play an important role in tissue homeostasis in general and the development of fibrosis in particular.

Liver Fibrosis

Liver fibrosis is characterized by the accumulation of myofibroblasts which produce excessive amounts of ECM such as collagens I, III and IV, fibronectin, laminin, hyaluronan and HSPGs (Gressner and Haarmann, 1988, Schuppan, 1990).This ongoing deposition of ECM leads to the formation of a scar and ultimately leads to cirrhosis, characterized by abnormal nodule formation and organ contraction (Lotersztajn et al., 2005).

Inflammatory lymphocytes infiltrate the liver parenchyma upon persistent injury, guided by chemokines presented by HSPGs. After the apoptotic cell death of a fraction of hepatocytes, Kupffer cells release fibrogenic mediators, which in turn activate hepatic stellate cells (HSC) (Bataller and Brenner, 2005). In normal liver, HSC function as Vitamin A storage. They are found in the space of Disse, but upon activation after chronic injury they lose Vitamin A and differentiate into myofibroblasts (Gabele et al., 2003), synthesizing collagen I rich matrix (Friedman et al., 1985). Platelet derived Growth factor (PDGF), mainly produced by Kupffer cells is the main mitogen for activated HSC. PDGF-B has been shown to bind to HS (Lindblom et al., 2003) and studies in mice revealed that N-sulphation and 6-O-sulphation are required for PDGF-B binding and subsequently for pericyte recruitment (Abramsson et al., 2007).

Other sources of ECM apart from HSC are portal fibroblasts (Beaussier et al., 2007) and also epithelial cells, which undergo epithelial-to mesenchymal transition, have been implicated as potential source, with TGFβ being a main

inducer of the EMT process (Liu, 2004, Rygiel et al., 2008).TGFβ also stimulates ECM production and inhibits its degradation in the liver (Shek and Benyon, 2004). Elevated levels of TGFβ are often found in fibrotic livers (Liu et al., 2006). Hepatocyte growth factor (HGF), which also requires HS as a cofactor (Catlow et al., 2008) can attenuate fibrosis by inhibiting TGFβ driven EMT (Xia et al., 2006). Fibrogenic liver tissue derived from chronic cholestatic diseased human livers revealed an increase of syndecan-1 and perlecan in ductular cells whereas HSC showed enhanced syndecan-3 expression; cultured HSC even showed increased expression of all 4 syndecans, perlecan and glypican, pointing out the important role of these matrix components in liver fibrogenesis (Roskams et al., 1996). Increased levels of perlecan have also been found in the ECM from chronically damaged livers of rats (Gallai et al., 1996). Another HSPG found overexpressed in cirrhotic livers is agrin (Tatrai et al., 2006). Recently, a study investigated changes in HS related to fibrogenesis in humans and rats and revealed an overall increase HS, specifically an increase in N-sulphation, 2-, 3- and 6-O-sulphation for both species. Also, levels of syndecan and perlecan were elevated in human cirrhotic livers (Tatrai et al., 2010).

Renal fibrosis

Chronic injury in kidneys, like chronic rejection, often leads to fibrosis, which is characterized by excessive accumulation and deposition of ECM, such as collagens I, III and IV, fibronectin, laminin and HSPGs (Klahr and Morrissey, 2002, Miyazaki et al., 2003). Ongoing deposition of ECM leads to fibrous scarring of the tissue and ultimately to graft dysfunction and failure (Liu, 2006).
Following injury, inflammatory lymphocytes, guided by pro-inflammatory chemokines presented by HSPGs, infiltrate the kidney. Proninflammatory cytokine and fibrogenic factors are released by inflammatory cells which in turn activate mesangial cells and fibroblasts and trigger EMT of tubular epithelial cells, which leads to the excessive production of ECM. TGFβ has been identified as main inducer of EMT (Schnaper et al., 2003). In *vitro,* TGFβ on its own can induce activation of mesangial cells and fibroblasts or activation of tubular epithelial cells (Yang and Liu, 2001). Elevated levels of both TGFβ-1 and its receptor have been found in renal tubular epithelial cells upon injury

(Yang and Liu, 2002). Hepatocyte growth factor can prevent renal fibrosis by inhibiting TGFβ-1 expression (Liu, 2002).

Recently, also endothelial cells were identified as origin of fibroblasts, after they underwent so called 'endothelial to mesenchymal transition' (Zeisberg et al., 2008).

Increased expression of HSPGs has been observed in renal fibrotic lesions (Born et al., 1996), which was accompanied by increased chemokine binding capacity by HS (Ali et al, 2005; Celie et al, 2007). Increased binding of L-selectin and CCL2 to tubulointerstitial HSPGs has been observed in an array of renal diseases; upregulation of syndecan 1 on tubular epithelial cells co-localizing with L-selectin and CCL2 binding HSPGs was shown (Celie et al, 2007). Recently, the role of HSPGs in tissue remodelling in chronic transplant dysfunction was demonstrated. Increased expression of HS was found in intrarenal arteries, glomeruli and the tubulointerstitium. Collagen XVIII and perlecan expression was induced in arteries with vasculopathy and sclerotic glomeruli, whereas versican, a chondroitin sulphate proteoglycan, was predominant in interstitial fibrosis. Glomerular remodelling was defined by pronounced expression of perlecan in the glomerular basement membrane. Collagen XVIII production was further induced in corticular tubular basement membranes (Rienstra et al, 2010).

As HS binds to growth factors, profibrogenic cytokines and also matrix metalloproteases (Yu and Woessner, 2000), which are involved in the degradation of the ECM, the changes in HSPG expression as well as HS modification are likely to modulate the tissue remodelling process.

1.13 Specific aims of this study

The endothelium can be regarded as a gatekeeper as its function is to separate tissues from peripheral blood leukocytes. The resting endothelium provides an anti-inflammatory environment. Therefore leukocyte infiltration can only occur if the endothelium is activated and promotes this process. During transplantation, ischemia/reperfusion syndrome and mechanical stress targets leukocytes into microvascular spaces (Ambrosio and Tritto, 1999, Linfert et al., 2009). The multistep process of leukocyte recruitment into the allograft is based on

interactions between adhesion molecules expressed both on the leukocyte as well as on the endothelium (Barreiro et al., 2010). Inflammatory mediators, such as TNFα, are produced and lead to an upregulation of adhesion molecules, which are responsible for leukocyte rolling and firm adhesion. The activation of leukocyte-expressed integrins by chemokines, bound to endothelial GAGs, leads to firm adhesion of the leukocyte on the endothelium (Middleton et al., 2002). Finally, chemokines promote the diapedesis of leukocytes. Once the leukocytes have entered the graft specific subpopulations can be further guided into the tissue by HS-immobilised chemokines.
The activation of these pro-inflammatory pathways can then lead to irreversible injury of the endothelium and of the graft, resulting in graft rejection.

This study aims to further elucidate the current understanding of Heparan Sulphate Proteoglycans during inflammation.

The specific aims of this study are as follows:

- Analysis of HS expression pattern in healthy tissues and tissues derived from organs undergoing rejection

- Investigation of the regulation of Heparan Sulphate biosynthesis at the protein level targeting the key enzyme NDST1

- Examine the consequence of modulation of NDST1 expression on HS structure and function

2 General Materials and Methods

2.1 General laboratory practice

All experimental procedures were conducted in accordance with 'Newcastle University safety policy' and 'Institute of Cellular Medicine safety policy'. Laboratory work was performed in accordance with University publication 'Safe working with biological hazards' and 'Safe working with chemicals in the laboratory'. Tissue culture was carried out in compliance with regulations for containment of class II pathogens and BIOCOSHH and COSHH risk assessments were conducted before commencing any work.

2.2 Cell culture

2.2.1 Culture media

Culture media used in this study included Dulbecco's Modified Eagle Medium (DMEM, 4.5g/l Glucose, 110mg/l sodium pyruvate, Cambrex); Roswell Park Memorial Institute 1640 (RPMI, Cambrex); Dulbecco's Modified Eagle Medium:Nutrient F12 Ham (DMEM-F12, Cambrex) and endothelial basal medium (MCDB-131, Sigma; supplemented with 10ng/ml epidermal growth factor (EGF) and 1µg/ml Hydrocortisone) . All media were supplemented with 2mM L-glutamine, 100U/ml Penicillin, 100µg/ml Streptomycin and 10% heat inactivated foetal calf serum (FCS) (all supplied by Sigma).
The antibiotic G418 sulphate (Calbiochem) was added in varying concentrations for transfectant selection (800µg/ml) and propagation (400µg/ml).

2.2.2 Cell lines

2.2.2.1 HEK 293

The human embryonic kidney cell line was obtained from the American Type Culture Collection (ATCC) and cultured in complete DMEM. Cells have been

transformed with adenovirus 5 DNA. They have epithelial appearance and are semi-adherent.

2.2.2.2 THP1

The monocytic suspension cell line was obtained from ATCC and cultured in complete RPMI. This cell line can easily differentiate into macrophages following stimulation. Cells were originally isolated from peripheral blood of a one year old boy with acute monocytic leukaemia.

2.2.2.3 PBMC

Peripheral blood mononuclear cells were extracted from fresh blood provided by healthy volunteers. After adding heparin (0.5U/ml) to the blood, an equal volume of serum-free medium was added. Density gradient separation was performed by underlaying the diluted blood with 3ml of Lympholyte-H (Cedarlane) and centrifuged it at 800 x g for 20 minutes. The interface layer containing PBMCs was carefully removed and washed once in serum free RPMI before being cultured in complete RPMI.

2.2.2.4 CHO

The Chinese hamster ovary cell line was cultured in complete DMEM-F12. Wild type cells are referred to as CHO-K1 whereas the CHO-745 cells refer to a glycosaminoglycan deficient strain lacking of xylosyltransferase, a key enzyme in HS biosynthesis. These cells were kindly provided by Prof. Jeff Esko, University of San Diego La Jolla, USA.

2.2.2.5 HMEC-1

The human microvascular endothelial cell line was obtained from ATCC and cultured in complete MCDB-131.

2.2.2.6 HK-2

This renal proximal tubular epithelial cell line has been isolated from normal human adult kidney and was immortalized by transduction with human papilloma virus 16 DNA. Cells were obtained from ATCC and cultured in complete DMEM-F12.

2.2.2.7 HepG2

The hepatocellular carcinoma cell line with epithelial morphology was obtained from ATCC and cultured in complete DMEM.
All cells were grown at 37ºC and 5% CO_2.

2.2.3 Sub-culturing of cells

Adherent cells were grown horizontally in tissue culture flasks (Corning) of variable sizes (25, 75, and 150 cm^2). Subculturing was performed in a ratio of 1:3 depending on cell density every 3 to 4 days.
Culture medium was removed and cells were washed with PBS (Sigma). Sufficient amounts of Trypsin-EDTA solution (Sigma) was added and cells were incubated at 37ºC for 5 minutes. The Trypsin/EDTA solution was then inactivated by addition of the same volume of culture media. This mixture was then transferred to a universal centrifuge tube (SLS). Cells were centrifuged at 500 x g for 5 minutes and the pellet was resuspended in fresh culture media.
Suspensions cells were grown vertically in tissue culture flasks and subcultured when necessary.

2.2.4 Cell counting

Cells were counted using an improved Neubauer chamber Haemocytometer (Reichert). Typically, 10µl of resuspended cells were allowed to diffuse beneath the coverslip. Cells in the 25 central squares of the grid were counted and the total multiplied by $1x10^4$ to obtain the number of cells per millilitre.

2.2.5 Cryopreservation of cells

Cells were cryopreserved in liquid nitrogen. Cells were detached from tissue culture flasks, pelleted and resuspended in 0.5ml of culture medium. To this 0.5ml of freezing medium was added, consisting of 20% dimethylsulfoxide (DMSO, Sigma) in FCS, resulting in a final DMSO concentration of 10%. This mixture was transferred into a cryovial (Corning) and slowly cooled at 1ºC/minute in a freezing vessel (Nalgene) containing isopropanol at -80ºC at least over night prior to final storage in liquid nitrogen.
Recovery of the cells was achieved by rapid thawing of the cryovial contents in a waterbath at 37ºC and their addition to 5-10ml of culture media in a 25cm^2 flask. After 24 hours DMSO-containing media was replaced with fresh culture media.

2.2.6 *Mycoplasma* testing and treatment

Mycoplasma sp. infection can affect a variety of cellular processes, including reduced cell proliferation and changes in gene expression. The origin of contamination is often the researcher himself, as one subspecies of *Mycoplasma* lives in the respiratory tract. Apart from fluorescence microscopy, which can detect the nuclei of *Mycoplasma* after 4',6-diamidino-2-phenylindole (DAPI) staining, a selective biochemical test was used in this study. The MycoAlert kit (LONZA) relies on the activity of certain mycoplasmal enzymes. After lysing mycoplasma the enzyme can react with the MycoAlert substrate catalyzing the conversion of ADP to ATP. This increase in ATP can be measured in a bioluminescent reaction, where the emitted light is linearly related to the ATP concentration. *Mycoplasma* testing was performed according to the manufactures instructions. In short, 100µl of culture supernatant were mixed with 100µl of MycoAlert reagent and after 5 minutes the first luminescence reading was taken (reading A). After the addition of 100µl of MycoAlert substrate a further 10 minutes of incubation time followed, after which the final luminescence reading was taken (reading B). The ratio of reading B to reading A was determined and ratios smaller than 1 were considered mycoplasma negative. If readings greater than 1 were obtained, cells were either replaced with healthy cells or if necessary cleaned up with

mycoplasma removal agent (MRA, Serotec). MRA shows strong anti-mycoplasma activity against many types of *mycoplasma,* including *Mycoplasma orale, M. arginini, M. hyorhinis* and *Acholeplasma laidlawii.* Cell culture media was supplemented with 0.5µg/ml MRA and cells were incubated for up to 10 days. Testing with the MycolAlert kit was repeated after removal of the agent.

2.3 General molecular biology techniques

2.3.1 Bacterial culture

E. coli were grown in LB-media (10g/L Bacto-tryptone, 5g/L Bacto yeast extract and 10g/L Sodium chloride; Sigma) at 37ºC in an orbital shaker. When grown on plates, LB Agar was used. After transformation of the bacteria the media was supplemented with antibiotics for selection of transformants. In these studies transformants were selected with Ampicillin (Sigma) at a final concentration of 100µg/ml or Kanamycin (Sigma) at a final concentration at 50µg/ml. For the stock solution, antibiotics were dissolved in sterile ddH_2O (100mg/ml ampicillin and 50mg/ml kanamycin).
For long term storage, 0.5ml of an overnight culture was mixed with 0.5ml 40% glycerol (Sigma), resulting in a final concentration of 20% glycerol. Cells were kept at -80ºC.

2.3.2 Preparation of competent cells and transformation

Transformation describes the uptake of foreign DNA into a prokaryotic cell. Cells which are capable of DNA uptake are naturally competent; other cells are not naturally competent or not competent under certain conditions (e.g. *E.coli* grown in full media in the labratory) and have to be treated in a certain way to gain competence.
In this study $CaCl_2$ competent *E.coli* JM109 cells were used, which were obtained from Promega or competent cells were prepared as described:
A single colony of *E.coli* XL-1-Bue was inoculated in 2ml of LB media and grown over night. 1ml of this suspension was transferred into 50ml of fresh LB

media. Cells were incubated in an orbital shaker until they reached an OD_{600} of 0.3-0.4. Cells were then chilled on ice for 10 minutes before harvesting at 2500 x g for 7 minutes at 4ºC. Cells were kept on ice all the time.

The pellet was carefully resuspended in 10ml of 100mM $CaCl_2$ solution and spinned at 2000 x g for 5 minutes at 4ºC. Again the pellet was carefully resuspended in 10ml of 100mM $CaCl_2$ solution and kept on ice for 30 minutes. After spinning at 2000 x g for 5 minutes at 4ºC the pellet was resuspended in ice cold $CaCl_2$ with 15% glycerol (Sigma). Cells were then aliquoted and frozen in liquid nitrogen. Until use, cells were stored at -80Cº.

Plasmid DNA (1-10µl; 10-100ng) was kept on ice for 5 minutes before 100 µl of chilled bacteria were added. After 30 minutes of incubation on ice the mixture was heat shocked at 42ºC for 2 minutes in a water bath. 0.9ml of LB media was added and after 30 minutes of regeneration time at 37ºC cells were plated onto LB-Agar plates containing appropriate antibiotics.

The plates were incubated upside down at 37ºC over night to allow single colonies to grow.

All strains used in these studies are listed in Table 2-1.

Table 2-1 Comparision of E. coli strains used in this study

Strain	Genotype	Origin
E. coli XL-1-Blue	endA1 gyrA96(nalR) thi-1 recA1 relA1 lac glnV44 F'[::Tn10 proAB+ lacIq Δ(lacZ)M15] hsdR17(rK-mK+)	Stratagene
E. coli JM 109	endA1 glnV44 thi-1 relA1 gyrA96 recA1 mcrB+ Δ(lac-proAB) e14- [F' traD36 proAB+ lacIq lacZΔM15] hsdR17(rK-mK+)	Promega
E. coli Solo pack	tetr ∆(mcrA)183 ∆(mcrCB-hsdSMR-mrr)173 endA1 supE44 thi-1 recA1 gyrA96 relA1 lac Hte [F´ proAB lacIqZ∆M15 Tn10 (Tetr) Amy Camr] cre	Stratgene

2.3.3 Plasmid DNA extraction

Plasmid DNA isolation from transformed bacteria was performed using kits based on the modified alkaline lysis method. Dependent on the required amount of DNA, DNA-Mini-, Midi- or Maxiprep kits (Qiagen) were used. When DNA was required for transfection an endotoxin free kit was used (Sigma).
Endotoxin consists of lipopolysaccharides and which are a major constituent of the outer membrane of gram-negative bacteria (*E. coli*). When they are released they initiate a host response in mammals which should be avoided.
DNA isolation was performed according to the manufactures instructions.
Briefly, transformed bacteria were grown over night under selection pressure. Cells were pelleted and resuspended and lysis was induced by the addition of NaOH and SDS. The addition of RNase to the buffer assured the degradation of all RNAs. The reaction was then neutralised and precipitated denatured proteins, chromosomal DNA and cell debris were removed. In the presence of a high salt concentration plasmid DNA was bound to a silica membrane and later eluted in a low salt buffer or H_2O.

2.3.4 Nucleic acid quantitation

DNA was quantified either using spectrophotometry at 260nm wavelength (Eppendorf BioPhotometer, Eppendorf or Nanodrop, Thermo Scientific) or by running an agarose gel and comparing the intensity of the bands to bands of a Hyperladder with known DNA concentrations.
When DNA or RNA were quantified spectrophotometrically, only samples with OD 260/280 and OD 260/230 ratios >1.8 were considered good quality. Measurements with 260/280 ratios <1.8 are indicative for protein contamination whereas 260/230 readings <1.8 indicate the presence of salts, solvents or proteins.

2.3.5 Precipitation of DNA

To increase the concentration of DNA and to remove impurities ethanol precipitation was performed. 3M Sodium Acetate (pH 5.2) was added to the DNA with a resulting final concentration of 0.3M. 2.5 volumes of ice-cold ethanol

absolute were added and this mixture was incubated at -80ºC for at least 20 minutes. The absolute ethanol precipitates DNA as well as salts. After a centrifugation step the pelleted DNA was washed in 70% ethanol to remove residual salts. The pellet was air dried and resuspended in an appropriate volume of sterile H_2O.

2.3.6 Agarose gel electrophoresis

Agarose gel electrophoresis was used to separate nucleic acid fragments according to their size. An electric field is applied to the gel and the negatively charged DNA molecules migrate through the matrix towards the positive electrode. Gels were routinely run at 85V with 1 x TAE (40mM Tris, 20mM acetic acid, 1mM EDTA; pH 8) as running buffer. The agarose (Bioline) was dissolved in 1 x TAE buffer whilst heating in a microwave. Dependent on the expected size of the DNA fragments 0.8 – 1.7% gels were used. The rate of migration is dependent on the size and form of the DNA. Smaller fragments migrate more quickly than larger ones and linear DNA migrates slower than supercoiled DNA. To determine the size of DNA fragments molecular weight markers with known fragment sizes are run on each gel. In this study either a 100bp ladder with fragments from 100bp to 1500bp (Promega) or Hyperladder 1 (200bp -10000bp) from Bioline were used. To allow the DNA to sink into the wells of the gel and for visualisation a DNA loading buffer was added, e.g. Orange G buffer (30% glycerol, 0.25% Orange G). For visualisation of the DNA on a UV screen the intercalating agent ethidium bromide was added to the gel at a final concentration of 0.5µg/ml.

2.3.7 Isolation of DNA fragments

DNA fragments were excised from agarose gels following electrophoresis separation using a sterile scalpel. The DNA was purified using the Wizard SV Gel and PCR Clean-up System (Promega). The gel slice was incubated with membrane Binding Solution at 60ºC until it was completely dissolved. This mixture was applied to a Minicolumn and the DNA bound to the silica membrane. After two washing steps with membrane Wash Solution the DNA was eluted in nuclease-free water. The DNA was then stored at -20ºC.

2.3.8 Cloning and use of restriction enzymes

Restriction enzymes are a group of endonucleases isolated from bacteria. They are able to hydrolyse DNA in a sequence specific manner. In the lab type II restriction endonucleases are of common use as they cleave DNA within the target sequence and do not posses methyltransferase activity. Target sequences are predominantly palindromic sequences consisting of 4, 6 or 8 basepairs. Hydrolysis of target DNA can result in blunt ends or single stranded 3' or 5' overhangs, so called sticky ends. All the restriction enzymes used in this study were obtained from Promega and were used according to the manufacture's guidelines. Per definition, one unit of restriction enzymes can cleave one µg of Lambda-DNA under optimal buffer conditions in one hour at 37ºC.

In general, restriction digestions were incubated for at least 2 hours at 37ºC or over night. If double digestions were performed, enzyme buffers which offered both enzymes the best conditions, were chosen.

Dependent on the enzyme heat inactivation was performed if necessary.

For the ligation of insert DNA into an appropriate vector a molar ratio of insert to vector of 3:1 was used. The T4 ligase (Promega) from Bacteriophage T4 catalyzes the formation of a phosphodiester bond between 5' phosphate and 3' hydroxyl termini in duplex DNA. Ligation reactions were generally performed over night at 16ºC.

2.3.9 DNA sequencing

Automated DNA sequencing was used to determine the sequence of the created construct. Sequencing was performed at Geneservice, Cambridge using the chain termination method originally developed by Sanger.

2.4 DNA transfection

Transfection of eukaryotic cells is a technique used to deliver foreign DNA molecules into cells to study gene expression.

It can be discriminated between two different types of transfection, transient and stable transfection.

Transiently transfected cells do not integrate foreign DNA into their genome therefore many copies of the gene of interest must be present in the cells. Transient transfection leads to high expression levels of the gene of interest, but this effect only lasts for a few days. Transiently transfected cells must be analysed within 24 to 96 hours after transfection, because cells lose their plasmids with every cell division.

Stable transfection is used to achieve a permanent expression of the gene of interest. Foreign DNA can either be incorporated into the host genome or the vector can be maintained episomally. Transfectants can be selected due to the antibiotic resistance marker of the plasmid. To avoid mixed populations, single clones must be picked and expanded.

Many different transfection kits are commercially available. In this study, the Effectene transfection kit (Qiagen) was used. At first, the DNA is condensed by interaction with the positive charged enhancer. Then, the condensed nucleic acid is coated with a cationic lipid micelle. This transfection complex is finally taken up into the cells by endocytosis.

Transfection was performed according to the manufacturer's instructions.

Briefly, 2 x 10^6 HEK 293 cells/100mm dish were seeded the day before transfection. On the day of transfection cells were 60-70% confluent. 2µg of DNA were mixed with the DNA condensation buffer EC and supplemented with enhancer to allow DNA condensation. This mixture was incubated at RT for 25 minutes and Effectene Transfection Reagent was added. In order to form transfection complexes, the sample was incubated for 10 minutes at RT. Different DNA:Effectene Transfection Reagent ratios were used (1:10, 1:30, 1:50). Culture medium was gently removed from the dishes, cells were washed with PBS and fresh culture media was added. The transfection complex was mixed with growth media and then added drop-wise onto the cells in the 100mm dishes. 48 hours after transfection antibiotics were added. The vector used has a neomycin resistance cassette. As neomycin is toxic, an analogous antibiotic, G418 sulphate (Calbiochem) was added (800µg/ml). Both antibiotics inhibit the protein biosynthesis by interfering with the 80S ribosome.

Single clones were selected and during expansion cells were kept under antibiotic selection (400µg/ml).

2.5 Protein chemistry

2.5.1 Protein extraction

For protein extraction cells from 1 subconfluent 75cm^2 flask were detached by trypsinisation. The cell suspension was washed twice in PBS. After centrifugation the pellet was resuspended in 200µl lysis buffer (50mM Tris, 150mM NaCl, 10mM Na_3VO_4 and 0.5-1%NP40; all supplied by Sigma, supplemented with Complete Mini Protease Inhibitor Cocktail tablet (Roche)). One tablet was added per 10ml of lysis buffer. Lysis occurred on ice for 30 minutes. If the cell pellet did not dissolve by mixing, the suspension was sheared mechanically by passing the lysate several times through a 21G needle. Cells were then sonicated until the DNA was disrupted. The sample was centrifuged at 20.000 x g for 20 minutes and the supernatant was collected. Proteins were stored at -80ºC prior to protein concentration estimation.

2.5.2 Protein precipitation

In order to increase protein concentration Trichloroacetic acid (TCA) precipitation was performed. In brief, TCA was added to the protein lysates to a final concentration of 25%. After incubating the mixture on ice for 10 minutes the sample was centrifuged at 14.000 x g for 5 minutes. Two washing steps with ice-cold acetone followed before the sample was left at 95°C degree to dry. To solubilise the proteins before SDS-PAGE, proteins were resuspended in loading buffer and incubated at 37°Celsius for further 30 minutes.

2.5.3 Protein concentration estimation

The protein concentration was determined by using the BCA kit from Pierce. This kit is based on the Biuret reaction, where Cu^{2+} gets reduced to Cu^{+} by proteins in an alkaline medium. The cuprous cation is selectively detected using a reagent containing BCA (bicinchoninic acid). A coloured chelate complex consisting of 2 BCA molecules and 1 cuprous ion is formed which exhibits absorbance at 562nm wavelength. The protein concentration is determined by spectrophotometry. To estimate the protein concentration of the sample its

absorbance is compared to the absorbance of the standard curve (made of serial dilutions of BSA with known concentration).
An appropriate amount of working reagent was prepared by mixing solution A and B in a ratio of 50:1. 10µl of protein sample were mixed with 200µl of working reagent, incubated for 30 minutes and absorbance was measured using a spectrophotometer (Eppendorf).

2.5.4 Sample preparation

The protein sample was made up to a concentration of 20 to 80µg/sample by adding H_2O. After adding 10x loading buffer (0.125M Tris-HCl, 2% (w/v) SDS, 10% (w/v) glycerol, 0.001% (w/v) bromophenolblue) and 10% β-mercaptoethanol the sample was boiled for 5 minutes at 100ºC and an aliquot was loaded onto a SDS-PAGE. The rest was kept at -80ºC.

2.5.5 SDS-PAGE

Proteins can be separated according to their size by SDS-PAGE. This protocol has been adopted from the original by Laemmli. Sodium dodecyl sulfate (SDS) is an anionic detergent which destroys secondary and non disulfide linked tertiary structures. SDS binds to the protein and gives the molecule an overall negative charge, so that the separation is solely dependent on the size of the protein. For SDS-PAGE a reducing agent such as dithiothreitol (DTT) or β-mercaptoethanol is added, which reduces disulfide linkages, which are responsible for some tertiary structures (typical composition of SDS-PAGE see Table 2-2). A molecular weight marker is run along side the protein to estimate its molecular size. In this study the ProSieve pre-stained protein marker was used which has a size range from 10 to 179 kDa.
SDS gels were run in a SDS-PAGE system from Bio-Rad which was filled with running buffer (0.025M Tris, 0.25M glycine pH 8.3, 0.1% (w/v) SDS).

Table 2-2 Composition of a typical SDS-PAGE

compound	**resolving gel 10%**	**stacking gel 4%**
H_20	4ml	1.4ml
Acrylamide 30%	3.3ml	0.33ml
1.5 M Tris pH 8.8	2.5ml	-
1.0 M Tris pH 6.8	-	0.25ml
SDS 10%	100µl	20µl
APS 10%	100µl	20µl
Temed	4µl	2µl

10% acrylamide gels were used because the protein of interest has an expected size of 100 kDa and 10% gels allow the separation of proteins from 15 to 100 kDa. APS (ammoniumpersulfate) and TEMED (tetramethyl-ethylenediamine) catalyse the polymerisation of the acrylamide, where APS acts as a source of free radicals.
Gels were run at 35mAMPs per gel with water cooling until the protein front reached the end of the gel.

2.5.5.1 Coomassie staining

In order to visualize protein bands on the SDS-PAGE gels were stained with Coomassie blue solution (10% acetic acid, 10% isopropanol, 0.1% Coomassie blue powder). Gels were immersed in stain for 24 hours before being destained in water.

2.5.6 Western Blot

Following SDS-PAGE the proteins were transferred to a HiBond-P PVDF (polyvinylidene) membrane (Amersham).
To activate the membrane it was soaked in methanol for 30 seconds and then washed in transfer buffer (20mM Tris, 1.92M glycine, 20% methanol) for 3

minutes. The resolving gel and the membrane were placed in a 'gel sandwich' in an immunoblotting cassette filled with transfer buffer. The transfer was carried out for 1 hour at 90V or over night at 20V with water cooling.

After the transfer the membrane was incubated for 1 hour in 5% non fat milk (Marvel) in TTBS (5mM Tris, 150mM NaCl, 0.005% Tween-20 (BDH Chemicals), pH 7.4) in order to block non-specific binding sites. The membrane was then washed 3 times in TTBS for 10 minutes before the addition of the antibody. The primary antibody NDST1 (Santa Cruz) was raised in goat and is able to detect an N-terminal sequence of human NDST1. Different dilutions of primary antibody were made up in 5% non-fat dry milk in TTBS and were incubated for 1 hour at room temperature or over night at 4ºC. After three washing steps in TTBS for 15 minutes the secondary antibody, donkey anti-goat HRP-conjugated (Santa Cruz) was added at a 1:5000 dilution and incubated for 1 hour at room temperature. Before antibody detection the membrane was washed again three times in TTBS.

All washing and incubating steps were carried out under gentle constant shaking of the membrane.

For the detection of the antibodies the ECL Plus system (Amersham) was used. In this system HRP and peroxide catalyse the oxidation of an acridan substrate to acridinium ester intermediates, which then further react with peroxide, producing high intensity chemiluminescence with maximum emission at 430nm. The resulting light was detected on an x-ray film (Kodak).

2.5.6.1 Regeneration of the membrane

Stripping was used to regenerate the membrane so it could be used for further detection. After washing twice in TTBS the membrane was incubated in stripping buffer (62.5mM Tris, 2% (w/v) SDS, 30mM β-mercaptoethanol, pH 6.7) for 20 minutes at 55º. Prior to reblocking, the membrane was washed twice in TTBS.

Reprobing with antibodies was used to prove equal loading.

2.5.6.2 Staining of the membrane

To visualize the proteins on the membrane and to ensure equal loading the membrane was stained in 0.05% copper-phtalocyanine in 12mM HCl for a few minutes (until bands appeared).

2.6 Statistical evaluation

Statistical analysis was performed using Graph Pad Prism 3.0 software. Data with normal distribution was analysed with student's t-test. One-way Anova with Tukeys post test was used to compare 3 or more independent groups. Tissue samples were analysed by non-parametric Krusak-Wallis test. Differences with $p<0.05$ were considered to be significant.

3 Role of Heparan sulphate in Transplantation

3.1 Introduction

HS regulates a variety of physiological as well as pathophysiological processes as it binds a plethora of growth factors, cytokines and other biomolecules. Its involvement in disease is manifold. It acts as a coreceptor for the entry of viruses, such as herpes simplex virus type 1, hepatitis B and C and human immunodeficiency virus (O'Donnell et al., 2010, Schulze et al., 2007, Barth et al., 2006, Saphire et al., 2001), bacteria (*Bacillus anthracis*) and parasites (*Toxoplasma gondii*) (Chen et al., 2008). In Alzheimer's disease, a neurodegenerative disorder, HS plays a role in plaque pathogenesis and ß-amyloid precursor protein processing (Scholefield et al., 2003, van Horssen et al., 2003). Evidence for a direct role in cancer was found by genetic analysis. Tumour suppressor genes which can lead to cancer once their function is impaired due to mutations were identified, namely the chain elongation enzymes EXT1 and EXT2 responsible for hereditary multiple exostoses, a benign bone tumour, and glypican 3, which is linked to Simpson-Golabi-Behmel syndrome. The HS degrading enzyme heparanase is also linked to cancer, as increased heparanase expression positively correlates with metastatic potential (Vlodavsky and Friedmann, 2001). Recently, an endothelial specific knock out of NDST1 in a lung carcinoma model resulted in decreased tumour angiogenesis and tumour growth, correlating with decreased association with FGF2 and VEGF (Fuster et al., 2007).

In inflammation, the role of HS in chemokine transcytosis and presentation has been discussed already, but an additional feature of HS is its shedding during inflammatory events. After crossing the endothelial cell layer, the subendothelial basement membrane represents a major obstacle for migrating leukocytes. An array of proteases has been implicated in this degradation process, heparanase being one of them (Madri and Graesser, 2000). Most likely the degradation of the basement membrane is accomplished in a collaborative process between endothelial cells, leukocytes and platelets; all contributing different enzymes involved in the breakdown of the membrane (Parish et al., 1998). Besides

helping leukocytes to migrate into the tissue, heparanase can bind to T cells in its enzymatically inactive proform presumably facilitating T cell migration through the basement membrane (Sotnikov et al., 2004). Heparanase is also involved in the inflammatory reaction by releasing cytokines, which would otherwise be inactive while bound to HS (Schonherr and Hausser, 2000). At the same time heparanase can also reduce inflammation, by decreasing chemokine levels on endothelial cells (Parish, 2006). In the context of transplantation, heparanse shed HS can lead to a breakdown of anticoagulant environment in the transplanted organ, possibly causing intravascular coagulation and fibrin deposits in the rejecting allograft (Ali et al., 2003).

3.1.1 Renal Heparan sulphate

HSPGs have been studied for their role in glomerular filtration for a while. Glomerular HS has been proposed to be a charge-selective barrier for proteins filtered from the blood. Negatively charged proteins, like albumin, would not be able to cross the barrier due to the highly negative charge of HS itself (Kanwar and Farquhar, 1979a, Kanwar and Farquhar, 1979b, Reeves et al., 1980). This concept has been supported by different approaches: Enzymatic digestion of HS of the glomerular basement membrane (GBM) increased permeability to albumin (Groffen et al., 1998) and an antibody directed against HS of the GBM resulted in proteinuria (van den Born et al., 1992). In patients with advanced diabetic nephropathy (DNP), GBM HS was partly or completely lost accompanied by increased proteinuria (Tamsma et al., 1994). However, recently the electrostatic barrier function of HS was questioned, as in a model of early human diabetic nephropathy and experimental diabetic nephropathy in rats no changes in HS content or composition were found. It was proposed that loss of HS from the GBM may be secondary to proteinuria and the involvement of glomerular podocytes in the capillary wall permeability was suggested (van den Born et al., 2006). In line with the later model a recent publication showed that removal of HS from the GBM did not result in acute albuminuria (Wijnhoven et al., 2007). Changes in glomerular endothelial HS expression have also been reported for human and murine lupus nephritis, where increased level of both N- and O-sulphation could be observed (Rops et al., 2007).

Relatively new is the interest in renal HS with regards to inflammation, but there is increasing evidence suggesting it plays a pivotal role. Studies of human renal allografts showed increased HS expression in acute rejecting kidneys compared to normal controls. HS was found in blood vessel walls and tubules, with the highest expression in the basement membrane, and colocalisation studies revealed co-expression of N-sulphated HS with CCL5. Apart from colocalisation, a positive correlation between HS and CCL5 expression levels was found (Ali et al., 2005a). This observation gives evidence that chemokines presented by HS direct leukocytes subsets to specific sites within a graft. An inflammatory response was simulated by stimulating primary endothelial cells with proiflammatory cytokines and an increase in NDST1 enzyme, which in turn led to increased N-sulphation on the cell surface, was the consequence. When these cells were examined for their ability to present CCL5, a significant increase in chemokine presenting capacity of the stimulated cells was revealed when compared to the unstimulated control, which was in line with the results obtained from kidney allograft biopsy studies (Ali et al., 2005a).

Murine renal HS has also been shown to be a ligand for L-selectin. This is interesting, as all leukocytes express this form of lectin. The interaction of L-selectin on the leukocyte and its binding partner HS on the endothelium initiate the first step of leukocyte extravasation. Binding assays in mouse kidney revealed collagen XVIII as ligand in the tubular basement membrane. In addition to the core protein, the HS chain length and the sulphation status (namely O-sulphation) were crucial for L-selectin binding (Celie et al., 2005). Based on the results from mouse experiments, human renal biopsies from primary kidney diseased patients were investigated for their ability to bind L-selectin and CCL2, a chemokine reported important in renal transplantation settings (Robertson et al., 1998, Ruster et al., 2004, Segerer et al., 2000). Both molecules showed increased binding to HS of the perivascular interstitial matrix which was associated with increased influx of leukocytes. Further more, increased binding of L-selectin and CCL2 to HS expressed on the basolateral side of tubular epithelial cells was observed (Celie et al., 2007).

As it has been suggested for chemokines (Ali et al., 2005a, Robertson and Kirby, 2003), HS in tubular basement membranes could display signals (chemokines, cytokines, L-selectin) which cause the infiltrating cell to penetrate

the tubular epithelium, resulting in tubulitis, an important feature of acute renal rejection.

3.1.2 Hepatic Heparan sulphate

HSPGs are the predominant form of proteoglycans in the liver and have been found to be highly sulphated compared to other organs or tissues (Lyon et al., 1994a, Vongchan et al., 2005). Changes in overall amounts of liver HS have been reported for cirrhosis (Murata et al., 1985), hepatocellular carcinoma (HCC) (Kovalszky et al., 1990) and cholestasis (Roskams et al., 1996). In addition to changes in the amounts of HS, a decrease in HS sulphation was observed in rats with experimental diabetes (Kjellen et al., 1983, Williams et al., 2005). Furthermore, impaired lipoprotein uptake by diabetic livers has been reported by different research groups (Ebara et al., 2000, Olsson et al., 2001). Highly sulphated HS domains in the liver have been reported to act as coreceptors for apolipoprotein E (Libeu et al., 2001). Recently, an elegant study demonstrated *in vivo* that hepatic HS acts as a coreceptor for triglyceride- and cholesterol-rich lipoproteins independently of the LDL-receptor family. Specific inactivation of NDST1 in hepatocytes resulted in partially undersulphated HS and plasma triglyceride accumulation (MacArthur et al., 2007). Similar results supporting the model of HS as lipoprotein coreceptor were obtained from mice lacking uronyl-2-O-sulphotransferase (Stanford et al., 2010). In a recent investigation, topological changes in fibrogenic liver disease and HCC have been revealed. Changes in a range of HS biosynthetic enzymes were recorded which resulted in overall increased 3-O-sulphation and slight 6-O-undersulphation in HCC (Tatrai et al., 2010). The role of liver HS with regards to transplantation has not been investigated so far, but as the bile duct is targeted during allograft rejection by inflammatory cells, which are guided into the tissue by chemokines, the role of ductular HS should be further explored.

3.1.3 Chemokines in transplantation

CCL2, formerly known as monocyte chemoattractant protein-1 (MCP-1), is a proinflammatory chemokine which binds to its receptor CCR2 and facilitates migration of subsets of leukocytes to sites of inflammation (Kruger et al., 2002).

CCL2 is produced by a range of cell types, including lymphocytes and vascular endothelial cells.

Elevated levels of CCL2 have been reported for an array of diseases, including multiple sclerosis, rheumatoid arthritis and cancer (Deshmane et al., 2009). In the kidney, weak basal expression of CCL2 in tubular epithelial cells has been reported and CCL2 expression was induced during renal allograft rejection (Prodjosudjadi et al., 1995, Robertson et al., 1998). Renal collagen XVIII has been identified as CCL2 ligand (Celie et al., 2007, Kawashima et al., 2003).

The amino acid residues representing the heparin-binding motif of CCL2 have been identified as Lys-58 and His-66 (Chakravarty et al., 1998), but less understood are the corresponding binding sites of HSPGs (Proudfoot et al., 2001, Severin et al., 2010). In general, all chemokines bind preferentially to saccharides with increased sulphation. In addition to N-sulphation, 2-O-sulphation has been shown to facilitate CCL2 binding (Sweeney et al., 2006). CCL2 also was shown to bind preferentially to N-acetylated residues among saccharides with constant sulphation (Schenauer et al., 2007). Recently, a heparin octasaccaride lacking 3-O-sulphate groups has been identified as minimal binding sequence (Meissen et al., 2009).

Taken together these data suggest that HS structure is highly flexible and can be altered upon interaction with various inflammatory stimuli in a cell/tissue dependent fashion, resulting in altered/new HS epitope expression with functional consequences for binding partners in the inflammatory response.

3.1.4 Specific aims

Organ and tissue specific HS have been described (Dennissen et al., 2002) as well as changes of HS between healthy and diseased organs (Ali et al., 2005a, Rops et al., 2007, Tatrai et al., 2010, Vongchan et al., 2005). However, most of the data (with the exception of findings by Ali and Tatrai and coworkers) does not include information about the structural changes and distribution of HS epitopes. This part of the work therefore aimed to investigate the changes in expression of differentially modified HS epitopes in human tissues during different stages of allograft rejection. Specific goals:

- Optimisation of antibody staining for HS (10e4, phage display antibodies) and CCL2 in human renal and liver tissue

- Staining of renal and liver human allograft biopsies for differentially modified HS and CCL2

- Determining changes in HS epitope expression and correlation with grades of rejection

3.2 Specific Materials and Methods

3.2.1 Human Tissue

Normal human kidney and liver tissue and allograft biopsies were obtained as formalin-fixed paraffin embedded blocks from the local transplant tissue archive in accordance with the Local Research Ethics Committee approval 06/Q0905/150. Samples were anonymised and coded before they were made available for the study.

3.2.2 Immunohistochemistry

Immunohistochemistry allows antigen visualisation within the tissue architecture. To analyze differences in HS composition and chemokine occurrence during rejection tissue samples from human kidneys and livers were examined immunohistologically.

Paraffin embedded formalin-fixed tissue sections were dewaxed for 10 minutes in xylene prior to rehydration in serial alcohol concentrations (100%, 95% and 70% ethanol) for 2 minutes each before immersing in water for 5 minutes.

Antigen retrieval was optimised for each antibody, 2 different methods were used in this study.

a) Antigen retrieval via heat (pressure cooking): After rehydration tissue sections were placed in a pressure cooker and antigens were retrieved whilst cooking for 1 minute in citrate buffer pH 6.

b) Enzymatic antigen retrieval (Trypsin): tissue sections were pre-warmed in TBS to 37ºC and incubated in a trypsin/calcium chloride solution (Sigma, pH 7.8) between 12 and 20 minutes at 37ºC.

Following several washes in TBS, sections were incubated with 2% BSA/TBS to block nonspecific binding of antibodies. After blocking, sections were incubated with the primary antibody over night at 4ºC.

Secondary antibodies were applied to the sections after a series of washes in TBS and incubated for 1h at room temperature. In order to visualize the cells nuclei DAPI solution (Sigma, 2µg/ml final concentration) was applied to the sections and they were incubated for 5 minutes.

In order to quench autofluorescent staining liver sections were further incubated in Sudan Black (0.3% Sudan black in 70% methanol).

After extensive washing in TBS sections were finally mounted in fluorescent mounting media (Dako) and stored until confocal analysis in the dark at 4ºC. Each time staining was performed a control staining, omitting the incubation with the primary antibody using the secondary antibody only, was carried along. Antibody specifications can be seen in Table 3-1 and Figure 3-1 (Rops et al., 2008, Smits et al., 2006).

Table 3-1 Antibodies used in this study and their binding requirements

Antibody	**Supplier**	**Subtype**	**Target sequence**	**Dilution**	**Secondary ab**
10e4	Seikagaku	Monoclonal Mouse IgM	GlcA-GlcNS-GlcA-GlcNAc	1/100	Anti-mouse-FITC (1/100), Dako
HS3A8	Gift from Prof. Kuppevelt, Nijmegen, Netherlands	Single chain phage display-derived	GlcNS6S-IdoA2S	1/6	Anti-VSV-Cy3 (1/300), Sigma
HS4C3	Gift from Prof. Kuppevelt, Nijmegen, Netherlands	Single chain phage display-derived	GlcNS3S6S-GlcA/Ido2S	1/6	Anti-VSV-Cy3 (1/300), Sigma
MCP-1	R&D	Monoclonal Mouse IgG2B	Human CCL2	1/20	Anti-mouse-FITC (1/100), Dako

Abbreviations GlcA: glucuronate; GlcNac: N-acteylated-glucosamine; GlcNS: N-sulphated-glucosamine; IdoA: iduronate; 2,3,6S: 2,3,6 sulphate (Smits et al, 2006; Rops et al, 2008)

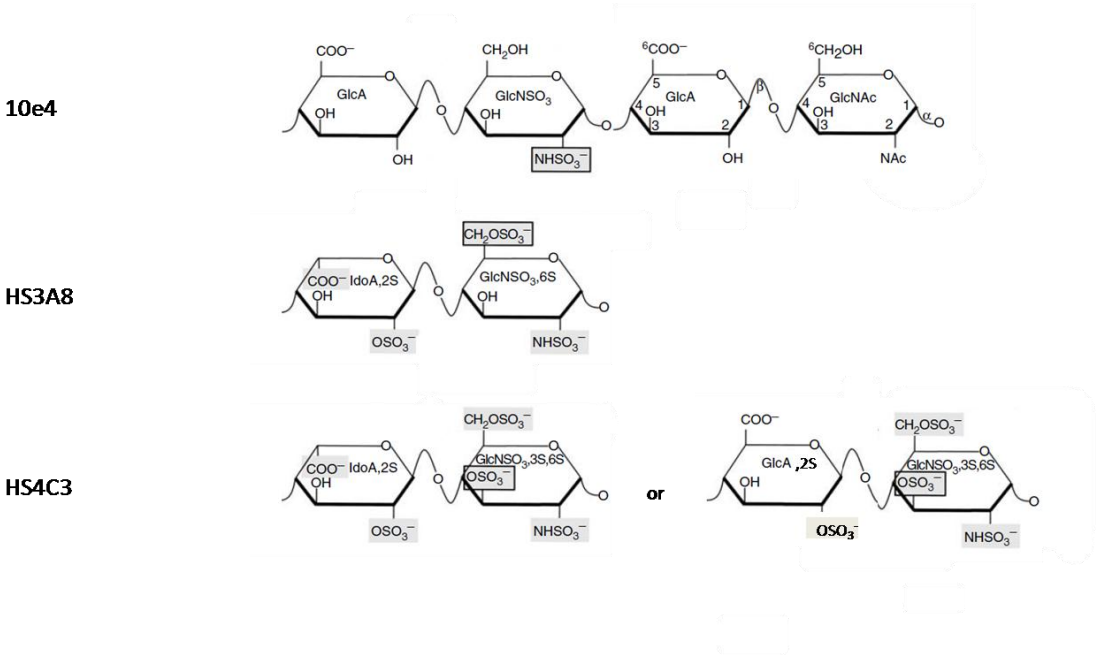

Figure 3-1 Structural motifs for HS antibody recognition

3.2.2.1 Confocal microscopy and data analysis

All fluorescent labelled samples were analysed with the Leica TCS-SP2UV confocal laser scanning microscope (Leica Lasertechnik). The excitation and emission wavelengths were 488nm and 530nm for FITC, 543nm and 580nm for TRITC and 358nm and 461nm for DAPI. Cy3 labelled samples were also visualized using TRITC filter settings as excition and emission spectra are almost identical to those of TRITC. Images were collected sequentially, frame by frame and finally combined to produce the final image.

Quantitative information of the renal sections analysed was obtained using COMOS software applying histogram analysis (as described by Wong et al, (Wong et al., 2003). 'Colour banding' allowed calculation of the median fluorescence intensity excluding the unstained areas such as tubular lumens. Median fluorescence was calculated by taking all fluorescent readings into account which where in-between 1 (threshold set manually) and 255 (maximum fluorescence). Whenever fluorescence readings were needed for quantification, staining was performed in parallel and readings were taken on the same day with the same settings applied.

Fluorescence readings of bile-duct-like structures of the liver were taken with Leica software by manually circling around ducts, therefore excluding other areas of the tissue and duct lumen.

3.2.3 Chemokine Binding

A chemokine binding assay was developed to investigate the ability of differentially modified HS to retain chemokines on the surface of cells and tissues.

For tissues, antigen retrieval was performed as described in materials and methods. The sections were blocked with 20% swine serum in TBS. In order to prevent binding of the secondary reagent avidin to endogenous biotin, an avidin-biotin blocking step (Vectorlabs) was introduced. Following this, chemokine was added to a final concentration of 100ng/ml in TBS and slides were incubated over night at 4ºC. Following two washing steps in TBS avidin-FITC was added for 1h at RT (BD, 1/100 dilution) before the slides were finally mounted in fluorescent mounting media (Dako).

In some cases cell surface HS was removed by heparinase III (Sigma) treatment. Therefore cells or tissues were incubated with 0.05U/ml of heparinase in a humified chamber for 1h at 37ºC.

3.2.4 Statistical analysis

Tissue samples were analysed by non-parametric Krusak-Wallis test with Tukey's post hoc test. Differences with $p<0.05$ were considered to be significant.

3.3 Results

3.3.1 Renal rejection

3.3.1.1 HS3A8 staining in kidney

3.3.1.1.1 Optimisation of HS3A8 staining

As the phage display derived antibodies have preferentially been used on frozen sections (personal communication Prof. van Kuppevelt, Harden conference, March 2009), antigen retrieval of formalin-fixed paraffin embedded tissues had to be optimised. Both enzymatic and heat mediated retrievals were used, with trypsin mediated antigen retrieval for 12 minutes resulting in precise and reliable staining results (Figure 3-2).

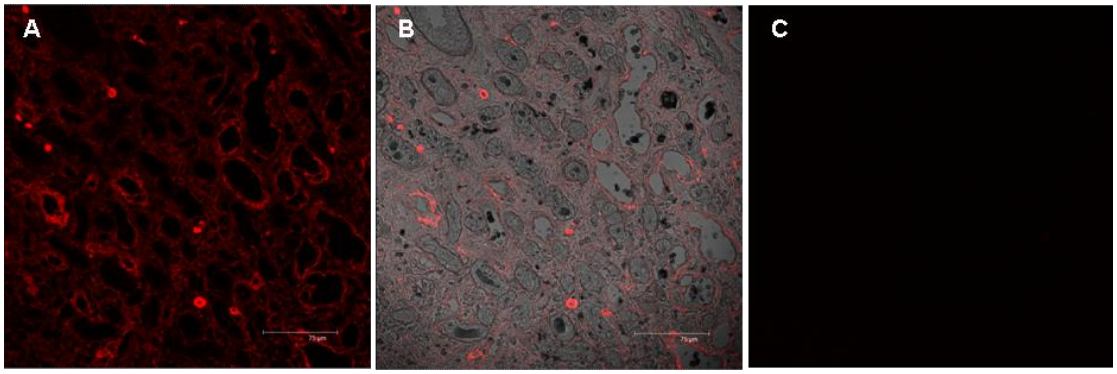

Figure 3-2 Optimisation of HS3A8 staining in human renal biopsies

HS3A8 antibody was used at 1/6 dilution and visualized by a Cy3-labelled secondary antibody. Fluorescent staining A, brightfield-fluorescent overlay B and control staining omitting the primary antibody C. Antigen retrieval was performed by trypsin digestion. Scale bar represents 75 µm.

Once the staining was optimised, additional sections were stained to further investigate the distribution of the HS3A8 (representing N-sulphation, 6-O-sulphation, C-5-epimerization and 2-O-sulphation) epitope in renal tissue. The most prominent staining was found on tubular epithelial cells and to some lesser extent in the interstitium and weak staining of the glomerulus (Figures 3-2 and 3-3).

3.3.1.1.2 Distribution of HS3A8 in normal renal tissue

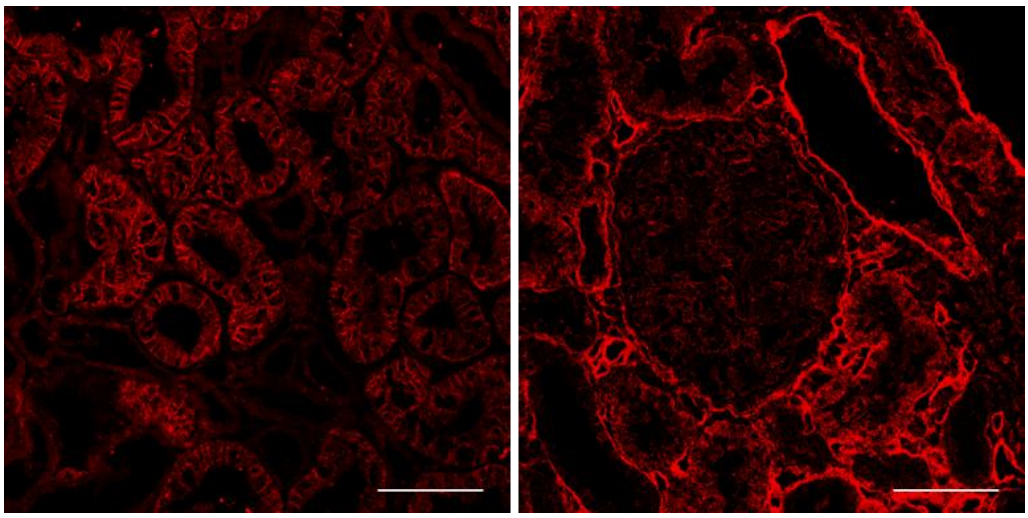

Figure 3-3 Distribution of HS3A8 epitope in human renal biopsies

HS3A8 antibody was used at 1/6 dilution and visualized by a Cy3-labelled secondary antibody. Antigen retrieval was performed by trypsin digestion. Scale bar represents 75 µm.

3.3.1.1.3 Changes in HS3A8 HS epitope expression during rejection

A series of renal allograft biopsies was investigated for the expression of HS3A8 during different stages of rejection. Figures 3-4 and 3-5 show slightly increased expression of HS3A8, but not significantly during acute rejection 1a. During chronic rejection, HS3A8 staining increased significantly ($p<0.05$) within the tubules and the interstitium.

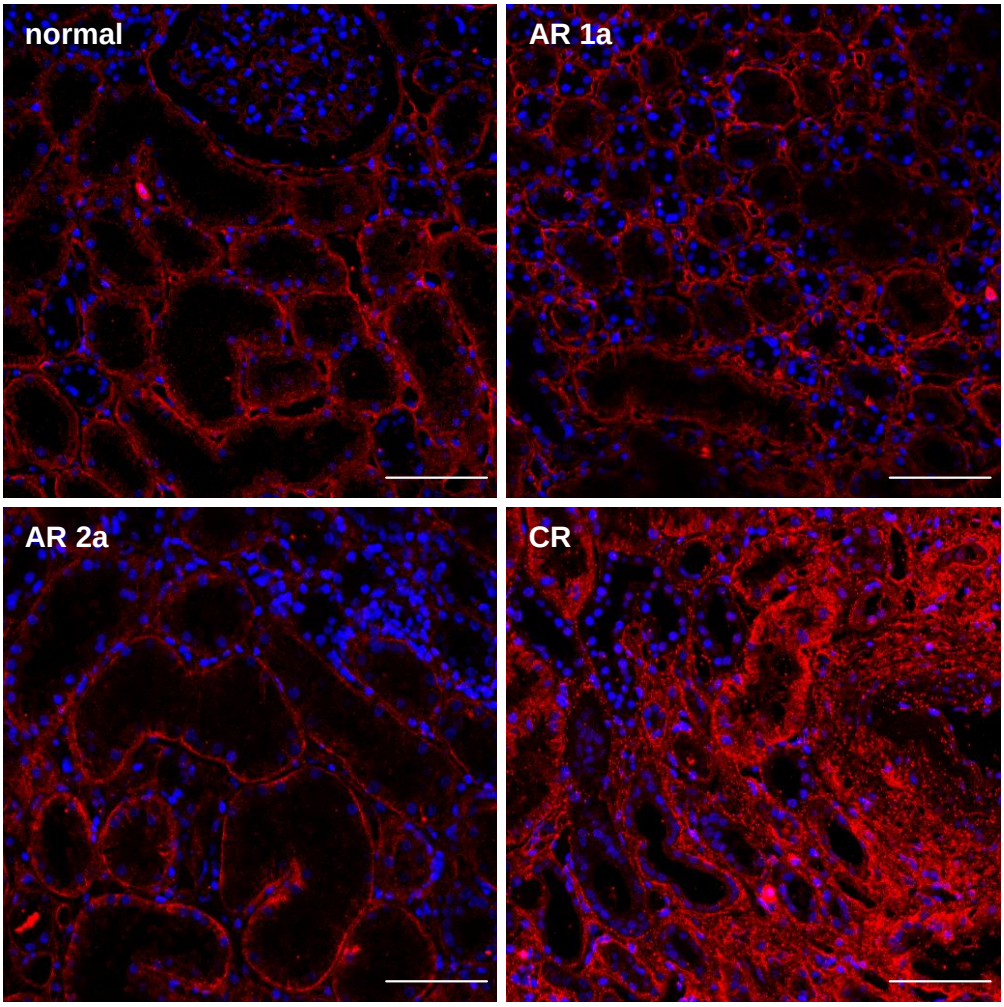

Figure 3-4 HS3A8 expression during renal allograft rejection

HS3A8 antibody was used at 1/6 dilution and visualized by a Cy3-labelled secondary antibody. Kidney sections are representative for the indicated stages of rejection (acute rejection 1a, acute rejection 2a, chronic rejection) with normal tissue as control. Scale bar represents 75 µm.

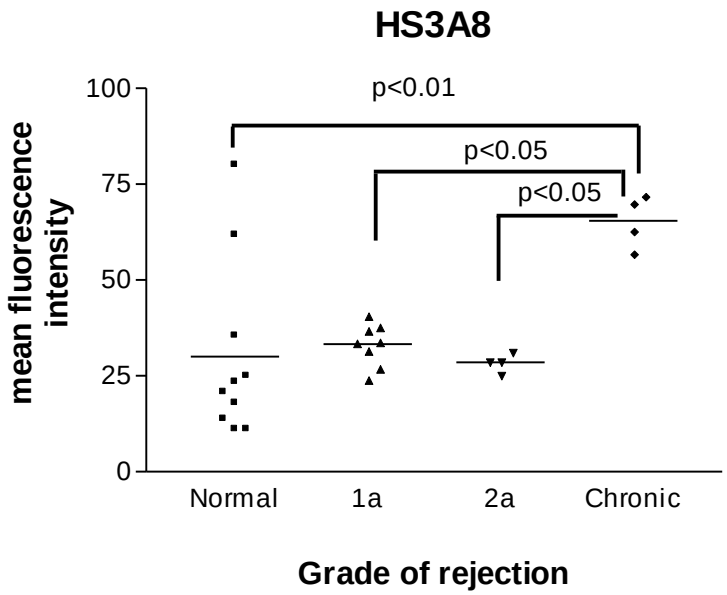

Figure 3-5 Mean fluorescent expression of HS3A8 during renal rejection

2-3 random fields per biopsy were chosen (dependent on size of the biopsy) and the mean fluorescence intensity analysis was performed using Comos software. Results represent data from 12 patients in total (5 normal, 3 acute rejection 1a, 2 acute rejection 2a and 2 chronic rejection). Statistical analysis was determinded by non-parametric Kruskal-Wallis test with differences p<0.05 considered to be significant.

In addition to the mean fluorescence intensity the median fluorescence intensity and the area covered by HS3A8 staining was determined. This was done to clarify if increased mean fluorescence was due to extremely intense staining of few, defined structures within the tissue or if staining also increased with regards to the area covered. This way it was believed to be able to distinguish between moderate staining covering large areas and intense staining of distinct, localised structures.

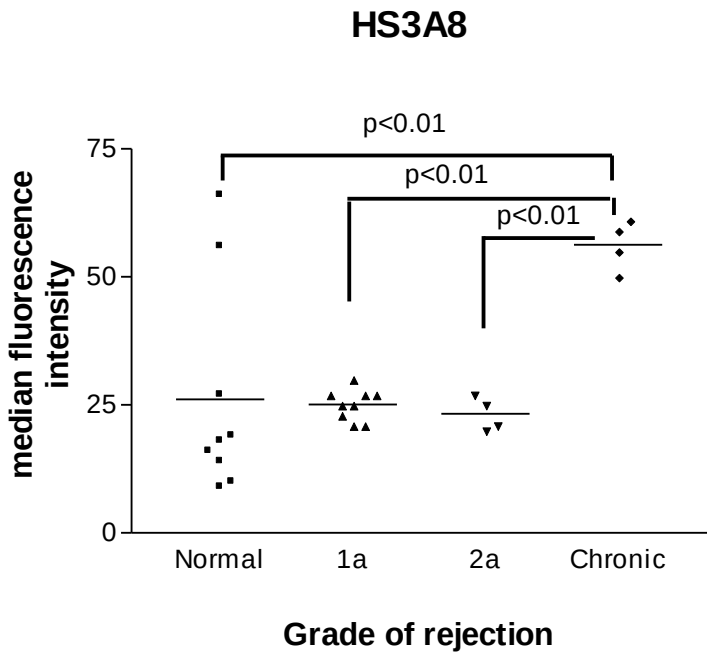

Figure 3-6 Median fluorescent expression of HS3A8 during renal rejection

2-3 random fields per biopsy were chosen (dependent on size of the biopsy) and the median fluorescence intensity was calculated by using the 'colour banding' mode of Comos software. Results represent data from 12 patients in total. (5 normal, 3 acute rejection 1a, 2 acute rejection 2a and 2 chronic rejection). Statistical analysis was determinded by non-parametric Kruskal-Wallis test with differences p<0.05 considered to be significant.

The analysis of median fluorescence intensity and area coverage confirmed the data from mean fluorescence intensity analysis in the way that both increased staining of individual structures as well as increased staining within the interstitial space covering an extended area was observed (Figures 3-6 and 3-7) during chronic rejection (all p-values < 0.05).

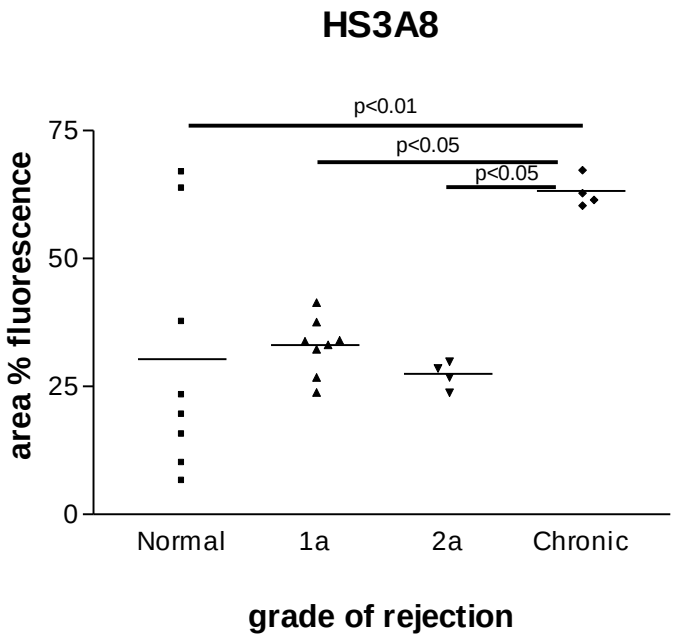

Figure 3-7 Graphic representation of area coverage by HS3A8 staining

2-3 random fields per biopsy were chosen and stained area was measured with Comos software. Results represent data from 12 patients in total (5 normal, 3 acute rejection 1a, 2 acute rejection 2a and 2 chronic rejection). Statistical analysis was determinded by non-parametric Kruskal-Wallis test with differences p<0.05 considered to be significant.

3.3.1.2 HS4C3 staining in kidney

3.3.1.2.1 Optimisation of HS4C3 staining

Antigen retrieval of formalin-fixed paraffin embedded tissue was performed both by enzymatic and heat mediated retrieval, with trypsin mediated antigen retrieval for 12 minutes (Figure 3-8) proving suitable for HS4C3 staining.

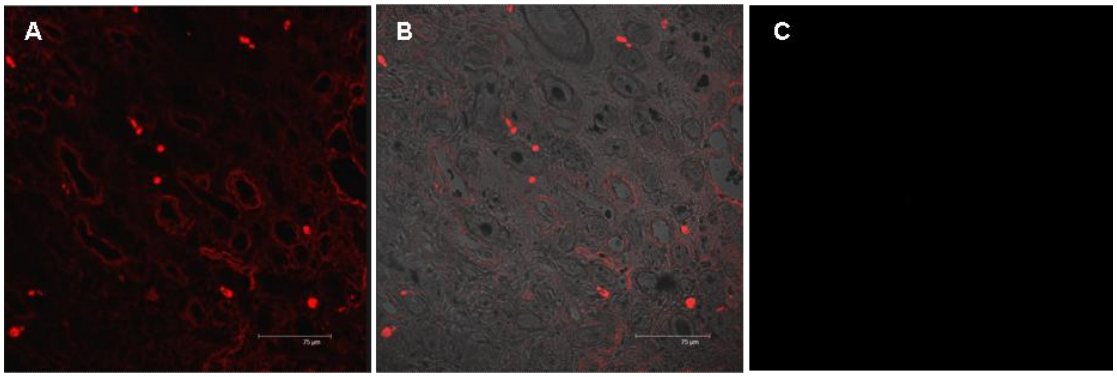

Figure 3-8 Optimisation of HS4C3 staining in human renal biopsies

HS4C3 antibody was used at 1/6 dilution and visualized by a Cy3-labelled secondary antibody. Fluorescent staining A, brightfield-fluorescent overlay B and staining control omitting primary antibody C. Antigen retrieval was performed by trypsin digestion. Scale bar represents 75 µm.

3.3.1.2.2 Distribution of the HS4C3 in normal renal tissue

Additional biopsies were stained to investigate the distribution of HS4C3 (representing N-sulphation, 6-O-sulphation, 2-O-sulphation and 3-O-sulphtion) in renal tissue.

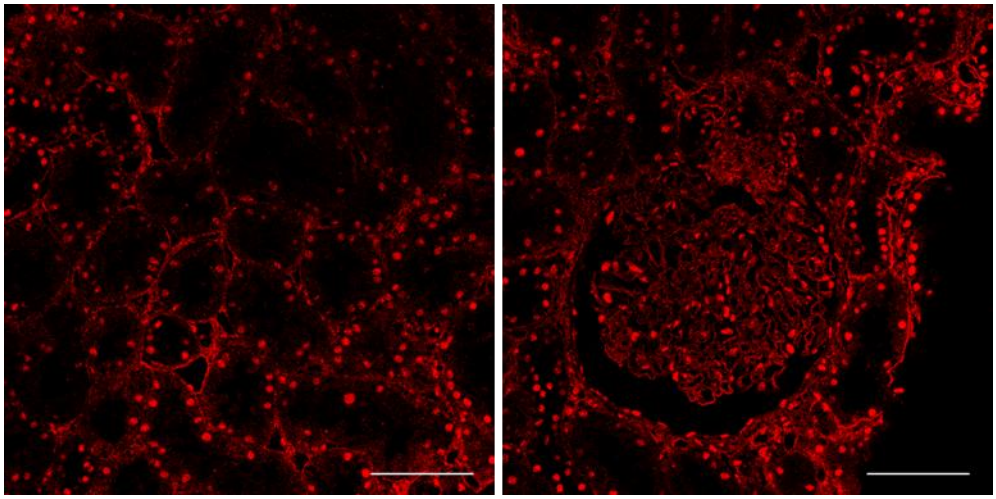

Figure 3-9 Distribution of HS4C3 epitope in human renal biopsies

HS4C3 antibody was used at 1/6 dilution and visualized by a Cy3-labelled secondary antibody. Antigen retrieval was performed by trypsin digestion. Scale bar represents 75 µm.

Figures 3-8 and 3-9 show the staining pattern of HS4C3. Antibody HS4C3 stained tubules in a similar fashion to antibody HS3A8. Glomerular staining appeared to be more prominent compared to HS3A8 staining and little interstitial staining was observed. In addition, nuclear staining was observed.

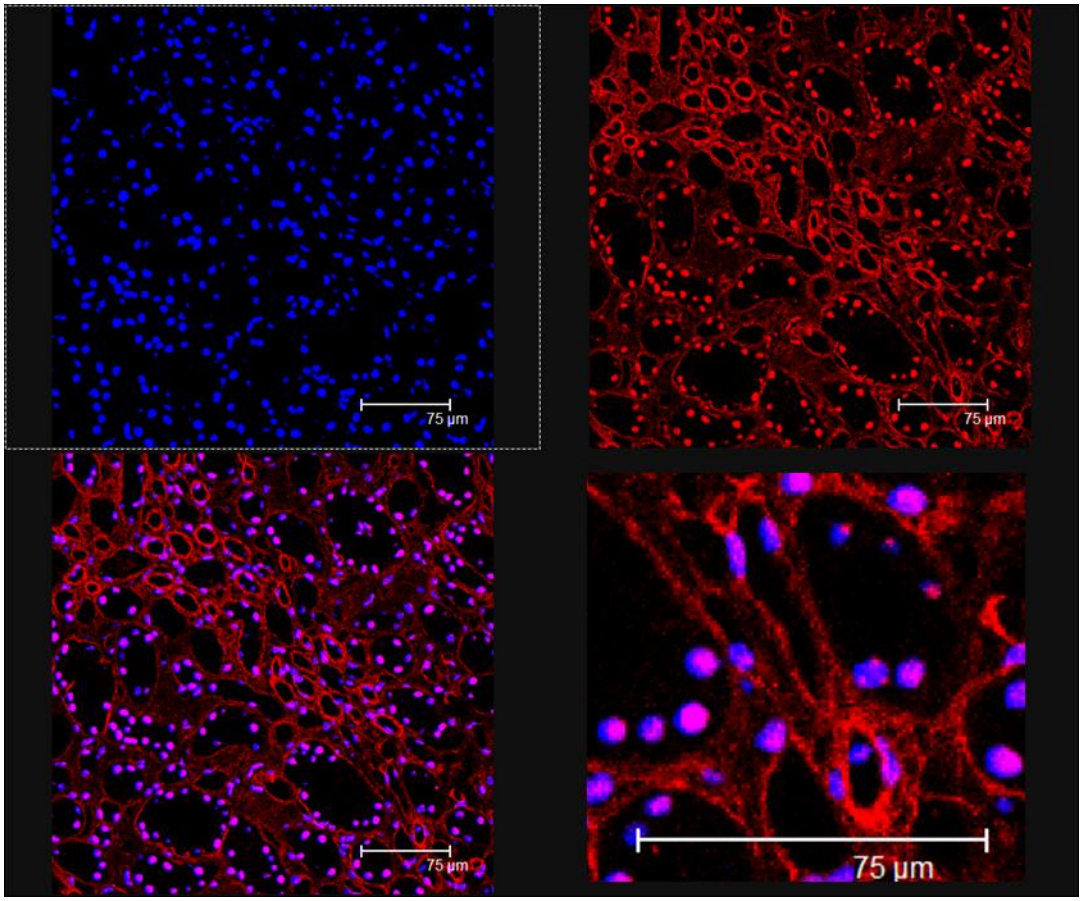

Figure 3-10 Nuclear staining of HS4C3 in human renal biopsies

HS4C3 antibody was used at 1/6 dilution and visualized by a Cy3-labelled secondary antibody. Antigen retrieval was performed by trypsin digestion. Scale bar represents 75 µm.

Inclusion of DAPI staining in following experiments confirmed the staining of nuclei with antibody HS4C3 (Figure 3-10). However, this nuclear staining was found to be present in most, but not all cases. Due to different degrees of nuclear staining a quantitative analysis could not be carried out for antibody HS4C3.

3.3.1.3 10e4 staining in kidney

Optimal antibody retrieval for the 10e4 antibody showed that citrate buffer boiling resulted in superior results compared to enzymatic mediated retrieval (Figure 3-11).

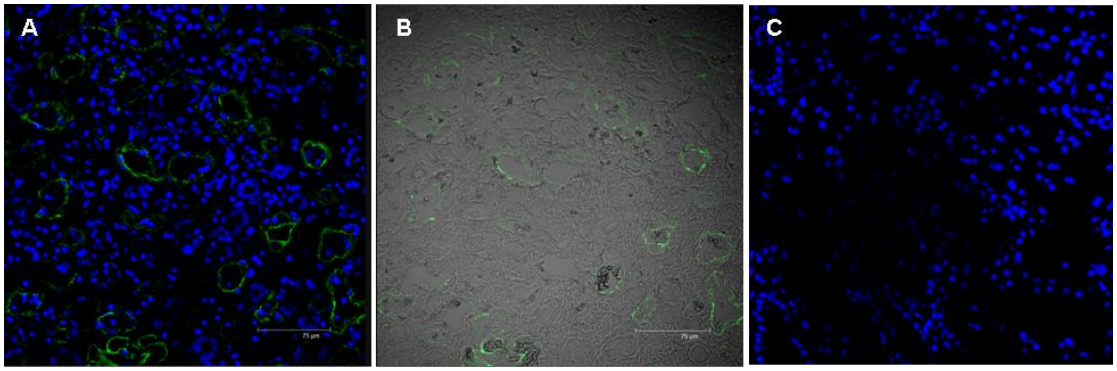

Figure 3-11 Optimisation of 10e4 staining in human renal biopsies

10e4 antibody was used at 1/100 dilution and visualized by a FITC-labelled secondary antibody. Fluorescent staining A, brightfield-fluorescent overlay B and control staining omitting primary antibody C. Antigen retrieval was performed by citrate buffer boiling. Scale bar represents 75 µm.

10e4 staining was found predominatly within tubules, with hardly any interstitial staining.

3.3.1.3.1 Changes in 10e4 HS epitope expression during renal rejection

A series of renal allograft biopsies were investigated for the expression of 10e4 HS epitope during different stages of rejection. Figures 3-12 and 3-13 show low level staining of 10e4 in normal kidney, whereas biopsies from patients with acute rejection 1a (cellular) exhibited much stronger staining throughout the tissue ($p<0.05$). Samples from acute rejection 2a (humoral) and chronic rejection patients revealed similar staining as the control.

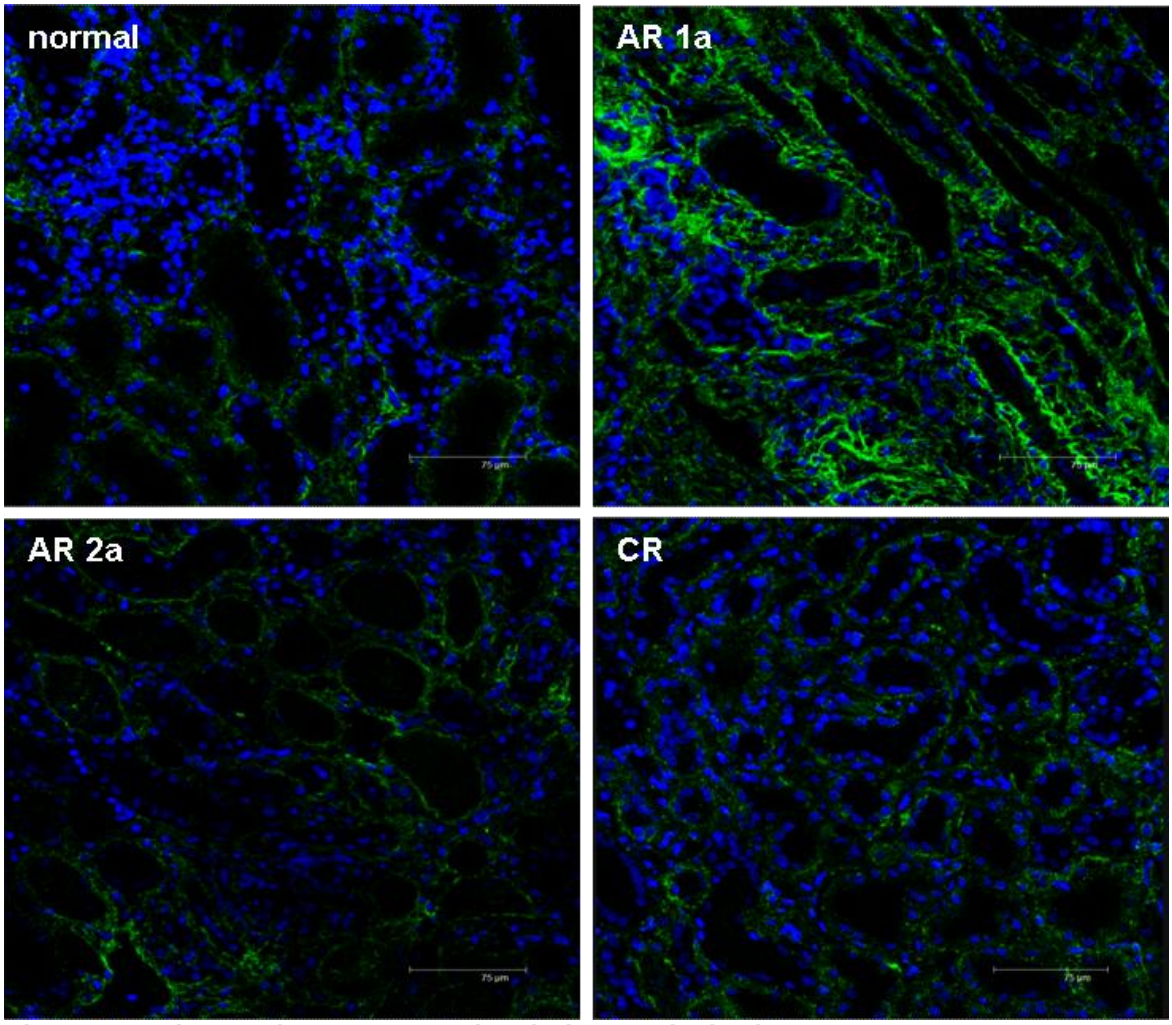

Figure 3-12 Changes in 10e4 expression during renal rejection

10e4 antibody was used at 1/100 dilution and visualized by a FITC-labelled secondary antibody. Kidney sections are representative for the indicated stages of rejection (acute rejection 1a, acute rejection 2a, chronic rejection) with normal tissue as a control. Scale bar represents 75 µm.

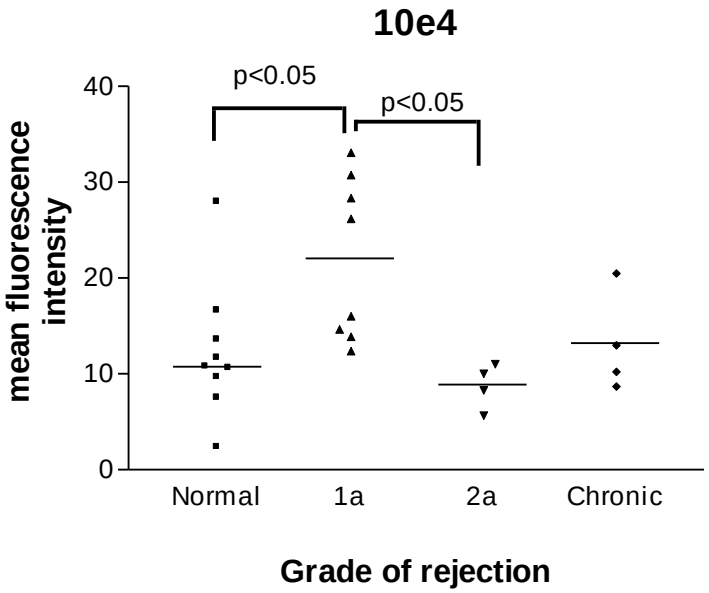

Figure 3-13 Mean fluorescent expression of 10e4 during renal rejection

2-3 random fields per biopsy were chosen (dependent on size of the biopsy) and the mean fluorescence intensity analysis was performed using Comos software. Results represent data from 12 patients in total (5 normal, 3 acute rejection 1a, 2 acute rejection 2a and 2 chronic rejection). Statistical analysis was determinded by non-parametric Kruskal-Wallis test with differences p<0.05 considered to be significant.

The analysis of median fluorescence intensity and area coverage confirmed the data from mean fluorescence intensity analysis in the way that both increased staining of individual structures as well as increased staining within the interstitial space covering an extended area was observed during acute rejection 1a, while levels of staining during chronic rejection were comparable to normal tissue (Figures 3-14 and 3-15).

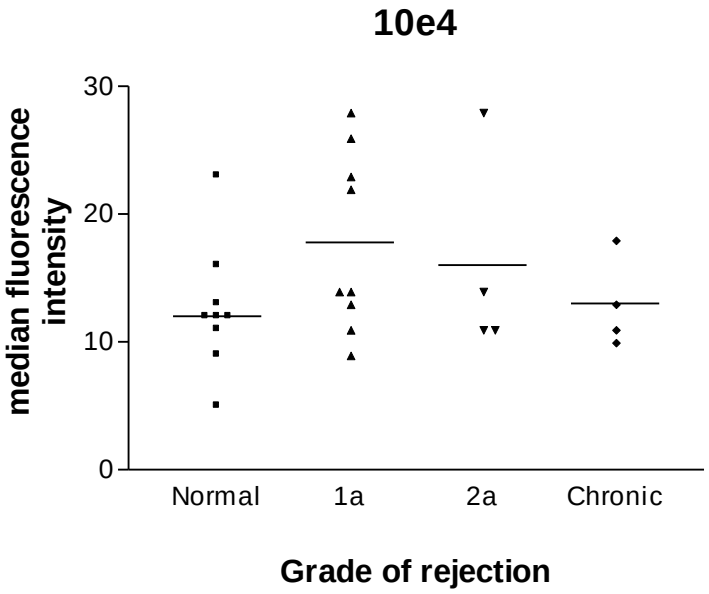

Figure 3-14 Median fluorescent expression of 10e4 during renal rejection

2-3 random fields per biopsy were chosen (dependent on size of the biopsy) and the median fluorescence intensity was calculated by using 'colour banding' mode of Comos software. Results represent data from 12 patients in total (5 normal, 3 acute rejection 1a, 2 acute rejection 2a and 2 chronic rejection). Statistical analysis was determinded by non-parametric Kruskal-Wallis test with differences p<0.05 considered to be significant.

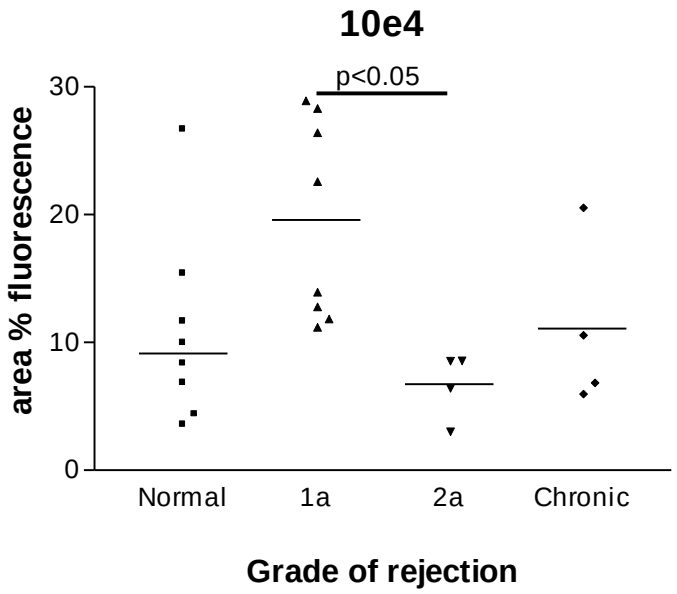

Figure 3-15 Graphic representation of area coverage by 10e4 staining

2-3 random fields per biopsy were chosen (dependent on size of the biopsy) and the stained area was measured with Comos software. Results represent data from 12 patients in total (5 normal, 3 acute rejection 1a, 2 acute rejection 2a and 2 chronic rejection). Statistical analysis was determinded by non-parametric Kruskal-Wallis test with differences p<0.05 considered to be significant.

This is in contrast to HS3A8 staining, which came up late during chronic stages of allograft rejection.

3.3.1.4 Optimisation of CCL2 antibody staining

CCL2 staining was first carried out as previously described by Roberson et al, (Robertson et al., 1998), but antigen retrieval by citrate buffer boiling did not result in appropriate staining (Figure 3-16A) and when a scan of fluorescence emission was performed, the residual staining was identified as autofluorescence, as no emission was collected at 530 nm, the emission wavelength of FITC (Figure 3-16B).

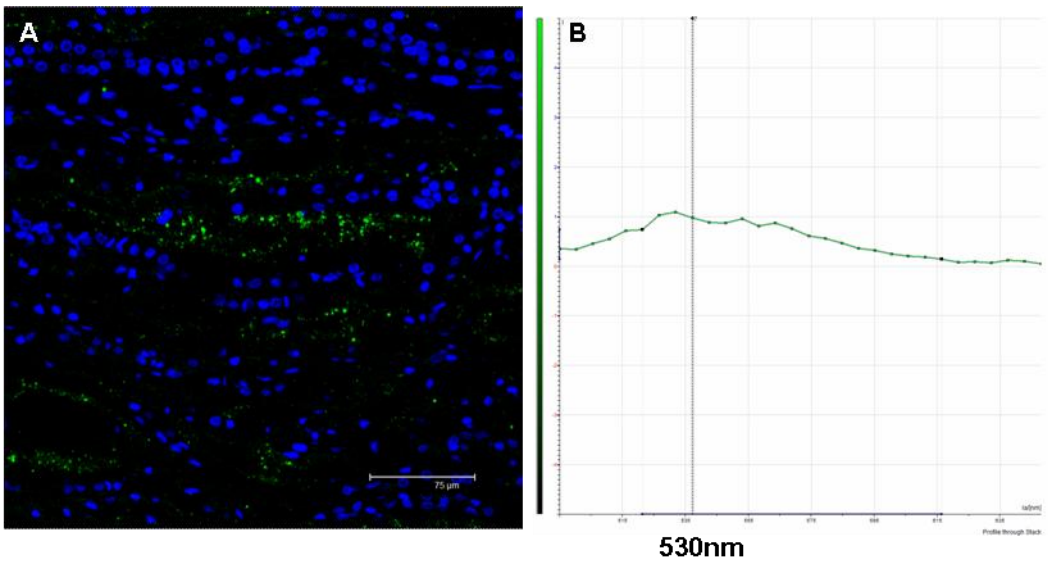

Figure 3-16 CCL2 expression in human renal biopsies

CCL2 antibody was used at 1/20 dilution and visualized by a FITC-labelled secondary antibody (A). Antigen retrieval was performed by citrate buffer boiling. Fluorescence spectra were collected and analysed using Leica software (B). Scale bar represents 75 µm.

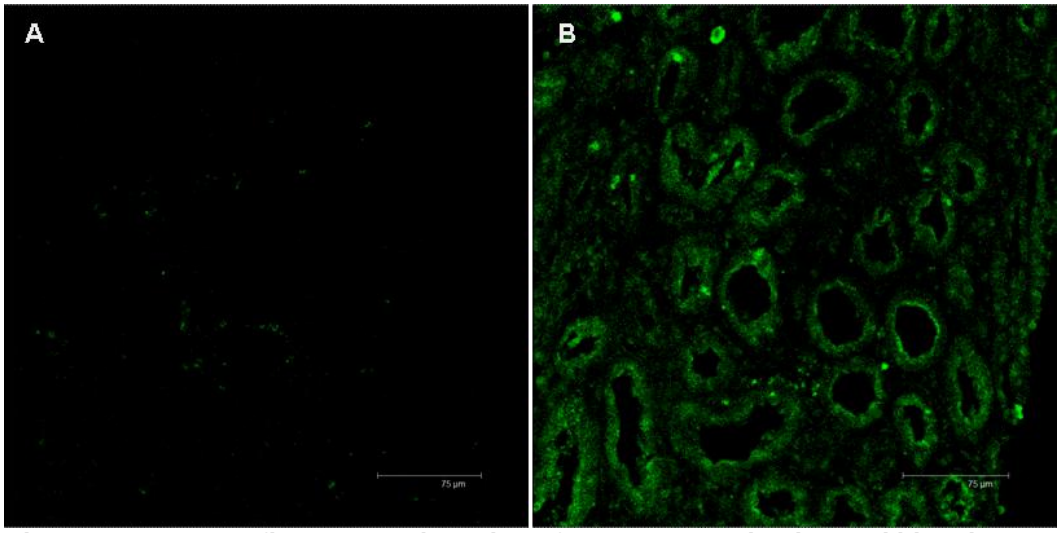

Figure 3-17 Immunofluorescent detection of CCL2 expression in renal biopsies

Secondary antibody control (A) and CCL2 staining (B).CCL2 antibody was used at 1/20 dilution and visualized by a FITC-labelled secondary antibody. Antigen retrieval was performed by trypsin digestion. Scale bar represents 75 µm.

CCL2 staining with trypsin mediated antigen retrieval showed better results; however, the staining pattern was different compared to the literature (Al-Hamidi et al., 2008, Lai et al., 2007, Robertson et al., 1998), where basolateral expression of CCL2 and other CC chemokines was reported (Figure 3-17). Instead of the basolateral surface of tubules, the luminal side revealed CCL2 staining. Repeated experiments resulted in similar staining pattern and a western blot was performed to verify the specificity of the antibody. The immunoblot revealed a clear band around 10kDa, which validated the specificity of the antibody (Figure 3-18).

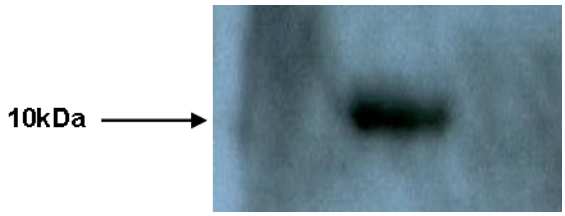

Figure 3-18 CCL2 expression by PBMCs

60 µg of total protein lysate from PBMCs were used for immunoblotting. Blots were probed with mouse monoclonal α-CCL2 antibody (1/20) and HRP-conjugated anti-mouse IgG (1/5000)

3.3.1.4.1 CCL2 expression during rejection

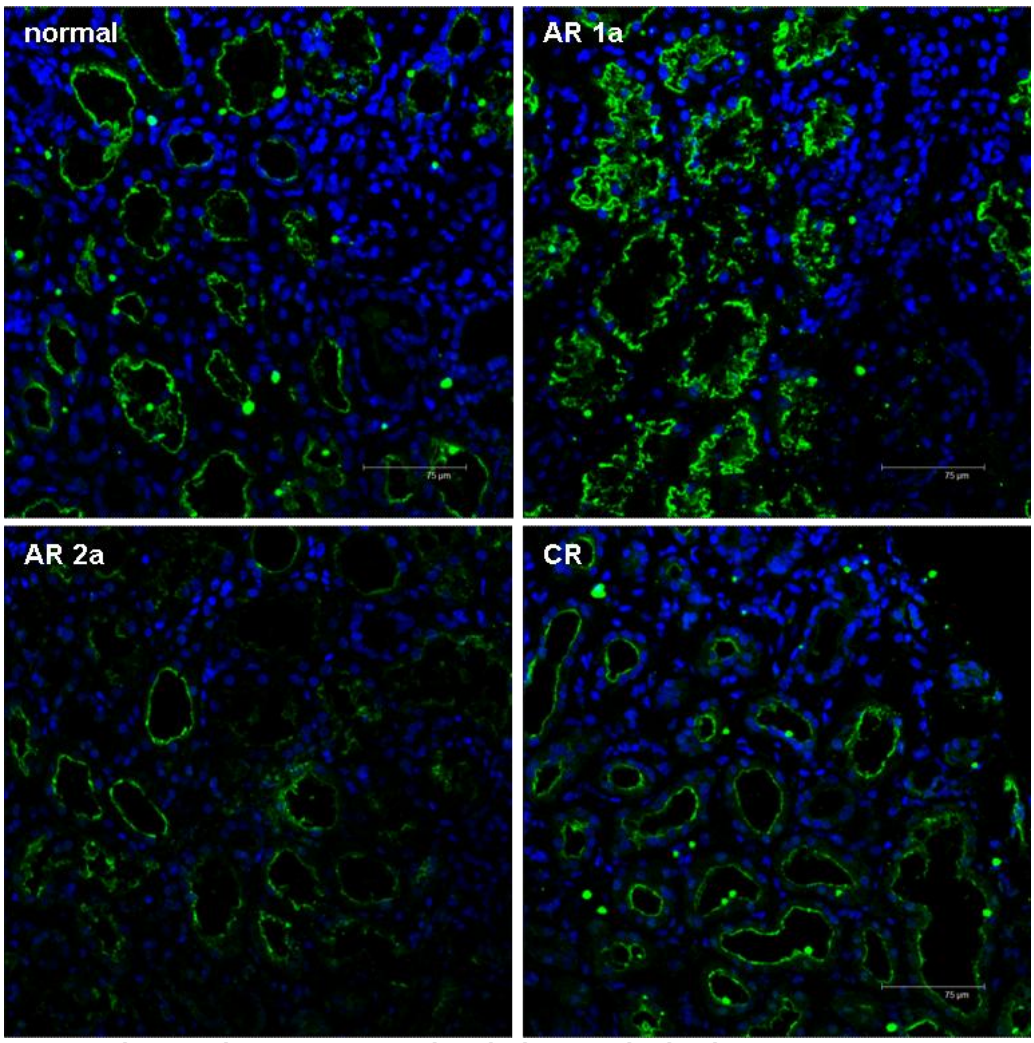

Figure 3-19 Changes in CCL2 expression during renal rejection

CCL2 antibody was used at 1/20 dilution and visualized by a FITC-labelled secondary antibody. Antigen retrieval was performed by trypsin digestion. Biopsies are representative for the indicated stages of disease (n=2). Scale bar represents 75 µm.

Figure 3-19 demonstrates that CCL2 was expressed in all groups of renal biopsies investigated. During renal acute rejection 1a an increase in CCL2 expression was observed, no differences between the other groups was found.

In addition to antibody staining, an antibody binding assay was developed to investigate the ability of differentially modified HS to present CCL5. This binding experiment was thought to give more insight into the physiology of HS during

rejection compared to staining (Segerer et al., 2007). Unfortunately the assay failed to work in these settings (data not shown).

3.3.2 Hepatic rejection

Expression of HS epitopes was also examined during liver rejection.

3.3.2.1 HS3A8 staining in liver

3.3.2.1.1 Optimisation HS3A8 staining in liver

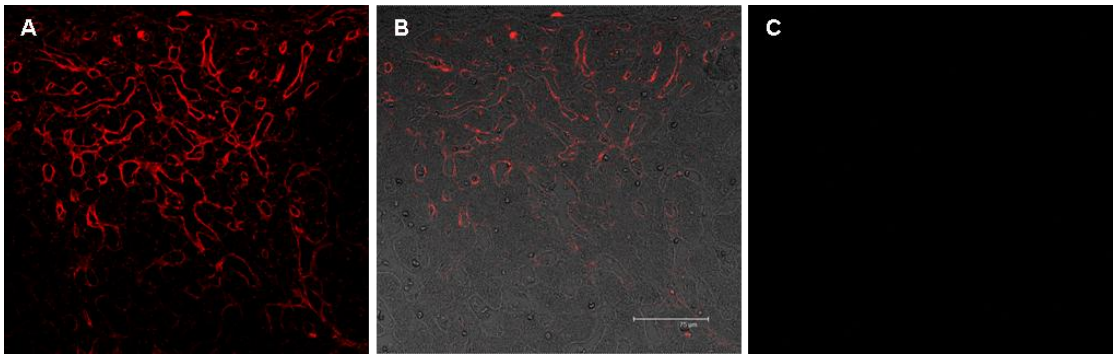

Figure 3-20 Optimisation of HS3A8 staining in liver biopsies

HS3A8 antibody was used at 1/6 dilution and visualized by a Cy3-labelled secondary antibody. Fluorescent staining A, brightfield-fluorescent overlay B and control staining omitting primary antibody C. Antigen retrieval was performed by trypsin digestion. Scale bar represents 75 µm.

Trypsin retrieval proved to work for HS3A8 in liver tissue and staining was found more or less uniformly in all sinusoids. HS3A8 antibody also labelled bile duct basement membranes (Figures 3-20 and 3-21).

3.3.2.1.2 Distribution of the HS3A8 in normal human liver

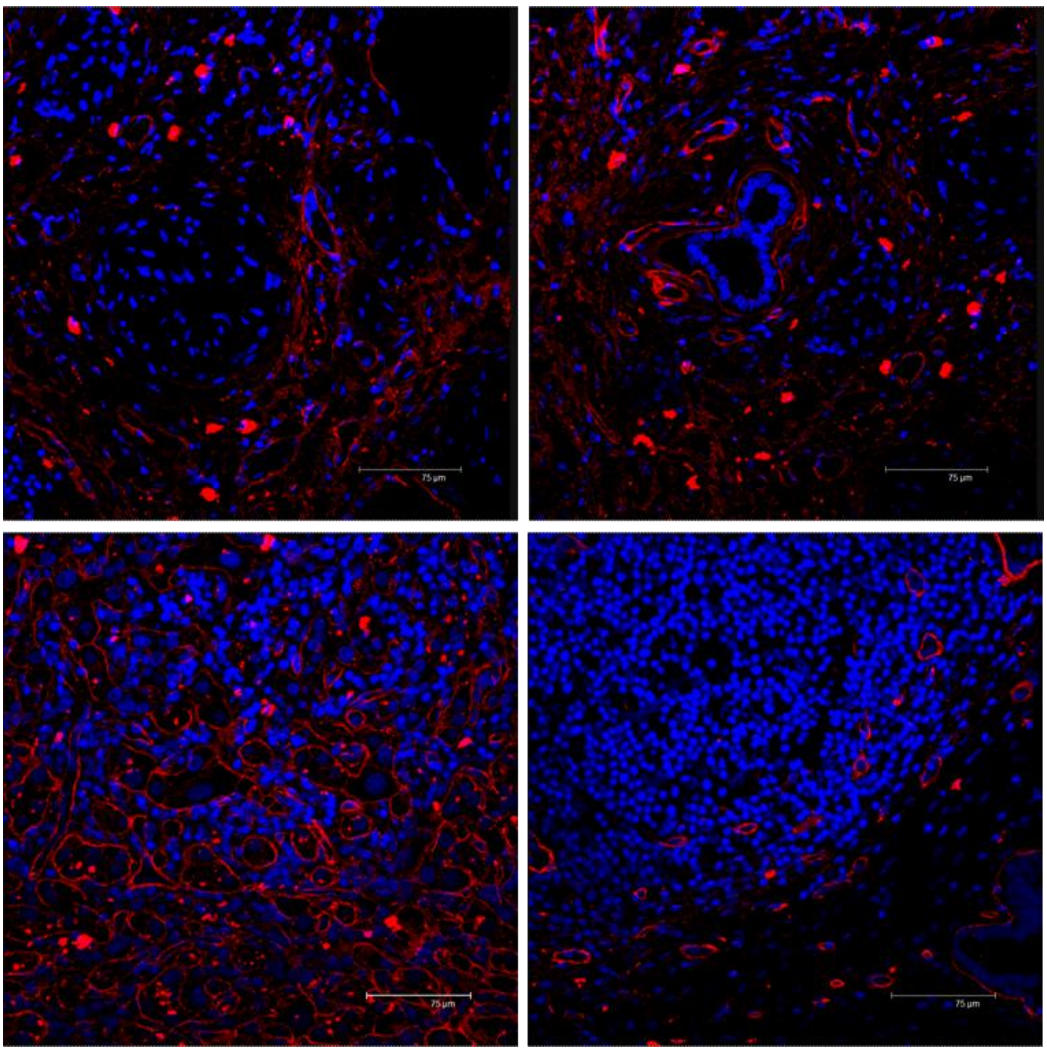

Figure 3-21 Distribution of HS3A8 epitope in human liver biopsies

Human liver biopsies were stained with HS3A8 antibody and the staining pattern analysed by confocal microscopy. Scale bar represents 75 µm.

3.3.2.1.3 Changes in HS3A8 HS epitope expression during liver rejection

A range of liver biopsies were investigated for their expression of HS epitopes during rejection. Changes in HS3A8 expression were examined and an increase in overall staining during late rejection could be observed. A more detailed quantitative analysis of bile duct staining confirmed the first impression and revealed rejection related changes. Ductular HS3A8 staining decreased slightly during moderate rejection ($p<0.01$), before it increased during late rejection and chronic hepatitis ($p<0.01$) (Figures 3-22 and 3-23).

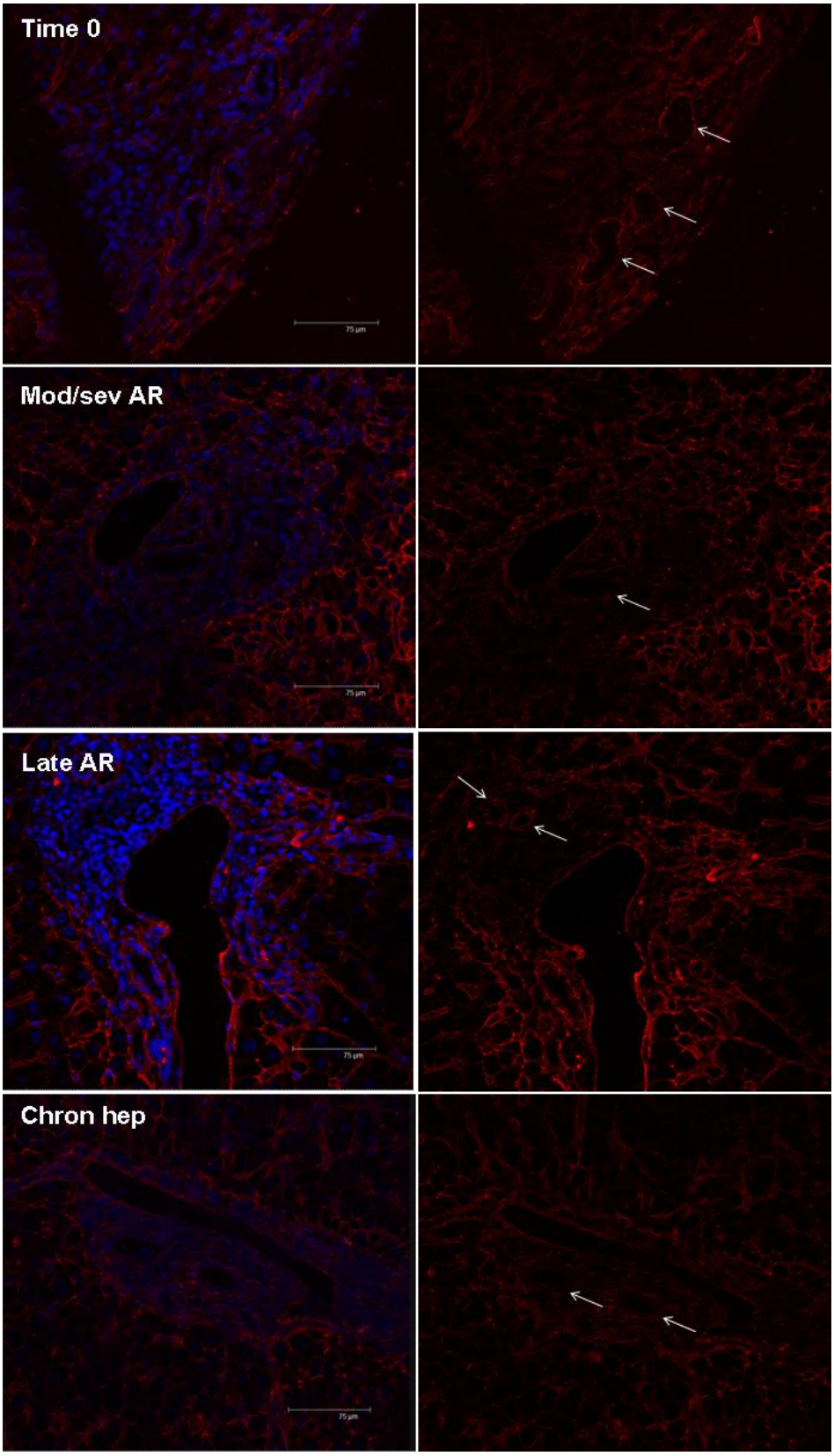

Figure 3-22 Changes in HS3A8 expression during liver rejection

HS3A8 antibody was used at 1/6 dilution and visualized by a Cy3-labelled secondary antibody. Liver sections are representative for the indicated stages of disease. Scale bar represents 75 µm. Arrows indicate bile duct-like structures.

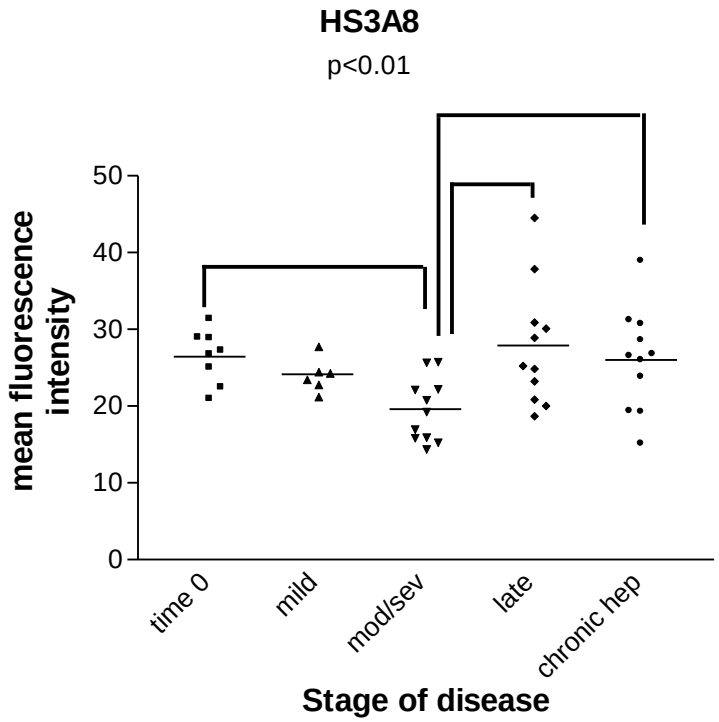

Figure 3-23 Quantitative analysis of ductular HS3A8 expression during liver disease

Ductular structures were examined manually and fluorescence readings taken by Leica software. Results represent data from 12 patients in total with varying numbers of bile duct readings in each group (time 0: n=8, mild acute rejection: n=6, moderate to severe acute rejection: n=13, late acute rejection: n=11 and chronic hepatitis: n=11). Statistical analysis was determinded by non-parametric Kruskal-Wallis test with differences p<0.05 considered to be significant.

3.3.2.2 HS4C3 staining in liver

3.3.2.2.1 Optimisation of HS4C3 staining in liver

HS4C3 antibody worked similar to HS3A8 antibody with trypsin mediated retrieval and staining patterns were comparable too. Sinusoids and bile ducts basement membranes were the main compartments stained in the biopsies (Figures 3-24 and 3-26). As it was shown for HS4C3 staining in kidney, the antibody labelled nuclei in livers as well (Figure 3-25). Again, nuclear staining was not uniform and therefore could not be used for quantitative analysis.

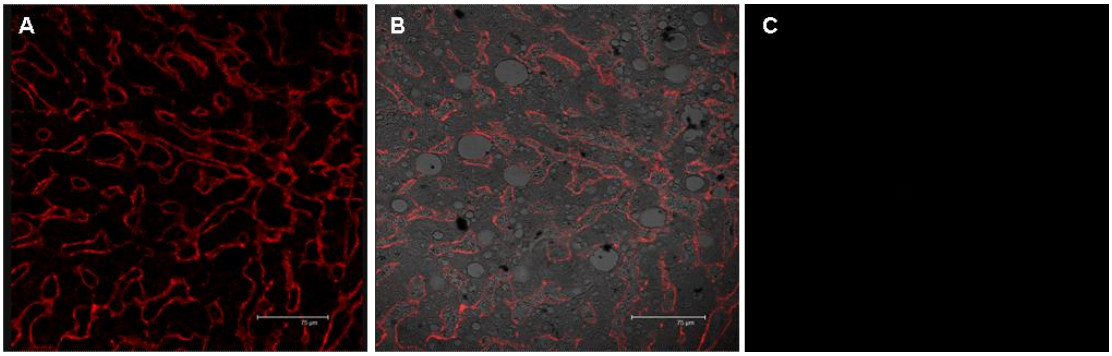

Figure 3-24 Optimisation of HS4C3 staining in human liver biopsies

HS4C3 antibody was used at 1/6 dilution and visualized by a Cy3-labelled secondary antibody. Fluorescent staining A, brightfield-fluorescent overlay B and control staining C. Antigen retrieval was performed by trypsin digestion. Scale bar represents 75 µm.

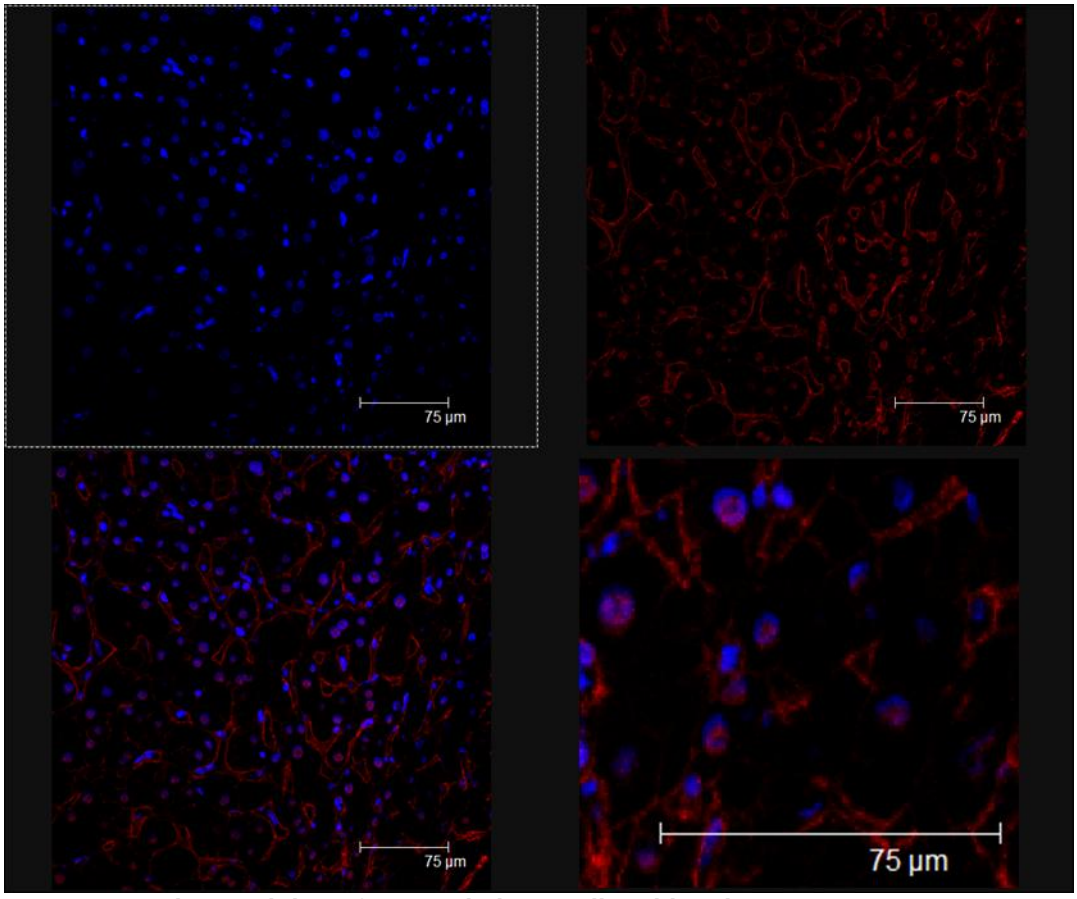

Figure 3-25 Nuclear staining of HS4C3 in human liver biopsies

HS4C3 antibody was used at 1/6 dilution and visualized by a Cy3-labelled secondary antibody. Antigen retrieval was performed by trypsin digestion. Scale bar represents 75 µm.

3.3.2.2.2 Distribution of the HS4C3 HS epitope in normal human liver tissue

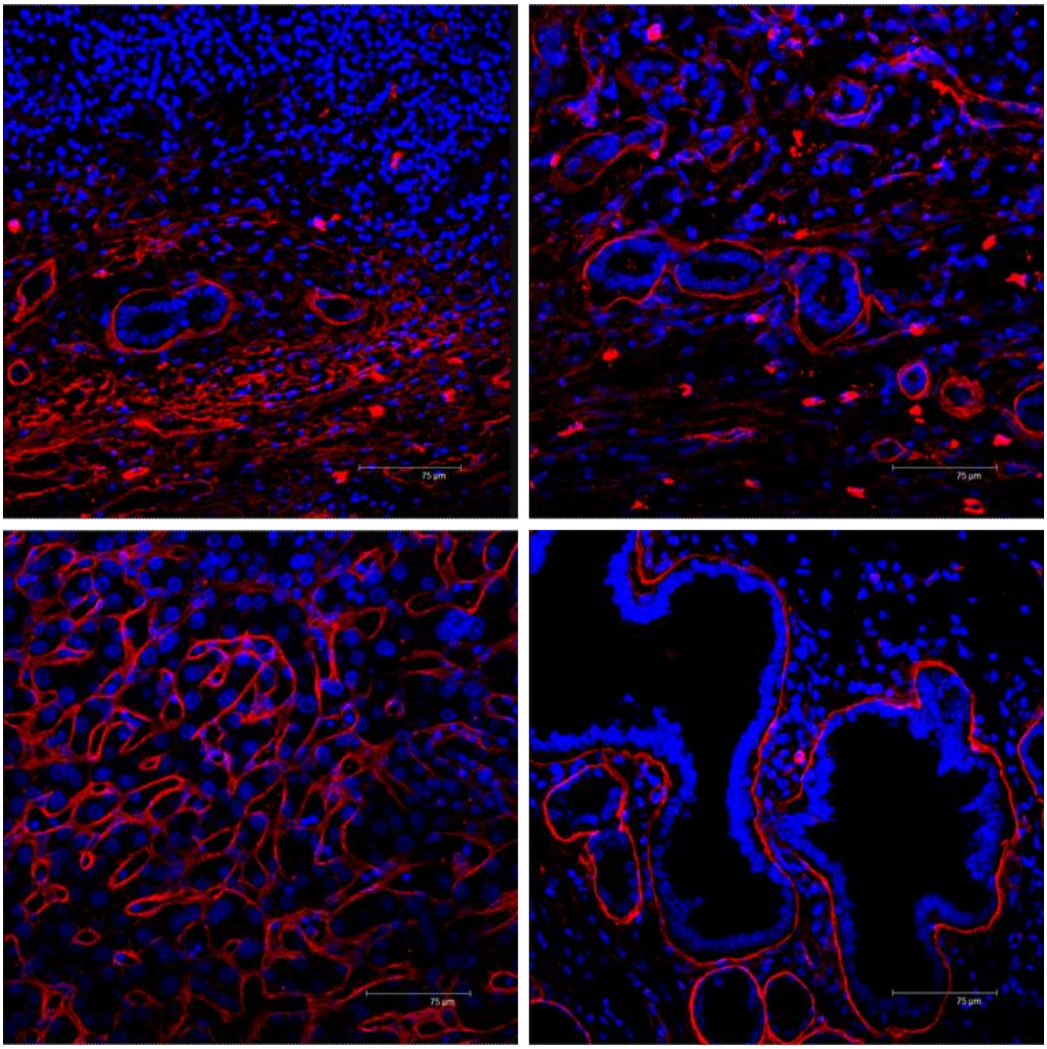

Figure 3-26 Distribution of HS4C3 epitope in human liver biopsies

Human liver biopsies were stained with HS4C3 antibody and the staining pattern analysed by confocal microsocopy. Scale bar represents 75 µm.

3.3.2.2.3 HS4C3 expression during liver disease

Even though no quantification of HS4C3 staining was feasible, qualitatively an increase in overall staining of time 0 transplants compared to chronic hepatitis biopsies was detectable (Figure 3-27).

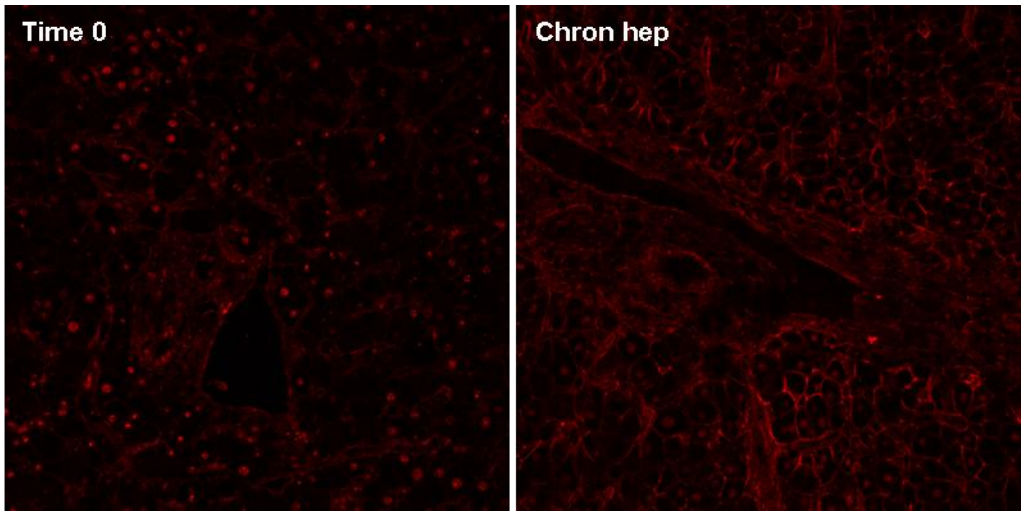

Figure 3-27 HS4C3 expression during liver disease

HS4C3 antibody was used at 1/6 dilution and visualized by a Cy3-labelled secondary antibody. Liver sections are representative for the indicated stages of disease. n = 3 each. Scale bar represents 75 µm.

3.3.2.3 10e4 HS staining in liver

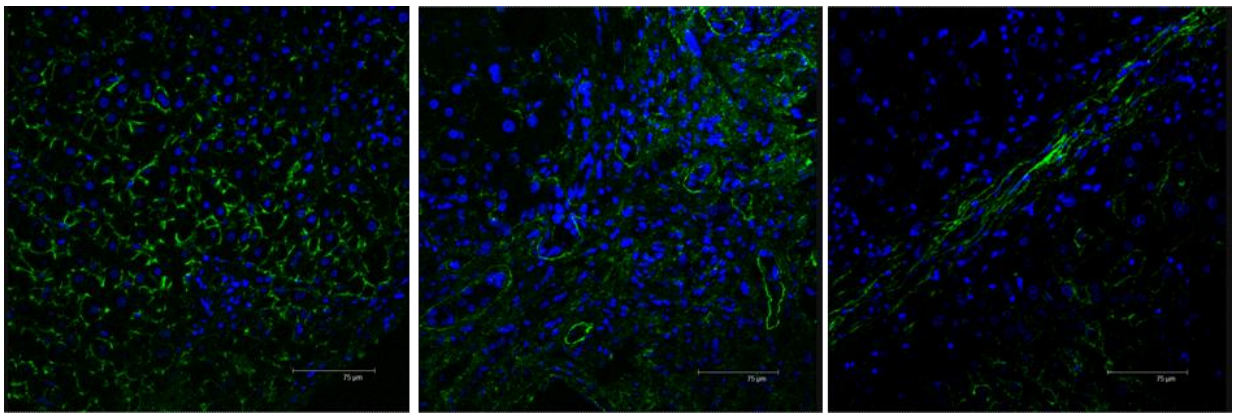

Figure 3-28 Distribution of 10e4 staining in human liver biopsies

10e4 antibody was used at 1/100 dilution and visualized by a FITC-labelled secondary antibody. Antigen retrieval was performed by citrate buffer boiling. The staining pattern was analysed by confocal microscopy. Scale bar represents 75 µm.

A range of liver biopsies were investigated for 10e4 HS epitope expression. 10e4 antibody staining was performed after the unmasking of antigens by citrate buffer boiling and appeared to be localised on sinusoids and bile ducts. When biopsies from rejecting livers were analysed for the expression of 10e4, no expression in time 0 transplants and hardly any expression in biopsies with mild rejection was observed. Expression of the 10e4 epitope seemed to be induced in time with the onset of moderate rejection. The staining was distributed throughout the tissue, with most pronounced increases in bile ducts. In sections from late stages of acute rejection and chronic hepatitis, a decline in overall staining, and a vanishing staining in bile ducts could be observed (Figures 3-28 and 3-29).

3.3.2.3.1 Changes in 10e4 HS epitope expression during liver disease

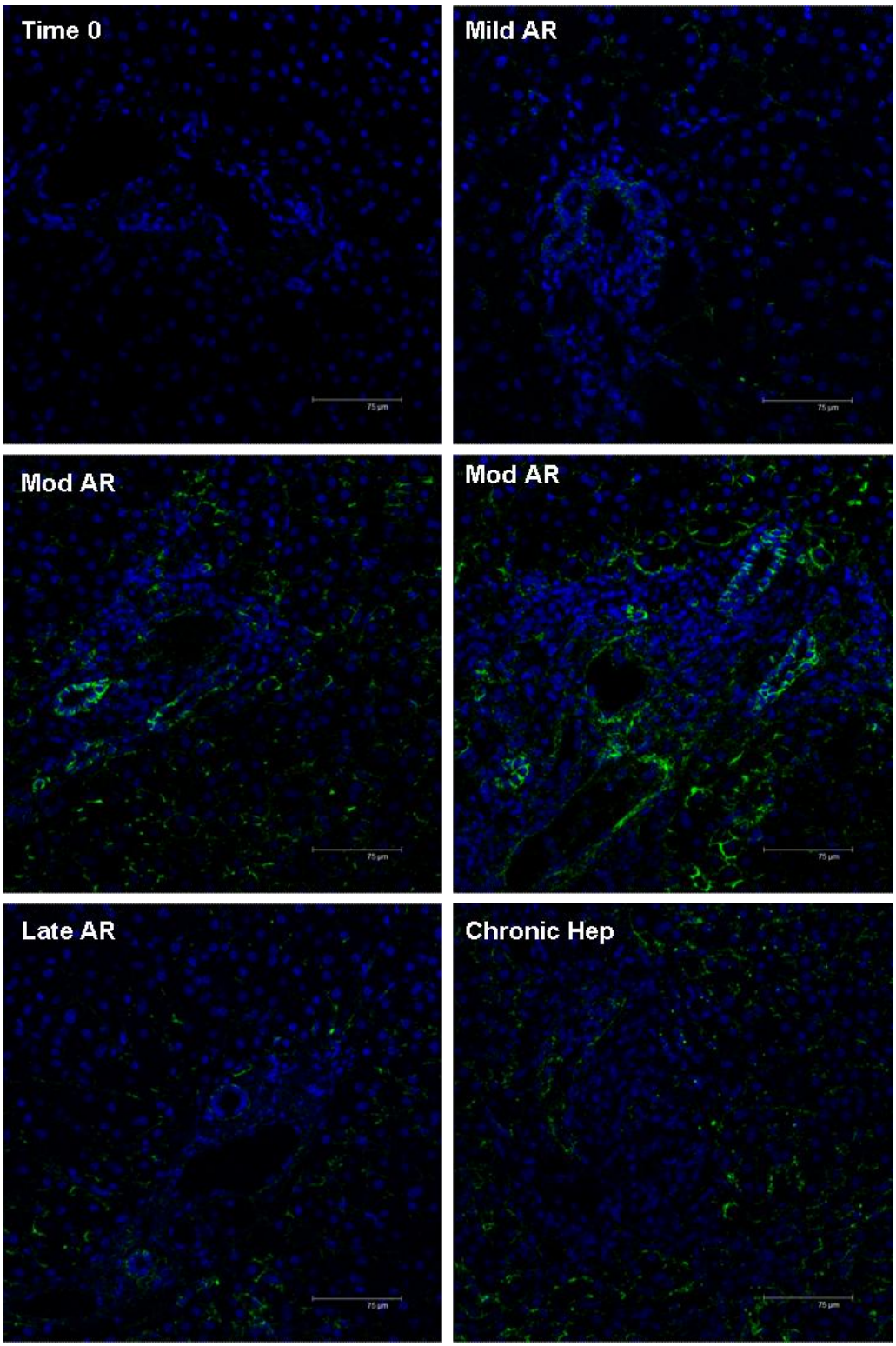

Figure 3-29 Changes in 10e4 expression during liver disease

10e4 antibody was used at 1/100 dilution and visualized by a FITC-labelled secondary antibody. Liver sections are representative for the indicated stages of disease. Scale bar represents 75 µm.

3.4 Discussion

HS structure is highly dynamic and variable in chain length and modification status. It is believed that the amount and arrangement of sulphated groups regulates the biological function of various proteins, including growth factors, cytokines and chemokines. These highly sulphated groups are created by a set of enzymes which are regulated at different levels. Transcriptional control (Carter et al., 2003, Krenn et al., 2008, Rops et al., 2008), translational control (Grobe and Esko, 2002) and control via the interaction and affinities of individual enzymes have been suggested (Esko and Selleck, 2002, Ledin et al., 2006).

HS has received increasing interest with regards to its role in inflammatory events. More or less accepted is the fact that HS is involved in all steps of leukocyte extravasation, primarily stabilising a chemokine gradient on the endothelium (Parish, 2006, Wang et al., 2005). Less attention is paid to other structures within the tissue, but as chemokines not only guide inflammatory cells into the graft, but also direct them once they have entered the graft, identification of HS species in different tissues involved in chemokine presentation seemed plausible. Different organs have been investigated for their HS content and differences between healthy and diseased organs were found. However, this data was based on overall HS content or modification status revealed by disaccharide analysis, none of which identifies physiological HS epitopes (Vongchan et al., 2005). A few research groups have started to investigate topological changes in HS (Dennissen et al., 2002, Rops et al., 2007) and the kidney is one of the organs investigated. In 2005 it was shown by Ali and coworkers that renal HS increased during acute rejection and described the distribution of HS within the tissue (Ali et al., 2005a). In general one can assume that changes between healthy and diseased organ mirror those of ligands which bind to HS in that particular situation. Altered or new binding sites for new interaction partners can be created by adopting chain length and modification status.

Observations in renal rejection

Based on these findings it was decided to examine HS expression during transplantation. First, antibody staining of human renal tissue had to be optimised. The process of antigen retrieval is of paramount importance, as antigens in formalin-fixed paraffin embedded tissues often have to be unmasked to be recognised by specific antibodies. HS3A8 and HS4C3 phage display antibodies required enzymatic retrieval with trypsin whereas 10e4 antibody worked best with heat-mediated retrieval by citrate buffer boiling. Renal tissues stained with the above mentioned phage display antibodies revealed similar staining patterns of tubules and the interstitium. The similarity in staining could be explained due to similar essential target modifications, being N-sulphation, C5-epimerization, 2O-sulphation and 6O-sulphation for HS3A8 and N-sulphation, 2O-sulphation, 6-O-sulphation and 3-O-sulphation for HS3C4. As 2-OST knock out mice lack kidneys (Bullock et al., 1998), the existence of 2-O-sulphation as indicated by HS3A8 staining was not surprising. Differential HS4C3 staining was observed in the glomerulus and the nucleus, with increased labelling of glomeruli and exclusive staining of nuclei. Changes in GBM and glomerular endothelial cell HS has been reported in other disease settings such as lupus nephritis or diabetes (Rops et al., 2007, van den Born et al., 2006) but were not further evaluated in this study. The existence of nuclear HS is quite disputable, but some research groups have reported nuclear localisation of HS (Richardson et al., 2001, Schubert et al., 2004). As the staining is quite variable results have to be interpreted carefully, non-specific interaction of the antibody cannot be excluded at this point.

10e4 staining revealed similar results to phage display antibody staining, differences only became apparent when changes of HS were analysed during rejection. Here, the 10e4 epitope increased significantly during acute rejection 1a, whereas the HS3A8 epitope increased significantly during chronic rejection. This observation supports the idea of regulated change in HS epitope expression during inflammatory responses. The 10e4 epitope could be induced during acute rejection to offer specific binding site to inflammatory molecules. After this process has taken place different HS species could be induced to offer binding sites to molecules involved in chronic settings, as HS3A8 during chronic rejection. 10e4 upregulation is consistent with observations of Ali et al,

who described increased 10e4 staining during acute kidney rejection (Ali et al., 2005a). As HSPGs are excreted with the urine, a link between HS expression and stage of disease could potentially give invaluable information about the progress of the disease and antibodies could be used as diagnostic tools.

To validate this idea a chemokine binding assay was developed. The theory was that chemokine binding could be observed in conjunction with appearance/disappearance of specific HS motifs. CCL5 was chosen because of its well defined GAG binding motif which has been described by various research groups (Ali et al., 2002, Kuschert et al., 1999, Proudfoot, 2006). A few binding assays employing CCL5 have been published (Ali et al., 2005a, Celie et al., 2007, Segerer et al., 2007), but the assay failed to work in our experimental settings. One reason could be that only paraffin embedded formalin-fixed tissue was available and binding studies are preferably performed on frozen tissues.

Instead of binding, chemokine staining was conducted. CCL2 was chosen as it has been reported to be involved in renal disease (Robertson et al., 1998, Ruster et al., 2004, Segerer et al., 2000). Staining was strongly increased during acute rejection 1a with moderate staining at later stages. The staining pattern of CCL2 in renal biopsies however was somehow unexpected as it was focused on the luminal side of the tubules rather than the basolateral surface, where it was reported previously (Al-Hamidi et al., 2008, Lai et al., 2007, Robertson et al., 1998). A western blot confirmed that the antibody was specific and one possible explanation could be that the CCL2 found in the tubules has been fixed during the fixation process while it was excreted with the urine. Indeed, increased urinary excretion of CCL2 during acute renal allograft rejection has been reported (Prodjosudjadi et al., 1995). As CCL2 is mainly produced by tubular epithelial cells, increased CCL2 expression possibly contributes to the damage of renal tubules (Morii et al., 2003a, Morii et al., 2003b).

Recently the significance of chemokine-HS interaction was highlighted in a model of mouse aortic allograft transplant. Either NDST1 or chemokine receptor 2 (CCR2) deficiency reduced inflammation and vasculopathy after aortic transplantation in a mouse model, proving GAG-chemokine interaction being the central regulatory step in inflammatory responses after transplantation. In addition, administration of the viral chemokine modulating protein M-T7, which

interferes with GAG binding for C, CC and CXC chemokines, resulted in prolonged survival and reduced inflammation in renal allograft transplants in mice (Dai et al., 2010).

Furthermore, the importance of HS during renal rejection was also demonstrated in a model of experimental renal transplantation in rats. Rather than the HS GAG-chains the HS core proteins were examined in this study and induction of perlecan in glomerular basement membranes and collagen XVIII in cortical tubular basement membranes was observed (Rienstra et al., 2010).

Observations in liver rejection

In order to investigate if the findings of differentially expressed HS during renal rejection would also apply to different organs, liver allografts were examined. Due to the unique properties of the liver (low immunogenicity, high regeneration capacity) chronic rejection is a rare event (Tiegs and Lohse, 2010). It was therefore decided to include a group of specimens with chronic hepatitis, representing a group of chronic inflammatory disease. HS3A8, HS4C3 and 10e4 antibodies stained in a similar fashion: sinusoids, bile ducts and basement membranes were the main compartments labelled by all the antibodies within the biopsies. Again, HS4C3 gave inconsistent results with regards to nuclear staining and was not analysed quantitatively. Inconsistency with HS4C3 staining pattern has also been reported previously by Toin van Kuppevelt (Harden conference, Cambridge UK, March 2009). The existence of the 3-O-sulphated domain on liver sinusoids has also been described previously (Ten Dam et al., 2006). Isoforms 3-OST-A, 3-OST-B and 3-OST-1 have been found in liver (Shworak et al., 2002, Tatrai et al., 2010). The distribution and alteration of the HS4C3 epitope is in line with data recently published on HS in normal liver (Tatrai et al., 2010).

When HS epitopes were compared during different stages of rejection, the 10e4 expression was induced during moderate acute rejection particularly of bile ducts while there was hardly any expression at time 0, mild rejection or in late rejection. HS3A8 staining on the other hand increased during late rejection and chronic hepatitis compared to moderate/severe rejection. HS4C3, which shares requirement for N- and O-sulphation with HS3A8, also showed increased expression during chronic hepatitis. A rise in 3-O sulphation correlating with

increased levels of 3-O-ST-1 has also been reported for fibrotic liver. In HCC, also a slight 6-O-undersulphation most likely caused by enhanced levels of 6-O-sulphatase 1 was observed (Tatrai et al., 2010).

Taken together, in both renal and liver allograft rejection, distinct HS epitopes are induced at specific time points during rejection. In both organs, the 10e4 N-sulphated HS epitope appeared at earlier times of the rejection whereas the HS3A8 (N-sulphation, 2-O- and 6-O-sulphation, epimerisation) and to some extent the HS4C3 (N-sulphation, 3-O- and 6-O-sulphation) motif was found to be induced at later time points, possibly providing differential binding sites for growth factors, cytokines or chemokines at that specific stage of the disease. Concluding from this preliminary case study, early inflammatory factors would be dependent on N-sulphation whereas during later events more sophisticated modification would be required.

Possible consequences of altered HS motifs on ligand binding

Although no binding experiments were carried out successfully, the consequences of the altered HS on ligand binding should be discussed.

L-selectin

L-selectin is expressed constitutively by leukocytes. Besides its role in lymphocytes homing it is involved in inflammation and expression of its ligands on the endothelium have been described in various diseases including rejection (Rosen, 1999). Endothelial HS has been identified as L-selectin ligand in a mouse model, where an endothelial specific NDST1 knockout resulted in reduced chemokine transcytosis, presentation and decreased leukocyte migration (Wang et al., 2005). Analysis of various tissues made clear that renal collagen XVIII, a HSPG found in the ECM, is the HS ligand in the kidney. It was also shown that L-selectin binding was dependent on chain length, O-sulphation and N-sulphation and inhibited by iduronate (Celie et al., 2005). This could suggest that L-selectin binds to NA/NS domains (alternating N-acetylated and N-sulphated residues), which are recognized by 10e4 antibody. It also has been shown that during acute renal rejection leukocytes enter the tissue and damage

the tubular epithelium, attracted by chemokines presented by HS on tubular basement membranes (Robertson and Kirby, 2003).

Indeed, induction of L-selectin and CCL2 ligands on tubular epithelial cells under inflammatory conditions have been demonstrated as well as increased binding of L-selectin and CCL2 to HSPGs in the interstitial matrix during renal disease (Celie et al., 2007). Recently, the expression of proinflammatory HSPGs was also demonstrated in an ischemia/reperfusion induced inflammatory response after kidney transplantation, where L-selectin and CCL2 binding domains where expressed under the endothelium on the basement membrane. The loss of SULF1, a 6-O-endosulphtase, is believed to be responsible for the induction of these inflammatory HS domains which require 6-O-sulphate groups which would not be expressed under normal conditions (Celie et al., 2007).

Overall, our findings in kidney support these models, as upregulation of the 10e4 epitope during acute rejection 1a was found in the interstitium and on the tubular epithelium, where L-selectin mediated damage to the tubules takes place. The early involvement of L-selectin in the rejection process is further supported by the expression of the HS3A8 epitope during chronic stages, as the iduronic acid represented by this antibody would be inhibitory for L-selectin binding during early events, as ischemia/reperfusion injury or acute rejection.

Chemokines

Chemokines are known to bind HS and the residues of chemokines responsible for GAG interaction have been described but very little is known about the corresponding region of GAGs (Proudfoot et al., 2001, Severin et al., 2010). It was long thought that the exact saccharide composition and modification pattern would determine the interaction of chemokines and HS, but so far there is no data regarding exact modification and distribution that would be mandatory. N- and O-sulphation are said to be required (Kuschert et al., 1999, Schenauer et al., 2007) and apart from the sulphation status itself the spacing of the NS-domains by less modified NA domains creating distinct charge topologies (Lortat-Jacob, 2009). For a few chemokines HS binding domains have been investigated and all bind preferentially to saccharides with increased sulphation. N-sulphation and 2-O-sulphation have been shown to facilitate

CCL2 binding (Sweeney et al., 2006). Among saccharides with constant sulphation CCL2 preferentially bound to an HS octasaccharide containing an N-acetylated residue (Schenauer et al., 2007). This would again be in agreement with our data, where CCL2 was found during acute rejection in conjunction with increased 10e4 staining, which represents N-sulphated and N-acetylated HS domains. Moreover, CCL2 was shown recently to bind to a heparin octasaccharide which is devoid of 3-O-sulphation, which is in agreement with our data where increased 3-O-sulphation, represented by HS4C3 staining, did only occur during chronic stages of rejection (Meissen et al., 2009).

AntithrombinIII

The antithrombinIII (ATIII) binding site is the only specific heparin binding site known so far. Although certain binding requirements have been reported for other molecules, including FGFs, IFNγ or chemokines, no exact sequence has been experimentally proven. Structural analysis revealed a unique pentasaccharide sequence containing a very rare 3-O-sulphation required for high affinity binding (Lindahl et al., 1984, Petitou et al., 2003). The binding causes conformational changes in the protein, which enhances the neutralization of thrombin leading to anticoagulant effects. This interaction is of great medical importance as heparin is widely used as anticoagulant.

3-OST-1 and to a lesser extent 3-OST-5 are the only isoforms of the 3-O-sulphotransferase family which are capable of synthesizing anticoagulant HS (Girardin et al., 2005, Xia et al., 2002). As HS4C3 antibody recognises 3-O-sulphation (Ten Dam et al., 2006), independent of the enzyme involved in generating the substitution, it is not clear if the identified domain has anticoagulant activity. In liver the existence of 3-OST-1, in addition to 3-OST-A and B, has been reported (Shworak et al., 1999, Tatrai et al., 2010) and therefore the existence of anticoagulant HS seems likable. The upregulation of the HS4C3 epitope during chronic hepatitis in conjunction with heparanse could lead to a breakdown of anticoagulant environment in the transplanted organ, possibly causing intravascular coagulation and fibrin deposits in the rejecting allograft (Shriver et al., 2000). Indeed, upregulation of heparanase has been demonstrated recently in fibrotic liver disease (Tatrai et al., 2010). The biopsies in this study representing chronic hepatitis have not been further characterized,

but as chronic hepatitis is often caused by infection with viruses, such as hepatitis B and C, it would be interesting to investigate the involvement of the upregulated 3-O-sulphate group with regards to these viruses. So far only dependency on N-sulphation has been reported for hepatitis infection (Barth et al., 2006) but as 3-O-sulphated epitopes are upregulated during chronic hepatitis this would appear an interesting new approach.

FGF2

Well studied interaction partners of HS are fibroblast growth factors (FGFs) and their receptors (FGFRs). Two FGF molecules and two FGFR must bind to HS forming a ternary complex in order to signal properly (Kan et al., 1993, Powell et al., 2002, Rapraeger et al., 1994) (Harmer, 2006). Although there is an oligosaccharide which is bound with preference, no unique or specific binding site has been described. The most favourable sequence is composed of N-sulphation on the non-reducing end glucosamine, 2-O-sulphation on iduronic acid and variable 6-O-sulphation on the reducing end glucosamine (Kreuger et al., 2001). The spatial arrangement of this binding motif is crucial for signalling of FGFs via their receptors. All of the above described modifications of HS necessary for FGF2 binding are represented by the antibody HS3A8. HS3A8 epitopes are significantly upregulated in tubules and the interstitium during chronic rejection of kidney and in bile ducts during late acute rejection as well as chronic hepatitis in liver. This would imply increased levels of FGF2 during chronic inflammatory events. Indeed, increased levels of FGF2 in interstitial and tubular renal cells (Strutz et al., 2000) were reported. Since allografts with chronic rejection undergo fibrotic changes, involvement of FGF2 is quite likely.

Although the phage display antibodies are a great tool for investigating changes in HS composition, nothing is known about the relative abundance of individual modifications (Rops et al., 2008, Smits et al., 2006).

An increase in staining could be due to high levels of N-sulphation and moderate levels of O-sulphation or vice versa. Therefore, disaccharide analysis in conjunction with staining would be very helpful in interpreting the data. In a recent study regarding phage display antibody specificity, significant differences between the existence of epitopes *in situ* (in tissue sections) and *in vitro* (in dot

blots of tissue extracts) were reported. A number of epitopes were not or only weakly recognized *in situ* but highly recognized in tissue extracts (and vice versa) (Thompson et al., 2009). This could be due to the masking of the HS epitope *in situ* by endogenous ligands and should be considered in the future.

In summary, distinct HS epitopes have been identified during different stages of rejection. Both organ systems analysed revealed a time dependent appearance/disappearance of distinct epitopes: N-sulphated domains came up at early time points during rejection in kidney and liver allografts whereas highly sulphated domains came up late during chronic rejection in kidney and chronic hepatitis in liver. In addition, increased expression of the chemokine CCL2 was observed during acute rejection 1a in kidney. The physiological consequence of these differentially modified motifs during rejection should be further explored by improved binding assays and matching studies between HS binding protein and distinct HS motives.

4 Regulation of Heparan Sulphate biosynthesis

4.1 Introduction

HS is a very heterogeneous molecule with a variety of functions. How the cell is capable of synthesizing such an information rich molecule in a cell/tissue as well as developmental stage/age specific manner (David et al., 1992, Ledin et al., 2006, Ledin et al., 2004) is still poorly understood. Unlike other molecules which carry biological information, such as DNA, there does not seem to be a code or any other form of template. So where does the regulation take place? At the transcriptional, translational or posttranslational level? Or is it assembly of the biosynthetic enzymes that determines their activity?

4.1.1 The sequential model of HS biosynthesis

In this established model it is believed that the HS biosynthetic enzymes act in a sequential manner. Therefore NDST1 would be regarded as the key player in HS biosynthesis (see section 1.6.3.1), as it is the first modifying enzyme to act on the HS chain. All other enzymes responsible for further modifications/sulphations would depend on prior action of NDST1. This model is based on observations that without N-sulphation no further modifications, such as C5-epimerization or O-sulphation, occur (Lindahl et al., 1998, Salmivirta et al., 1996).

4.1.2 The GAGosome model of HS biosynthesis

Recently, a different model of HS biosynthesis was suggested by Esko and Selleck, which was later experimentally investigated by Ledin and co-workers. Based on studies in embryonic mouse liver tissue it was suggested that no regulation at the transcriptional, translational or posttranslational level takes place at all. Regulation is rather due to the assembly of the enzyme complex and the selection of enzymes into this complex, called the GAGosome (Esko and Selleck, 2002, Ledin et al., 2006). This model would offer a more flexible way of modification where enzymes involved in HS chain processing can act

simultaneously or before or after each other. The GAGsome is thought to offer a limited number of binding sites for NDSTs and that their affinity will predict which isoform gets incorporated.
Even though the GAGosome model is a recent concept, there is some evidence to support it. In 2004 it was demonstrated that HS synthesised from embryonic stem cells deficient in NDST1 and NDST2 lack N-sulphation but still contain 6-O-sulphate groups (Holmborn et al., 2004), indicating modification of HS without prior N-sulphation. However, different research groups have shown transcriptional, translational and post-translational control of HS biosynthesis and it would be almost unbelievable that a molecule as complex as HS would be generated 'by chance', solely depending on the enzymes available and their affinities.

Translational control of NDST enzymes has been suggested; sequence analysis revealed that all 4 murine isoforms of NDST have extremely long and complex 5' untranslated regions (5'UTRs) with a high degree of secondary structures and contain several upstream AUG codons which interfere with normal cap-dependent ribosome scanning and translation initiation. These Internal Ribosome Entry Sites (IRES) offer regulation on the translational level. Interestingly, some of the growth factors that bind to HS (FGF2, VEGF) reveal very similar 5'UTRs. This could suggest the possibility of a coordinated regulation of growth factors and their co-receptors HS (Grobe and Esko, 2002).

A few research groups have also shown that HS biosynthetic enzymes can be regulated by exogenous stimuli, such as proinflammatory cytokines. Mouse glomerular endothelial cells were activated with either TNF-α or IL-ß and an upregulation of a range of enzymes involved in HS biosynthesis (NDST1, NDST2, 6-OST) was the consequence (Rops et al., 2008). This is consistent with data from TNF-α and IFN-γ stimulated human microvascular endothelial cells which also showed upregulation of NDST1 transcript (Carter et al., 2003). In agreement with that, stimulation of dermal human microvascular endothelial cells with LPS also resulted in upregulation of NDST1 (Krenn et al., 2008).

4.1.3 Protein-protein interaction of HS biosynthetic enzymes

The GAGosome model is based on the formation of a complex involving the HS biosynthetic enzymes. So far only a few protein-protein interactions of HS enzymes have been identified.

The first interaction between HS synthesizing enzymes has been demonstrated by affinity chromatography (Schwartz et al., 1974), where the xylosyltransferase and the galactosyltransferase1 have been shown to interact.

The chain elongation enzymes EXT1 and EXT2 have been shown to form a heterooligomeric complex in the Golgi compartment, which is said to be the biologically active form of the chain elongation machinery (Munro, 1998, Nilsson et al., 1994, Salmivirta et al., 1996).

Relocation studies where the C5 epimerase was relocated from the Golgi to the ER in CHO cells caused parallel redistribution of the 2-O-sulphotransferase, providing evidence for physiological interaction and complex formation (Pinhal et al., 2001).

Recently, immunoprecipitation experiments revealed that EXT2 and NDST1 interact with each other. This model suggests that EXT2 is acting as a chaperone, responsible for the transport of NDST1 to the Golgi apparatus. In this model, supporting the GAGosome concept, EXT1 and NDST1 compete for binding sites of EXT2 and the relative amount of the proteins decides which one gets incorporated, thus greatly influencing the sulphation pattern of HS (Presto et al., 2008).

4.1.3.1 Protein-protein interaction: Tandem Affinity Purification (TAP)

Different experimental approaches have been used to study protein-protein interactions, including co-immunoprecipitation, mammalian 2-hybrid systems and various fusion tags. The TAP-tag is the latest technology to analyse protein-protein interactions. Originally developed for purification of yeast protein complexes (Puig et al., 2001), this method has now been refined for use in mammalian systems. The tandem affinity purification method uses two different affinity purification tags that are fused to the protein of interest. After two consecutive purification steps, the targeted complex can be gently eluted and the interacting protein partners can then be identified by mass spectrometry.

The advantages of this system are that it allows purification under native conditions and the proteins recovered are very pure. It is now the method of choice for purification of recombinant protein complexes.
As NDST1 plays a crucial role in HS biosynthesis it was decided to investigate its regulation on the level of protein-protein interaction.

4.1.4 Specific aims

This part of the work aimed to investigate the regulation of HS biosynthesis by studying the regulation of NDST1 at the protein level. Specific goals:

- Design and cloning of the NDST1-TAP-tag construct
- Optimisation of protein purification conditions
- Purification of protein complexes and identification of interacting partners
- Validation of the interaction

4.2 Specific Materials and Methods

4.2.1 PCR

PCR (polymerase chain reaction) is a simple method used to amplify DNA. The target DNA is bordered by a pair of oligonucleotide primers. PCR primers are usually 18-35 nucleotides in length and both primers should have approximately the same GC content and share a similar melting temperature. Primers should not be self-complemetary or complemetary to other primers used in the reaction to avoid homo- or heterodimerization.

There are three basic steps in PCR cycles.
Initially, the DNA is denatured at 95ºC. After that primers can anneal to the single stranded DNA template at a temperature 5ºC below their melting temperature. Finally, elongation of the DNA takes place at 72ºC.
For PCRs using *taq* polymerase and Platinum *taq* the temperature settings shown in Table 4-1 were used.

Table 4-1 Temperature settings of typical PCR reactions

***Taq* polymerase**	**Platinum *Taq***
15 min 95 °C	2 min 94 °C
1 min 94 °C	30 sec 94°C
1 min 56°C	30 sec 55°C
3 min 72°C	2.6 min 68°C
10 min 72	---------

Despite the temperature settings and the amount of template, the concentration of primers and nucleotides are of importance.

A typical PCR reaction was set up as shown in Table 4-2:

Table 4-2 Composition of a typical PCR reaction

compound	volume (µl)	final concentration
DNA template	1	1-10ng plasmid DNA
dNTPs 10µM	1	200nM each
fw primer 10 µM	1	200nM
rev primer 10 µM	1	200nM
Buffer 10x	5	1x
polymerase	0.5	2.5U
H_20	40.5	
final volume	50	

For routine PCR, *Taq* polymerase from Qiagen was used. As this enzyme has no proofreading activity, mutations are quite common (error rate $1.1x10^4$/bp (Tindall and Kunkel, 1988). For PCR reactions where the amplified fragment was needed for expression, an enzyme with proofreading activity was used, such as Platinum *Taq* high fidelity polymerase from Invitrogen. This enzyme mixture is composed of a recombinant *Taq* polymerase and a second polymerase with proof reading activity which increases fidelity approximately six times over that of *Taq* polymerase alone (invitrogen.com). Due to the *Taq* polymerase the amplified product ends with an A overhang at the 3' end, which makes it applicable for TA-overhang cloning and the 3' exonuclease activity from the second enzyme reduces the error rate.

A plasmid (pcDNA3) containing the entire reading frame of human NDST1 including 3' untranslated region was kindly provided by Dr. Humphries, Boston University, USA). Primers for PCR amplification were designed using Primer3 open source software (frodo.wi.mit.edu). In order to subclone the DNA fragment directionally, restriction sites were added to each primer. In addition to PCR

primers also sequencing primers were designed to ensure integrity of the whole insert and not just the fusion region.

Table 4-3 Primer design for NDST1 amplification and sequencing

	primer	**5' addition**	**sequence 5'→ 3'**
PCR primers	forward	*Eco*RI (gaattc)	ggaggccaggatgcctg
	reverse	*Xho*I (ctcgag)	cctggtgttctggaggtcct
Sequencing primers	forward	-	cgtggatgccgtggccttcc
	reverse	-	aatcatcaacgggggcgagctc

4.2.2 TA-cloning

In order to facilitate subcloning of a PCR fragment, a PCR cloning kit (Stratagene) was used. This technology allows cloning without the use of restriction enzymes and ligase. It is based on the fact that topoisomerase is able to cleave and rejoin DNA molecules. *Taq* polymerase amplified products contain a 3' adenosine overhang which allows ligation into the TA-vector through A-T base-pairing followed by topoisomerase mediated strand ligation. The resulting vector contains a LacZ' α-complementation cassette to allow blue-white screening on agar plates containing 20µg/ml X-gal (5-bromo-4-chloro-3-indolyl-ß-D-galactopyranoside). The host strain used here does not require the addition of IPTG as inducer for the *lac* operon. As two *Eco*RI sites flank the MCS, vectors containing an insert can easily be verified by *Eco*RI digestion followed by agarose gel electrophoresis.

4.2.3 Protein cross-linking

Protein cross-linking was performed to investigate the formation of multi-protein complexes. Two amine-reactive crosslinkers were employed.

4.2.3.1 Formaldehyde

Formaldehyde (methanol-free, Pierce) was used as a cross-linking agent as it is highly reactive and cell permeable. The single carbonyl group of formaldehyde functions as a homobifunctional crosslinker. It reacts with the nitrogen of the lysine residues of the protein forming a methylene bridge. Cells were seeded in 100mm dishes, grown to ~80% confluency and incubated with Formaldehyde (0-1%) for 20 minutes at 37°C. Following extensive washing in PBS, the reaction was stopped by the addition of glycine to a final concentration of 0.125M. After washing the cells twice, lysis buffer was added and cells were scraped on ice. After spinning for 20 minutes at 16.000 x g, the supernatant was collected and analysed by Western blotting.

4.2.3.2 DST (disuccinimidyl tartrate)

DST is a membrane permeable homobifunctional crosslinker, suitable for intracellular or intramembrane protein conjugation. Cells were seeded in 100mm dishes, grown to ~80% confluency and incubated with 1mM DST in DMSO for 30 and 45 minutes at RT after extensive washing in PBS. The reaction was stopped by the addition of glycine. After washing the cells twice, lysis buffer was added and cells were scraped on ice. After spinning for 20 minutes at 16.000 x g, the supernatant was collected and analysed by Western blotting.

4.2.4 Tandem affinity purification

The tandem affinity purification method uses two different affinity purification tags that are fused to the protein of interest. After two purification steps, the targeted complex can be gently eluted. The interacting protein partners are then identified by mass spectrometry.

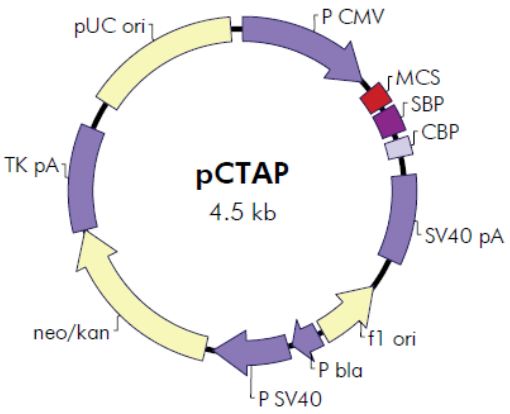

Figure 4-1 Schematic representation of the pCTAP vector

In this study the InterPlay mammalian TAP system from Stratagene has been used. In this system the protein of interest is fused to a streptavidin binding peptide (SBP) and a calmodulin binding peptide (CBP). The SBP tag has a high affinity for the streptavidin resin and can be eluted with biotin. The CBP tag has a high affinity for the calmodulin resin in the presence of calcium. When calcium is removed, the tagged protein complex can be eluted.

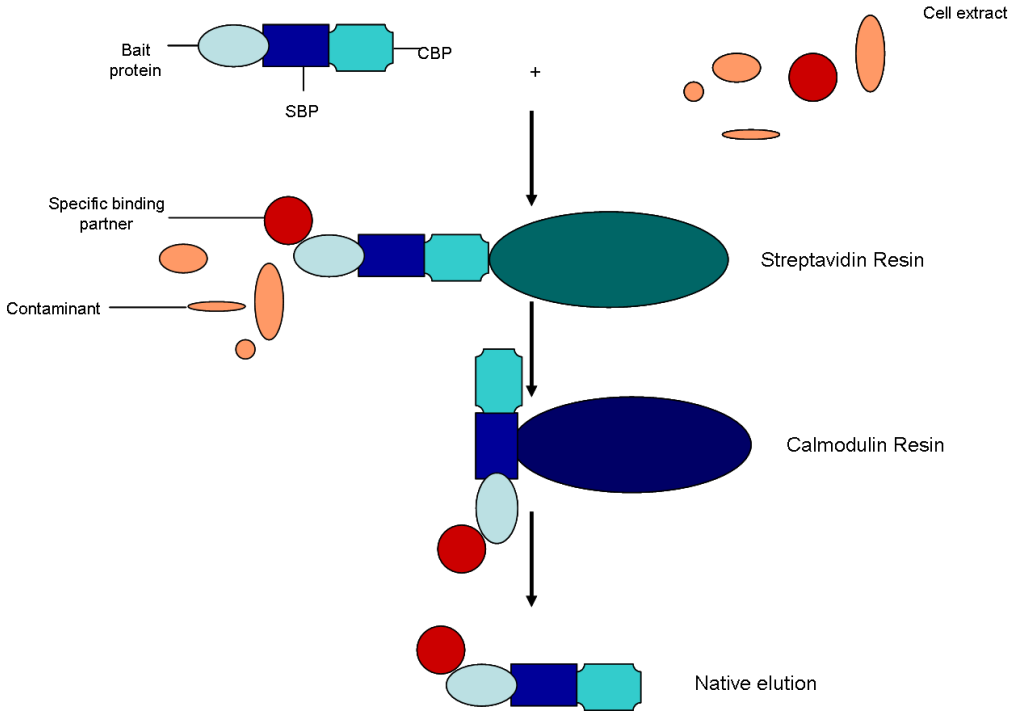

Figure 4-2 Overview of TAP-technology

The protein of interest is fused to the strepatvidin binding peptide (SBP) and the calmodulin binding peptide (CBP). After incubation with cell extracts the bound proteins are purified in two consecutive steps and interacting proteins are eluted under native conditions.

In brief, approximately 6 x 10^7 cells were harvested. After two washes with ice-cold PBS, the cells were removed mechanically from the culture flasks and maintained at 4ºC during the whole purification process. Cells were resuspended in lysis buffer and were then subjected to three successive cycles of freeze-thawing by incubating cells at -80ºC for 20 minutes followed by incubating cells in a cold water bath at 4ºC for 10 minutes. Cells were harvested at 16.000 x g for 10 minutes to pellet cell debris and the supernatant was supplemented with 4µl of 0.5M EDTA and 0.7µl of 14.4M β-mercaptoethanol per ml of lysate. 50 µl of washed streptavidin resin slurry (25 µl resin) was added to 1ml of protein lysate and the mixture was incubated at 4ºC for 2h whilst rotating to allow the tagged protein to bind to the resin. After collecting the resin by centrifugation at 1500 x g and two further washes, 100 µl streptavidin elution buffer was added. Proteins were eluted by rotating the tube for 30 minutes. After collecting the supernatant via centrifugation at 500 x g for 5 minutes it was supplemented with 2 µl streptavidin supernatant supplement and 25 µl washed calmodulin resin slurry (12.5 µl resin) per ml of supernatant. After 2 additional hours of incubation and rotation, the resin was collected by centrifugation for 5 minutes at 1500 x g. The supernatant was discarded and the tagged proteins bound to the calmodulin resin were eluted by rotating the tube for 30 minutes after adding 50 µl calmodulin elution buffer. Finally, the resin was collected by centrifugation for 5 minutes at 1500 x g and the supernatant containing the Tandem Affinity Purified complexes was stored at -20 ºC until further processing.

In order to concentrate the sample, the TAP-purified protein complexes were TCA precipitated and then loaded onto a 4-12% gradient SDS-PAGE (Invitrogen).

4.2.4.1.1 Staining of the SDS-PAGE

The SDS-PAGE was stained with colloidal coomassie blue (SimplyBlue SafeStain, Invitrogen). In brief, the gel was rinsed 3 times for 5 minutes in deionised water before staining for 1h at room temperature. After washing the gel in deionised water for 1h at room temperature, bands were excised and sent for MS analysis.

4.2.4.1.2 Mass spectrometric analysis

After enzymatic (trypsin) digestion of the excised bands, proteins were identified by peptide-mass fingerprinting (PINNACLE, Newcastle University).
The individual samples from peptide mass fingerprinting were analysed using the Mascot Mowse score, which basically compares the calculated peptide masses of all entries in the sequence database with the experimental data of the sample and if the calculated value falls within the set mass tolerance it counts as a match. The Mascot protein score is -10*Log (P), where P is the probability that the match observed is random. The e-value in Mascot corresponds to the number of times one would expect this score by chance alone (Pappin et al., 1993, Perkins et al., 1999). The settings for the identification of unknown proteins by peptide mass fingerprint were as follows:

Taxonomy: the taxonomy was set to 'all entries' and not restricted to a specific species albeit only samples from human origin were analysed as restricting the taxonomy could prevent finding a match if for instance the protein is not present in database yet. In that case, a homologous protein match from a different species could give invaluable information about the protein identity. Further, not all databases do have a rigorous taxonomy system.

Enzyme: the serine protease trypsin was used for all digestions.

Variable modifications: with variable modifications, which may but may not be present in the samples, each potential site is tested with or without the modification. Variable modifications were: *Carbamidomethyl* (cystein), which is as a result of the alkylating reaction with iodoacetamide during sample preparation; *Oxidation M* (methionine either normal or methionine+oxygen) and *Peptide N-terminal Gln to pyro-glu* N-terminal either glutamine or pyro-glutamic acid)

Mass values: Monoisotopic was chosen, where mass is determined by the masses of the most abundant isotopes

Protein Mass: Unrestricted

Peptide mass tolerance: the mass tolerance was expressed as fraction as parts per million (ppm) and individual settings can be seen in the results tables

Peptide charge state: 1+

Max missed cleavage: a perfect digestion would mean that no partial fragments are present, but as often samples are only partially digested, this parameter was routinely set to 1.

(www.matrixscience.com)

4.2.5 Co-IP

Antibody immobilisation

The AminoLink Plus coupling resin was equilibrated at room temperature and 50µl of the resin slurry was added into a spin column, which was centrifuged at 1000 x g for 1 minute to collect the resin. After the flow-through was discarded, the resin was washed twice in 200 µl of coupling buffer and excess liquid was removed carefully with a paper towel. 75 µg of affinity purified beta tubulin antibody (Abcam) in 200µl of coupling buffer (10 µl of antibody at a concentration of 1 µg/µl plus 190 µl of coupling buffer) was added directly to the resin. 3µl of Sodium Cyanoborohydride solution was added and the column was incubated for 120 minutes on a rotator at room temperature. After centrifuging the column once at 1000 x g for 1 minute, the column was washed twice with 200 µl coupling buffer and once with 200 µl of quenching buffer. The column was incubated with 3µl of Sodium Cyanoborohydride in 200 µl of quenching buffer for 15 minutes with gentle shaking at room temperature before the column was washed with 200 µl of quenching buffer twice. After six additional washes with 150 µl of washing solution the resin was ready for the following Co-IP.

Cell Lysis

Cells were grown to ~80% confluency in 100mm dishes, washed twice in PBS and lysed in 500 µl of lysis/wash buffer for 10 minutes on ice with periodic mixing. After lysis, the supernatant was collected at 13.000 x g for 10 minutes and transferred into a fresh tube for protein concentration determination. Cell lysate was adjusted to 400 µl with lysis/wash buffer.

Co-IP

All steps were performed at 4°C. The column, containing the antibody-coupled resin, was washed twice with 500 µl of lysis/wash buffer and excess liquid was carefully removed with a paper towel. Lysate and controls were added to the resins and incubated with gentle rocking for 2 hours. The column was centrifuged (flow-through was saved for later analysis), placed in a new collection tube and washed three times with 500 µl of lysis/wash buffer.

Elution of Co-IP

The column was placed in a new collection tube and 10 µl of elution buffer were added. After centrifuging, 70 µl of elution buffer was added and columns were incubated for 5 minutes at room temperature. Finally, the column was centrifuged and the flow-through was collected for further analysis.

Protein samples were analysed by Western blotting probed for NDST1.

The control resin, which is composed of the same material as the Co-IP resin but is not activated, was carried along as negative control.

4.3 Results

4.3.1 Cloning of NDST1-pCTAP

4.3.1.1 Cloning of NDST1 into the pCTAP-vector

In order to create a C-terminal tagged form of NDST1 the stop codon of the human NDST1 cDNA was removed by PCR. Prior to PCR amplification of NDST1 cDNA the sequence was verified by sequencing using routine sequencing primers T7 and Sp6 (see appendix section 8.1). Figure 4-3 shows successful amplification of the PCR product.

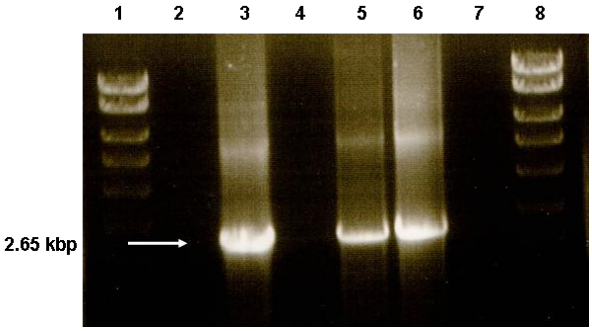

Figure 4-3 Representative agarose gel of PCR products

Lanes 1 and 8 contain DNA hyperladder, lanes 3, 5 and 6 containing amplified ORF of NDST1, lane 2 containing no enzyme control and lane 4 and 7 contain no template controls.

To facilitate subcloning, *Taq* polymerase was used for the PCR reaction with an additional proof reading enzyme in the reaction mix. Due to the A overhang provided by the *Taq* polymerase the PCR product was subcloned into a TA-vector. Blue-white screening allowed identification of positive clones (Figure 4-4).

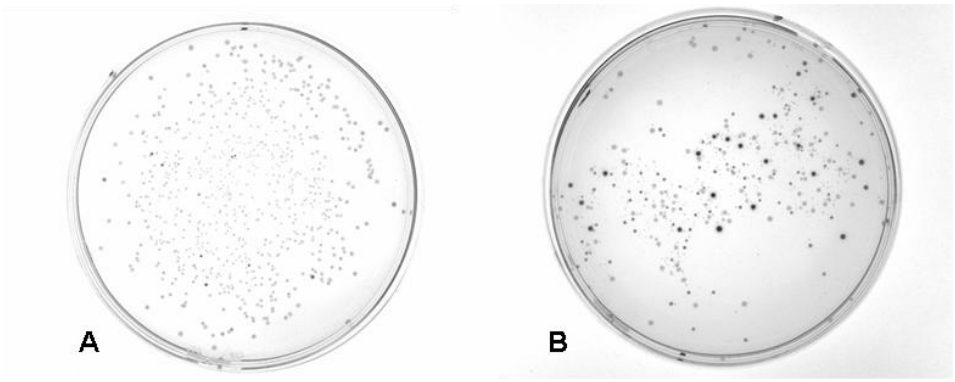

Figure 4-4 Blue white screening of TA clones

PCR- amplified NDST1 cDNA was cloned into the TA-vector and transformed into competent *E.coli*. Blue-white screening was performed using agar plates containing X-gal. A) representing the positive control transformation and B) clones transformed with the PCR-amplified NDST1 cDNA.

Positive (white) clones were selected, expanded and DNA extracted. The DNA was *Eco*RI digested (two *Eco*RI sites flank the MCS in the TA-vector) to identify clones carrying the insert (Figure 4-5).

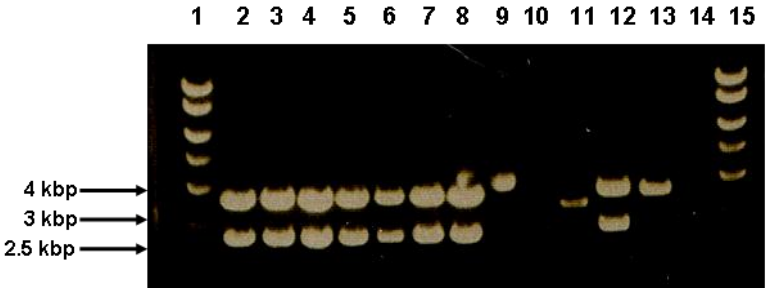

Figure 4-5 Representative agarose gel of restriction digests of TA-clones

Lane 1 and 15 contain DNA hyperladders with fragment sizes as indicated, lane 2-8 and 12 contain *Eco*R1 digested plasmid plus insert (approximately 2.6 kbp), lane 9 contains uncut plasmid as a control, lane 13 contains *Eco*R1 digested plasmid without insert and lane 10 and 14 were used as spacers.

NDST1 DNA fragments of the correct size (approximately 2.65 kbp) were excised from the gel, purified and ligated into the pCTAP vector which previously had been linearized with the corresponding enzymes (*Eco*RI and *Xho*I). After transformation into competent *E. coli*, colonies were picked from agar plates, DNA was isolated and restriction digestion was performed to screen for positive clones (Figure 4-6).

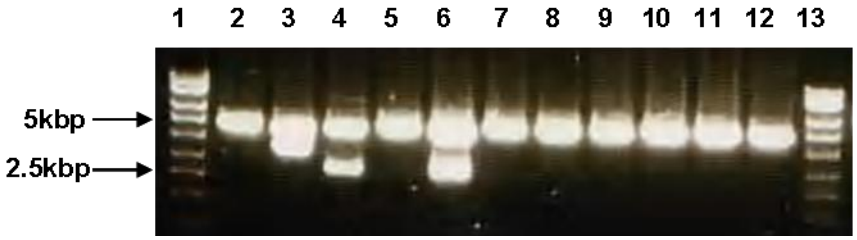

Figure 4-6 Representative agarose gel of restriction digests of pCTAP-NDST1 clones

Clones were analysed by *Not*1 and *Xho*1 restriction mapping. Lane 1 and 13 contain DNA hyperladder, lanes 4 and 6 contain clones carrying NDST1 insert, lanes 2, 3, 5 and 7-12 containing false-positive clones without insert.

DNA of 2 clones, which appeared to have correctly sized fragments, was excised and sent for sequencing to ensure the integrity of the amplified product. As the insert exceeds 2400bp internal sequencing primers were designed to ensure integrity of the whole insert. Figure 4-7 shows a schematic representation of the NDST1-TAP-tag construct (the complete sequence of the construct can be found in the appendix section 8.2).

a

b

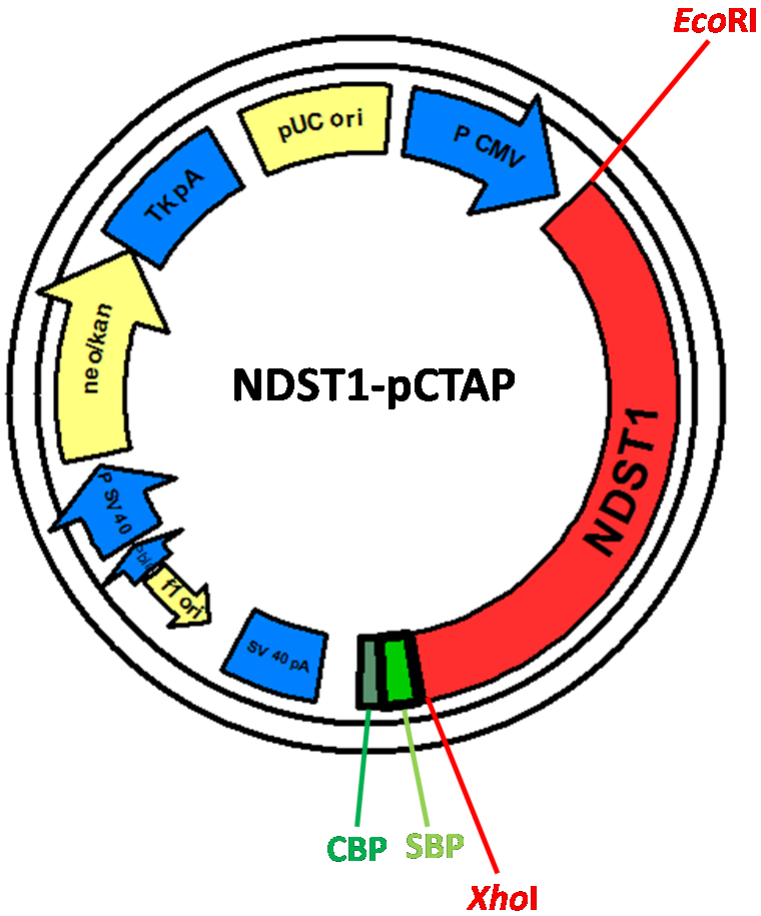

Figure 4-7 Schematic representation of NDST1-pCTAP construct

NDST1 cDNA has been cloned between *EcoR*I and *Xho*I restriction sites in frame with the SBP-tag of the pCTAP vector. DNA sequence of fusion region with restriction sites (a) and schematic representation of the cloned construct (b).

Prior to transfection of HEK 293 cells the NDST1-pCTAP construct was linearized to improve integration frequency into the host genome. As there was no singular restriction site available for linearization, the *Mlu*I site which

overlapped with 1 base at the end with the SV40 polyA signal was chosen (Figure 4-8).

Figure 4-8 Linearisation of pCTAP and pCTAP-NDST1

Lane 1 and 4 containing hyperladder, lane 2 containing NDST1-pCTAP in circular form and lane 3 containing pCTAP-NDST1 which was linearized by *MluI* restriction digestion.

4.3.1.2 Transfection of HEK 293 cells with NDST1-pCTAP and control plasmid

Various DNA:Effectene ratios were used for transfection without any significant effect on the efficiency. Transfectants were selected with 800µg/ml of G418 and kept under selection pressure (400µg/ml) whilst expanding.

4.3.1.3 Screening of NDST1 transfectants

The 20 surviving clones were screened via Western blotting for the expression of NDST1 protein with antibodies raised against NDST1 (NDST1 antibody Santa Cruz, see section 2.5.6) and against the calmodulin binding peptide (Santa Cruz). Figure 4-9 shows that neither the C-terminal tag nor the linearization of the DNA prior to transfection interfered with the expression of NDST1, as the protein was expressed correctly sized and non-degraded. Transfectant 15 revealed upregulation of NDST1 protein and was used for further experiments.

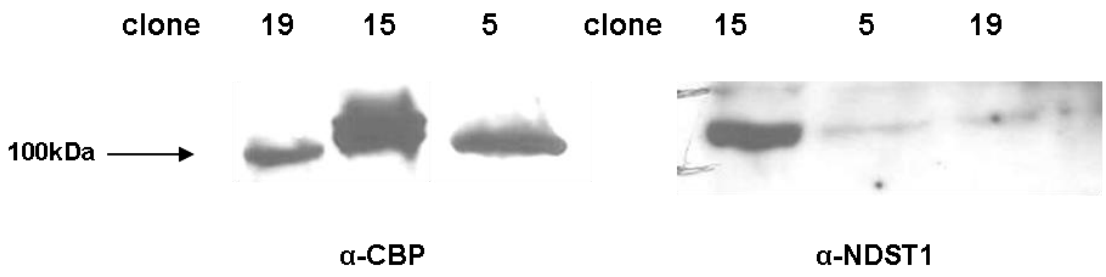

Figure 4-9 Expression of pCTAP-NDST1

Western blots of pCTAP-NDST1 stably transfected HEK 293 cells (Transfectant 5, 15 and 19). 70µg of total cell lysates were used, blots were probed with α-CBP- and α-NDST1-specific antibodies as indicated. Representative for n=2.

FACS analysis revealed functionality of the tagged enzyme as F15 cells showed significantly increased staining for 10e4 (Figure 4-10).

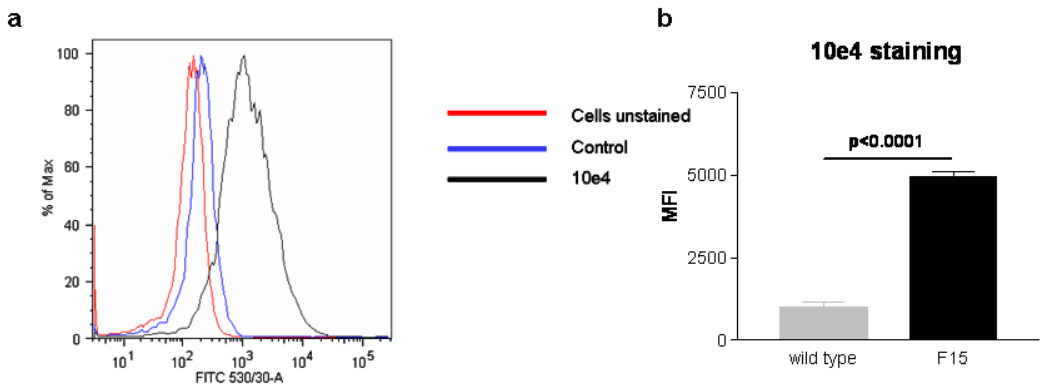

Figure 4-10 10e4 epitope expression of NDST1 overexpressing F15 cells

F15 cells were incubated with 10e4 antibody (1/50) and anti-mouse-FITC conjugated secondary antibody. Unstained cells were incubated in FACS buffer (5% FCS/PBS) and cells incubated with the secondary antibody, omitting the primary antibody incubation step, served as a control. Representative flow cytometry plots (a). Differential expression of 10e4 HS epitope of wild type and NDST1 overexpressing F15 cells (b). Data representative for 2 individual experiments performed in duplicates. Statistical analysis was determinded by student's t-test with differences p<0.05 considered to be significant.

4.3.2 Protein complex formation

4.3.2.1 Formaldehyde crosslinking

Proteins crosslinking was used to study protein complex formation. As formaldehyde is membrane permeable it can be added to living cells and proteins in close proximity (within 2 Å distance) are able to form bonds. Prior to the Tandem affinity purification, NDST1 overexpressing cells were used for these chemical cross-linking experiments, as it seemed plausible that due to overexpression of NDST1, complex formation with interacting protein partners could be observed.

Subconfluent flasks of HEK 293 NDST1 transfectant cells were incubated with 0.5% or 1% of methanol-free formaldehyde and incubated for 20 minutes at 37°C before glycine was added to stop the reaction. Reaction time and temperature were chosen as they have been shown to work in similar settings (Vasilescu et al., 2004).

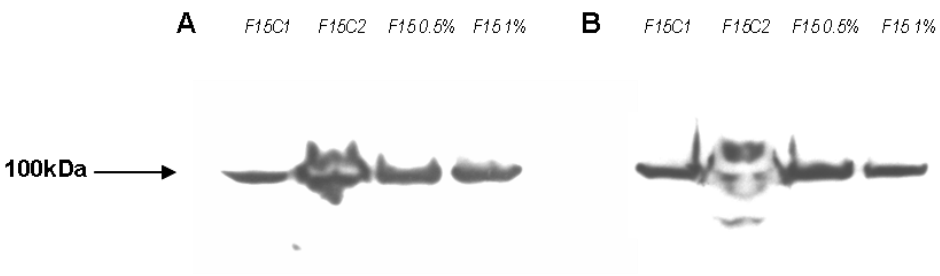

Figure 4-11 Western Blot of formaldehyde crosslinked protein lysates

NDST1 overexpressing clone F15 was incubated with varying concentrations of Formaldehyde for 20 minutes at 37°C. Blots were probed with NDST1 specific antibodies. SDS-PAGE was run under denaturing (A) or non-denaturing (B) conditions. F15C1 served as a control without formaldehyde treatment, whereas F15C2 served as a control without formaldehyde treatment but addition of glycine. Representative for n=2.

As seen in Figure 4-11, no protein complex formation was observed under either denaturing or non-denaturing conditions. If NDST1 had interacted with other proteins, one would expect a shift towards higher molecular weight on the Western blot. Similar experiments were also carried out with DST as

crosslinking agent but also failed to reveal protein complex formation (data not shown).

4.3.2.2 Screen for protein-interacting partners: Tandem Affinity Purification

As no protein complex formation was observed using chemical cross-linking, NDST1 overexpressing HEK 293 cells were used for affinity purification. In this study a purification kit optimized for cytoplasmatic proteins was used. As NDST1 is a non-soluble membrane protein with one transmembrane domain lysis conditions had to be optimized. In the first approach, the lysis buffer provided with the kit was supplemented with nonidet NP40 to a final concentration of 1%, as suggested by Seraphin and co-workers, who initially developed this method (Puig et al., 2001).

4.3.2.2.1 Purification using original lysis buffer

The purification was carried out according to the standard protocol, starting with 6 x 10^7cells. After the purification, total protein lysates were separated by a gradient SDS-PAGE.

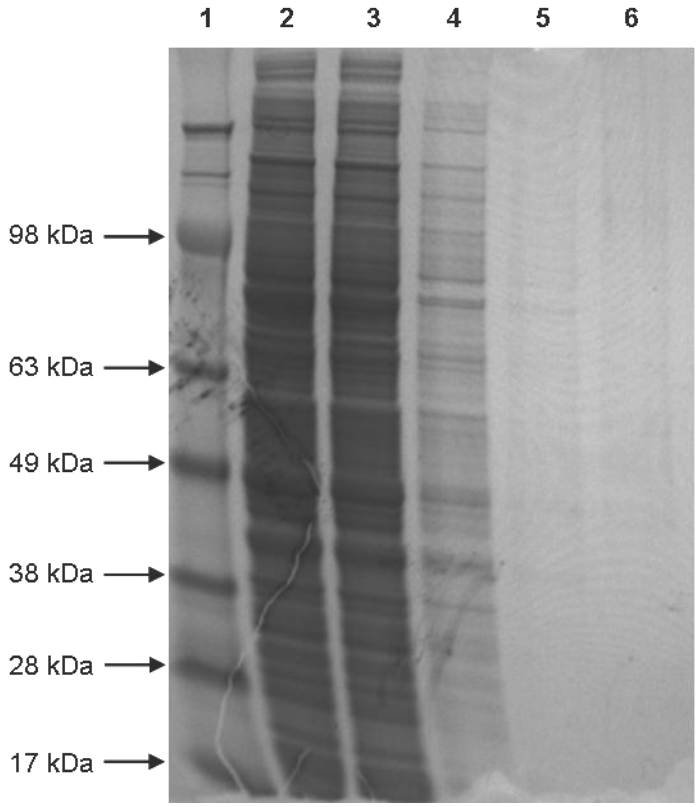

Figure 4-12 Affinity purification using original lysis buffer

4-12% colloidal coomassie-stained SDS-PAGE loaded with TAP-purified proteins. Approximately 6 x10^{7}cells were used. Lane 1: protein ladder, lane 2: whole lysate (2µl loaded), lane 3: SBP-wash (2µl loaded), lane 4: SBP-eluate (20µl loaded), lane 5: CBP-wash (20µl loaded),, lane 6: final eluate (all loaded after TCA precipitation).

Figure 4-12 shows no evidence of NDST1 purification. In the final eluate (lane 6), no band around 100kDa, where NDST1 would be expected, is visible. This suggests that the addition of NP40 to the original lysis buffer is incompatible with the purification process. As the composition of the lysis buffer provided with the kit is proprietary, it was decided to develop completely new lysis conditions.

4.3.2.2.2 Purification using 'home-made' lysis buffer

As the original lysis conditions failed to purify NDST1, a new lysis buffer was used for the next purification (50mM Tris, 150mM NaCl, 10mM Na_3VO_4 and 1%NP40) based on the method originally developed by Puig (Puig et al., 2001). Again, 6 x 10^{7}cells were used as starting material.

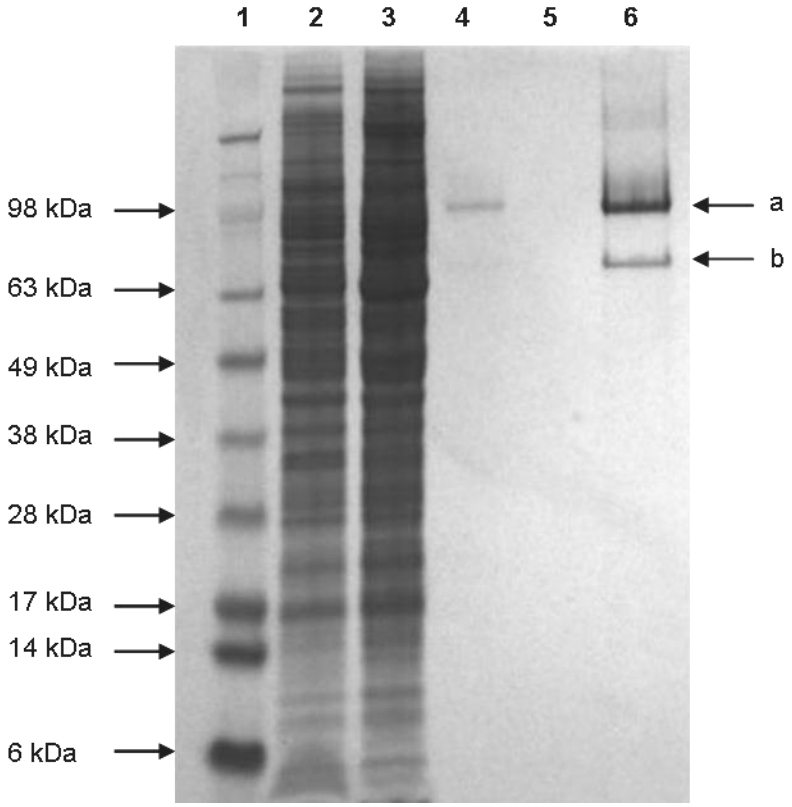

Figure 4-13 Affinity purification using modified lysis buffer

4-12% colloidal coomassie-stained SDS-PAGE loaded with TAP-purified proteins. Approximately 6 x10^{7}cells were used. Lane 1: protein ladder, lane 2 whole lysate (2µl loaded), lane 3: SBP-wash (2µl loaded), lane 4: SBP-eluate (20µl loaded), lane 5: CBP-wash (20µl loaded), lane 6: final eluate (all loaded after TCA precipitation).

Figure 4-13 proves that the new lysis conditions worked well in conjunction with the purification kit and a distinct band around 100kDa plus one smaller band were visible in the finale eluate. Both bands were excised with a clean scalpel and sent for MS-identification.

Table 4-4 MS-analysis of TAP-purified, co-eluted proteins using modified lysis conditions

band	identified as	e-score	protein score (significance)	queries matched/total nr of queries	mass tolerance (+/- ppm)
a	NDST1	1e -26	325 (>78)	44/83	55
b	HSP 70 precursor	3e -13	177 (>64)	16/25	50

The band around 100kDa was identified as NDST1 (Table 4-4), which proved that the new lysis buffer worked in conjunction with the purification kit (representation of NDST1 MS peptide mass fingerprinting analysis can be found in the appendix 8.3). The second band was identified as a precursor of HSP70. Heat shock proteins have been found as common contaminants in almost every purification reported and therefore have to be accepted with reservation (Gavin et al., 2002, Shevchenko et al., 2002).

The protein score is -10*Log (P), where P is the probability that the match observed is random and the e-value corresponds to the number of times one would expect this score by chance alone therefore making high p-scores and low e-scores desirable.

4.3.2.2.3 Purification using optimised lysis conditions and increased cell number

Having shown that the system works in principle and NDST1 can be purified by this technique, the next step was to increase the cell number, as apart from HSP70 no other proteins were co-eluted together with NDST1 from the resin.

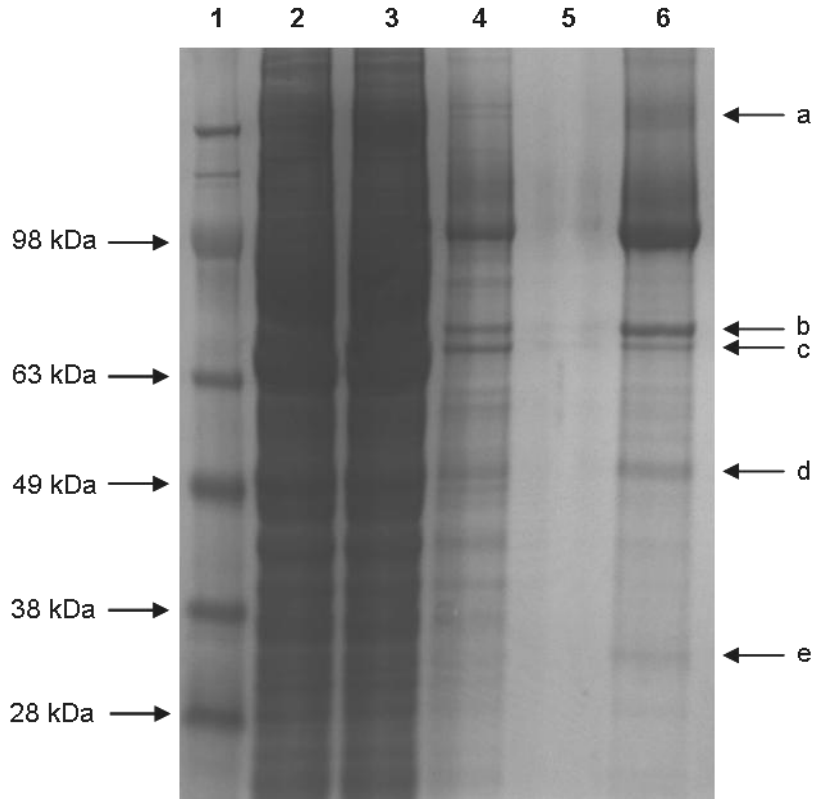

Figure 4-14 Affinity purification using optimised lysis buffer and increased cell number

4-12% colloidal coomassie-stained SDS-PAGE loaded with TAP-purified proteins. Approximately 1.2 x10^{8}cells were used. Lane 1: protein ladder, lane 2: whole lysate (2µl loaded), lane 3: SBP-wash (2µl loaded), lane 4: SBP-eluate (20µl loaded), lane 5: CBP-wash (20µl loaded), lane 6: final eluate (all loaded after TCA precipitation).

Approximately 1.2 x 10^8cells were used for purification and the resins for purification were pooled. With increased cell number, more proteins were co-eluted with NDST1 from the resin. Figure 4-14 shows five distinct lanes which were excised as indicated (a-e) and identified by MS analysis (Table 4-5).

Table 4-5 MS-analysis of TAP-purified, co-eluted proteins using increased cell number

band	identified as	e-score	protein score (significance)	queries matched/total nr of queries	mass tolerance (+/- ppm)
a	NDST1	6.52 -16	217 (>78)	29/52	100
b	Hsp 70 precursor	8.1e -06	116 (>78)	17/48	100
c	Hsp 70 precursor	0.0002	102 (>78)	16/50	100
d	Beta-tubulin	1.2e -15	201 (>64)	28/48	50
e	ADP-ATP translocase	0.0017	93 (>78)	12/46	100

Using increased number of cells a band was detected above the 100kDa band of NDST1. This was later identified as NDST1 by MS analysis. This could mean that proteins were not fully denatured when loaded onto the PAGE and NDST1 is still in complex with a protein binding partner, therefore appearing at a higher molecular weight. Similar to the first purification, heat shock proteins were identified.

Beta tubulin was also co-eluted. This is interesting, as NDST2 has been reported to interact with beta tubulin in mice (Ledin et al., 2006). The last protein to be identified in this mixture was ADP-ATP translocase.

4.3.2.2.4 Purification using optimised lysis conditions and optimised cell number

After optimising lysis conditions and cell number, a control transfectant (C7) was used along with transfectant F15 for purification. The control transfectant was created by transfecting HEK 293 cells with an empty pCTAP vector (not carrying the NDST1 insert). This is important, as this control helps to discriminate between specific binding partners of NDST1 and proteins, which eventually stick to the streptavidin binding peptide or the calmodulin binding peptide on its own. This seemed to be an appropriate control and of more

informative value than a mock transfectant for instance. Figure 4-15 shows the pattern of eluted proteins of F15 and control cells.

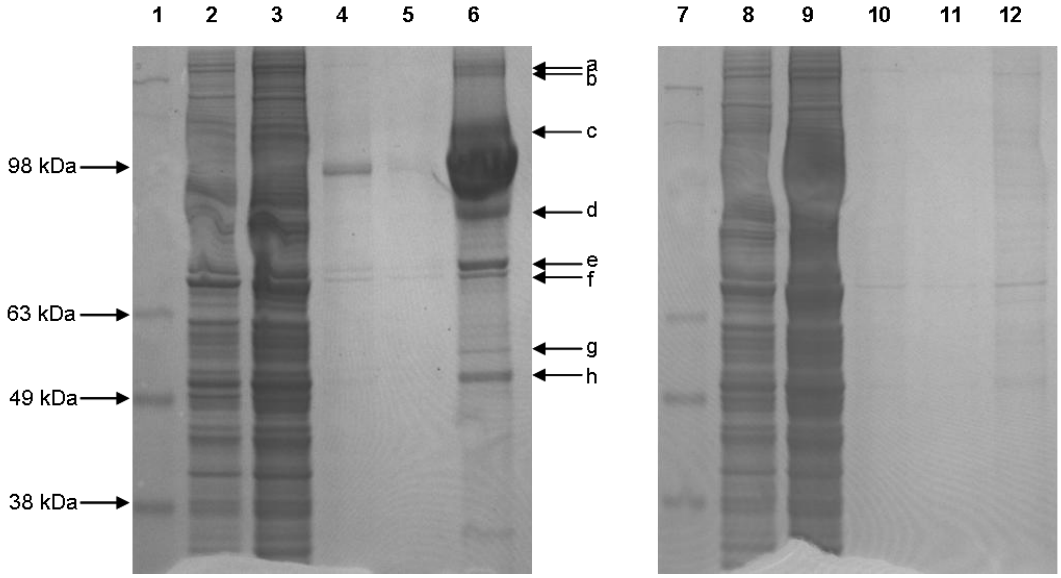

Figure 4-15 Affinity purification using optimised conditions of NDST1-pCTAP and control

4-12% colloidal coomassie-stained SDS-PAGE loaded with TAP-purified proteins. Approximately 1.2 x10^8 cells were used. Lanes 2-6 were loaded with proteins from NDST1-pCTAP clone 15, whereas lanes 7-12 were loaded with proteins from vector control clone 7.
Lane 1: protein ladder, lane 2: whole lysate (0.5µl loaded), lane 3: SBP-wash(1µl loaded), lane 4: SBP-eluate (20µl loaded), lane 5: CBP-wash (20µl loaded), lane 6: final eluate (all loaded after TCA precipitation), lane 7: protein ladder, lane 8 whole lysate (0.5µl loaded), lane 9: SBP-wash (0.5µl loaded), lane 10: SBP-eluate (20µl loaded), lane 11: CBP-wash(20µl loaded), lane 12: final eluate (all loaded after TCA precipitation).

Both clones, transfectant F15 and control transfectant C7, were grown in parallel under the same conditions and the same number of cells was used for cell lysis and subsequent purification. When the patterns of the two SDS-PAGEs (Figure 4-15) are compared, a lack of the 100kDa band corresponding to NDST1 in the control can be observed. Hardly any bands, apart from one around 70kDa, probably representing a heat shock protein, can be detected in the control purification.
Eight bands from transfectant F15 were excised and sent for MS identification (Table 4-6).

Table 4-6 MS-analysis of TAP-purified, co-eluted proteins using optimised conditions

band	identified as	e-score	protein score (significance)	queries matched/total nr of queries	mass tolerance (+/- ppm)
a	NDST1	4.1e-18	239 (>78)	22/27	100
b	NDST1	2e-18	242 (>78)	22/28	50
c	NDST1	6.5e-12	177 (>78)	17/23	50
d	NDST1	1e-18	239 (>78)	21/25	50
e	HSP70 precursor	0.0089	62 (>64)	8/18	80
f	HSP70 precursor	1.3e-8	144 (>78)	12/23	20
g	ATP synthase subunit + NDST1	8.1e-11	166 (>78)	17/20	50
h	Beta tubulin	9.3e-22	262 (>64)	25/30	50

Surprisingly, NDST1 peptides were detected in five out of the eight samples. Three were of a higher molecular weight than NDST1 whereas two migrated below NDST1. For the higher molecular weight samples, this could again mean that NDST1 is still in complex with other proteins which were not fully denatured before loading onto the PAGE. However, this cannot fully explain the existence of the smaller bands. Maybe they are remains of proteins complexes which have been partially degraded. In one case NDST1 was found as a mixture with a subunit of the ATP synthase. Beta tubulin was again identified by MS.

4.3.2.2.5 Purification using optimised lysis conditions and cell number under stringent denaturation conditions

Further alterations were introduced to the standard protocol for the last purification. The cell number was increased to 1.5 x 10^8 cells and resins for

purification were pooled. Additionally, the washing steps were doubled (4 instead of 2 five minute washes) at each individual step of the purification.
In an attempt to dissolve the higher molecular weight bands more stringent denaturation conditions were chosen. After the purification, protein lysates were boiled for 30 minutes in 4 x loading buffer supplemented with 2% LDS (lithium dodecyl sulphate) and ß-mercaptoethanol as a reducing agent. Figure 4-16 reveals a similar protein elution profile compared to the previous one.

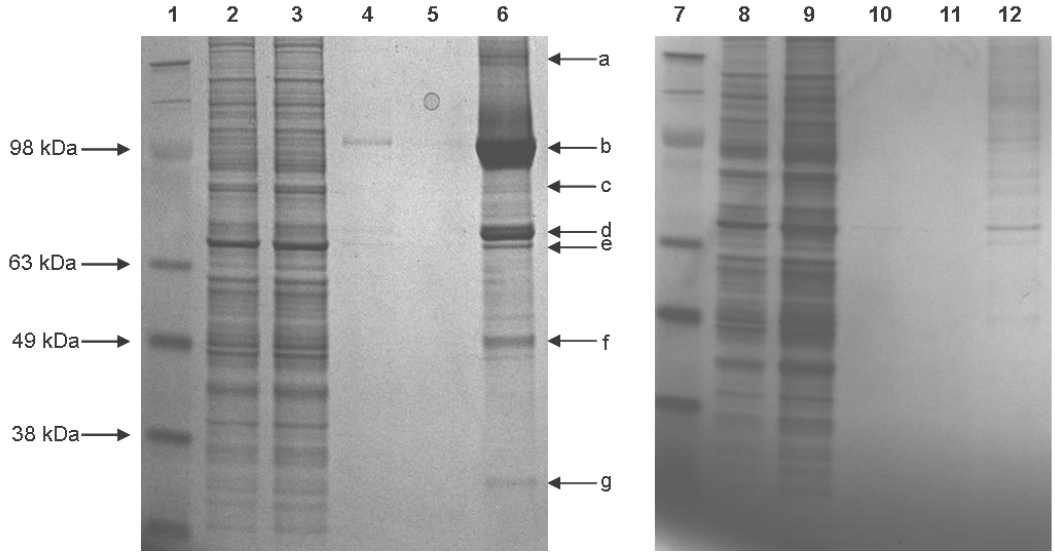

Figure 4-16 Affinity purification under stringent denaturation conditions

4-12% colloidal coomassie-stained SDS-PAGE loaded with TAP-purified proteins. Approximately 1.5 x10^8 cells were used. Lanes 2-6 were loaded with proteins from NDST1-pCTAP clone 15, whereas lanes 9-12 were loaded with proteins from vector control clone 7. Prior to loading protein samples they were denatured in 4xNU-PAGE sample buffer containing 2% LDS and β-mercaptoethanol by boiling for 30 minutes.
Lane 1: protein ladder, lane 2: whole lysate (0.5µl loaded), lane 3: SBP-wash (1µl loaded), lane 4: SBP-eluate (20µl loaded), lane 5: CBP-wash (20µl loaded), lane 6: final eluate (all loaded after TCA precipitation), lane 7: protein ladder, lane 8 whole lysate (0.5µl loaded), lane 9: SBP-wash (0.5µl loaded), lane 10: SBP-eluate (20µl loaded), lane 11: CBP-wash (20µl loaded), lane 12: final eluate(all loaded after TCA precipitation).

The control lacked the 100kDa band indicative for NDST1 and did not show too many distinct protein bands apart from the ~70kDa band (most likely to be a member of the HSP superfamily). Six unknown bands plus the 100kDa NDST1 band were sent for MS analysis. Despite the harsh denaturation conditions higher as well as lower molecular weight bands were identified as NDST1

(Table 4-7). Members of the HSP70 superfamily were found on their own (HSP70 and BiP) and in conjunction with NDST1. Additionally, beta tubulin was detected again in the protein preparation.

Table 4-7 MS-analysis of TAP-purified, co-eluted proteins under stringent conditions

band	identified as	e-score	protein score (significance)	queries matched/total nr of queries	mass tolerance (+/- ppm)
A	NDST1	7e-21	255 (>66)	30/45	100
B	NDST1	1.8e-13	181 (>66)	27/66	100
C	BiP	64.4e-20	247 (>66)	29/44	100
D	HSP70	3.5e-18	230 (>66)	27/36	100
E	HSP70 and NDST1	1.4e-27	322 (>66)	42/64	100
F	Beta tubulin	5.6e-25	269 (>78)	27/43	100
G	Non-specific	-	-	-	-

Beta tubulin and NDST1 were the only two proteins which were found consistently in all the protein preparations with reliable p- and e-scores. Figures 4-17 and 4-18 illustrate typical protein sequence alignments used to identify proteins in this study using Mascot software, a sample of Mascot data analysis can be found in the appendix.

1 MPALACLRRL CRHVSPQAVL FLLFIFCLFS VFISAYYLYG WKRGLEPSAD
51 APEPDCGDPP PVAPSR**LLPL KPVQAATPSR** TDPLVLVFVE SLYSQLGQEV
101 VAILESSRFK YRTEIAPGKG DMPTLTDKGR GRFALIIYEN ILK**YVNLDAW**
151 **NR**ELLDKYCV AYGVGIIGFF KANENSLLSA QLK**GFPLFLH SNLGLK**DCSI
201 NPK**SPLLYVT RPSEVEK**GVL PGEDWTVFQS NHSTYEPVLL AKTR**SSESIP**
251 **HLGADAGLHA ALHATVVQDL GLHDGIQRVL FGNNLNFWLH KLVFVDAVAF**
301 **LTGKR**LSLPL DRYILVDIDD IFVGKEGTRM KVEDVK**ALFD TQNELR**AHIP
351 NFTFNLGYSG K**FFHTGTNAE DAGDDLLLSY VK**EFWWFPHM WSHMQPHLFH
401 NQSVLAEQMA LNKKFAVEHG IPTDMGYAVA PHHSGVYPVH VQLYEAWK**QV**
451 **WSIRVTSTEE YPHLKPAR**YR **RGFIHNGIMV LPR**QTCGLFT HTIFYNEYPG
501 GSSELDKIIN GGELFLTVLL NPISIFMTHL SNYGNDRLGL YTFKHLVR**FL**
551 **HSWTNLRLQT LPPVQLAQK**Y FQIFSEEKDP LWQDPCEDKR HKDIWSKEKT
601 CDRFPKLLII GPQKTGTTAL YLFLGMHPDL SSNYPSSETF EEIQFFNGHN
651 YHKGIDWYME FFPIPSNTTS DFYFEK**SANY FDSEVAPR**RA AALLPKAK**VL**
701 **TILINPADRA YSWYQHQR**AH DDPVALK**YTF HEVITAGSDA SSK**LRALQNR
751 CLVPGWYATH IER**WLSAYHA NQILVLDGK**L LRTEPAKVMD MVQK**FLGVTN**
801 **TIDYHK**TLAF DPK**KGFWCQL LEGGK**TKCLG KSKGR**KYPEM DLDSRAFLKD**
851 **YYR**DHNIELS KLLYK**MGQTL PTWLR**EDLQN TR

Figure 4-17 Sequence alignment of NDST1 peptide mass fingerprinting

Matching peptides highlighted in red.

1 MREIVHLQAG QCGNQIGAKF WEVISDEHGI DPTGTYHGDS DLQLERINVY
51 YNEATGGKYV PR**AVLVDLEP GTMDSVRSGP FGQIFRPDNF VFGQSGAGNN**
101 **WAKGHYTEGA ELVDSVLDVV R**KEAESCDCL QGFQLTHSLG GGTGSGMGTL
151 LISKIREEYP DRIMNTFSVV PSPKVSDTVV EPYNATLSVH QLVENTDETY
201 CIDNEALYDI CFRTLK**LTTP TYGDLNHLVS ATMSGVTTCL RFPGQLNADL**
251 **R**K**LAVNMVPF PRLHFFMPGF APLTSR**GSQQ YR**ALTVPELT QQMFDAK**NMM
301 AACDPRHGR**Y LTVAAVFR**GR MSMKEVDEQM LNVQNK**NSSY FVEWIPNNVK**
351 TAVCDIPPRG LKMSATFIGN STAIQELFKR **ISEQFTAMFR** RKAFLHWYTG
401 EGMDEMEFTE AESNMNDLVS EYQQYQDATA EEEGEFEEEA EEEVA

Figure 4-18 Sequence alignment of beta tubulin peptie mass fingerprinting

Matching peptides highlighted in red.

Thus, beta tubulin was regarded as the only possible specific interacting protein found in this study as it appeared consistently in all purifications with extremely low e-values.

4.4 Discussion

HSPGs regulate a huge variety of functions, both during embryonic development and adult (patho-) physiology. As a multitude of proteins and biomolecules rely on HSPGs to exert their function, HSPGs have become a major therapeutic target.

Different approaches have been made to modulate HS biology. Targets could be directly activated or inactivated with glycomimetics, as shown for PI-88, an inhibitor of heparanase (Khachigian and Parish, 2004), which currently is in use in clinical trials for various cancers based on its anti-angiogenic properties by inhibiting VEGF and FGF stimulated tumour angiogenesis (Khachigian and Parish, 2004, Liu et al., 2009). Furthermore these glycomimetics could be used as competitive ligands, thus preventing 'specific' protein-HS interaction.

In theory, HS could be prevented from activating specific inflammatory molecules, such as cytokines and chemokines, by blocking with monoclonal antibodies. However, efforts in that direction have failed so far, which could be due to the fact that HS is hardly immunogenic and antibodies are very difficult to raise. An exception are the phage display derived anti-HS antibodies (Jenniskens et al., 2000, van Kuppevelt et al., 1998, van Kuppevelt et al., 2001), but these are not at a therapeutic stage yet.

A more generic approach would be the inhibition/modulation of HS biosynthesis by targeting the sulphotransferases, hence affecting HS sulphation. Targeting HS biosynthesis for therapeutic intervention relies on understanding the biosynthesis. So far, not much is known about the regulatory network. A few research groups have demonstrated that HS biosynthetic enzymes are under transcriptional control. In various experiments it was shown that under inflammatory conditions NDST1 expression increases significantly (Carter et al., 2003, Krenn et al., 2008, Rops et al., 2008).

Translational control of NDST enzymes was proposed by Esko and co-workers. They identified unusually long 5'-Untranslated Regions (5'UTR) with embedded Internal Ribosome Entry Sites (IRES), allowing regulation at the level of translation (Grobe and Esko, 2002).

The GAGosome model, which was introduced recently, describes the formation of an enzyme complex where concentrations of individual enzymes and their

affinity for each other decides which isoform gets incorporated into the complex. This formation would rely on protein-protein interactions, of which a few have been discovered so far (for example xylosyltransferase and galactosyltransferase (Schwartz et al., 1974); EXT1 and EXT2 (Munro, 1998); C5 epimerase and 2-O-sulphotransferase (Pinhal et al., 2001); EXT2 and NDST1 (Presto et al., 2008).

In order to further our understanding of the regulation of HS biosynthesis, it was decided to investigate biosynthetic enzyme regulation at the protein level. NDST1 was chosen as it is thought to be the key enzyme in HS biosynthesis.
A number of experimental procedures to study protein-protein interaction are available, all with their individual advantages and disadvantages. The yeast two-hybrid system is based on gene activation by a transcription factor. A transcription factor can be separated into an activating (AD) and a DNA binding domain (DBD). If proteins are tested for their interaction, one is fused to the activating domain (AD) and the other one to the DBD. Only if the two proteins interact the reporter gene can be transcribed. The advantages of this system are that many proteins can be tested for interaction and yeast is an easy model to use. However, as this system is based on the transcription of a gene, the proteins studied have to be soluble and targeted to the nucleus, which makes it unsuitable for membrane proteins Another disadvantage is that it only produces binary interactions. In addition, the protein interaction may depend on post-translational modifications which might not occur in the heterologous yeast environment (Bruckner et al., 2009).
Another method of studying protein-protein interaction is Co-Immunoprecipitation (Co-IP). This is a purification procedure where an antibody is directed against a specific protein and any proteins that interact with the first protein can be precipitated out of the solution and identified by Western Blotting. The advantage of this system is that it is independent of cloning (which can be time consuming) and physiological, as it is not dependent on overexpression of a protein but works on the endogenous level. The disadvantage is the availability and quality of specific antibodies. Other problems are antibody bleeding, where the heavy and the light chains of the protein A/G, which is used

as a substrate, are obscuring the bands of interacting proteins during electrophoresis.

The TAP-system was chosen for this study as it allows the purification of protein complexes under native conditions. Also, the proteins eluted are very pure as two consecutive affinity tags are employed which strongly reduce the background. An advantage is also the possibility to gain complex composition data and that the existence of specific antibodies is not vital. The technique has been successfully adopted for the use in mammalian systems and a variety of tag-combinations has been employed (Burckstummer et al., 2006, Knuesel et al., 2003), with the combination of CBP and SBP being the only commercially available at this time.

On the downside, the tag itself can hinder or even prevent protein-protein interactions and the tagged protein competes with the endogenous, untagged form.

NDST1 is a bifunctional enzyme, with its N-deacetylase activity located at the N-terminus and its N-sulphotransferase activity at the C-terminus. As N-deacetylation is a prerequisite for N-sulphation it was decided to place the TAP-tag at the C-terminal end of NDST1. At this point it could not be excluded that the tag itself could impair the viability/stability or function of the protein. A different problem arose from the fact that the pCTAP vector did not offer any singular site for linearization. Linearization is important, as it hugely increases the integration efficiency into the host genome which is desirable for the creation of stable transfectants. Generation of stable transfectants was essential as cell numbers necessary for TAP (starting with 6×10^7 cells) would not be reached with serial transient transfections. The only linearization site available overlapped with the SV40-polyA signal by a single base, which is important for protein stability, but was used anyway due to the absence of an alternative. Western blotting experiments revealed that NDST1 was expressed by HEK 293 transfectants despite the C-terminal tag and linearization. Before the cells with the tagged NDST1 were used for TAP, an additional experiment was carried out to investigate the formation of a protein complex by chemical crosslinking. The intention was to incubate the cells overexpressing NDST1 in the presence of a chemical crosslinker, which would then crosslink the proteins

interacting with each other at the time. Formaldehyde and DST were chosen as they are membrane permeable and have been reported to work in similar settings (Vasilescu et al., 2004). Complex formation would have been detected by a shift towards higher molecular weight on the Western blot when probed with NDST1 antibody. However, no such shift was observed. This could be due to the number and availability of lysine residues, which are responsible for bond formation and maybe due to the existence of the tag itself, which could obstruct binding site(s).

In the first TAP experiment cell number and lysis conditions were examined. As the system has been developed for cytoplasmic proteins, a few changes had to be introduced to optimise it for NDST1, a non-soluble protein in the Golgi compartment with one transmembrane domain. In order to not alter the conditions specified by the kit too much, the original lysis buffer was adjusted from 0.1 to 1% detergent, namely nonidet NP40. As a result no NDST1 was purified at all. No distinct protein lanes were visible in the final eluate on the stained SDS-PAGE after purification. As the company did not reveal the composition of the lysis buffer new lysis conditions had to be developed.
A basic lysis buffer consisting of 50mM Tris, 150mM NaCl, 10mM Na_3VO_4 and 1%NP40 based on the method originally developed by Puig (Puig et al., 2001) was applied for the next purification. With these conditions the system seemed to work in principle as two distinct bands with high p- and low e-scores were detected. The band around 100kDa was identified as NDST1 and the second one around 70 kDa as heat shock protein 70 precursor by mass spectrometry. With cell lysis conditions resolved the cell number was adjusted from 6×10^7 to 1.2×10^8 cells for the next purification. With increased cell number, more bands were visible on the SDS-PAGE. In addition to the previously found HSP a second HSP appeared. A band was detected above the 100kDa band of NDST1, which was later identified as NDST1 by MS analysis. Beta tubulin and ADP-ATP translocase were also identified within the co-eluted proteins. Up to this point any results had to be accepted with reservations, as no appropriate controls were included. Based on the conditions optimized in the initial two purifications the next TAP was conducted with a control run in parallel. The control cells were transfected with the pCTAP vector alone without NDST1

insert. This control provides information about non-specific protein binding due to affinity for the tags rather than the protein expressed. An additional control could be a mock transfectant or cells previously transfected with an unrelated protein.

The control was run alongside the actual purification and revealed that the protein band pattern was distinct and hardly any proteins were purified in the control settings. Again, bands above the 100kDa size of NDST1 were detectable and identified as NDST1. This could be due to complex formation which survived the brief denaturation step before loading onto the gel. Complexes could be NDST1 plus interacting partners or maybe NDST1 in a dimeric/oligomeric form. The existence of NDST1 homo-oligomers has not been reported, but at the same time could not be excluded.

The last purification was performed under stringent denaturation conditions with extensive boiling in 4 x loading buffer supplemented with LDS and beta-mercaptoethanol. The cell number was again increased to 1.5 x 10^8 and purifications were pooled. Unfortunately, bands above 100kDa were still detected as NDST1. It appears that conditions were not harsh enough to break up the protein complexes.

As beta tubulin was the only protein found throughout all purifications with consistent high p- and low e-values, it is considered the most likely genuine interaction partner of NDST1. Beta tubulin together with alpha tubulin represents the functional unit of microtubules responsible for the structure and function of the Golgi complex (Thyberg and Moskalewski, 1999). These microtubules play a crucial role in transportation of newly synthesized proteins from the ER to the Golgi. Validation of this interaction was attempted using Co-IP. Unfortunately the Co-IP failed to work, which is most likely due to the unavailability of good quality antibodies against NDST1. If specific antibodies of good quality were available, Co-IP experiments could be carried out with NDST1 as ‘fishing’ antibody. If beta tubulin was found as the interacting partner again, a reciprocal Co-IP with the antibody against the interacting protein as fishing antibody could confirm the results.

FRET (Förster resonance energy transfer) would be another method of investigating protein-protein interaction. Confocal microscopy would be able to determine if the fluorescence signals overlap, thus proving protein interaction.

To avoid the dependence on antibodies of poor quality the two proteins of interest could be labelled with fluorescent dyes. This, however, would again involve lengthy cloning procedures.

Interestingly, two more glycosylation enzymes have been reported to interact with beta tubulin, namely NDST2 (Ledin et al., 2006) and β-1,4-galactosyltransferase (Yamaguchi and Fukuda, 1995). This could possibly indicate a role in Golgi transport, with tubulin acting as some kind of receptor for the type-II-transmembrane glycosylation enzymes which do not possess a Golgi retention signal, thereby regulating their rate of transport.

5 Modulation of NDST1 and cell surface Heparan Sulphate

5.1 Introduction

5.1.1 Diversity of HSPGs

HSPGs are expressed abundantly and ubiquitously in a tissue- and development-specific manner at the cell surface and in the ECM of all mammalian cells. They are involved in the regulation of a range of biological processes, including inflammation (Bernfield et al., 1999, Parish, 2006). Distinct HS epitopes are created during biosynthesis which in turn determine the interaction profile of HS with its protein ligands. Modification includes N-deaceylation and N-sulphation of the N-acetylglucosamine, C5-epimerzation of the glucuronic acid and various O-sulphations at positions C2, C3 and C6 of the chain. In addition, the chain can be even further modified by the action of the endoglucuronidase heparanase, which cleaves the chain at specific sites and 6-O-endosulphtases, which remove 6-O-sulphate groups (Bishop et al., 2007). Overall, the interplay of different enzymes involved gives rise to an extraordinary structural diversity of the molecule. How this complex biosynthetic machinery is regulated is still poorly understood.

5.1.2 Differential regulation of HS biosynthesis

Different levels of control have been suggested for HS biosynthesis, including control at the transcriptional and translational level as well as regulation of HS biosynthesis controlled by the interaction of individual enzymes based on their affinities for each other (see section 4.1.1 and 4.1.2)

Changes of HS composition in response to exogenous stimuli have been reported by various research groups. In most models, the inflammatory response was mimicked by stimulation of endothelial cells with proinflammatory cytokines. Activation of mouse glomerular endothelial cells with TNFα or IL-1ß resulted in upregulation of several core proteins and sulphation specific antibodies revealed increased N- and O-sulphation in conjunction with upregulation of corresponding HS biosynthetic enzymes (namely NDST1 and 2

and 6-OST-1 and 2). The addition of antibodies that recognise the N- and O-sulphated regions in an *in vitro* dynamic flow leukocyte adhesion assay caused increased rolling velocity and decreased numbers of adhering cells (Rops et al., 2008). These observations are in agreement with previous studies where increased levels of NDST1 and N-sulphation after stimulation of HMEC-1 cells with proinflammatory cytokines were reported (Carter et al., 2003).

5.1.3 Interaction of HS with protein ligands

Although the importance of overall sulphation is unquestionable, the existence of specific binding sites has not been demonstrated yet with the exception of the antithrombin III binding domain. There is dispute if selective domain spacing and distribution rather than individually tailored sequences are responsible for complex formation (Kreuger et al., 2006). It seems likely that individual interactions can be either granted by specific and rare modifications (such as 3-O-sulphation for ATIII) or by the spatial arrangement of common modifications (such as N- and O-sulphation for FGF2).

5.1.3.1 L-Selectin

L-selectin is a cell adhesion molecule which is involved in lymphocytes homing in high endothelial venules (HEVs) and leukocyte migration under inflammatory conditions. It is a type I transmembrane glycoprotein and consists of a N-terminal lectin-like domain, an epidermal growth factor (EGF)-like domain, a variable number of consensus repeats and a single membrane domain with a short cytoplasmatic tail (Barthel et al., 2007). It binds to a range of sialomucins, with sulphation being an important factor for ligand binding (Imai et al., 1993). An endothelial specific NDST1 knockout in mice led to the discovery of endothelial HS as L-selectin ligand (Wang et al., 2005) and collagen XVIII was identified as a ligand in the kidney (Celie et al., 2005). Binding of L-selectin to HS was shown to be dependent on chain length, 2-O-, 6-O- and N-sulphation and iduronic acid proved to be inhibitory (Celie et al., 2005, Kawashima et al., 2003).

5.1.3.2 CCL5

CCL5 is a proinflammatory chemokine which binds to its receptors CCR1, 3, 4, and 5 and facilitates the migration of monocytes and activated T-cells (Murphy et al., 2000). Two clusters of basic amino acid residues, representing GAG-binding sites, have been identified, a BBXB motif in the 40s loop and a BBXXB motif in the 50s loop of the amino acid sequence, both of which contribute to the biological function of CCL5 *in vivo* (Proudfoot et al., 2001, Segerer et al., 2009). While the residues involved in the interaction on the chemokine site have been described extensively, little is known about the corresponding region of GAGs. However, N- and O-sulphation have been reported to be involved (Kuschert et al., 1999, Schenauer et al., 2007). Crystallization studies of CCL5 in the presence of differently modified heparin disaccharides demonstrated that N-sulphation is more important than 6-O-sulphation (Shaw et al., 2004). Apart from the sulphation status itself the spacing and the distribution of the groups involved will influence the binding.

CCL5 is presented by GAGs on the surface of the endothelium and GAG binding facilitates cooperative oligomerisation of the chemokine which is crucial for biological activity *in vivo* (Proudfoot et al., 2003). HS dp (degree of polymerization) 14 was recently identified as minimal oligosaccharide binding sequence (Rek et al., 2009). On the endothelium CCL5 directs inflammatory cells through the endothelial barrier into the tissue. It has been reported to be involved in a variety of inflammatory diseases, including renal allograft rejection (Ali et al., 2005a, Ruster et al., 2004) and chronic inflammatory liver disease (Goddard et al., 2001, Karlmark et al., 2008).

5.1.3.3 FGF2

Fibroblast growth factor 2 (FGF2) is a member of the FGF family and is produced by many cell types with a variety of biological functions. It acts as a mitogenic and angiogenic factor and is involved in tissue remodelling and regeneration. It can be secreted into the ECM where it can act in an autocrine or paracrine way via binding to its high affinity receptors FGFR1-4 (Okada-Ban et al., 2000). The formation of a ternary complex composed of FGF2, FGFR and HS is crucial for FGF2 signalling (Kan et al., 1993, Rapraeger et al., 1994).

The FGF2 binding motif of HS typically contains N-sulphation at the non-reducing end glucosamine, 2-O-sulphated iduronic acid and variable 6-O-sulphation on the reducing end glucosamine (Kreuger et al., 2001). The minimal FGF2 binding domain has been described as a tetrasaccharide which is not sulphated at the C6 position (Guglieri et al., 2008). 2-O-sulphation appears to be sufficient for binding but 6-O-sulphation is vital for receptor activation (Ornitz, 2000). These N- and O-sulphated groups are clustered in domains where the interaction with the ligand takes place and their abundance, length and overall sulphation seem to be more important than selective saccharide sequence. Together with FGF1, FGF2 appears to be more promiscuous in the HS binding requirements than other members of the FGF family (Allen and Rapraeger, 2003, Jastrebova et al., 2006).

5.1.4 Specific Aims

This part of the work aimed to investigate changes in cell surface HS expression after modulation of NDST1 expression, the key enzyme in HS biosynthesis. Further, changes in HS expression have been reported for inflammatory conditions. Therefore cell surface HS expression following experimental ischemia and inflammation and potential outcome of altered HS expression on ligand binding should be investigated. Specific goals:

Examination of transfectants following overexpression and silencing of NDST1:

- design and cloning of NDST1 silencing construct
- analysis of HS expression of NDST1 modulated cells
- physiological consequences of altered HS expression

Characterization of cell surface HS of cell lines following experimental inflammation:

- analysis of changes in HS expression of various cell lines upon hypoxia and proinflammatory stimulation with IFNγ and TNFα

- physiological consequences of altered HS expression

5.2 Specific Materials and Methods

5.2.1 Gene silencing technology

Silencing is a method to mediate specific suppression of gene expression. RNA interference is based on the introduction of double stranded RNA, which leads to a functional inactivation of the target gene. Its origin is believed to be a defence mechanism of plants against viral pathogens or uncontrolled transposon mobilization (Cerutti and Casas-Mollano, 2006).

The basic mechanism relies on a pair of custom made oligonucleotides that contains a unique 19bp long sequence that corresponds to a 19bp target sequence within the mRNA of interest. The dsRNA is subsequently processed into 21-25bp small interfering RNAs by an RNaseIII-like enzyme called Dicer. This siRNA is then incorporated into the RNA-induced-silencing-complex (RISC). Binding of the antisense strand of the processed siRNA duplex to the mRNA mediates cleveage of the molecule and inhibits target gene expression.

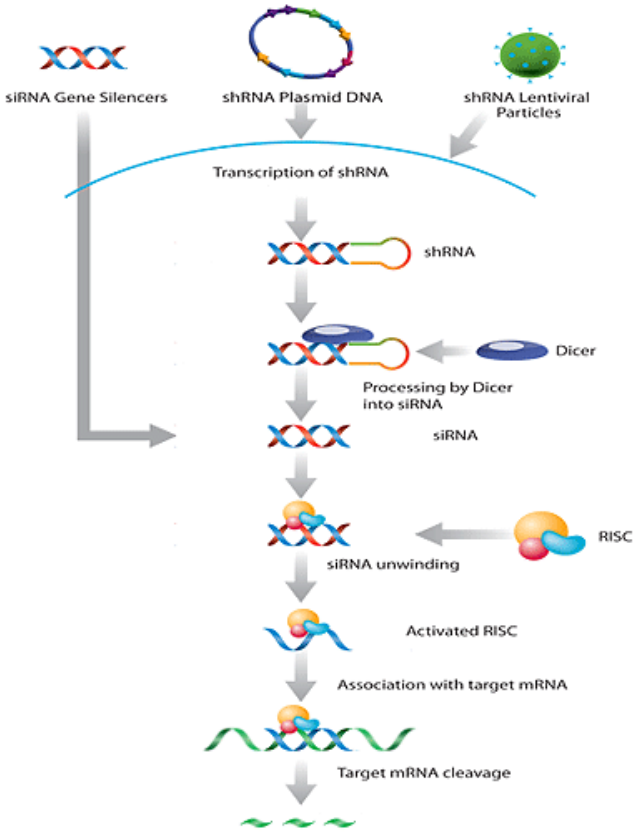

Figure 5-1 Principle mechanism of RNAi

(adapted from Santa Cruz www.scbt.com)

In this study the pSUPER.neo vector system (Oligoengine) was used (Figure 5-2).

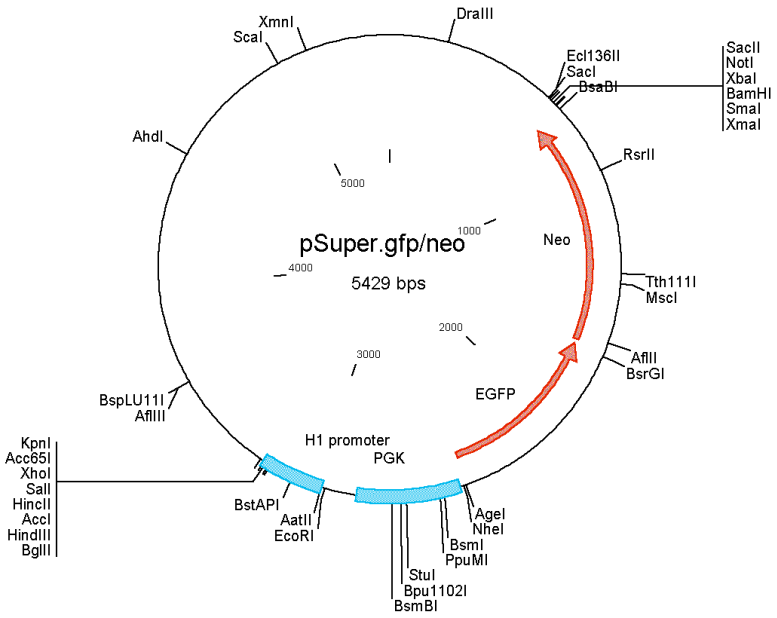

Figure 5-2 shRNA vector map of pSUPER.gfp-neo

In contrast to siRNA, which is administered to the cells directly and gets degraded quickly, the Oligoengine pSUPER systems directs intracellular synthesis of short hairpin RNAs (shRNA) driven by a vector, which allows stable suppression of gene expression.

Briefly, 3 µg of forward and reverse oligonucleotide containing the 19bp target sequence (5'GCCGCTTCAAATACCGCAC3', designed by a former member of the group) were annealed in annealing buffer (100mM NaCl and 50nM HEPES) (Sigma). The mixture was incubated at 90ºC for 4 minutes and then at 70ºC for 10 minutes. The annealed oligos were cooled slowly to 10ºC before using them in the ligation reaction. The vector was linearized before the ligation using *Bgl*II and *Hind*III restriction enzymes. After ligation of the oligonucleotides into the vector the construct was transformed into competent *E. coli*.

5.2.2 RNA isolation and cDNA generation

For mRNA isolation and cDNA generation the µMACS technology was used (Miltenyi). This kit was developed for the direct isolation of mRNA without prior preparation of total RNA. The isolation is achieved by adding Oligo(dT) MicroBeads to the cell lysates which bind to the polyA-tail of the mRNA. This

magnetically labelled mRNA can be easily separated from the rest of RNAs in the μMACS column and cDNA synthesis can follow subsequently.

In short, cells were harvested and a maximum number of 10^7 cells were lysed in 1ml of Lysis/Binding buffer. To avoid any clumps, lysate was sheared mechanically by passing the lysate several times through a 21G needle. The sheared lysate was applied on a LysateClear column and centrifuged for 3 minutes at 13.000 x g. 50μl of Oligo(dT) MicroBeads were added to the lysate. After rinsing the column with Lysis/Binding buffer the lysate was applied on the column. Magnetically labelled mRNA was retained in the column. For the removal of proteins and DNA, the column was rinsed twice with Lysis/Binding buffer. During the last four washing steps residual DNA and rRNA were removed.

For cDNA synthesis the column was rinsed with Equilabration/Wash buffer. After that the resuspended enzyme mixture was applied onto the column and the column was sealed with Sealing Solution to avoid evaporation. Following 1 hour of incubation at 42ºC the column was rinsed twice with Equilabration/Wash buffer. After an additional incubation step with cDNA Release Solution for 10 minutes at 42ºC, the synthesised cDNA was eluted with cDNA Elution buffer.

cDNA was quantified using a nanodrop system. All cDNAs showed a ratio of A260/280 equal or greater than 1.8.

5.2.3 Quantitative Real-Time PCR

Real-time PCR is an advanced form of conventional PCR which allows very sensitive and accurate measurement of gene expression. It quantifies the initial amount of the template specifically rather than measuring the endpoint.

Real-time PCR is based on the detection and quantification of a fluorescent signal, produced proportionally during the target amplification. By measuring the fluorescence at each cycle it is possible to examine the first significant increase in target amplification proportional to the initial amount of template.

In this study hydrolysis probes, such as TaqMan probes, were used. A TaqMan assay comprises of a set of specific primers and a probe. Wherever possible primers are designed exon spanning to minimise amplification of possible contaminating DNA. The probe anneals to the DNA in a region in between the

primer binding sites. The probe contains a fluorescent dye on its 5' end and a quencher on the 3' end. When the probe gets excited by irradiation the fluorescent dye transfers energy to the adjacent quencher dye. When the Taq polymerase amplifies the template DNA its 5' exonuclease activity cleaves the probe, resulting in a separation of the reporter and the quencher. The quencher is no longer active and the reporter dye can emit fluorescence. This fluorescence signal increases with every cycle proportional to the accumulation of template. In the first cycles of the reaction no significant increase in fluorescence can be observed. The threshold cycle (Ct) is defined as the fractional number of cycles where fluorescence increases beyond the fixed threshold (exceeds background fluorescence). This increase in fluorescence is based on the exponential growth of the amplicon within the log-linear phase. The higher the initial amount of template, the lower the Ct.

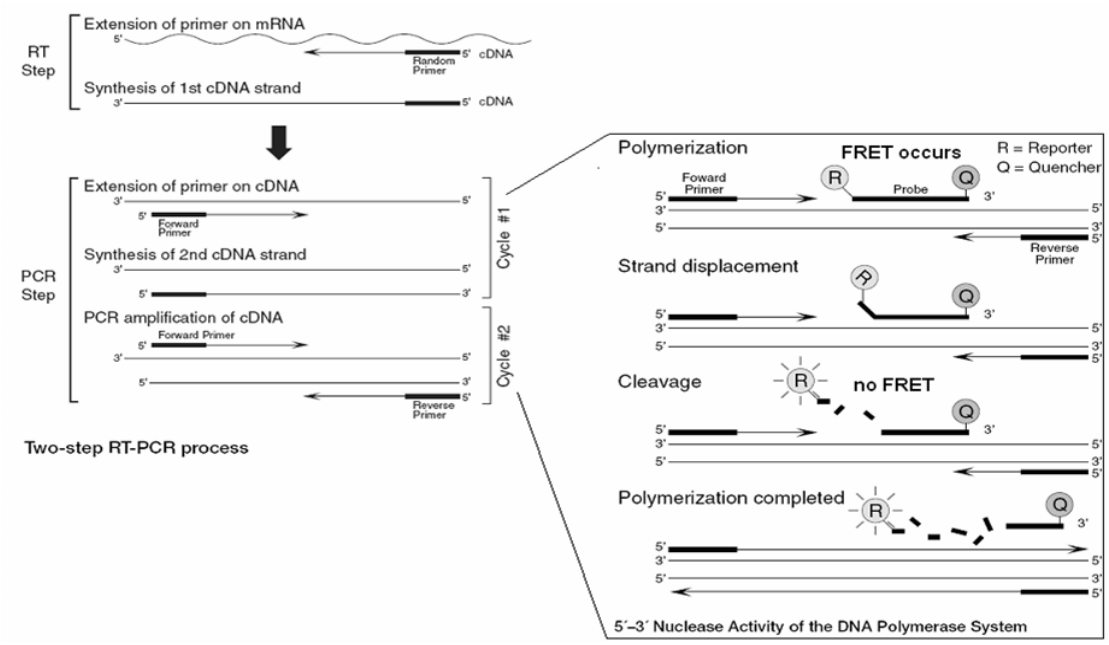

Figure 5-3 Principles of Real-Time PCR

(adapted from Applied Biosystems)

In this study primers and probe as well as the PCR mastermix were obtained from Applied Biosystems. Primers were exon spanning and the probe contained the 5' fluorescence probe FAM and the 3' quencher TAMRA. The concentrations of the primers and probes were 900nM and 250nM, respectively. The comparative Ct method (ΔΔCt) for relative quantitation of gene expression

was used. The level of gene expression of the gene of interest is normalised by including an endogenous control, which is usually a housekeeping gene such as β-actin (used in this study), GAPDH or tubulin.
A typical qRT-PCR reaction was set up as shown in Table 5-1:

Table 5-1 Composition of a typical qRT-PCR reaction

compound	**volume (µl)**
primers and probe	1
2x Mastermix	10
cDNA	2
H_20	7
final volume	20

Every time a qRT-PCR reaction was run a NTC (no template control) was performed in parallel.

The parameters of the qRT-PCR were as shown in Table 5-2:

Table 5-2 Temperature settings of a typial qRT-PCR reaction

temperature (degree ºC)	**time**	**cycles**
50	2 min	1
95	10 min	1
95	15 sec	40
60	1 sec	40
4	hold	-

The reaction was performed in an ABI Prism 7000 Sequence Detection System (Applied Biosystems). Data analysis was carried out using the ABI prism

software. As the comparative Ct method (ΔΔCt) was used the housekeeping gene β-actin served as a normalizer for expression of the gene of interest. Target gene expression can be calculated according to the following formula: relative expression = $2^{-\Delta\Delta Ct}$, where ΔΔCt = ΔCt target - ΔCt normaliser. In order to use the ΔΔCt method the efficiencies of the target gene and the reference control should be equal. This can be assessed by plotting ΔCt values against cDNA dilutions. A slope of -3.32 indicates 100% efficiency of the PCR reaction. In general efficiencies should be between 90 and 100% which equals to a slope between -3.6 and -3.1. (calculation: Eff = $10^{(-1/slope)} - 1$) (Livak and Schmittgen, 2001).

A different option for relative quantification without the need for calibration curves would be the mathematical model by Pfaffl, where the relative expression ratio is calculated from Real-time PCR efficiencies and the crossing point deviation of an unknown sample versus control (Pfaffl, 2001).

5.2.4 Immunocytochemistry

Immunocytochemistry is a technique used for antigen visualisation within the cell compound. To analyze differences in HS of wild type and NDST1 silenced cells immunofluorescent staining was utilized.

Cells were seeded on 4-chamber slides (Nunc) at 60.000 cells/chamber and grown under normal conditions for 48h. Cells were rinsed with cold PBS and fixed in 4% PFA for 25 minutes at RT. After two washes with PBS the chamber structure was removed from the slides and the chambers were circled with a hydrophobic marker. The cells were incubated in 5% BSA in PBS for 1h to minimize non-specific binding. Incubation with the primary antibody took place over night at 4ºC. After decanting the primary antibody (anti-HS antibody 10e4, 1/100, Seikagaku) slides were washed in 0.2% Tween 20 in PBS three times for 5 minutes. An additional wash step in PBS was carried out before incubation with the secondary (anti-mouse TRITC, 1/20, Dako) for one hour at room temperature. Three washing steps for 5 minutes in 0.2% Tween 20 in PBS were followed by washes in PBS for 5 minutes. The slides were then mounted wet in fluorescence mounting medium (DakoCytomation, DAKO) and stored in the dark at 4ºC.

To ascertain the levels of background fluorescence appropriate negative controls were carried out. These consisted of an unstained population of cells and cells stained with the secondary antibody only.

5.2.5 Flow cytometry

Flow cytometry is a technique to analyse suspensions of cell populations qualitatively and quantitatively. A range of different parameters such as cell size, cell-cycle status and expression of extra- as well as intracellular markers can be assessed. All flow cytometry experiments in this study were performed using a BD (Becton Dickinson) LSRII flow cytometer. Data were collected and analysed using FloJo Software.

5.2.5.1 Staining of cell surface antigens by FACS

Adherent cells were split using non-enzymatic cell dissociation media (Sigma). Cells in suspension were transferred into a FACS tube and following a washing step incubated with primary antibodies in 5%FCS/PBS for 45 minutes. All incubation steps were performed at 4ºC. After another two washing steps fluorescently labelled secondary antibodies were added and incubated for further 30 minutes. For the phage display antibodies, a tertiary fluorescently labelled antibody incubation step was necessary (anti-mouse-FITC, 1/100, Sigma, for further 30 minutes). Cells were resuspended in 200µl of 5%FCS/PBS and analysed using appropriate laser and filter settings (488nm emission, 530nm extinction for FITC). All flow cytometry data is expressed as mean fluorescent intensity (MFI).

Antibodies used in this study are listed in Table 5-3.

Table 5-3 Antibodies used in this study and their specific binding requirements

Antibody	Subtype	Target sequence	Dilution	Supplier	Secondary ab
10e4	Monoclonal Mouse IgM	GlcA-GlcNS-GlcA-GlcNAc	1/100	Seikagaku	Anti-mouse-FITC (1/100), Dako
HS3A8	Single chain phage display-derived	GlcNS6S-IdoA2S	1/6	Gift from Prof. Kuppevelt, Nijmengen, Netherlands	Anti-VSV-Cy3 (1/300), Sigma
HS4C3	Single chain phage display-derived	GlcNS3S6S-GlcA/Ido2S	1/6	Gift from Prof. Kuppevelt Nijmengen, Netherlands	Anti-VSV-Cy3 (1/300), Sigma

Abbreviations GlcA: glucuronate; GlcNac: N-acteylated-glucosamine; GlcNS: N-sulphated-glucosamine; IdoA: iduronate; 2,3,6S: 2,3,6 sulphate (Smits et al, 2006; Rops et al, 2008)

5.2.6 Chemotaxis assay

To compare the chemotactic potential of the biotinylated CCL5 to the wild type CCL5 a chemotaxis assay was employed. 3µm filter in corresponding 24 well plates (Falcon) were used for migration experiments. 800µl of RPMI 1640 medium supplemented with 0.1% BSA containing the desired concentrations of chemokine was added to the lower chamber. 500.000 THP-1 cells were resuspended in 200 µl of complete RPMI 1640 and added to the upper chamber. The filters were incubated at 37ºC and 5%CO_2 for 90 minutes. Before fixing and staining, the filters were wiped with a cotton bud to remove cells which have not migrated. Then the filters were fixed in methanol at -20ºC over night. After few washes with water the filters were stained with haematoxylin (Sigma) for 5 minutes. The stained filters were immersed for 10 minutes in

Scotts' Tap Water (166mM $MgSO_4$, 24mM $NaHCO_3$).They were then dehydrated through increasing concentrations of ethanol (50%, 75%, 90% and 100%). The filters were air dried and mounted onto glass-slides with DPX mountant (Fluka).

5.2.7 Adhesion assay

To compare the influence of HS expression on adhesion to L-selectin, a well known HS-binding molecule, a solid phase adhesion assay was developed. Flat bottomed 96-well ELISA plates were coated with 10µg/ml goat anti-human IgG Fc-antibody (Sigma) over night at 4°C. After two washes in PBS, L-selectin-Fc fusion protein (10µg/ml, R and D) was added in HBSS buffer (Sigma) for a further 18h at 4°C. Excess protein was washed twice with HBSS buffer and non-specific binding was blocked with 1% BSA in HBSS for 2 h. $1x10^6$ cells were labelled with 1.5 µM BCECF-AM (Sigma) for 20 min at 37°C in the dark. After washing twice in HBSS, $4x10^4$ cells were resuspended in HBSS and added to each well and plates were centrifuged at 80 x g for 2 minutes to allow cells to adhere. After 45 min of incubation at 37°C in the dark, fluorescence was measured with wavelengths set at 488 and 535nm using a plate fluorimeter (Fluostra Optima, BMG Labtech) . Following removal of non-adherent cells by mechanical oscillation, plates were carefully washed with HBSS and fluorescence readings were taken again.

5.2.8 ELISA

An enzyme linked immunosorbent assay was employed to quantify the amounts of chemokine eluted from the heparin column. Samples were incubated over night at 4ºC in coating buffer (15mM Na_2CO_3, 35mM $NaHCO_3$, ph 9.6; Sigma), allowing the proteins to adhere to the plate. After two washes with 0.05% Tween/PBS plates were blocked with 5%BSA/PBS for 1 hour. 100µl of primary antibody (anti-CCL5, R and D) made up in 0.5%BSA/PBS was added and incubated for 3 hours at RT. Plates were then washed again twice with 0.05% Tween/PBS before secondary antibody (anti-goat-HRP, 1/5000, Abcam) was added and incubated for 1h at RT. Plates were washed twice before being

incubated with substrate solution (Fast OPD, Sigma) for 30 minutes. Plates were read at 450nm using an Opsys MR plate reader (Dynex).

5.2.9 FPLC

To investigate if the addition of the biotin group to CCL5 would affect its ability to bind to heparin a heparin-sepharose column was used. 1µg of chemokine in 500µl of 10mM phosphate buffer was loaded onto a 1mlHiTrap heparin HP column (Amersham) which was linked to a FPLC system (Amersham). The chemokine was eluted from the column by the application of salt gradient (0-1M NaCl in phosphate buffer) at a flow rate of 1ml/minute in 30 fractions. 50µl of the eluent were used for ELISA.

5.2.10 Calcium Flux

In this study, CCL5 and CCL5-biotin were assessed for their ability to induce a calcium flux. Changes in calcium mobilization are considered a direct consequence of chemokine activity. This can be monitored by using calcium binding dyes, such as Indo-1-AM (Molecular probes). The acetyloxymethylester form is taken up by the cells passively, as it can permeate the cell membranes. Cell endogenous esterases hydrolyze the dye rendering the indo-1 form which is non-permeant. Indo-1 is excited by UV and changes in fluorescence refer to calcium bound (440nm) or calcium unbound (530nm) state. The ratio of these wavelengths indicates changes in intracellular calcium concentrations.
In this study, THP-1 cells were serum starved over night and 500.000 cells were resuspended in HBSS containing 1mM $CaCl_2$, 1mM $MgCl_2$ and 1% FCS. Cells were labelled with 3µg/ml Indo-1-AM for 45 minutes at RT in the dark. Following a washing step cells were resuspended in HBSS and warmed to 37ºC before taking the basal reading. Following stimulation with chemokine changes in flux were recorded before ionomycin (1mg/ml, Sigma) was added as a positive control. Calcium flux was analysed with LSRII flow cytometer.

5.2.11 Stimulation of cell lines

HEK 293, HK-2, HepG2 and HMEC-1 cells were grown to 80% confluency and stimulated with TNFα and IFNγ (100ng/ml each, Sigma) for 18h in full media before cell surface Heparan sulphate was analysed by flow cytometry. Due to the lack of an incubator with hypoxic conditions, hypoxia was mimicked by replacing vented caps of tissue flasks with unvented caps for the duration of 18h.

5.2.12 Binding assays

5.2.12.1 FGF2 binding assay

The binding of FGF2 has been investigated intensively and relies on the formation of a trimeric complex of FGF2, FGF2-receptor and HS. It has been shown recently that binding of FGF2 relies on the number of chains and their degree of sulphation. A Fluorokine FGF2 flow cytometry kit was used in this study (R and D).

In brief, cells were detached using cell dissociation media and after 2 washes in PBS 100.000 cells were mixed with FGF2 at a final concentration of 570ng/ml and incubated for 60 min at 4ºC. Avidin-FITC was added without prior wash to the cells and further incubated for 30 min at 4ºC. After two more washes cells were resuspended in 200µl of wash buffer and analysed by flow cytometry. As a negative control, cells were incubated with an unrelated biotinylated soybean protein. FGF2 binding was analysed with LSRII flow cytometer.

5.2.12.2 CCL5 binding assay

A chemokine binding assay similar to the FGF binding assay was developed to investigate the ability of differentially modified HS to retain chemokines on the surface of cells.

Biotinylated CCL5 (Almac) was added to a final concentration of 100ng/ml in PBS and cells were incubated for 60 min at 4ºC. Streptavidin-FITC (1/100, BD) was added without prior wash to the cells and further incubated for 30 min at

4ºC. After two more washes cells were resuspended in 200µl of wash buffer und analysed by flow cytometry. As a negative control cells were incubated with FACS buffer instead of chemokine solution. CCL5 binding was analysed with LSRII flow cytometer.

5.2.13 Statistical analysis

Student's t-test was used to compare data that followed the Gaussian distribution. A one-way Anova (analysis of variance) with Tukey's post test was used to compare the means of 3 or more independent groups and differences with $p<0.05$ were considered to be significant. Error bars represent the standard error of the mean (SEM).

5.3 Results

5.3.1 Silencing of NDST1

5.3.1.1 Cloning of the NDST1 silencing construct

In an attempt to suppress NDST1 expression and investigate its effect on HS expression, a NDST1 silencing construct was employed, which was designed by a former member of the group. The 19bp target sequence (5'GCCGCTTCAAATACCGCAC3') corresponding to exon 1 of the NDST1 mRNA was previously chosen according to the guidelines of the Oligoengine website.

The pSUPER silencing vector was linearized using *Bgl*II and *Hind*III restriction enzymes and after DNA purification the annealed oligonucleotides, flanked by corresponding restriction sites, were incorporated into the vector in a ligation reaction. The resulting construct was transformed into chemically competent *E. coli* and 3 colonies were isolated from ampicillin containing agar plates. Resistant clones were picked, propagated and isolated DNA was subjected to restriction digestion with *EcoR*I and *Xho*I in order to identify clones carrying the correct insert. DNA digests were run on a 2% agarose gel and fragment sizes were analysed. Positive clones comprised a fragment of 281bp, whereas false positive clones were expected to reveal a 248bp fragment (Figure 5-4).

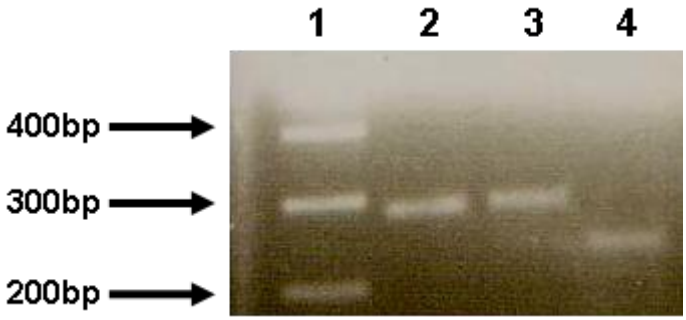

Figure 5-4 Cloning of NDST1silencing construct

Representative agarose gel of restriction digests of NDST1 silencing constructs. Lane 1 containing DNA hyperladder with fragment sizes as indicated. Lane 2 and 3 containing DNA fragments excised by EcoRI and XhoI restriction enzymes revealing positive clones carrying the insert. Lane 4 representing EcoRI and XhoI digested DNA fragment without the insert revealing a negative clone.

Plasmids revealing correctly sized fragments were sent for sequencing and after sequence verification used for further transfection experiments.

5.3.1.2 Transfection of HEK 293 cells with NDST1 silencing construct

Various DNA:Effectene ratios were used for transfection of HEK 293 cells without any significant effect on the efficiency. 50 transfectants were selected with 800µg/ml of G418 and kept under selection pressure (400µg/ml) whilst expanding. In total 7 clones survived the selection process.

5.3.1.3 Screening of NDST1 silenced clones by q-RT-PCR

The 7 remaining clones were assayed for NDST1 downregulation on the mRNA level using quantitative RT-PCR. cDNA was generated and ß-actin served as an internal control. To avoid amplification of eventually contaminating genomic DNA, exon spanning primers were selected. The expression of NDST1 mRNA derived from transfectants was calculated relative to the control (untransfected cells). Ideally, it would have been calculated relative to a mock transfectant, but unfortunately none of the mock transfectants survived the selection process.

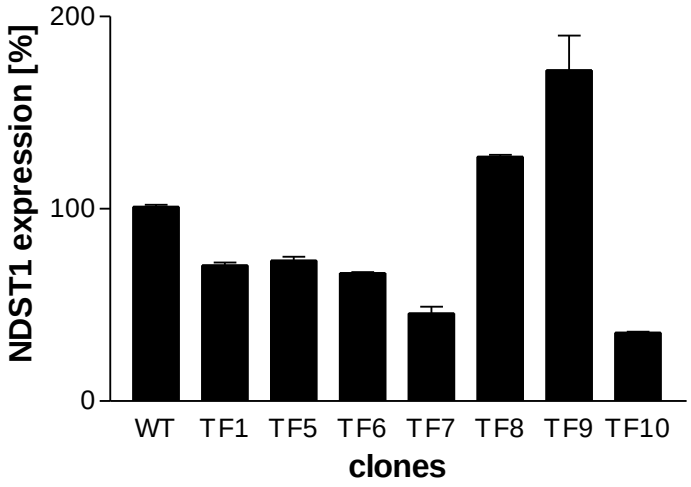

Figure 5-5 Relative expression of NDST1 mRNA of NDST1 silenced clones

NDST1 expression of HEK 293 wild type cells and stably silenced NDST1 transfectants was assessed by q-RT-PCR. NDST1 mRNA expression was normalized to the endogenous control ß-actin. Experiment was performed in triplicates.

The attempt to suppress NDST1 expression resulted in both up- and downregulation of NDST1 transcript (Figure 5-5) with transfectant 10 revealing the highest reduction by 64%.

5.3.1.4 Verification of NDST1 silencing by Western blotting

To ensure that the reduction of NDST1 mRNA is accompanied by a reduction on the protein level, Western blot analysis was carried out. This was of importance as mRNA levels do not always correlate with protein levels, especially when translational regulation, as suggested for NDST1, could be involved.

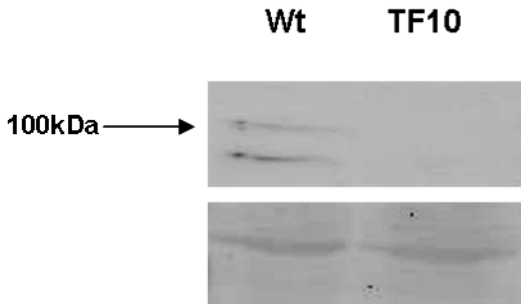

Figure 5-6 Western Blot analysis of wild type and NDST1 silenced clones

Western blot of wild type HEK 293 and NDST1 stably silenced cells (upper panel). 60µg of total cell lysates were used, blots were probed with α-NDST1 antibody (1/200) and HRP-conjugated anti-goat IgG (1/5000). Copper-phtalocyanine stained membrane verifying equal loading (bottom panel). Representative for n=2.

Wild type protein lysates revealed two bands, corresponding to the two human NDST1 isoforms. No NDST1 protein was detectable in cell lysates of NDST1 silenced clone, confirming the results obtained from RT-PCR and transfectant 10 was chosen for further analysis (Figure 5-6).

5.3.1.5 Cell surface HS expression of NDST1 silenced clones

To investigate the effect of NDST1 suppression on HS expression transfectant 10 was immunostained for HS epitope 10e4.

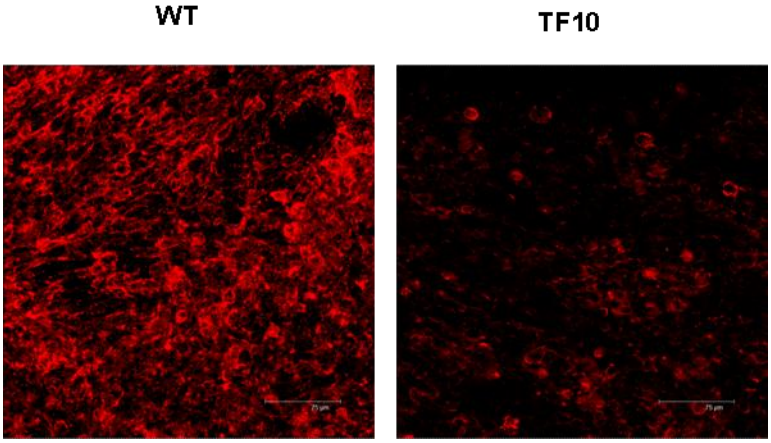

Figure 5-7 Immunofluorescent 10e4 staining of HEK wild type and NDST1 silenced transfectant 10

Cells were stained with mouse anti-Heparan sulphate antibody 10e4 (1/100) and visualized by anti-mouse TRITC conjugated secondary antibody (1/20). Representative for n=2. Scale bar represents 75 µm.

10e4 staining revealed a prominent reduction of cell surface HS of the NDST1 silenced clone compared to wild type cells (Figure 5-7).

5.3.2 Overexpression of NDST1

5.3.2.1 Cell surface HS expression of NDST1 overexpressing clone F15

In addition to the NDST1 silenced TF10 the NDST1 overexpressing clone F15, characterized for protein purification studies (see section 4.3.1.), was assessed for HS expression as well.

Overexpression of NDST1 in F15 cells resulted in increased expression of N-sulphated HS domains ($p<0.0001$) demonstrated by 10e4 staining (Figure 5-8). However, the same cells revealed a significant decrease in HS3A8 and HS4C3 staining (Figure 5-9), indicating that increased levels of N-sulphation do not necessarily correspond with increased levels of further modifications, such as 2-O- and 6-O-sulphation.

a

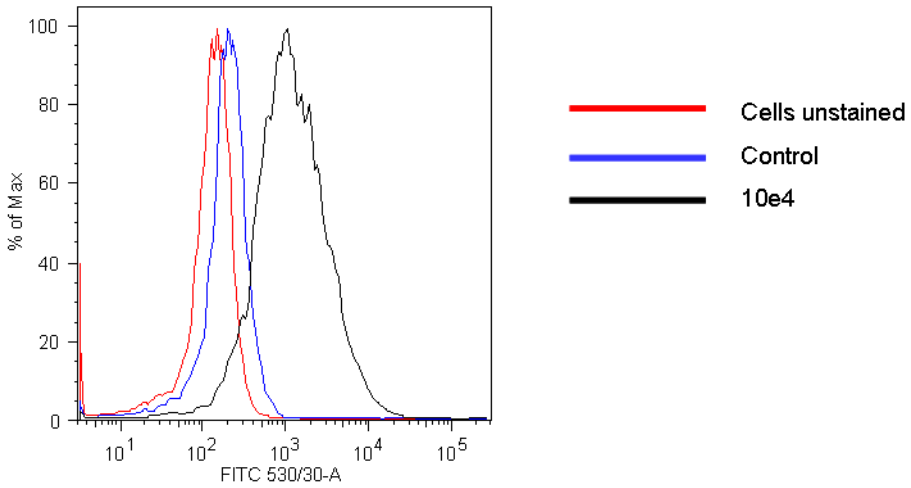

b

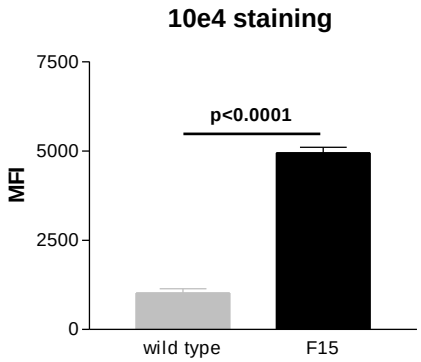

Figure 5-8 10e4 epitope expression of NDST1 overexpressing F15 cells

F15 cells were incubated with 10e4 antibody (1/50) and anti-mouse-FITC conjugated secondary antibody. Unstained cells were incubated in FACS buffer (5% FCS/PBS) and cells incubated with the secondary antibody, omitting the primary antibody incubation step, served as a control. Representative flow cytometry plots (a). Differential expression of 10e4 HS epitope of wild type and NDST1 overexpressing F15 cells (b). Data representative for 2 individual experiments performed in duplicates. Statistical analysis was determinded by student's t-test with differences $p<0.05$ considered to be significant.

a

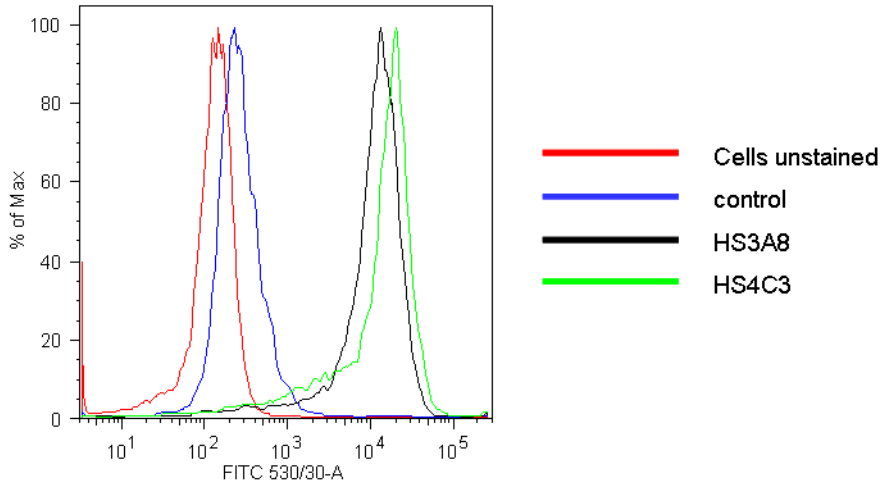

b

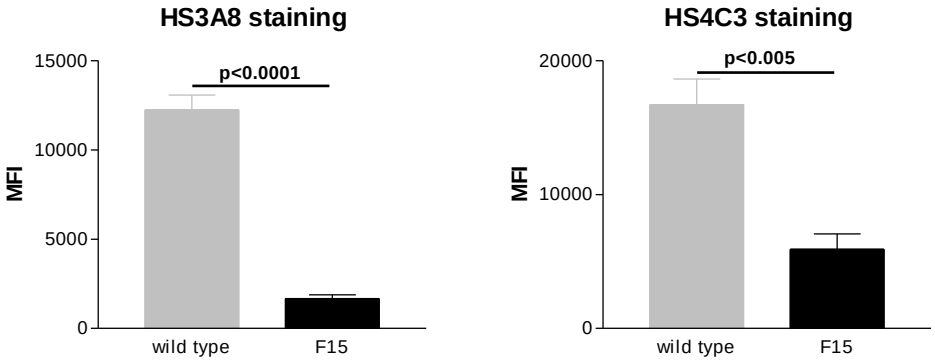

Figure 5-9 HS3A8 and HS4C3 epitope expression of NDST1 overexpressing F15 cells

F15 cells were incubated with HS3A8 and HS4C3 primary antibody (1/5), anti-VSV-tag secondary antibody (1/300) and anti-mouse-FITC tertiary antibody. Unstained cells were incubated in FACS buffer (5% FCS/PBS) and cells incubated with the secondary and tertiary antibody, omitting the primary antibody incubation step, served as a control. Representative flow cytometry plot of HS3A8 and HS4C3 HS epitope expression of NDST1 transfected F15 cells (a). Histograms of differential expression of HS3A8 and HS4C3 HS epitopes of wild type and NDST1 transfected F15 cells (b). Data representative for 2 individual experiments performed in duplicates. Statistical analysis was determinded by student's t-test with differences $p<0.05$ considered to be significant.

A set of experiments was designed to investigate the physiological consequences of altered HS expression of NDST1 transfectants. In the first instance, a chemotaxis assay was employed to test if altered cell surface HS would favour or hinder trans-cellular migration of monocytes.

5.3.3 Examination of chemokine presentation during chemotaxis

The transfectant cells were seeded on 3µm chemotaxis filters and grown to confluency. Chemokine (10nM) was added to the lower well and monocytes were added to the upper well in order to migrate through the monolayer of transfectant cells towards the chemotactic stimulus. However, no cells migrated through the monolayer of HEK 293 cells. Incubation times varied from 90 minutes to over night, but even after 24 h of incubation, no migrant cells could be found in the bottom well or the bottom side of the filter. To ensure that chemokine was still present and not degraded after longer incubation time, an ELISA was employed which proved that chemokine was present and functional in the system (Figure 5-10).

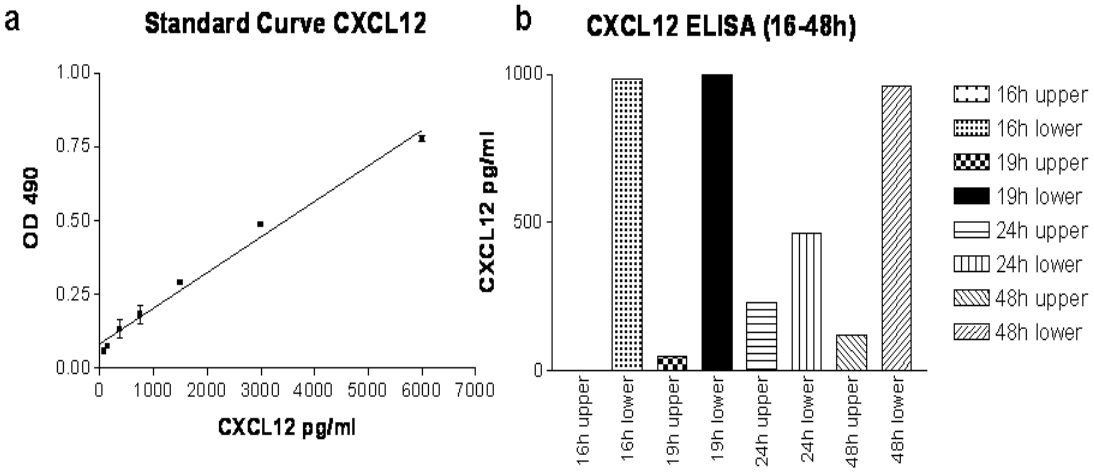

Figure 5-10 Examination of chemokine presentation during chemotaxis

CXCL12 standard curve (a) and chemokine presence in upper und bottom well during 48h of incubation (b).

Despite the presence of chemokine, no chemotaxis of monocytes occurred independent of incubation time. It appeared that HEK 293 cells forming a monolayer were blocking the pores of the filter, not allowing monocytes to

migrate through. Therefore, the model proved to be unsuitable to investigate the effect of altered HS expression on chemokine presentation and migration.

5.3.4 Adhesion of wild type and NDST1 transfected cells

In a different approach to test the physiology of differentially expressed HS a static adhesion assay was developed. L-selectin, a well known HS binding protein was coated onto ELISA plates and fluorescently labelled HEK293 cells were tested for their ability to adhere to the molecule. After the optimal BCECF dye concentration of 1.5µM was established a series of adhesion assays were performed with varying incubation times from 45 up to 120 minutes. Independent of the incubation time, hardly any cells adhered to the L-selectin coated surface after a washing step (Figure 5-11). It seemed that HEK 293 cells, which are classed as semi-adherent, were not sufficiently adherent for this type of experiment. The influence of HS expression on the adhesion potential could not be tested in this setting, as labelled cells only gave background readings almost identical to unstained cells or even buffer alone.

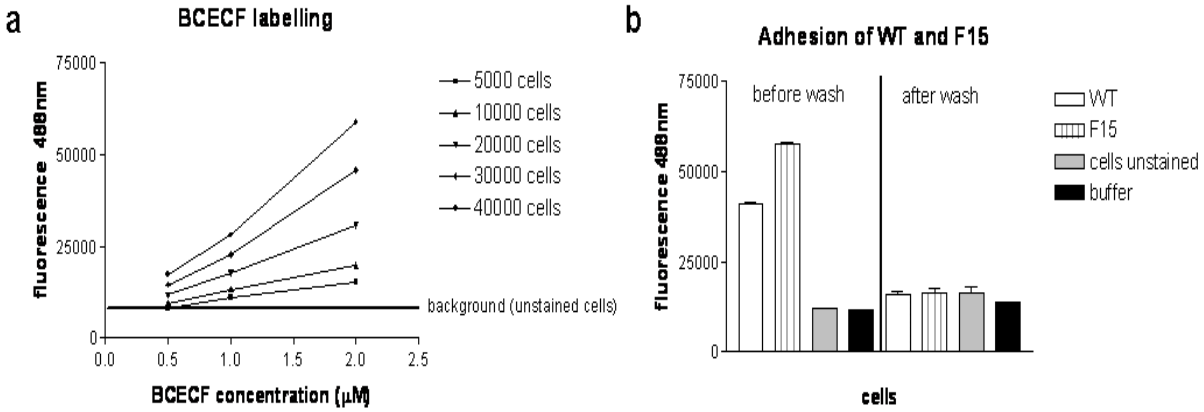

Figure 5-11 Adhesion of wild type and F15 HEK 293 cells

Optimisation of BCECF labelling of cells (a) and static adhesion assay (b). 40.000 cells were incubated on L-selectin coated 96-well plate for 45 minutes at 37° degree and fluorescence readings were taken before and after washing. Unstained cells (cells which were not incubated with BCECF but buffer alone) and wells containing PBS without cells served as controls.

To test the biological differences of HS expression of NDST1 transfected cells chemokine presentation should be investigated. In this assay a biotinylated form of the chemokine CCL5 was used to test the potential of HS to sequester

chemokines on the cell surface. Even though the biotin group was placed apart from the GAG binding motif in CCL5 it first had to be tested for biological activity.

5.3.5 Analysis of CCL5-biotin

As later experiments would rely on the detection of CCL5-biotin it had to be ensured that the altered chemokine would be detectable in a similar fashion to the wild type. Primary and secondary antibodies were titrated using wild type CCL5 and optimal concentrations were established. ELISA analysis of CCL5-biotin revealed a reduction in detection but a similar curve shape (Figure 5-12).

a

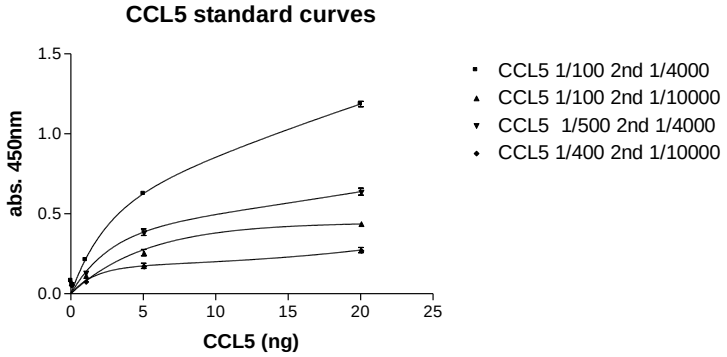

b

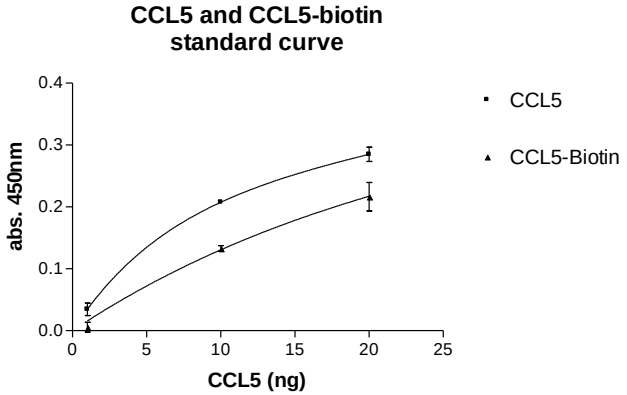

Figure 5-12 Titration of CCL5 antibodies for ELISA

Goat anti-CCL5 and anti-goat antibodies have been used in different concentrations (as indicated) for the development of a CCL5 ELISA (top panel). CCL5 and CCL5-biotin were used under optimised conditions (bottom panel). CCL5 wild type and CCL5-biotin were incubated with anti-CCL5 antibody (1/150) and anti-goat antibody (1/5000).

5.3.5.1 Determination of heparin affinity

Having established a methodology capable of quantifying chemokines an ELISA was set up again and employed to test the heparin affinity of CCL5 biotin by FPLC.

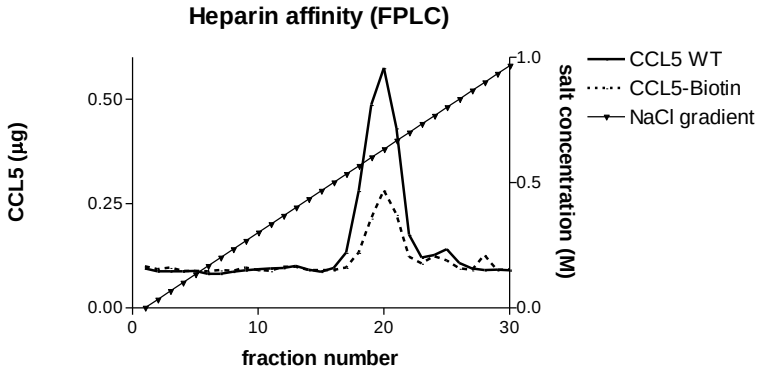

Figure 5-13 Determination of CCL5-biotin heparin affinity

FPLC was performed to compare the heparin affinities of wild type CCL5 and CCL5-biotin. 1µg of chemokine in phosphate buffer was loaded onto a heparin column. The chemokine was eluted from the column by a salt gradient (0-1M NaCl) in 30 fractions. 50µl of the eluent were used for an ELISA.

Even though no 280nm readings could be recorded during the elution of the proteins from the column the ELISA analysis confirmed the elution of the protein fractions. Wild type CCL5 was eluted in fractions 19-21, corresponding to ~0.7M NaCl. The biotinylated from was eluted in the same fraction numbers, although with a smaller peak (Figure 5-13). This can be explained by the lower detection rate of CCL5-biotin as previously demonstrated in analogous ELISA experiments

5.3.5.2 Determination of biological activity of CCL5-biotin

Establishing that CCL5-biotin was binding to heparin its ability to further induce mobilisation of intracellular calcium was investigated. THP1 monocytes were stimulated with 1nM and 10nM CCL5 and CCL5-biotin and changes in florescence were recorded. Both forms of CCL5 were capable of causing transient calcium fluxes, proving the biotinylated form to be functional (Figure 5-14).

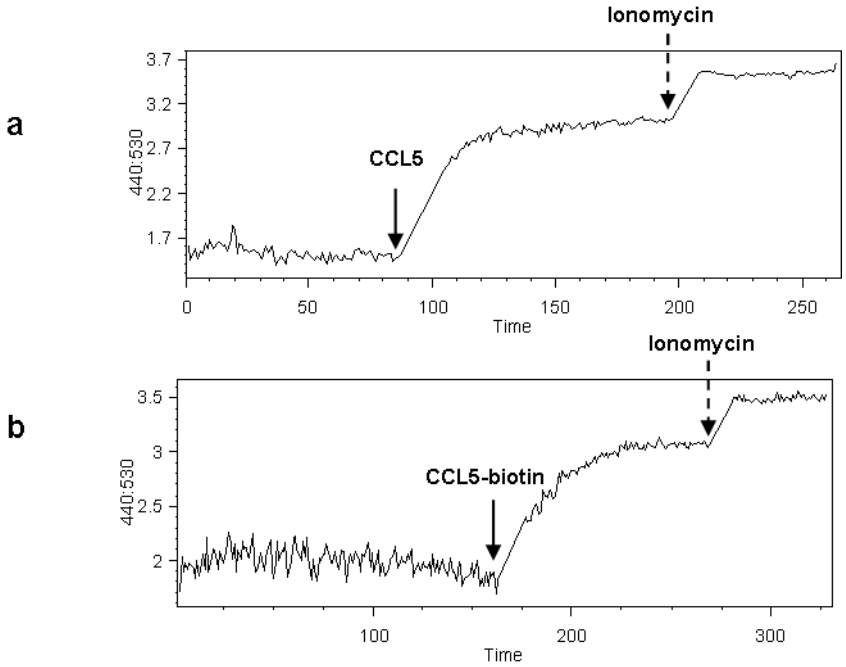

Figure 5-14 Examples of CCL5 induced Calcium flux.

THP1 monocytes were loaded with 3µg/ml of the Calcium sensitive dye Indo-1-AM prior to stimulation with 10nM CCL5 wild type (a) or CCL5-biotin (b). The second peak after chemokine addition is due to ionomycin addition (1µg/ml) serving as positive control.

5.3.5.3 Chemotactic ability of CCL5 wild type and CCL5-biotin

Having demonstrated that CCL5-biotin was binding to heparin in a similar fashion to the wild type and proving its functionality by calcium flux studies chemotaxis assays were carried out to assay the ability of CCL5-biotin to induce cell migration. Chemotaxis assays (Figure 5-15) demonstrated that 1nM of wild type or biotinylated chemokine did not drive significant chemotaxis above background levels, however, 10 and 50nM of either chemokine was sufficient to elicit migration ($p < 0.05$). Wild type and biotinylated chemokine did induce migration to the same extent at 1 and 10nM, however, at 50nM the biotinylated form did induce migration to a lesser extent compared to the wild type ($p<0.01$).

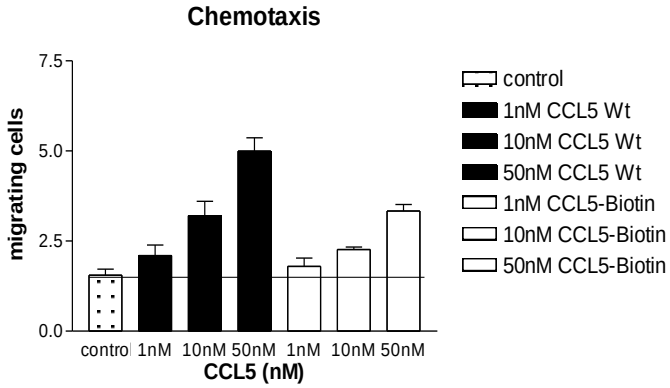

Figure 5-15 Chemotaxis mediated by CCL5 and CCL5-biotin

500.000 THP1 cells were migrated across a 3µm transwell filter towards the indicated amounts of chemokine for 90 minutes. Wells containing RPMI medium and no chemokine served as control. Results representative for 3 independent experiments performed in triplicates.

5.3.5.4 Chemokine presentation by HEK 293 cells

After the validation of CCL5-biotin, NDST1 transfected cells with altered HS expression on the cell surface were investigated for their ability to sequester and present the biotinylated chemokine. The dependency on HS for chemokine presentation was shown by other members of the group previously by the use of CHO cells, which demonstrated that wild type CHO cells were capable of sequestering chemokines whereas a GAG deficient mutant was not (unpublished data from PhD thesis of Dr. Graeme O'Boyle).

Wild type HEK and NDST1 overexpressing cells were grown to 70-80% confluency on chamber slides and incubated with CCL5-biotin. Visualization with strepatvidin–FITC revealed a stronger capability of F15 cells with increased HS expression to present chemokine on the cell surface (Figure 5-16) compared to the wild type cells.

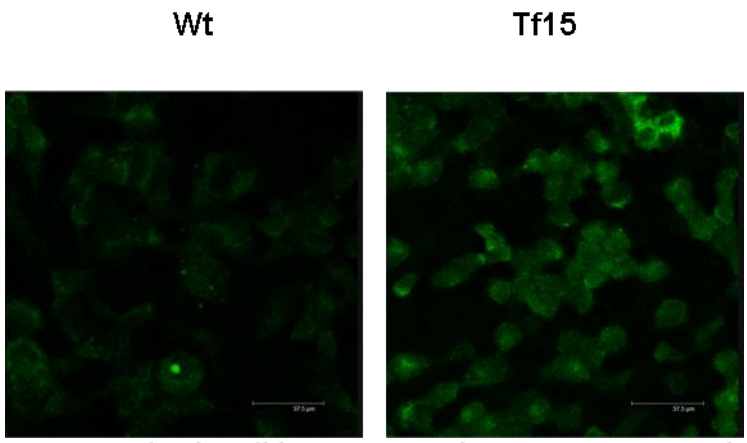

Figure 5-16 CCL5 presenation by wild type HEK and NDST1 overexpressing cells

Cells were incubated for 60 minutes at RT with exogenous, biotinylated CCL5 (100ng/ml) which was visualised with strepatvidin –FITC. Scale bar represents 75 µm.

5.3.6 Optimisation FGF binding

In addition to the CCL5 binding assay which was established previously an FGF2 binding assay was employed. To verify the dependency of FGF2 binding on HS, CHO wild type and GAG-deficient CHO cells were used for initial experiments. The GAG deficiency of the CHO-745 cells was confirmed by the lack of signal when stained for HS epitope 10e4 and the cells were incapable of sequestering FGF2 on the cell surface. CHO wild type cells however showed positive staining for 10e4 and FGF2 was retained on the cell surface. FACS plots clearly demonstrate the correlation between HS expression and FGF2 binding capacity (Figures 5-17 and 5-18).

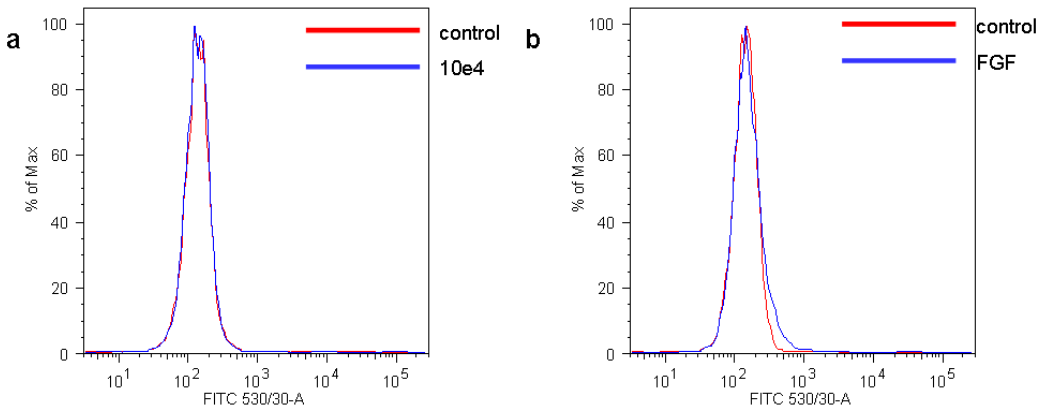

Figure 5-17 10e4 staining and FGF2 binding of HS deficient CHO-745 cells

Representative flow cytometry plots of GAG deficient cells stained for 10e4 HS epitope (a) and analysed for FGF2 binding capacity (b).

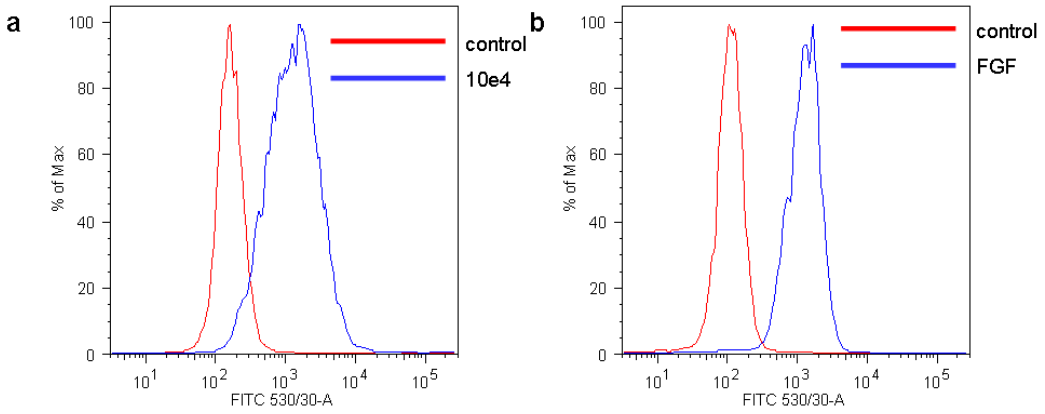

Figure 5-18 10e4 staining and FGF2 binding of CHO wild type cells

Representative flow cytometry plots of CHO wild type cells stained for 10e4 HS epitope (a) and analysed for FGF2 binding capacity (b).

As the buffer provided with the FGF2 kit was of unknown composition an experiment with buffer provided and PBS was carried out which highlighted that the provided buffer was not highly stringent, as no differences in FGF2 binding between the two washing conditions could be observed (Figure 5-19).

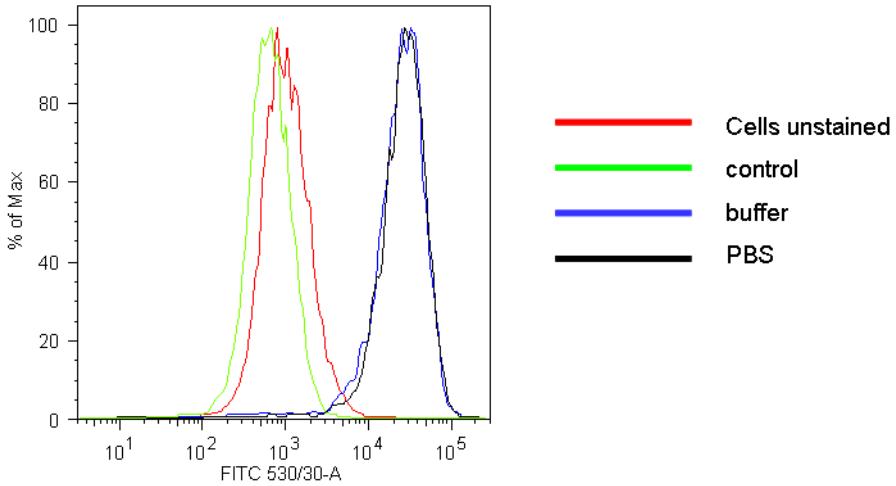

Figure 5-19 Influence of washing conditions on FGF2binding

Representative flow cytometry plots of HK2 cells binding FGF2. The difference of washing conditions (buffer provided with FGF binding kit versus PBS) was investigated.

5.3.6.1 FGF2 binding of HEK 293 cells

After the validation of FGF2 binding NDST1 transfected cells with altered HS expression were investigated for their ability to sequester and present FGF2 on the cell surface. Wild type HEK 293 cells were capable of binding slightly more FGF2 compared to F15 cells, although significance was not reached (Figure 5-20).

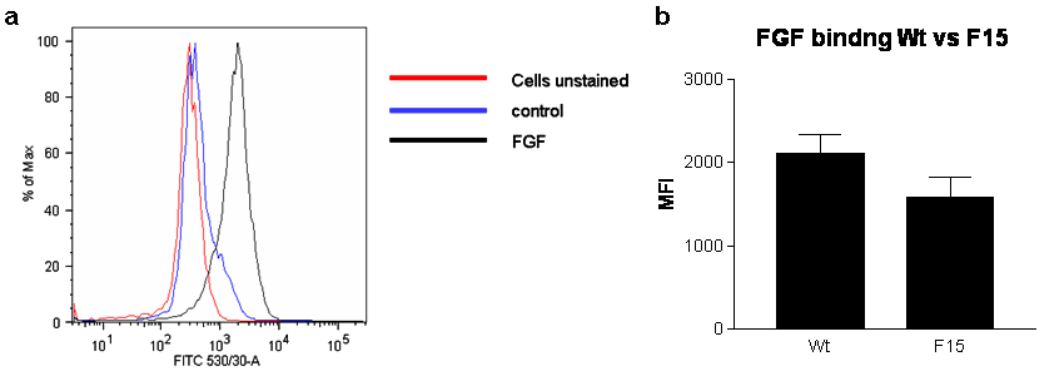

Figure 5-20 FGF2 binding of wild type HEK versus NDST1 overexpression F15 cells

Flow cytometry plots of HEK wild type cells binding FGF2 (a) and histograms of differential binding of FGF2 to HEK wild type versus NDST1 overexpressing F15 cells (b). Statistical analysis was determinded by student's t-test with differences $p<0.05$ considered to be significant.

5.3.7 Profiling of HS epitope expression and ligand binding upon experimental inflammation and hypoxia

After the analysis of NDST1 HEK transfectants various cell lines were assayed for potential changes in HS expression upon induction of hypoxia and inflammatory stimulation, mimicking ischemia and an inflammatory response. Furthermore the physiological consequences of altered HS expression were investigated by chemokine and growth factor binding studies, which have been validated previously.

5.3.7.1 Screening of the embryonic kidney cell line (HEK 293)

HEK 293 cells were analysed by FACS to measure the levels of cell surface HS of resting cells and after hypoxia/stimulation for 18 hours. Basal expression of

10e4 epitope was moderate and a significant increase could be observed in both groups of stimulated cells and cells undergoing hypoxic stress ($p<0.05$) (Figure 5-21). No significant changes in HS3A8 staining could be observed between the groups and HS4C3 staining revealed increased expression after hypoxia ($p<0.01$), but not after stimulation with IFNγ and TNFα (Figure 5-22). To see if overall changes in HS expression would have an effect on the binding capacity a FGF2 binding assay was performed. Resting cells were capable of sequestering slightly more FGF2 than stimulated cells (Figure 5-23). CCL5 binding experiments were carried out but experimental conditions appeared to be too harsh for CCL5 as no readings above the background were taken (data not shown).

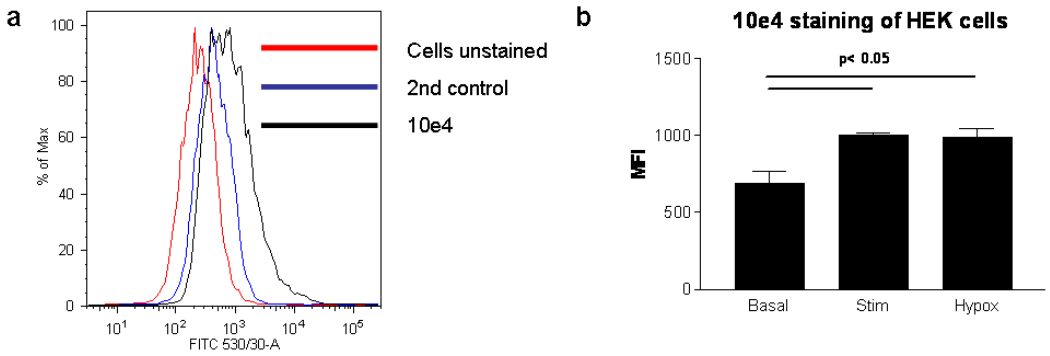

Figure 5-21 10e4 staining of HEK 293 cells at basal level and following stimulation

Representative flow cytometry plot of 10e4 HS epitope expression of HEK cells (a) and histograms of differential 10e4 expression after stimulation with proinflammatory cytokines (18h IFNγ and TNFα) or induction of hypoxia. Data representative for 2 individual experiments performed in duplicates. Statistical analysis was determinded by 1-way Anova with differences $p<0.05$ considered to be significant.

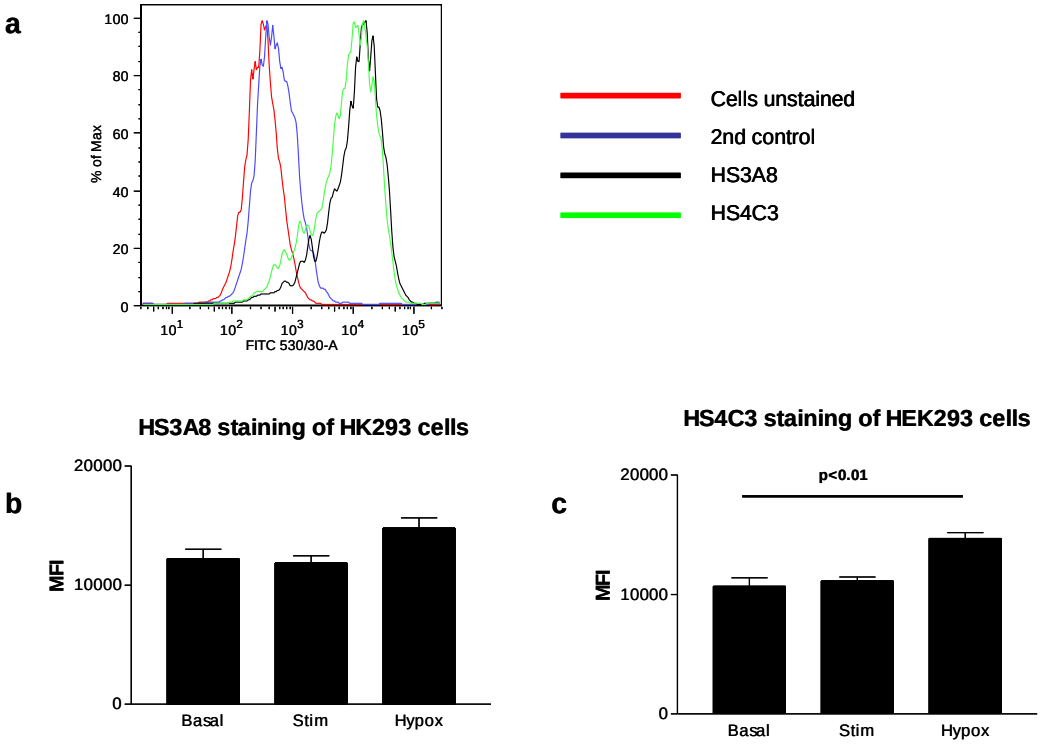

Figure 5-22 HS3A8 and HS4C3 staining of HEK 293 cells at basal level and following stimulation

Representative flow cytometry plot of HS3A8 and HS4C3 HS epitope expression of HEK cells (a) and histograms of differential HS3A8 expression (b) and HS4C3 expression (c) after stimulation with proinflammatory cytokines (18h IFNγ and TNFα) or induction of hypoxia. Data representative for 2 individual experiments performed in duplicates. Statistical analysis was determinded by 1-way Anova with differences p<0.05 considered to be significant.

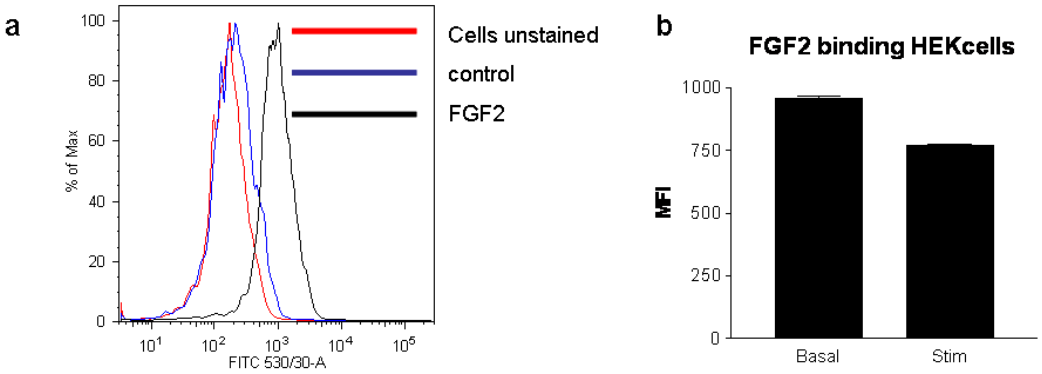

Figure 5-23 FGF2 binding of stimulated HEK 293 cells

Representative flow cytometry plot of HEK 293 cells binding FGF2 (a) and differential binding of FGF2 after stimulation (18h IFNγ and TNFα).

5.3.7.2 Screening of renal proximal tubular epithelial cells (HK-2)

HK-2 cells were analysed analogous to HEK 293 cells by FACS. HK-2 cells were chosen as changes in tubular epithelial HS have been shown to occur during rejection (Ali et al., 2005a, Celie et al., 2008) and it should be investigated if the changes observed in the tissue are reflective of changes in tubular epithelial cells.

Basal expression of all three HS epitopes were higher than in HEKs and a decrease in 10e4 ($p<0.01$), HS3A8 ($p<0.01$) and HS4C3 ($p<0.05$ between basal and hypoxic group) staining could be observed in both groups of stimulated cells and cells undergoing hypoxic stress (Figures 5-24 and 5-25).The decrease in HS domains was accompanied by a decrease in FGF2 and CCL5 binding (Figures 5-26 and 5-27).

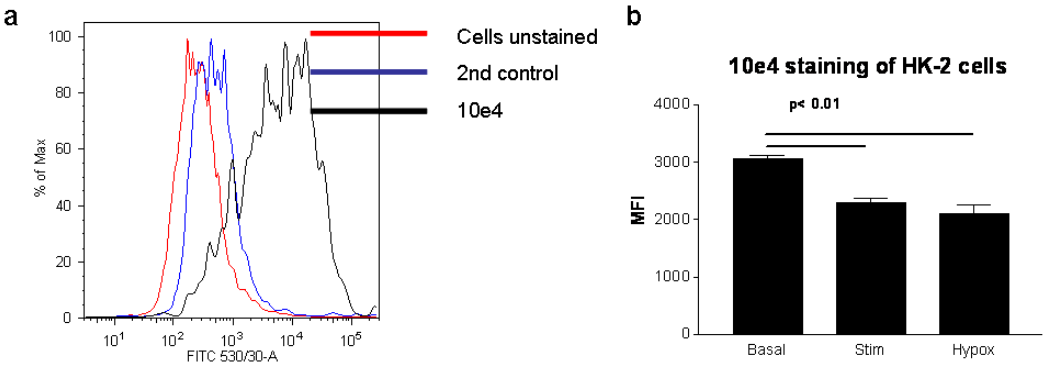

Figure 5-24 10e4 staining of HK-2cells at basal level and following stimulation

Representative flow cytometry plot of 10e4 HS epitope expression of HK-2 cells (a) and differential expression of 10e4 HS epitope after stimulation with proinflammatory cytokines (18h IFNγ and TNFα) or induction of hypoxia. Data representative for 2 individual experiments performed in duplicates. Statistical analysis was determinded by 1-wayAnova with differences $p<0.05$ considered to be significant.

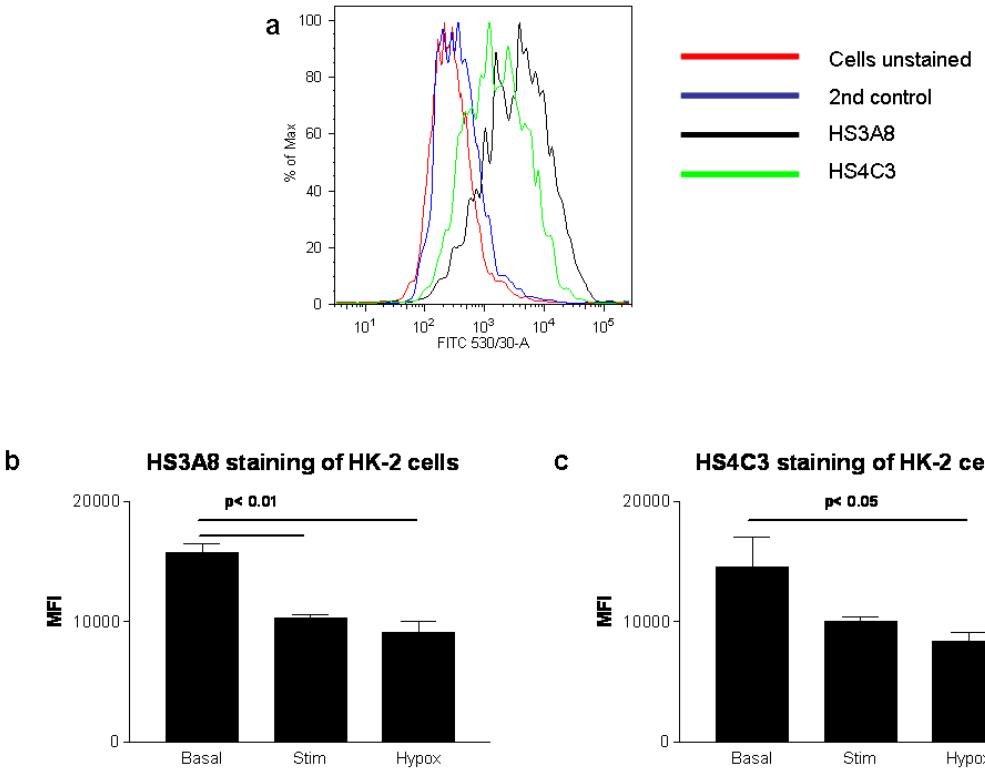

Figure 5-25 HS3A8 and HS4C3 staining of HK-2 cells at basal level and following stimulation

Representative flow cytometry plot of HS3A8 and HS4C3 HS epitope expression of HK-2 cells (a) and differential expression of HS3A8 (b) and HS4C3 (c) HS epitope after stimulation with proinflammatory cytokines (18h IFNγ and TNFα) or induction of hypoxia. Data representative for 2 individual experiments performed in duplicates. Statistical analysis was determinded by 1-way Anova with differences p<0.05 considered to be significant.

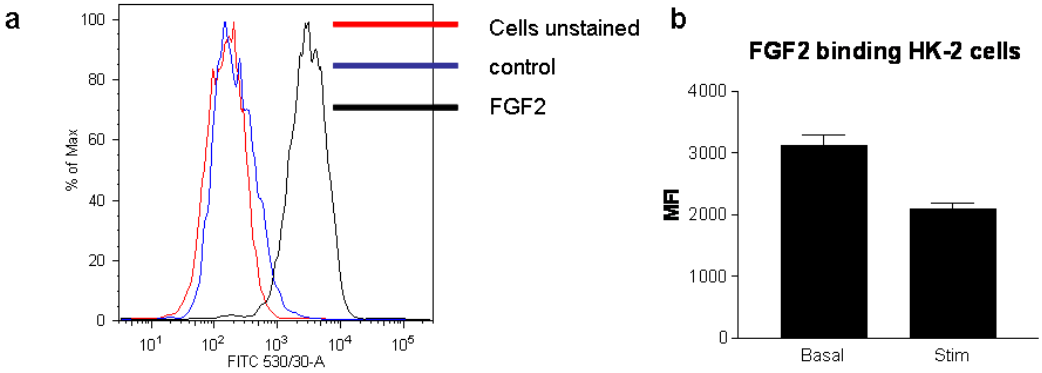

Figure 5-26 FGF2 binding of stimulated HK-2 cells

Representative flow cytometry plot of HK-2 cells binding FGF2 (a) and differential binding of FGF2 after stimulation (18h IFNγ and TNFα).

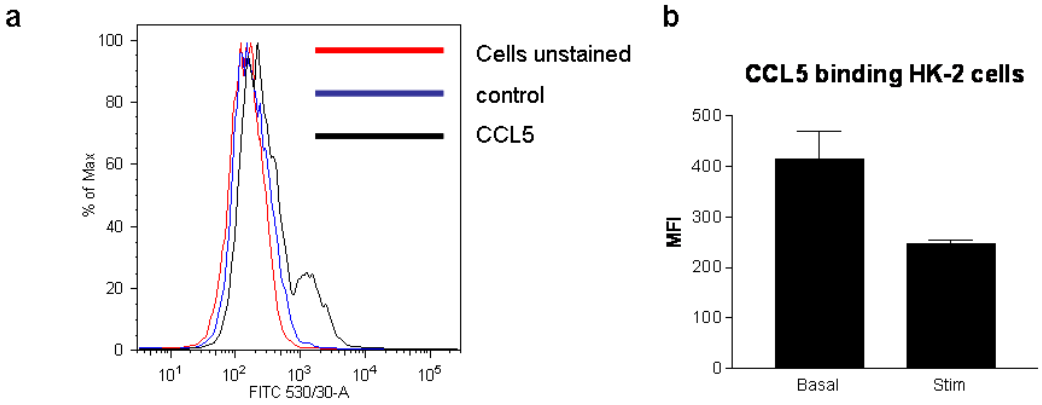

Figure 5-27 CCL5 binding of stimulated HK-2 cells

Representative flow cytometry plot of HK-2 cells binding CCL5 (a) and differential binding of CCL5 after stimulation (18h IFNγ and TNFα).

5.3.7.3 Screening of the hepatocellular carcinoma cell line (HepG2)

HepG2 cells were employed as changes in liver HS have been reported in chronic inflammatory liver diseases (Murata et al., 1985, Tatrai et al., 2010). Stimulation and hypoxic stress of HepG2 cells resulted in a pronounced reduction of all HS domains (p-values <0.001) with stimulated cells revealing the lowest amount of HS (Figures 5-28 and 5-29). Despite the decrease of all HS species analysed the stimulated cells showed a slight increase in binding of FGF2 and CCL5 (Figures 5-30 and 5-31).

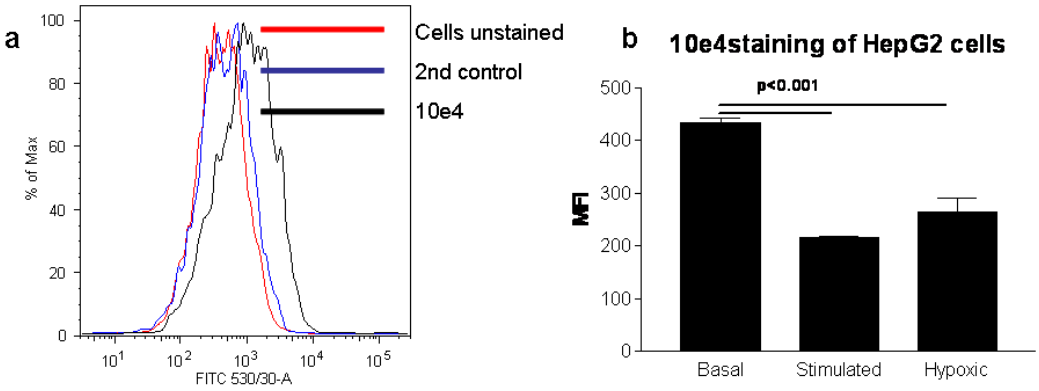

Figure 5-28 10e4 staining of HepG2 cells at basal level and following stimulation

Representative flow cytometry plot of 10e4 HS epitope expression of HepG2 cells (a) and differential expression of 10e4 HS epitope after stimulation with proinflammatory cytokines (18h IFNγ and TNFα) or induction of hypoxia. Data representative for 2 individual experiments performed in duplicates. Statistical analysis was determinded by 1-way Anova with differences $p<0.05$ considered to be significant.

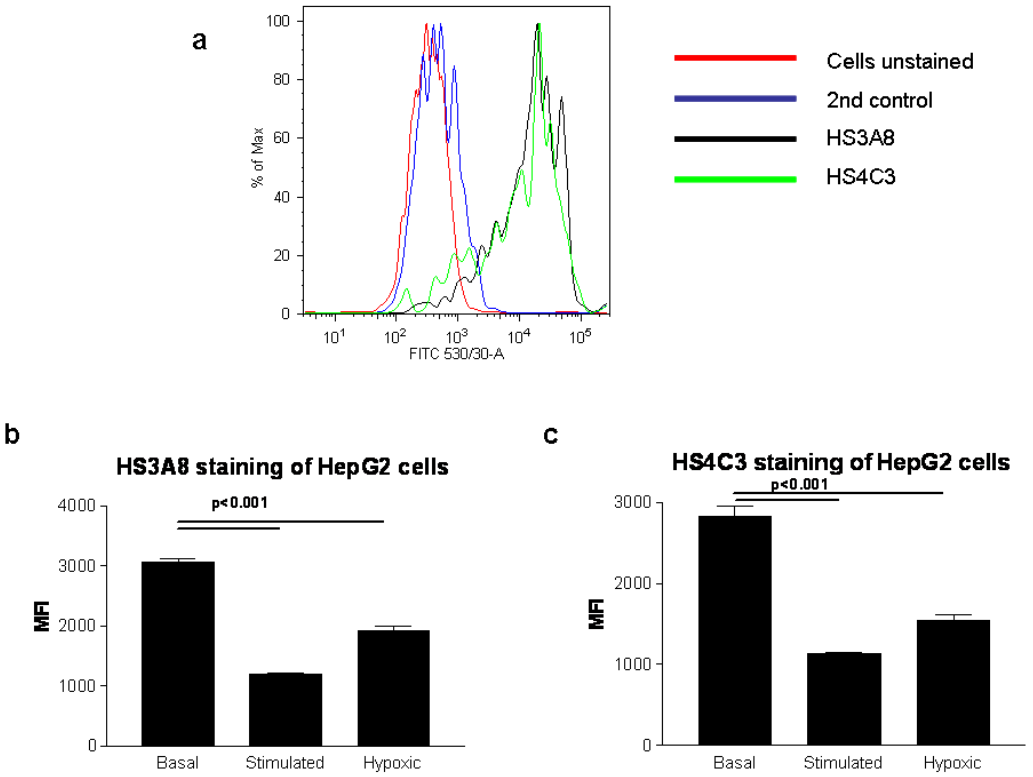

Figure 5-29 HS3A8 and HS4C3 staining of HepG2 cells at basal level and following stimulation

Representative flow cytometry plot of HS3A8 and HS4C3 HS epitope expression of HepG2 cells (a) and differential expression of HS3A8 (b) and HS4C3 (c) HS epitope after stimulation with proinflammatory cytokines (18h IFNγ and TNFα) or induction of hypoxia. Data representative for 2 individual experiments performed in duplicates. Statistical analysis was determinded by 1-way Anova with differences p<0.05 considered to be significant.

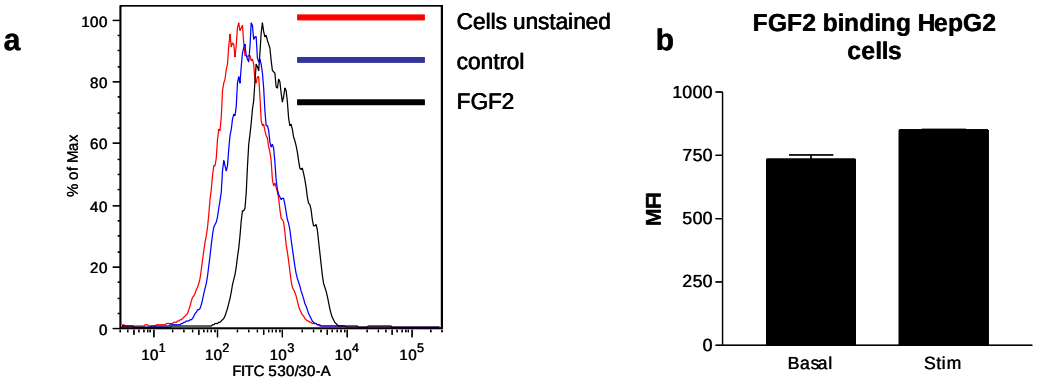

Figure 5-30 FGF2 binding of stimulated HepG2 cells

Representative flow cytometry plot of HepG2 cells binding FGF2 (a) and differential binding of FGF2 after stimulation (18h IFNγ and TNFα).

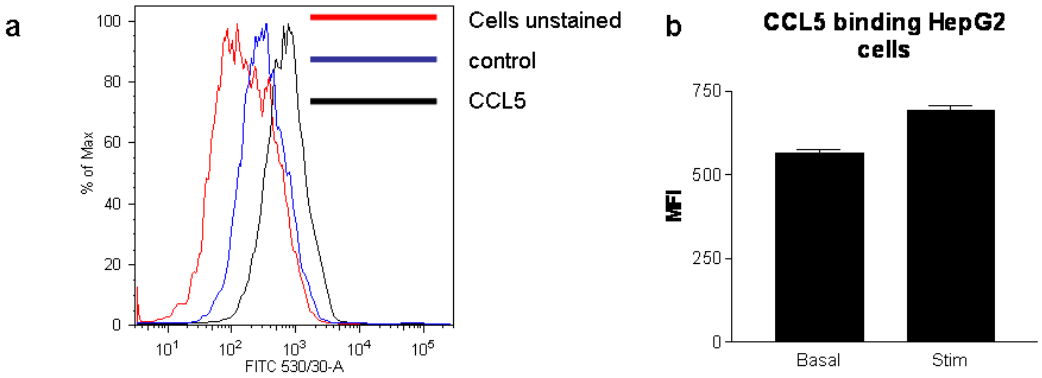

Figure 5-31 CCL5 binding of stimulated HepG2 cells

Representative flow cytometry plot of HepG2 cells binding CCL5 (a) and differential binding of CCL5 after stimulation (18h IFNγ and TNFα).

5.3.7.4 Screening of the microvascular endothelial cell line (HMEC-1)

Stimulation of HMEC-1 cells led to a small decrease ($p<0.01$) in 10e4 staining whereas no changes were found for cells grown under hypoxic conditions. Neither did HS3A8 or HS4C3 staining differ significantly between any of the groups (Figures 5-32 and 5-33). FGF2 binding was unaltered as well, only a small increase in CCL5 binding of stimulated HMEC-1 cells could be observed (Figures 5-34 and 5-35).

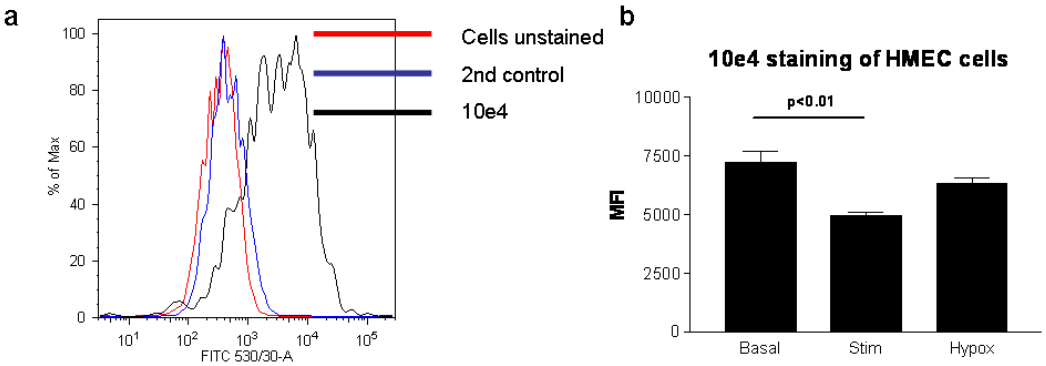

Figure 5-32 10e4 staining of HMEC-1 cells at basal level and following stimulation

Representative flow cytometry plot of 10e4 HS epitope expression of HMEC-1 cells (a) and differential expression of 10e4 HS epitope after stimulation with proinflammatory cytokines (18h IFNγ and TNFα) or induction of hypoxia. Data representative for 2 individual experiments performed in duplicates. Statistical analysis was determinded by 1-way Anova with differences $p<0.05$ considered to be significant.

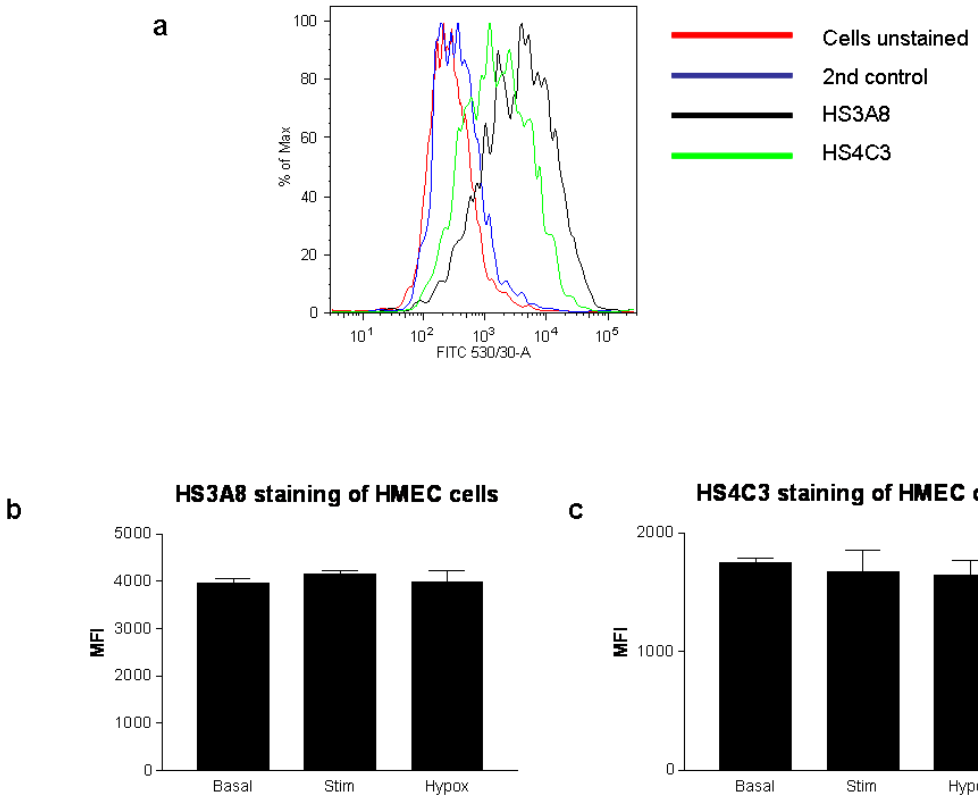

Figure 5-33 HS3A8 and HS4C3 staining of HMEC-1 cells at basal level and following stimulation

Representative flow cytometry plot of HS3A8 and HS4C3 HS epitope expression of HMEC cells (a) and differential expression of HS3A8 (b) and HS4C3 (c) HS epitope after stimulation with proinflammatory cytokines (18h IFNγ and TNFα) or induction of hypoxia. Data representative for 2 individual experiments performed in duplicates. Statistical analysis was determinded by 1-way Anova with differences $p<0.05$ considered to be significant.

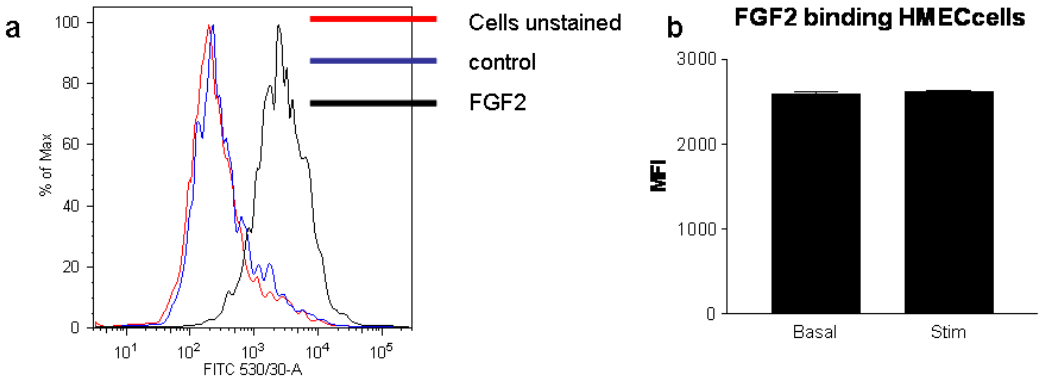

Figure 5-34 FGF2 binding of stimulated HMEC-1 cells

Representative flow cytometry plot of HMEC-1 cells binding FGF2 (a) and differential binding of FGF2 after stimulation (18h IFNγ and TNFα).

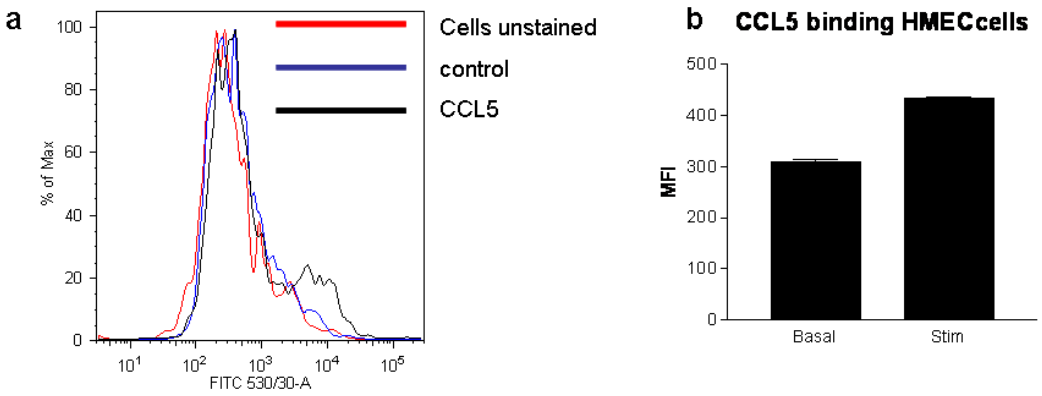

Figure 5-35 CCL5 binding of stimulated HMEC-1 cells

Representative flow cytometry plot of HMEC cells binding CCL5 (a) and differential binding of CCL5 after stimulation (18h IFNγ and TNFα).

Tables 5-4 and 5-5 give an overview of the observed changes upon hypoxia and stimulation of the employed cell lines.

Table 5-4 Summaryof HS expression of cell lines after stimulation

	stimulation			**hypoxia**		
	10e4	HS3A8	HS4C3	10e4	HS3A8	HS4C3
HEK 293	↑	↔	↔	↑	↔	↑
HK-2	↓	↓	↓	↓	↓	↓
HepG2	↓	↓	↓	↓	↓	↓
HMEC-1	↓	↔	↔	↔	↔	↔

(arrows indicating up- or downregulation or unchanged)

Table 5-5 Summary of ligand binding of cell lines upon stimulation

	stimulation	
	FGF2	CCL5
HEK 293	↓	-
HK-2	↓	↓
HepG2	↑	↑
HMEC-1	↔	↑

5.4 Discussion

HS is a multifunctional molecule which can adapt to a changing environment quickly. The changes in HS structure reflect changes in HS biosynthetic enzymes, which can be influenced by external factors (Carter et al., 2003, Rops et al., 2008). In the sequential model of HS biosynthesis, NDST1 is regarded as the key enzyme and its activity is a prerequisite for all other enzymes (Lindahl et al., 1998). It was therefore decided to investigate how modulation of NDST1 would affect HS expression in general and further the ability of altered HS to interact with HS binding molecules, such as chemokines, growth factors or adhesion molecules.

5.4.1 Modulation of NDST1

In the attempt to suppress NDST1 expression a silencing construct was transformed into *E. coli*. Once the sequence of the positive transformant was verified the construct was used for the transfection of HEK 293 cells. Ideally a different cell line, preferably an endothelial one, would have been the cell line of choice but due to difficulties in transfecting and establishing stable clones of endothelial origin (Lindemann and Schnittler, 2009), HEK 293 cells were used as an easy to handle alternative. Initially 50 clones were picked and propagated. Only 7 survived the selection process and screening for NDST1 mRNA expression revealed that both up- and downregulation of NDST1 occurred in transfected cells. The transfectant with the most prominent effect revealed a reduction of 64% on the mRNA level. Higher levels of NDST1 reduction might not be reached due to the essential role of NDST1 in mammalian cells and due to the fact that cells are stably transfected, which means they have been cultured for a certain time whereas up to 80% of NDST1 reduction have been reported for transient transfection (Deligny et al., 2010). The transfectant with the highest reduction was chosen for further experiments and the reduction in mRNA level was confirmed at the protein level by Western blotting. Even though stable clones with NDST1 gene knockdown were generated, only clones from early passage numbers were used for further experiments as it is unknown how long shRNA induced gene silencing lasts.

The influence of NDST1 reduction was investigated immunocytochemically by the application of the 10e4 antibody which revealed a marked reduction in N-sulphation. The concurrent reduction of NDST1 and 10e4 levels was in line with the literature where reduced levels of N-sulphation were reported after silencing of NDST1 in cell lines such as L6 muscle cells or Jurkat T cells (Deligny et al., 2010, Pankonin et al., 2005). In general, the NDST1 silenced transfectants were very difficult to handle as they were hardly adherent. Therefore, immunofluorescent staining proved very challenging as cells lifted off the chamber slides during the staining procedure, often even during the initial washes in PBS. Because of this fact 10e4 immunofluorescent staining was only successful twice (despite numerous attempts) and as there was quite a time span between the two successfull stainings no quantification of the fluorescence intensity was performed.

As a stable cell line with decreased HS expression was established, comparative studies using NDST1 overexpressing F15 cells, which were originally generated for the protein-protein interaction studies, were carried out. Analysed for N-sulphated HS those cells demonstrated a marked increase in 10e4 staining. This has been reported previously for HEK 293 cells overexpressing NDST1 (Bengtsson et al., 2003, Pikas et al., 2000). The NDST1 overexpressing clone F15 also revealed a drastic reduction in both other HS domains, namely HS3A8 (indicative for N-sulphation, 2-O- and 6-O-sulphation, C5-epimerisation) and HS4C3 (N-sulphation, 3-O- and 6-O-sulphation). This is interesting, as according to the sequential model one would expect increased amounts of other modifications, such as O-sulphation or epimerization after an increase of N-sulphation. However, this was clearly not the case. A possible explanation could be that the other endogenous HS modifying enzymes were present only at low endogenous levels in the cell and therefore could not make use of the increased N-sulphated template. Similarly, due to the overexpression of NDST1, NDST1 molecules were present at high levels possibly masking the nascent HS chain thus hindering other enzymes gaining access. Increased N-sulphation does not always go in line with increases in other modifications; disaccharide analysis of NDST1 overexpressing HEK 293 cells revealed no change in iduronic acid content or O-sulphation despite high levels of N-

sulphation (Pikas et al., 2000). Similar observations were also made by Rops et al., in a model of glomerular endothelial inflammation they found that increase in 10e4 staining was not correlated with HS3A8 and HS4C3 staining (Rops et al., 2008). A direct comparision of the HS expression profile of NDST1 over- and underexpressing cells was unfortunately not feasible as the tranfectants were created at different time points and NDST1 silenced clones were already growing for some time before NDST1 overexpressing clones and phage-display derived antibodies became available. Due to this fact and the general handling problems with the silenced clones (bad adherence to culture flasks and chamber slides as well as the GFP signal derived from the GFP-tag of the silencing vector) only NDST1 overexpressing cells were employed in further experiments.

5.4.2 Physiological consequence of altered HS of NDST1 transfectants

5.4.2.1 Chemotaxis

Having established stable cell lines with altered HS expression the functional consequences of the differentially modified HS should be investigated. One option was to test the potential of chemokines to induce vectorial migration of monocytes across the monolayer of transfected cells with altered HS. This model proved unfortunately to be unsuitable as no migration of cells occurred at all independent of incubation time. This could be due to HEK 293 cells penetrating the pores; a scenario which has been reported for epithelial cells when seeded at high densities (Mul et al., 2000). Seeding at high densities is however inevitable to avoid the possibility that monocytes would migrate directly through the pores on the filter which would not be covered by cells seeded at low densities.

5.4.2.2 Adhesion

In a different approach the transfected cell lines expressing different amounts of HS were tested for their potential to interact with the adhesion molecule L-selectin, a well known HS binding protein (Wang et al., 2005), and mediate adhesion. Again, this assay failed to work as cells did not adhere to the L-

selectin coated plate. One possible explanation could be that L-selectin only binds to a subset of HSPGs with a collagen XVIII backbone (Celie et al., 2005), which might not be expressed by HEK 293 cells. Also, besides N-sulphation, binding of L-selectin also depends on 2-O- and 6-O-sulphation (Celie et al., 2005, Kawashima, 2006), which have been shown to be greatly reduced in F15 cells. Overall, the lack of adherent potential of semi-adherent HEK 293 cells in general does not favour such an assay which involves washing steps and mechanic oscillation.

5.4.2.3 Chemokine presenation

As chemotaxis failed to work a different way of demonstrating chemokine presentation on the cell surface HS was developed. In a chemokine presentation assay a biotinylated form of CCL5, a well studied HS binding chemokine (Ali et al., 2002, Rek et al., 2009), was used. The biotinylated form allows endogenous and exogenous chemokine to be distinguished in the assay and facilitated direct visualization via a fluorescently labelled streptavidin; avoiding a signal merged with endogenous CCL5, which would have been recognised by the application of a specific anti-CCL5 antibody. Although the CCL5 was not labelled in house with the biotin but was supplied HPLC purified by a company, its biological activity had to be validated.

The most common method to assay chemokine-HS interaction is determining the amount of salt required to elute the bound chemokine from a heparin-Sepharose column. Heparin can be seen as uniformly highly sulphated form of HS and this assay demonstrates some degree of specificity for the interaction. When wild type and CCL5-biotin were eluted from the heparin column by the application of a salt gradient they both eluted at the same fraction numbers corresponding to 0.7M NaCl which is slightly lower than the reported value of 0.8M in the literature (Proudfoot, 2006). The smaller peak of CCL5-biotin can be explained by the reduced recognition of the modified molecule by the antibodies employed in the ELISA quantification. Although the biotin group is placed distant from the GAG-binding motifs it can not be excluded that it interferes with the anti-CCL5 antibody recognition site.

It was further necessary to demonstrate that CCL-5 biotin was functional and calcium flux analysis proved receptor activation, as binding of the chemokine ligand to its receptor lead to mobilisation of intracellular calcium. In a final validation experiment CCL5-biotin was assessed for its ability to induce trans-filter migration of THP1 monocytes. CCL5-biotin did support migration of monocytes at 1nM and 10nM to the same level as wild type chemokine, although with a significant decrease at 50nM. This could mean that the modified chemokine is not capable of activating all signalling pathways necessary for directing vectorial migration but was employed in the chemokine presentation assay as this assay relies on the heparin affinity and does not examine migration.

When analysed for chemokine presentation F15 cells showed an enhanced capacity to retain CCL5-biotin on its surface due to increased expression of N-sulphated HS. At the same time, F15 cells showed slightly decreased potential to sequester FGF2 on the cell surface in line with decreased levels of HS3A8 and HS4C3. N-sulphation as represented by 10e4 staining therefore appears to be more important for CCL5 binding (Schenauer et al., 2007, Sweeney et al., 2006) whereas 2-O- and 6-O-sulphation (Guglieri et al., 2008, Kreuger et al., 2001) as represented by antibodies HS3A8 and HS4C3 appear to be involved in FGF2 binding. Therefore one has to be cautious in attempting indirect measurements of HS content by FGF2 binding, as suggested by Garner (Garner et al., 2008).

Unfortunately the transfected cells with decreased HS N-sulphation (TF10) could not be tested for their potential to sequester chemokine or FGF as they required a TRITC-conjugated streptavidin for visualization due to the GFP encoded by the plasmid in the cells, which resulted in very high background fluorescence.

5.4.3 Alteration of HS expression upon experimental inflammation

Having investigated changes in cell surface HS of HEK 293 transfectants it was decided to examine relevant cell lines in physiological settings for changes in HS in response to external stimuli. Hypoxia was chosen to mimic ischemia, a condition donor organs undergo e.g. in transplantation settings, and stimulation of cell lines with the proinflammatory cytokines IFNγ and TNFα to simulate an inflammatory response. HEK 293 cells were included in the study as they were used extensively in previous experiments as they are easy to transfect.
HMEC-1 cells were chosen as a representative for an endothelial cell line, as endothelial HS is involved in almost every step of an inflammatory response, such as chemokine transcytosis and chemokine binding and presentation at the luminal surface (Wang et al., 2005). HK-2 cells are renal proximal tubular epithelial cells and are involved in the presentation of chemokines and other signal molecules on the basement membrane causing an influx of infiltrating cells into tubules (see section 3.1.1). The HepG2 cell line was selected to represent a liver epithelial cell line, as changes in liver HS have been shown to occur during rejection (see section 3.1.2).

In addition to changes in HS the biological significance of these changes should be tested by the application of binding experiments. To reassure that binding of CCL5 and FGF2 is indeed due to HS, CHO cells were employed. CHO wild type cells expressing HS were capable of sequestering chemokine and growth factor on its surface whereas CHO 745 cells, a mutant cell line lacking GAGs due to deleting the xylosyltransferase, was unable. This system is especially useful as CHOs lack FGFRs and CCRs (Di Marzio et al., 2005, Yayon et al., 1991), thus making the reaction solely dependent on HS and not any receptors.

Stimulation with proinflammatory cytokines TNFα and IFNγ and hypoxia of HEK 293 cells lead to an increase in 10e4 ($p<0.05$) and HS4C3 ($p<0.01$) staining whereas HS3A8 levels stayed unaltered. FGF2 binding decreased only slightly after stimulation and CCL5 did not bind to the cells at all. As HS3A8 expression did not change it seems plausible that FGF2 binding did not change

dramatically, as HS3A8 represents all modifications required for FGF2-binding (N-sulphation, C5-epimerization, 2O-sulphation and 6-sulphation).

HK-2 renal cells showed a decrease of all different HS epitopes after hypoxia/stimulation (10e4 and HS3A8 staining $p<0.01$; HS4C3 staining $p<0.05$ basal versus hypoxic). Again, a reduction in HS3A8 level is in line with decreased FGF2 binding. CCL5 binding, which is dependent on N-sulphation and O-sulphation, was reduced as well.

Lack of oxygen and stimulation resulted in a reduction of all HS domains of HepG2 cells ($p<0.01$); however, binding of FGF2 and CCL5 was increased marginally. This was surprising, as changes of HS3A8 seemed to correlate with changes in binding studies previously.

The observed decrease in cell surface HS could be due to shedding of syndecans and glypicans from the cell surface (Fux et al., 2009, Rehm et al., 2007), which also can be induced by growth factors such as FGF2 (Ding et al., 2005).

HMEC-1 cells did not alter HS3A8 or HS4C3 expression, but demonstrated a significant reduction in 10e4 staining ($p<0.01$). This is not consistent with earlier results which demonstrated an increase in 10e4 expression after stimulation with IFNγ and TNFα over time (Carter et al., 2003); however, it has to be pointed out that different time points have been analysed and therefore the results cannot be directly compared. In a very similar model the stimulation of dermal derived human microvascular endothelial cells with TNFα also resulted in a slight overall decrease in sulphation with unaltered levels of NDST1 (Krenn et al., 2008) which again would be in line with results obtained in this study. One possible explanation could be that cells were exposed to cytokines after serum starvation in one case (Carter et al., 2003) whereas cells were stimulated without prior starvation in the other case. FGF2 binding stayed unaltered but a small subset of cells showed increased capacity of CCL5 retention.

In summary, exogenously administered proinflammatoy cytokines and induction of hypoxia did result in distinct changes of the HS expression profile in conjunction with changes in ligand binding. As HS is regulated in a tissue/cell specific manner it could mean that cell lines exhibiting similar antibody staining profiles still differ in their fine structure, thus influencing the reactivity with its

ligands. The modifications essential for antibody recognition do give evidence about the existence of those modifications, not about their spatial arrangement which is crucial for protein binding. Furthermore, nothing is known about the hierarchy of the individual modifications. An increase in HS3A8 staining could be due to high levels of N-sulphation and moderate levels of O-sulphation, as well as little N-sulphation in combination with high levels of C5-epimerization.

In the future chain length and disaccharide composition analysis could, in conjunction with antibody staining and protein binding data, shed light into the complex biology of HS-protein interaction.

6 Final Discussion

6.1 Summary of Findings

- Role of Heparan Sulphate in Transplantation

Besides its involvement in embryonic development and adult physiology, HS regulates a range of pathophysiological processes as it binds a variety of biomolecules, including proinflammatory cytokines and chemokines, thereby shaping the inflammatory response (Parish, 2006). HS was shown to be involved in all steps of leukocyte extravastion, primarily by stabilising a chemokine gradient on the surface of the vascular endothelium (Wang et al., 2005). But HS is not only crucial for guiding inflammatory cells from the blood into the tissue, it is thought that different HS species also further direct immune cells to specific subcompartments within the tissue. Differential expression of HSPGs has been reported for renal allografts, where an increase in HS expression was observed during acute rejection (Ali et al., 2005a). It can be proposed that changes in HS expression resemble those of ligands at the specific stage of rejection. Therefore, the spatio-temporal expression of distinct HS epitopes in human renal and hepatic allografts were investigated in this part of the study.

HS expression in the kidney

An initial series of experiments were performed to optimise staining procedures and different retrieval methods were found to be effective for individual antibodies. Following optimisation, normal tissue was employed to determine the staining pattern of the HS antibodies.

The phage-display derived antibodies HS3A8 and HS4C3 revealed a similar staining pattern, which can be explained by similar essential target modifications, being N-sulphation, C5-epimerisation, 2-O-sulphation and 6-O-sulphation for HS3A8 and N-sulphation, 2-O-sulphation 6-O-sulphation and 3-O-sulphation for HS4C3. In addition, 10e4 staining, which is mostly dependent on N-sulphation, revealed similar results to phage display antibody staining. All

antibodies employed exhibited staining of tubules, the interstitium and glomeruli in renal biopsies. In addition, HS4C3 staining was also observed in the nucleus. Even though nuclear HS has been reported previously (Schubert et al., 2004), its role is not fully understood. One possible role for nuclear HS could be to function as a shuttle for nuclear transport for heparin binding factors, which once in the nucleus can directly influence cellular activities (Hsia et al., 2003). As nuclear staining of HS4C3 was not consistent during the studies, results had to be interpreted with reservation to this point and quantification of HS4C3 staining was therefore not feasible.

A total of 12 patients samples (5 cases of normal control biopsies, 3 cases of acute rejection 1a, 2 cases of acute rejection 2a and 2 cases of chronic rejection) were assayed for differential expression of HS epitopes in this study. While all HS species were expressed in normal control tissue, differential expression of distinct HS epitopes during different stages of rejection could be observed. 10e4 staining was significantly increased during acute rejection 1a, which is consistent with observations by Ali et al, 2005 who reported increased expression of N-sulphated HS during acute rejecting kidney allografts (Ali et al., 2005a). In contrast to 10e4 staining, HS3A8 staining (which represents N-sulphation, C5-epimerisation, 2-O-sulphation and 6-O-sulphation) did not alter during acute rejection, it did however increase significantly during chronic rejection. In order to investigate if changes in HS expression reflect changes in ligand binding, renal biopsies were assessed for the expression of the chemokine CCL2, whose involvement in renal disease has been reported previously (Robertson et al., 1998). CCL2 was found to be strongly upregulated during acute rejection 1a with moderate expression during later stages.

HS expression in the liver

After optimising the staining procedure, normal liver tissue was assessed for the expression and distribution of HS epitopes. HS3A8, HS4C3 and 10e4 antibodies all stained in a similar fashion in normal tissue and labelled sinusoids, bile ducts and basement membranes.

A total of 12 patients were examined for HS expression during liver rejection and chronic hepatitis in this study. The N-sulphated 10e4 epitope was hardly expressed at time 0 in transplants, but was induced at the time of moderate rejection with the most pronounced increase in bile ducts.
Ductular HS3A8 expression decreased slightly but significantly during moderate rejection before it increased during late rejection and chronic hepatitis. As previously experienced for renal tissue, antibody HS4C3 revealed inconsistent nuclear staining and could not be analysed quantitatively, qualitatively an increase in HS3A8 staining during chronic hepatitis could however be observed.

Physiological consequences of altered HS expression

Distinct HS epitopes, offering new or altered binding sites, have been identified during different stages of the rejection process in both organ systems investigated. N-sulphated HS domains appeared to be important during early time points of rejection whereas highly sulphated and heavily modified HS was expressed at later stages during chronic rejection in kidney and chronic hepatitis in liver. Changes of HS expression are believed to mirror those of its ligands and therefore it makes sense to discuss the consequences of altered HS epitope expression.

N-sulphation, represented by 10e4 staining, was increased during acute rejection 1a in kidney allografts and moderate acute rejection in liver allografts. As N-sulphation is the main requirement for L-selectin binding (Wang et al., 2005), it appears only logical that the expression of the specific HS species occurs at early time points. L-selectin expressed on leukocytes could encounter its HS ligand expressed on the endothelium, initiating the extravasation of leukocytes into the graft. Once the leukocytes have entered the graft, N-sulphated HS displayed by tubules (kidney) or bile ducts (liver) could guide subsets of immune cells further into the tissue (Celie et al., 2007). In line with this idea increased expression of CCL2 in conjunction with increased N-sulphation was found during acute renal rejection 1a, as CCL2, similar to L-selectin, binds to primarily N-sulphated HS (Schenauer et al., 2007).
In agreement with this model are also the findings that heavily modified HS, represented by HS3A8 and HS4C3 staining, was upregulated during chronic

stages of the rejection process. Modifications essential for HS3A8 staining resemble accurately the binding requirements for FGF2, with 2-O-sulphation being essential (Guglieri et al., 2008, Ornitz, 2000). The increased expression of HS3A8 epitope in interstitial and renal tubular cells during chronic rejection and bile ducts undergoing late rejection or chronic hepatitis could lead to a fibrotic environment involving FGF2. These fibrotic changes could be further facilitated by a breakdown of the anticoagulant environment as HS4C3 staining was upregulated during chronic rejections processes and represents ATIII binding sites due to existence of the rare 3-O-sulphation.

- Modulation of NDST1 and Cell Surface Heparan Sulphate

Many enzymes are involved in the biosynthesis of HS and the interplay of these enzymes determines the interaction profile of HS and its protein ligands. NDST1 is believed to be the key enzyme as it initiatites the modification process. Therefore, it was decided to investigate the effect of NDST1 modulation on HS expression and the consequences on ligand binding. Further, the changes observed in human allografts should be investigated *in vitro* using representative cell lines.

To start with, NDST1 over- and underexpressing constructs had to be created. Once stable clones were established, they were assayed for NDST1 expression. NDST1 silenced clones revealed a reduction of 64% on the mRNA level, which was confirmed at the protein level by Western blotting. Further, the reduction of NDST resulted in a decrease of N-sulphation, as demonstrated by 10e4 staining. This is in accordance with the literature where decreased N-sulphation after NDST1 silencing was reported (Deligny et al., 2010, Pankonin et al., 2005). Unfortunately NDST1 silenced cells could not be employed for further experiments due to the existence of the GFP within in the cells and problems with high background fluorescence of TRITC conjugated secondary reagents.

Similarly to NDST1 silenced cells, NDST1 overexpressing transfectants revealed increased NDST1 expression in conjunction with increased 10e4

staining, which is also in line with the literature (Bengtsson et al., 2003, Pikas et al., 2000). Interestingly, when assessed for HS3A8 and HS4C3 expression, the NDST1 overexpressing clone showed a marked reduction in both HS domains. The observation that increased N-sulphation is not necessarily accompanied by an increase of other modifications was also made by other research groups (Pikas et al., 2000, Rops et al., 2008).

Different approaches were undertaken to investigate the physiological outcome of altered HS expression. An FGF2 binding kit was employed and NDST1 overexpressing cells showed a slight decrease in FGF2 binding on the cell surface in agreement with a reduction in HS3A8 and HS4C3 staining, albeit an increased expression of N-sulphated domains. This shows that one has to be careful in determining HS expression indirectly by FGF2 binding, as suggested by some research groups (Garner et al., 2008).

In addition, the potential of NDST1 overexpressing cells to retain and present chemokines on their surface was investigated. An initial series of experiments were performed to validate the chemokine CCL5-biotin *in vitro*. Heparin affinity chromatography demonstrated that the biotinylated form of CCL5 had the same affinity as the wild type form and Calcium-flux analysis confirmed receptor activation. A series of migration assays proved that CCL-biotin was able to induce migration. Employed in a chemokine presentation assay, NDST1 overexpressing cells were capable of retaining more CCL5 on their surface when compared to wild type cells.

Ligand binding data of NDST1 transfectants resembled the ligand binding profile in transplant tissue. In both circumstances, increased N-sulphation correlated with increased potential to sequester and present chemokines, namely CCL2 in renal tissue and CCL5 in NDST1 overexpressing transfectant cells, confirming the dependency of chemokines on N-sulphation, whereas increased expression of the HS3A8 epitope was concurrent with increased FGF2 binding in both transplant tissue and the transfectant cell line.

To mimic the changes seen in transplant settings, appropriate cell lines representing the individual organs were chosen (HMEC-1 cells representing the endothelium, HK-2 renal tubular epithelial cells and HepG2 hepatocytes) and

inflammatory conditions were simulated by stimulation of cell lines with the proinflammatory cytokines TNFα and IFNγ. In addition, hypoxia mimicking ischemia after transplantation was induced by non-vented tissue culture flasks. Besides the changes in HS expression binding experiments with FGF2 and CCL5 were employed.

Overall, exogenous administered proinflammatory cytokines and induction of hypoxia resulted in almost identical changes in HS epitope expression. HK2 and HepG2 cells revealed a decrease in expression of all HS species. The reduction of cell surface HS could be due do constitutive shedding of syndecans and glypicans from the cell surface of cultured cells (Fux et al., 2009). In addition, inducible shedding of syndecans dependent on FGF2 has been reported, which could also explain the apparent reduction of HS in conjunction with reduced FGF2 binding (Ding et al., 2005). Ischemia, which was simulated by hypoxia in this study, is a condition organs undergo upon removal from the donor. Shedding of HS chains and syndecans has been reported for patients during ischemia (Rehm et al., 2007). Functionally, shed HS is capable of activating antigen presenting cells (APC) which further may initiate the T-helper 1 type response in transplant rejection (Ali et al., 2003).
Interestingly, while this decrease in HS resulted in decreased ligand binding for HK-2 cells, the same decrease in HS resulted in an increased binding of HS ligand for HepG2 cells. As for HMEC-1 cells, levels of HS stayed almost unaltered with a small increase of CCL5 binding, which is dependent on N- and O-sulphation (Schenauer et al., 2007, Shaw et al., 2004) of a small subset of cells. This implies that albeit similar HS profile, reactivity with protein ligands can still differ due to the spatial arrangements of the residues involved in binding.

- Regulation of Heparan Sulphate biosynthesis

The GAGosome model of HS biosynthesis is based on the interaction of individual enzymes with each other rather then the strict sequential model.

In both models, NDST1 is a key enzyme in HS biosynthesis and was therefore targeted for studying the regulation of HS biosynthesis on the protein level by Tandem affinity purification.

Initially, a tagged form of NDST1 was created for the intended affinity purification studies. After transfection of the construct into HEK 293 cells, stable clones with increased NDST1 expression were established. In a series of experiments, cell number and lysis conditions were optimised carefully.
In all affinity purifications carried out beta tubulin was the only partner to constantly co-elute with NDST1 and reliable p- and e-scores from Mascot analysis confirmed the genuine interaction. Previous studies have shown other glycosylation enzymes to interact with beta tubulin, namely NDST2 and ß-1,4-galactosyltransferase (Ledin et al., 2006, Schonherr and Hausser, 2000, Yamaguchi and Fukuda, 1995). This could mean that beta tubulin is acting as a receptor for these enzymes, as no Golgi retention signals are known, thus influencing their rate of transport.
The finding that no other HS biosynthetic enzyme co-eluted with NDST1 would rather oppose the GAGosome model and strengthen the idea of a more generic role in cell movement and migration, as indicated by the interaction with beta tubulin. This view is further supported by the findings of altered HS epitope expression in various cell lines upon induction of hypoxia or experimental inflammation, where transcriptional control of individual enzymes appears to be involved. Even though no analysis of mRNA expression of individual enzymes was performed at the time, the observed changes in HS expression pattern most likely reflect changes in enzyme expression and/or activity. As HS expression in different cell lines was due to endogenous levels of enzymes rather than exogenous, the change in expression profile must be due to transcriptional regulation rather than aberrant expression of proteins as often seen for transfected cell lines.

6.2 Implications of this Study

It is well established today that HSPGs regulate normal physiology as well as pathophysiology by binding a large array of molecules, including those involved

in inflammatory responses and rejection. It seems that certain species of HS can be linked to certain disease states, such as allograft rejection or cancer (Ali et al., 2005a, Rienstra et al., 2010, Tatrai et al., 2010), thus making HS a target for therapeutic intervention.
Modulation of chemokine-HS interaction may allow the blockade of an array of proinflammatory cytokines in a localised fashion and would therefore be hugely desirable as current immunosuppressive calcineurin inhibitors such as cyclosporine A predominantly target IL-2 (interleukin-2) and γ-interferons.

Trying to prevent immune cells from invading the graft can be achieved either by targeting chemokines, the molecules guiding the cells from the blood into the tissue, or HSPGs, which offer binding sites allowing chemokines to build up gradients crucial for leukocyte extravasation. Due to the redundancy within the chemokine system HS was chosen for investigations with regards to inflammation in this study.

A few studies have highlighted the importance of differential expression of HS during various diseases and experiments were carried out to determine the changes related to allograft rejection. Distinct HS epitopes could be linked to different stages of graft rejection and results from renal allografts where similar to results obtained with liver allografts. Changes observed in transplant tissue were also partially confirmed by *in vitro* studies employing appropriate cell lines and NDST1 transfectants for binding studies.
Exploring changes in renal HS during rejection could also be hugely beneficial in the clinical setting. As HSPGs are secreted via the kidney with the urine, they could potentially be used as some kind of biomarker in the future.

In the clinic, antibodies recognizing distinct HS domains could be administered, blocking corresponding binding sites for protein ligands thus preventing leukocytes from entering the tissue, limiting the inflammatory response.
Likewise, chemokines with improved HS binding capacity and knocked out GPCR activity could be used to displace the wild type chemokines, as already shown by one research group (Potzinger et al., 2006).

Alternatively, one could target the biosynthetic enzyme responsible for the modification essential for ligand binding directly with small inhibitory peptides which requires a deeper understanding of the regulation of HS biosynthesis. In case of NDST1 and other glycosyltransferases beta tubulin has been proposed as interacting partner and interfering with HS biosynthesis might have an overall greater consequence on cell movement and migration.

Taken together, this study indicates that the chemokine–GAG interaction proves an attractive target for therapeutic intervention.

6.3 Future directions

It is evident that future work will be required to further the understanding of chemokine-HS interplay.

Besides the insightful results from allograft studies, an increase in sample size is required and the descriptive results of HS epitope expression during rejection should be matched with physiological ligand binding studies. Therefore, binding assays employing molecules relevant to rejection processes (such as CCL5, CCL2 and other chemokines, FGF2, L-selectin and antithrombin III) should be optimised to allow matching of ligands to selective HS species. Also, H&E (haematoxylin and eosin) staining should be incorporated in the future, which amongst others would help identifying blood vessels.

Overall, also other tissues and cell lines should be examined for inflammation related changes in HS. In addition to optimised binding studies, cell lines with modified HS could also be employed in a leukocyte rolling assay under controlled shear using a dynamic flow chamber model simulating leukocyte rolling and adhesion in blood vessels. This would be more appropriate than a static adhesion assay.
In addition, a HS ELISA could clarify if reduced levels of HS expression following ischemia and inflammation are indeed due to HS shedding rather than a decrease in cell surface expression. Although HS shedding can be mediated

by proteases and phospholipases, evaluation of heparanase could also help to understand this process.

Cell lines with altered HS expression as well as NDST transfectants could be analysed for HS composition by disaccharide analysis by reverse-phase HPLC (high-performance liquid chromtatography) and ESI-MS (electrospray ionisation mass spectrometry). This, in conjunction with antibody staining and ligand binding, would allow identification of specific binding sites.

Finally, the interaction of NDST1 with beta tubulin should be verified by Co-IP studies or FRET. A NDST1 silenced transfectant could also help verifying this interaction, preferably with a viral-based system as this would yield better results and a broader range of transfectable cell lines compared to a plasmid based approach.

6.4 Conclusions

In summary, this study aimed to further our understanding of HS biology. A number of different approaches have been made to highlight the importance of HSPGs in inflammation and rejection. Distinct HS epitopes have been identified which could be linked to different stages of allograft rejection in both kidney and liver allografts. Observations from transplant tissues were partially confirmed by *in vitro* studies employing relevant cell lines and NDST1 transfectants in HS composition and binding assays. An interesting observation was the interaction of the HS biosynthetic enzyme NDST1 with beta tubulin. This interaction could well be of general importance beside HS biology, as it possibly illuminates a model of Golgi localisation and retention of glycosylation enzymes.

7 References

References

ABRAMSSON, A., KURUP, S., BUSSE, M., YAMADA, S., LINDBLOM, P., SCHALLMEINER, E., STENZEL, D., SAUVAGET, D., LEDIN, J., RINGVALL, M., LANDEGREN, U., KJELLEN, L., BONDJERS, G., LI, J. P., LINDAHL, U., SPILLMANN, D., BETSHOLTZ, C. & GERHARDT, H. (2007) Defective N-sulfation of heparan sulfate proteoglycans limits PDGF-BB binding and pericyte recruitment in vascular development. *Genes Dev,* 21**,** 316-31.

AI, X., DO, A. T., KUSCHE-GULLBERG, M., LINDAHL, U., LU, K. & EMERSON, C. P., JR. (2006) Substrate specificity and domain functions of extracellular heparan sulfate 6-O-endosulfatases, QSulf1 and QSulf2. *J Biol Chem,* 281**,** 4969-76.

AIKAWA, J. & ESKO, J. D. (1999) Molecular cloning and expression of a third member of the heparan sulfate/heparin GlcNAc N-deacetylase/ N-sulfotransferase family. *J Biol Chem,* 274**,** 2690-5.

AIKAWA, J., GROBE, K., TSUJIMOTO, M. & ESKO, J. D. (2001) Multiple isozymes of heparan sulfate/heparin GlcNAc N-deacetylase/GlcN N-sulfotransferase. Structure and activity of the fourth member, NDST4. *J Biol Chem,* 276**,** 5876-82.

AL-HAMIDI, A., PEKALSKI, M., ROBERTSON, H., ALI, S. & KIRBY, J. A. (2008) Renal allograft rejection: the contribution of chemokines to the adhesion and retention of alphaE(CD103) beta7 integrin-expressing intratubular T cells. *Mol Immunol,* 45**,** 4000-7.

ALEXANDER, C. M., REICHSMAN, F., HINKES, M. T., LINCECUM, J., BECKER, K. A., CUMBERLEDGE, S. & BERNFIELD, M. (2000) Syndecan-1 is required for Wnt-1-induced mammary tumorigenesis in mice. *Nat Genet,* 25**,** 329-32.

ALI, S., FRITCHLEY, S. J., CHAFFEY, B. T. & KIRBY, J. A. (2002) Contribution of the putative heparan sulfate-binding motif BBXB of RANTES to transendothelial migration. *Glycobiology,* 12**,** 535-43.

ALI, S., HARDY, L. A. & KIRBY, J. A. (2003) Transplant immunobiology: a crucial role for heparan sulfate glycosaminoglycans? *Transplantation,* 75**,** 1773-82.

ALI, S., MALIK, G., BURNS, A., ROBERTSON, H. & KIRBY, J. A. (2005a) Renal transplantation: examination of the regulation of chemokine binding during acute rejection. *Transplantation,* 79**,** 672-9.

ALI, S., PALMER, A. C., FRITCHLEY, S. J., MALEY, Y. & KIRBY, J. A. (2001) Multimerization of monocyte chemoattractant protein-1 is not required for glycosaminoglycan-dependent transendothelial chemotaxis. *Biochem J,* 358**,** 737-45.

ALI, S., ROBERTSON, H., WAIN, J. H., ISAACS, J. D., MALIK, G. & KIRBY, J. A. (2005b) A non-glycosaminoglycan-binding variant of CC chemokine ligand 7 (monocyte chemoattractant protein-3) antagonizes chemokine-mediated inflammation. *J Immunol,* 175**,** 1257-66.

ALLEN, B. L. & RAPRAEGER, A. C. (2003) Spatial and temporal expression of heparan sulfate in mouse development regulates FGF and FGF receptor assembly. *J Cell Biol,* 163**,** 637-48.

AMBROSIO, G. & TRITTO, I. (1999) Reperfusion injury: experimental evidence and clinical implications. *Am Heart J,* 138**,** S69-75.

ANAND, A. C., HUBSCHER, S. G., GUNSON, B. K., MCMASTER, P. & NEUBERGER, J. M. (1995) Timing, significance, and prognosis of late acute liver allograft rejection. *Transplantation,* 60**,** 1098-103.

ARIKAWA-HIRASAWA, E., WATANABE, H., TAKAMI, H., HASSELL, J. R. & YAMADA, Y. (1999) Perlecan is essential for cartilage and cephalic development. *Nat Genet,* 23**,** 354-8.

BAME, K. J. (2001) Heparanases: endoglycosidases that degrade heparan sulfate proteoglycans. *Glycobiology,* 11**,** 91R-98R.

BARREIRO, O., MARTIN, P., GONZALEZ-AMARO, R. & SANCHEZ-MADRID, F. (2010) Molecular cues guiding inflammatory responses. *Cardiovasc Res,* 86**,** 174-82.

BARTH, H., SCHNOBER, E. K., ZHANG, F., LINHARDT, R. J., DEPLA, E., BOSON, B., COSSET, F. L., PATEL, A. H., BLUM, H. E. & BAUMERT, T. F. (2006) Viral and cellular determinants of the hepatitis C virus envelope-heparan sulfate interaction. *J Virol,* 80**,** 10579-90.

BARTHEL, S. R., GAVINO, J. D., DESCHENY, L. & DIMITROFF, C. J. (2007) Targeting selectins and selectin ligands in inflammation and cancer. *Expert Opin Ther Targets,* 11**,** 1473-91.

BASHKIN, P., DOCTROW, S., KLAGSBRUN, M., SVAHN, C. M., FOLKMAN, J. & VLODAVSKY, I. (1989) Basic fibroblast growth factor binds to subendothelial extracellular matrix and is released by heparitinase and heparin-like molecules. *Biochemistry,* 28**,** 1737-43.

BATALLER, R. & BRENNER, D. A. (2005) Liver fibrosis. *J Clin Invest,* 115**,** 209-18.

BATTAGLIA, C., MAYER, U., AUMAILLEY, M. & TIMPL, R. (1992) Basement-membrane heparan sulfate proteoglycan binds to laminin by its heparan sulfate chains and to nidogen by sites in the protein core. *Eur J Biochem,* 208**,** 359-66.

BATTS, K. P. (1999) Acute and chronic hepatic allograft rejection: pathology and classification. *Liver Transpl Surg,* 5**,** S21-9.

BEAUSSIER, M., WENDUM, D., SCHIFFER, E., DUMONT, S., REY, C., LIENHART, A. & HOUSSET, C. (2007) Prominent contribution of portal mesenchymal cells to liver fibrosis in ischemic and obstructive cholestatic injuries. *Lab Invest,* 87**,** 292-303.

BELENKAYA, T. Y., HAN, C., YAN, D., OPOKA, R. J., KHODOUN, M., LIU, H. & LIN, X. (2004) Drosophila Dpp morphogen movement is independent of dynamin-mediated endocytosis but regulated by the glypican members of heparan sulfate proteoglycans. *Cell,* 119**,** 231-44.

BENGTSSON, J., ERIKSSON, I. & KJELLEN, L. (2003) Distinct effects on heparan sulfate structure by different active site mutations in NDST-1. *Biochemistry,* 42**,** 2110-5.

BERNFIELD, M., GOTTE, M., PARK, P. W., REIZES, O., FITZGERALD, M. L., LINCECUM, J. & ZAKO, M. (1999) Functions of cell surface heparan sulfate proteoglycans. *Annu Rev Biochem,* 68**,** 729-77.

BERNFIELD, M., KOKENYESI, R., KATO, M., HINKES, M. T., SPRING, J., GALLO, R. L. & LOSE, E. J. (1992) Biology of the syndecans: a family of transmembrane heparan sulfate proteoglycans. *Annu Rev Cell Biol,* 8**,** 365-93.

BISHOP, J. R., SCHUKSZ, M. & ESKO, J. D. (2007) Heparan sulphate proteoglycans fine-tune mammalian physiology. *Nature,* 446**,** 1030-7.

BOHMIG, G. A., EXNER, M., WATSCHINGER, B., WENTER, C., WAHRMANN, M., OSTERREICHER, C., SAEMANN, M. D., MERSICH, N., HORL, W. H., ZLABINGER, G. J. & REGELE, H. (2001) C4d deposits in renal allografts are associated with inferior graft outcome. *Transplant Proc,* 33**,** 1151-2.

BORN, J., JANN, K., ASSMANN, K. J., LINDAHL, U. & BERDEN, J. H. (1996) N-Acetylated domains in heparan sulfates revealed by a monoclonal antibody against the Escherichia coli K5 capsular polysaccharide. Distribution of the cognate epitope in normal human kidney and transplant kidney with chronic vascular rejection. *J Biol Chem,* 271**,** 22802-9.

BRUCKNER, A., POLGE, C., LENTZE, N., AUERBACH, D. & SCHLATTNER, U. (2009) Yeast two-hybrid, a powerful tool for systems biology. *Int J Mol Sci,* 10**,** 2763-88.

BULLOCK, S. L., FLETCHER, J. M., BEDDINGTON, R. S. & WILSON, V. A. (1998) Renal agenesis in mice homozygous for a gene trap mutation in the gene encoding heparan sulfate 2-sulfotransferase. *Genes Dev,* 12**,** 1894-906.

BURCKSTUMMER, T., BENNETT, K. L., PRERADOVIC, A., SCHUTZE, G., HANTSCHEL, O., SUPERTI-FURGA, G. & BAUCH, A. (2006) An efficient tandem affinity purification procedure for interaction proteomics in mammalian cells. *Nat Methods,* 3**,** 1013-9.

BUSSE, M. & KUSCHE-GULLBERG, M. (2003) In vitro polymerization of heparan sulfate backbone by the EXT proteins. *J Biol Chem,* 278**,** 41333-7.

BUTCHER, E. C. & PICKER, L. J. (1996) Lymphocyte homing and homeostasis. *Science,* 272**,** 60-6.

CANO-GAUCI, D. F., SONG, H. H., YANG, H., MCKERLIE, C., CHOO, B., SHI, W., PULLANO, R., PISCIONE, T. D., GRISARU, S., SOON, S., SEDLACKOVA, L., TANSWELL, A. K., MAK, T. W., YEGER, H., LOCKWOOD, G. A., ROSENBLUM, N. D. & FILMUS, J. (1999) Glypican-3-deficient mice exhibit developmental overgrowth and some of the abnormalities typical of Simpson-Golabi-Behmel syndrome. *J Cell Biol,* 146**,** 255-64.

CAREY, D. J. (1997) Syndecans: multifunctional cell-surface co-receptors. *Biochem J,* 327 (Pt 1) **,** 1-16.

CARLSSON, P., PRESTO, J., SPILLMANN, D., LINDAHL, U. & KJELLEN, L. (2008) Heparin/heparan sulfate biosynthesis: processive formation of N-sulfated domains. *J Biol Chem,* 283**,** 20008-14.

CARTER, N. M., ALI, S. & KIRBY, J. A. (2003) Endothelial inflammation: the role of differential expression of N-deacetylase/N-sulphotransferase enzymes in alteration of the immunological properties of heparan sulphate. *J Cell Sci,* 116**,** 3591-600.

CATLOW, K. R., DEAKIN, J. A., WEI, Z., DELEHEDDE, M., FERNIG, D. G., GHERARDI, E., GALLAGHER, J. T., PAVAO, M. S. & LYON, M. (2008) Interactions of hepatocyte growth factor/scatter factor with various glycosaminoglycans reveal an important interplay between the presence of iduronate and sulfate density. *J Biol Chem,* 283**,** 5235-48.

CELIE, J. W., KEUNING, E. D., BEELEN, R. H., DRAGER, A. M., ZWEEGMAN, S., KESSLER, F. L., SOININEN, R. & VAN DEN BORN, J. (2005) Identification of L-selectin binding heparan sulfates attached to collagen type XVIII. *J Biol Chem,* 280**,** 26965-73.

CELIE, J. W., REIJMERS, R. M., SLOT, E. M., BEELEN, R. H., SPAARGAREN, M., TER WEE, P. M., FLORQUIN, S. & VAN DEN BORN, J. (2008) Tubulointerstitial heparan sulfate proteoglycan changes in human renal diseases correlate with leukocyte influx and proteinuria. *Am J Physiol Renal Physiol,* 294**,** F253-63.

CELIE, J. W., RUTJES, N. W., KEUNING, E. D., SOININEN, R., HELJASVAARA, R., PIHLAJANIEMI, T., DRAGER, A. M., ZWEEGMAN, S., KESSLER, F. L., BEELEN, R. H., FLORQUIN, S., ATEN, J. & VAN

DEN BORN, J. (2007) Subendothelial heparan sulfate proteoglycans become major L-selectin and monocyte chemoattractant protein-1 ligands upon renal ischemia/reperfusion. *Am J Pathol,* 170**,** 1865-78.

CERUTTI, H. & CASAS-MOLLANO, J. A. (2006) On the origin and functions of RNA-mediated silencing: from protists to man. *Curr Genet,* 50**,** 81-99.

CHAKRAVARTY, L., ROGERS, L., QUACH, T., BRECKENRIDGE, S. & KOLATTUKUDY, P. E. (1998) Lysine 58 and histidine 66 at the C-terminal alpha-helix of monocyte chemoattractant protein-1 are essential for glycosaminoglycan binding. *J Biol Chem,* 273**,** 29641-7.

CHEN, P., ABACHERLI, L. E., NADLER, S. T., WANG, Y., LI, Q. & PARKS, W. C. (2009) MMP7 shedding of syndecan-1 facilitates re-epithelialization by affecting alpha(2) beta(1) integrin activation. *PLoS One,* 4**,** e6565.

CHEN, Y., GOTTE, M., LIU, J. & PARK, P. W. (2008) Microbial subversion of heparan sulfate proteoglycans. *Mol Cells,* 26**,** 415-26.

COLE, G. J. & HALFTER, W. (1996) Agrin: an extracellular matrix heparan sulfate proteoglycan involved in cell interactions and synaptogenesis. *Perspect Dev Neurobiol,* 3**,** 359-71.

COLVIN, R. B. (2006) C4d in liver allografts: a sign of antibody-mediated rejection? *Am J Transplant,* 6**,** 447-8.

COLVIN, R. B. (2007) Antibody-mediated renal allograft rejection: diagnosis and pathogenesis. *J Am Soc Nephrol,* 18**,** 1046-56.

CORNELL, L. D., SMITH, R. N. & COLVIN, R. B. (2008) Kidney transplantation: mechanisms of rejection and acceptance. *Annu Rev Pathol,* 3**,** 189-220.

CRESPO, M., PASCUAL, M., TOLKOFF-RUBIN, N., MAUIYYEDI, S., COLLINS, A. B., FITZPATRICK, D., FARRELL, M. L., WILLIAMS, W. W., DELMONICO, F. L., COSIMI, A. B., COLVIN, R. B. & SAIDMAN, S. L. (2001) Acute humoral rejection in renal allograft recipients: I. Incidence, serology and clinical characteristics. *Transplantation,* 71**,** 652-8.

D'AMBROSIO, D., PANINA-BORDIGNON, P. & SINIGAGLIA, F. (2003) Chemokine receptors in inflammation: an overview. *J Immunol Methods,* 273**,** 3-13.

D'ANTIGA, L., DHAWAN, A., PORTMANN, B., FRANCAVILLA, R., RELA, M., HEATON, N. & MIELI-VERGANI, G. (2002) Late cellular rejection in paediatric liver transplantation: aetiology and outcome. *Transplantation,* 73**,** 80-4.

DAI, E., LIU, L. Y., WANG, H., MCIVOR, D., SUN, Y. M., MACAULAY, C., KING, E., MUNUSWAMY-RAMANUJAM, G., BARTEE, M. Y., WILLIAMS, J., DAVIDS, J., CHARO, I., MCFADDEN, G., ESKO, J. D. & LUCAS, A. R. (2010) Inhibition of chemokine-glycosaminoglycan interactions in donor tissue reduces mouse allograft vasculopathy and transplant rejection. *PLoS One,* 5**,** e10510.

DAVID, G., BAI, X. M., VAN DER SCHUEREN, B., CASSIMAN, J. J. & VAN DEN BERGHE, H. (1992) Developmental changes in heparan sulfate expression: in situ detection with mAbs. *J Cell Biol,* 119**,** 961-75.

DELIGNY, A., DENYS, A., MARCANT, A., MELCHIOR, A., MAZURIER, J., VAN KUPPEVELT, T. H. & ALLAIN, F. (2010) Synthesis of heparan sulfate with cyclophilin B-binding properties is determined by cell type-specific expression of sulfotransferases. *J Biol Chem,* 285**,** 1701-15.

DEMETRIS, A., ADAMS, D., BELLAMY, C., BLAKOLMER, K., CLOUSTON, A., DHILLON, A. P., FUNG, J., GOUW, A., GUSTAFSSON, B., HAGA, H., HARRISON, D., HART, J., HUBSCHER, S., JAFFE, R., KHETTRY, U., LASSMAN, C., LEWIN, K., MARTINEZ, O., NAKAZAWA, Y., NEIL, D., PAPPO, O., PARIZHSKAYA, M., RANDHAWA, P., RASOUL-ROCKENSCHAUB, S., REINHOLT, F., REYNES, M., ROBERT, M., TSAMANDAS, A., WANLESS, I., WIESNER, R., WERNERSON, A., WRBA, F., WYATT, J. & YAMABE, H. (2000) Update of the International Banff Schema for Liver Allograft Rejection: working recommendations for the histopathologic staging and reporting of chronic rejection. An International Panel. *Hepatology,* 31**,** 792-9.

DEMETRIS, A. J. & MARKUS, B. H. (1989) Immunopathology of liver transplantation. *Crit Rev Immunol,* 9**,** 67-92.

DENNISSEN, M. A., JENNISKENS, G. J., PIEFFERS, M., VERSTEEG, E. M., PETITOU, M., VEERKAMP, J. H. & VAN KUPPEVELT, T. H. (2002) Large, tissue-regulated domain diversity of heparan sulfates demonstrated by phage display antibodies. *J Biol Chem,* 277**,** 10982-6.

DESAI, M. & NEUBERGER, J. (2009) Chronic liver allograft dysfunction. *Transplant Proc,* 41**,** 773-6.

DESHMANE, S. L., KREMLEV, S., AMINI, S. & SAWAYA, B. E. (2009) Monocyte chemoattractant protein-1 (MCP-1) : an overview. *J Interferon Cytokine Res,* 29**,** 313-26.

DHOOT, G. K., GUSTAFSSON, M. K., AI, X., SUN, W., STANDIFORD, D. M. & EMERSON, C. P., JR. (2001) Regulation of Wnt signaling and embryo patterning by an extracellular sulfatase. *Science,* 293**,** 1663-6.

DI MARZIO, P., DAI, W. W., FRANCHIN, G., CHAN, A. Y., SYMONS, M. & SHERRY, B. (2005) Role of Rho family GTPases in CCR1- and CCR5-induced actin reorganization in macrophages. *Biochem Biophys Res Commun,* 331**,** 909-16.

DING, K., LOPEZ-BURKS, M., SANCHEZ-DURAN, J. A., KORC, M. & LANDER, A. D. (2005) Growth factor-induced shedding of syndecan-1 confers glypican-1 dependence on mitogenic responses of cancer cells. *J Cell Biol,* 171**,** 729-38.

DIXON, J., LOFTUS, S. K., GLADWIN, A. J., SCAMBLER, P. J., WASMUTH, J. J. & DIXON, M. J. (1995) Cloning of the human heparan sulfate-N-deacetylase/N-sulfotransferase gene from the Treacher Collins syndrome candidate region at 5q32-q33.1. *Genomics,* 26**,** 239-44.

DOWSLAND, M. H., HARVEY, J. R., LENNARD, T. W., KIRBY, J. A. & ALI, S. (2003) Chemokines and breast cancer: a gateway to revolutionary targeted cancer treatments? *Curr Med Chem,* 10**,** 579-92.

EBARA, T., CONDE, K., KAKO, Y., LIU, Y., XU, Y., RAMAKRISHNAN, R., GOLDBERG, I. J. & SHACHTER, N. S. (2000) Delayed catabolism of apoB-48 lipoproteins due to decreased heparan sulfate proteoglycan production in diabetic mice. *J Clin Invest,* 105**,** 1807-18.

ECHTERMEYER, F., STREIT, M., WILCOX-ADELMAN, S., SAONCELLA, S., DENHEZ, F., DETMAR, M. & GOETINCK, P. (2001) Delayed wound

repair and impaired angiogenesis in mice lacking syndecan-4. *J Clin Invest,* 107**,** R9-R14.

EL-SAWY, T., FAHMY, N. M. & FAIRCHILD, R. L. (2002) Chemokines: directing leukocyte infiltration into allografts. *Curr Opin Immunol,* 14**,** 562-8.

ESCOBAR GALVIS, M. L., JIA, J., ZHANG, X., JASTREBOVA, N., SPILLMANN, D., GOTTFRIDSSON, E., VAN KUPPEVELT, T. H., ZCHARIA, E., VLODAVSKY, I., LINDAHL, U. & LI, J. P. (2007) Transgenic or tumor-induced expression of heparanase upregulates sulfation of heparan sulfate. *Nat Chem Biol,* 3**,** 773-8.

ESKO, J. D. & LINDAHL, U. (2001) Molecular diversity of heparan sulfate. *J Clin Invest,* 108**,** 169-73.

ESKO, J. D. & SELLECK, S. B. (2002) Order out of chaos: assembly of ligand binding sites in heparan sulfate. *Annu Rev Biochem,* 71**,** 435-71.

ESKO, J. D. & ZHANG, L. (1996) Influence of core protein sequence on glycosaminoglycan assembly. *Curr Opin Struct Biol,* 6**,** 663-70.

FAN, G., XIAO, L., CHENG, L., WANG, X., SUN, B. & HU, G. (2000) Targeted disruption of NDST-1 gene leads to pulmonary hypoplasia and neonatal respiratory distress in mice. *FEBS Lett,* 467**,** 7-11.

FARACH-CARSON, M. C. & CARSON, D. D. (2007) Perlecan--a multifunctional extracellular proteoglycan scaffold. *Glycobiology,* 17**,** 897-905.

FILMUS, J., CAPURRO, M. & RAST, J. (2008) Glypicans. *Genome Biol,* 9**,** 224.

FILMUS, J. & SELLECK, S. B. (2001) Glypicans: proteoglycans with a surprise. *J Clin Invest,* 108**,** 497-501.

FITZGERALD, M. L., WANG, Z., PARK, P. W., MURPHY, G. & BERNFIELD, M. (2000) Shedding of syndecan-1 and -4 ectodomains is regulated by multiple signaling pathways and mediated by a TIMP-3-sensitive metalloproteinase. *J Cell Biol,* 148**,** 811-24.

FODOR, W. L., WILLIAMS, B. L., MATIS, L. A., MADRI, J. A., ROLLINS, S. A., KNIGHT, J. W., VELANDER, W. & SQUINTO, S. P. (1994) Expression of a functional human complement inhibitor in a transgenic

pig as a model for the prevention of xenogeneic hyperacute organ rejection. *Proc Natl Acad Sci U S A,* 91**,** 11153-7.

FORSBERG, E. & KJELLEN, L. (2001) Heparan sulfate: lessons from knockout mice. *J Clin Invest,* 108**,** 175-80.

FORSBERG, E., PEJLER, G., RINGVALL, M., LUNDERIUS, C., TOMASINI-JOHANSSON, B., KUSCHE-GULLBERG, M., ERIKSSON, I., LEDIN, J., HELLMAN, L. & KJELLEN, L. (1999) Abnormal mast cells in mice deficient in a heparin-synthesizing enzyme. *Nature,* 400**,** 773-6.

FRIEDMAN, S. L., ROLL, F. J., BOYLES, J. & BISSELL, D. M. (1985) Hepatic lipocytes: the principal collagen-producing cells of normal rat liver. *Proc Natl Acad Sci U S A,* 82**,** 8681-5.

FRITCHLEY, S. J., KIRBY, J. A. & ALI, S. (2000) The antagonism of interferon-gamma (IFN-gamma) by heparin: examination of the blockade of class II MHC antigen and heat shock protein-70 expression. *Clin Exp Immunol,* 120**,** 247-52.

FUKAI, N., EKLUND, L., MARNEROS, A. G., OH, S. P., KEENE, D. R., TAMARKIN, L., NIEMELA, M., ILVES, M., LI, E., PIHLAJANIEMI, T. & OLSEN, B. R. (2002) Lack of collagen XVIII/endostatin results in eye abnormalities. *Embo J,* 21**,** 1535-44.

FUSTER, M. M., WANG, L., CASTAGNOLA, J., SIKORA, L., REDDI, K., LEE, P. H., RADEK, K. A., SCHUKSZ, M., BISHOP, J. R., GALLO, R. L., SRIRAMARAO, P. & ESKO, J. D. (2007) Genetic alteration of endothelial heparan sulfate selectively inhibits tumor angiogenesis. *J Cell Biol,* 177**,** 539-49.

FUX, L., ILAN, N., SANDERSON, R. D. & VLODAVSKY, I. (2009) Heparanase: busy at the cell surface. *Trends Biochem Sci,* 34**,** 511-9.

GABELE, E., BRENNER, D. A. & RIPPE, R. A. (2003) Liver fibrosis: signals leading to the amplification of the fibrogenic hepatic stellate cell. *Front Biosci,* 8**,** d69-77.

GALLAI, M., KOVALSZKY, I., KNITTEL, T., NEUBAUER, K., ARMBRUST, T. & RAMADORI, G. (1996) Expression of extracellular matrix proteoglycans perlecan and decorin in carbon-tetrachloride-injured rat liver and in isolated liver cells. *Am J Pathol,* 148**,** 1463-71.

GARNER, O. B., YAMAGUCHI, Y., ESKO, J. D. & VIDEM, V. (2008) Small changes in lymphocyte development and activation in mice through tissue-specific alteration of heparan sulphate. *Immunology,* 125**,** 420-9.

GAUTAM, M., NOAKES, P. G., MOSCOSO, L., RUPP, F., SCHELLER, R. H., MERLIE, J. P. & SANES, J. R. (1996) Defective neuromuscular synaptogenesis in agrin-deficient mutant mice. *Cell,* 85**,** 525-35.

GAVIN, A. C., BOSCHE, M., KRAUSE, R., GRANDI, P., MARZIOCH, M., BAUER, A., SCHULTZ, J., RICK, J. M., MICHON, A. M., CRUCIAT, C. M., REMOR, M., HOFERT, C., SCHELDER, M., BRAJENOVIC, M., RUFFNER, H., MERINO, A., KLEIN, K., HUDAK, M., DICKSON, D., RUDI, T., GNAU, V., BAUCH, A., BASTUCK, S., HUHSE, B., LEUTWEIN, C., HEURTIER, M. A., COPLEY, R. R., EDELMANN, A., QUERFURTH, E., RYBIN, V., DREWES, G., RAIDA, M., BOUWMEESTER, T., BORK, P., SERAPHIN, B., KUSTER, B., NEUBAUER, G. & SUPERTI-FURGA, G. (2002) Functional organization of the yeast proteome by systematic analysis of protein complexes. *Nature,* 415**,** 141-7.

GETHER, U., ASMAR, F., MEINILD, A. K. & RASMUSSEN, S. G. (2002) Structural basis for activation of G-protein-coupled receptors. *Pharmacol Toxicol,* 91**,** 304-12.

GIRARDIN, E. P., HAJMOHAMMADI, S., BIRMELE, B., HELISCH, A., SHWORAK, N. W. & DE AGOSTINI, A. I. (2005) Synthesis of anticoagulantly active heparan sulfate proteoglycans by glomerular epithelial cells involves multiple 3-O-sulfotransferase isoforms and a limiting precursor pool. *J Biol Chem,* 280**,** 38059-70.

GODDARD, S., WILLIAMS, A., MORLAND, C., QIN, S., GLADUE, R., HUBSCHER, S. G. & ADAMS, D. H. (2001) Differential expression of chemokines and chemokine receptors shapes the inflammatory response in rejecting human liver transplants. *Transplantation,* 72**,** 1957-67.

GOTTING, C., KUHN, J., ZAHN, R., BRINKMANN, T. & KLEESIEK, K. (2000) Molecular cloning and expression of human UDP-d-Xylose:proteoglycan core protein beta-d-xylosyltransferase and its first isoform XT-II. *J Mol Biol,* 304**,** 517-28.

GRESSNER, A. M. & HAARMANN, R. (1988) Regulation of hyaluronate synthesis in rat liver fat storing cell cultures by Kupffer cells. *J Hepatol,* 7**,** 310-8.

GROBE, K. & ESKO, J. D. (2002) Regulated translation of heparan sulfate N-acetylglucosamine N-deacetylase/n-sulfotransferase isozymes by structured 5'-untranslated regions and internal ribosome entry sites. *J Biol Chem,* 277**,** 30699-706.

GROBE, K., INATANI, M., PALLERLA, S. R., CASTAGNOLA, J., YAMAGUCHI, Y. & ESKO, J. D. (2005) Cerebral hypoplasia and craniofacial defects in mice lacking heparan sulfate Ndst1 gene function. *Development,* 132**,** 3777-86.

GROBE, K., LEDIN, J., RINGVALL, M., HOLMBORN, K., FORSBERG, E., ESKO, J. D. & KJELLEN, L. (2002) Heparan sulfate and development: differential roles of the N-acetylglucosamine N-deacetylase/N-sulfotransferase isozymes. *Biochim Biophys Acta,* 1573**,** 209-15.

GROFFEN, A. J., RUEGG, M. A., DIJKMAN, H., VAN DE VELDEN, T. J., BUSKENS, C. A., VAN DEN BORN, J., ASSMANN, K. J., MONNENS, L. A., VEERKAMP, J. H. & VAN DEN HEUVEL, L. P. (1998) Agrin is a major heparan sulfate proteoglycan in the human glomerular basement membrane. *J Histochem Cytochem,* 46**,** 19-27.

GROFFEN, A. J., VEERKAMP, J. H., MONNENS, L. A. & VAN DEN HEUVEL, L. P. (1999) Recent insights into the structure and functions of heparan sulfate proteoglycans in the human glomerular basement membrane. *Nephrol Dial Transplant,* 14**,** 2119-29.

GUGLIERI, S., HRICOVINI, M., RAMAN, R., POLITO, L., TORRI, G., CASU, B., SASISEKHARAN, R. & GUERRINI, M. (2008) Minimum FGF2 Binding Structural Requirements of Heparin and Heparan Sulfate Oligosaccharides As Determined by NMR Spectroscopy (dagger) . *Biochemistry*.

HABUCHI, H., HABUCHI, O. & KIMATA, K. (2004) Sulfation pattern in glycosaminoglycan: does it have a code? *Glycoconj J,* 21**,** 47-52.

HABUCHI, H., HABUCHI, O., UCHIMURA, K., KIMATA, K. & MURAMATSU, T. (2006) Determination of substrate specificity of sulfotransferases and glycosyltransferases (proteoglycans) . *Methods Enzymol,* 416**,** 225-43.

HABUCHI, H., MIYAKE, G., NOGAMI, K., KUROIWA, A., MATSUDA, Y., KUSCHE-GULLBERG, M., HABUCHI, O., TANAKA, M. & KIMATA, K. (2003) Biosynthesis of heparan sulphate with diverse structures and functions: two alternatively spliced forms of human heparan sulphate 6-O-sulphotransferase-2 having different expression patterns and properties. *Biochem J,* 371**,** 131-42.

HABUCHI, H., TANAKA, M., HABUCHI, O., YOSHIDA, K., SUZUKI, H., BAN, K. & KIMATA, K. (2000) The occurrence of three isoforms of heparan sulfate 6-O-sulfotransferase having different specificities for hexuronic acid adjacent to the targeted N-sulfoglucosamine. *J Biol Chem,* 275**,** 2859-68.

HAFEZI-MOGHADAM, A., THOMAS, K. L., PROROCK, A. J., HUO, Y. & LEY, K. (2001) L-selectin shedding regulates leukocyte recruitment. *J Exp Med,* 193**,** 863-72.

HAGNER-MCWHIRTER, A., LINDAHL, U. & LI, J. (2000) Biosynthesis of heparin/heparan sulphate: mechanism of epimerization of glucuronyl C-5. *Biochem J,* 347 Pt 1**,** 69-75.

HAIMOV-KOCHMAN, R., FRIEDMANN, Y., PRUS, D., GOLDMAN-WOHL, D. S., GREENFIELD, C., ANTEBY, E. Y., AVIV, A., VLODAVSKY, I. & YAGEL, S. (2002) Localization of heparanase in normal and pathological human placenta. *Mol Hum Reprod,* 8**,** 566-73.

HALLORAN, P. F., WADGYMAR, A., RITCHIE, S., FALK, J., SOLEZ, K. & SRINIVASA, N. S. (1990) The significance of the anti-class I antibody response. I. Clinical and pathologic features of anti-class I-mediated rejection. *Transplantation,* 49**,** 85-91.

HARDY, L. A., BOOTH, T. A., LAU, E. K., HANDEL, T. M., ALI, S. & KIRBY, J. A. (2004) Examination of MCP-1 (CCL2) partitioning and presentation during transendothelial leukocyte migration. *Lab Invest,* 84**,** 81-90.

HARMER, N. J. (2006) Insights into the role of heparan sulphate in fibroblast growth factor signalling. *Biochem Soc Trans,* 34**,** 442-5.

HILEMAN, R. E., FROMM, J. R., WEILER, J. M. & LINHARDT, R. J. (1998) Glycosaminoglycan-protein interactions: definition of consensus sites in glycosaminoglycan binding proteins. *Bioessays,* 20**,** 156-67.

HOLMBORN, K., LEDIN, J., SMEDS, E., ERIKSSON, I., KUSCHE-GULLBERG, M. & KJELLEN, L. (2004) Heparan sulfate synthesized by mouse embryonic stem cells deficient in NDST1 and NDST2 is 6-O-sulfated but contains no N-sulfate groups. *J Biol Chem,* 279**,** 42355-8.

HOOGEWERF, A. J., KUSCHERT, G. S., PROUDFOOT, A. E., BORLAT, F., CLARK-LEWIS, I., POWER, C. A. & WELLS, T. N. (1997) Glycosaminoglycans mediate cell surface oligomerization of chemokines. *Biochemistry,* 36**,** 13570-8.

HSIA, E., RICHARDSON, T. P. & NUGENT, M. A. (2003) Nuclear localization of basic fibroblast growth factor is mediated by heparan sulfate proteoglycans through protein kinase C signaling. *J Cell Biochem,* 88**,** 1214-25.

HU, Z., YU, M. & HU, G. (2007) NDST-1 modulates BMPR and PTHrP signaling during endochondral bone formation in a gene knockout model. *Bone,* 40**,** 1462-74.

HUMPHRIES, D. E., LANCIOTTI, J. & KARLINSKY, J. B. (1998) cDNA cloning, genomic organization and chromosomal localization of human heparan glucosaminyl N-deacetylase/N-sulphotransferase-2. *Biochem J,* 332 (Pt 2) **,** 303-7.

HUMPHRIES, D. E., WONG, G. W., FRIEND, D. S., GURISH, M. F., QIU, W. T., HUANG, C., SHARPE, A. H. & STEVENS, R. L. (1999) Heparin is essential for the storage of specific granule proteases in mast cells. *Nature,* 400**,** 769-72.

HUMPHRIES, M. J. (2000) Integrin structure. *Biochem Soc Trans,* 28**,** 311-39.

IHRCKE, N. S., WRENSHALL, L. E., LINDMAN, B. J. & PLATT, J. L. (1993) Role of heparan sulfate in immune system-blood vessel interactions. *Immunol Today,* 14**,** 500-5.

IMAI, Y., LASKY, L. A. & ROSEN, S. D. (1993) Sulphation requirement for GlyCAM-1, an endothelial ligand for L-selectin. *Nature,* 361**,** 555-7.

INATANI, M., IRIE, F., PLUMP, A. S., TESSIER-LAVIGNE, M. & YAMAGUCHI, Y. (2003) Mammalian brain morphogenesis and midline axon guidance require heparan sulfate. *Science,* 302**,** 1044-6.

IOZZO, R. V. (2005) Basement membrane proteoglycans: from cellar to ceiling. *Nat Rev Mol Cell Biol,* 6**,** 646-56.

IOZZO, R. V. & SAN ANTONIO, J. D. (2001) Heparan sulfate proteoglycans: heavy hitters in the angiogenesis arena. *J Clin Invest,* 108**,** 349-55.

ISEMURA, M., SATO, N., YAMAGUCHI, Y., AIKAWA, J., MUNAKATA, H., HAYASHI, N., YOSIZAWA, Z., NAKAMURA, T., KUBOTA, A., ARAKAWA, M. & ET AL. (1987) Isolation and characterization of fibronectin-binding proteoglycan carrying both heparan sulfate and dermatan sulfate chains from human placenta. *J Biol Chem,* 262**,** 8926-33.

ISHIGURO, K., KADOMATSU, K., KOJIMA, T., MURAMATSU, H., NAKAMURA, E., ITO, M., NAGASAKA, T., KOBAYASHI, H., KUSUGAMI, K., SAITO, H. & MURAMATSU, T. (2000) Syndecan-4 deficiency impairs the fetal vessels in the placental labyrinth. *Dev Dyn,* 219**,** 539-44.

ISHIGURO, K., KOJIMA, T. & MURAMATSU, T. (2002) Syndecan-4 as a molecule involved in defense mechanisms. *Glycoconj J,* 19**,** 315-8.

JASTREBOVA, N., VANWILDEMEERSCH, M., RAPRAEGER, A. C., GIMENEZ-GALLEGO, G., LINDAHL, U. & SPILLMANN, D. (2006) Heparan sulfate-related oligosaccharides in ternary complex formation with fibroblast growth factors 1 and 2 and their receptors. *J Biol Chem,* 281**,** 26884-92.

JENNISKENS, G. J., OOSTERHOF, A., BRANDWIJK, R., VEERKAMP, J. H. & VAN KUPPEVELT, T. H. (2000) Heparan sulfate heterogeneity in skeletal muscle basal lamina: demonstration by phage display-derived antibodies. *J Neurosci,* 20**,** 4099-111.

JIA, J., MACCARANA, M., ZHANG, X., BESPALOV, M., LINDAHL, U. & LI, J. P. (2009) Lack of L-iduronic acid in heparan sulfate affects interaction with growth factors and cell signaling. *J Biol Chem,* 284**,** 15942-50.

JOHNSON, L. A., CLASPER, S., HOLT, A. P., LALOR, P. F., BABAN, D. & JACKSON, D. G. (2006) An inflammation-induced mechanism for leukocyte transmigration across lymphatic vessel endothelium. *J Exp Med,* 203**,** 2763-77.

JOHNSON, P., MAITI, A., BROWN, K. L. & LI, R. (2000) A role for the cell adhesion molecule CD44 and sulfation in leukocyte-endothelial cell adhesion during an inflammatory response? *Biochem Pharmacol,* 59**,** 455-65.

JORDAN, S. C. & PESCOVITZ, M. D. (2006) Presensitization: the problem and its management. *Clin J Am Soc Nephrol,* 1**,** 421-32.

KAMIYAMA, S., SASAKI, N., GODA, E., UI-TEI, K., SAIGO, K., NARIMATSU, H., JIGAMI, Y., KANNAGI, R., IRIMURA, T. & NISHIHARA, S. (2006) Molecular cloning and characterization of a novel 3'-phosphoadenosine 5'-phosphosulfate transporter, PAPST2. *J Biol Chem,* 281**,** 10945-53.

KAMIYAMA, S., SUDA, T., UEDA, R., SUZUKI, M., OKUBO, R., KIKUCHI, N., CHIBA, Y., GOTO, S., TOYODA, H., SAIGO, K., WATANABE, M., NARIMATSU, H., JIGAMI, Y. & NISHIHARA, S. (2003) Molecular cloning and identification of 3'-phosphoadenosine 5'-phosphosulfate transporter. *J Biol Chem,* 278**,** 25958-63.

KAN, M., WANG, F., XU, J., CRABB, J. W., HOU, J. & MCKEEHAN, W. L. (1993) An essential heparin-binding domain in the fibroblast growth factor receptor kinase. *Science,* 259**,** 1918-21.

KANWAR, Y. S. & FARQUHAR, M. G. (1979a) Anionic sites in the glomerular basement membrane. In vivo and in vitro localization to the laminae rarae by cationic probes. *J Cell Biol,* 81**,** 137-53.

KANWAR, Y. S. & FARQUHAR, M. G. (1979b) Presence of heparan sulfate in the glomerular basement membrane. *Proc Natl Acad Sci U S A,* 76**,** 1303-7.

KARLMARK, K. R., WASMUTH, H. E., TRAUTWEIN, C. & TACKE, F. (2008) Chemokine-directed immune cell infiltration in acute and chronic liver disease. *Expert Rev Gastroenterol Hepatol,* 2**,** 233-42.

KAWASHIMA, H. (2006) Roles of sulfated glycans in lymphocyte homing. *Biol Pharm Bull,* 29**,** 2343-9.

KAWASHIMA, H., WATANABE, N., HIROSE, M., SUN, X., ATARASHI, K., KIMURA, T., SHIKATA, K., MATSUDA, M., OGAWA, D., HELJASVAARA, R., REHN, M., PIHLAJANIEMI, T. & MIYASAKA, M. (2003) Collagen XVIII, a basement membrane heparan sulfate proteoglycan, interacts with L-selectin and monocyte chemoattractant protein-1. *J Biol Chem,* 278**,** 13069-76.

KHACHIGIAN, L. M. & PARISH, C. R. (2004) Phosphomannopentaose sulfate (PI-88) : heparan sulfate mimetic with clinical potential in multiple vascular pathologies. *Cardiovasc Drug Rev,* 22**,** 1-6.

KIM, B. T., KITAGAWA, H., TAMURA, J., SAITO, T., KUSCHE-GULLBERG, M., LINDAHL, U. & SUGAHARA, K. (2001) Human tumor suppressor EXT gene family members EXTL1 and EXTL3 encode alpha 1,4- N-acetylglucosaminyltransferases that likely are involved in heparan sulfate/ heparin biosynthesis. *Proc Natl Acad Sci U S A,* 98**,** 7176-81.

KITAGAWA, H., TONE, Y., TAMURA, J., NEUMANN, K. W., OGAWA, T., OKA, S., KAWASAKI, T. & SUGAHARA, K. (1998) Molecular cloning and expression of glucuronyltransferase I involved in the biosynthesis of the glycosaminoglycan-protein linkage region of proteoglycans. *J Biol Chem,* 273**,** 6615-8.

KJELLEN, L., BIELEFELD, D. & HOOK, M. (1983) Reduced sulfation of liver heparan sulfate in experimentally diabetic rats. *Diabetes,* 32**,** 337-42.

KJELLEN, L. & LINDAHL, U. (1991) Proteoglycans: structures and interactions. *Annu Rev Biochem,* 60**,** 443-75.

KLAHR, S. & MORRISSEY, J. (2002) Obstructive nephropathy and renal fibrosis. *Am J Physiol Renal Physiol,* 283**,** F861-75.

KNUESEL, M., WAN, Y., XIAO, Z., HOLINGER, E., LOWE, N., WANG, W. & LIU, X. (2003) Identification of novel protein-protein interactions using

a versatile mammalian tandem affinity purification expression system. *Mol Cell Proteomics,* 2**,** 1225-33.

KOENIG, A., NORGARD-SUMNICHT, K., LINHARDT, R. & VARKI, A. (1998) Differential interactions of heparin and heparan sulfate glycosaminoglycans with the selectins. Implications for the use of unfractionated and low molecular weight heparins as therapeutic agents. *J Clin Invest,* 101**,** 877-89.

KOLSET, S. O. & TVEIT, H. (2008) Serglycin--structure and biology. *Cell Mol Life Sci,* 65**,** 1073-85.

KOVALSZKY, I., POGANY, G., MOLNAR, G., JENEY, A., LAPIS, K., KARACSONYI, S., SZECSENY, A. & IOZZO, R. V. (1990) Altered glycosaminoglycan composition in reactive and neoplastic human liver. *Biochem Biophys Res Commun,* 167**,** 883-90.

KRENN, E. C., WILLE, I., GESSLBAUER, B., POTESER, M., VAN KUPPEVELT, T. H. & KUNGL, A. J. (2008) Glycanogenomics: a qPCR-approach to investigate biological glycan function. *Biochem Biophys Res Commun,* 375**,** 297-302.

KREUGER, J., SALMIVIRTA, M., STURIALE, L., GIMENEZ-GALLEGO, G. & LINDAHL, U. (2001) Sequence analysis of heparan sulfate epitopes with graded affinities for fibroblast growth factors 1 and 2. *J Biol Chem,* 276**,** 30744-52.

KREUGER, J., SPILLMANN, D., LI, J. P. & LINDAHL, U. (2006) Interactions between heparan sulfate and proteins: the concept of specificity. *J Cell Biol,* 174**,** 323-7.

KRUGER, B., SCHROPPEL, B., ASHKAN, R., MARDER, B., ZULKE, C., MURPHY, B., KRAMER, B. K. & FISCHEREDER, M. (2002) A Monocyte chemoattractant protein-1 (MCP-1) polymorphism and outcome after renal transplantation. *J Am Soc Nephrol,* 13**,** 2585-9.

KUSCHERT, G. S., COULIN, F., POWER, C. A., PROUDFOOT, A. E., HUBBARD, R. E., HOOGEWERF, A. J. & WELLS, T. N. (1999) Glycosaminoglycans interact selectively with chemokines and modulate receptor binding and cellular responses. *Biochemistry,* 38**,** 12959-68.

LAI, K. N., LEUNG, J. C., CHAN, L. Y., GUO, H. & TANG, S. C. (2007) Interaction between proximal tubular epithelial cells and infiltrating monocytes/T cells in the proteinuric state. *Kidney Int,* 71**,** 526-38.

LAMANNA, W. C., KALUS, I., PADVA, M., BALDWIN, R. J., MERRY, C. L. & DIERKS, T. (2007) The heparanome--the enigma of encoding and decoding heparan sulfate sulfation. *J Biotechnol,* 129**,** 290-307.

LANGER, H. F. & CHAVAKIS, T. (2009) Leukocyte-endothelial interactions in inflammation. *J Cell Mol Med,* 13**,** 1211-20.

LE MOINE, A., GOLDMAN, M. & ABRAMOWICZ, D. (2002) Multiple pathways to allograft rejection. *Transplantation,* 73**,** 1373-81.

LEBARON, R. G., HOOK, A., ESKO, J. D., GAY, S. & HOOK, M. (1989) Binding of heparan sulfate to type V collagen. A mechanism of cell-substrate adhesion. *J Biol Chem,* 264**,** 7950-6.

LEDIN, J., RINGVALL, M., THUVESON, M., ERIKSSON, I., WILEN, M., KUSCHE-GULLBERG, M., FORSBERG, E. & KJELLEN, L. (2006) Enzymatically active N-deacetylase/N-sulfotransferase-2 is present in liver but does not contribute to heparan sulfate N-sulfation. *J Biol Chem,* 281**,** 35727-34.

LEDIN, J., STAATZ, W., LI, J. P., GOTTE, M., SELLECK, S., KJELLEN, L. & SPILLMANN, D. (2004) Heparan sulfate structure in mice with genetically modified heparan sulfate production. *J Biol Chem,* 279**,** 42732-41.

LEE, J. S. & CHIEN, C. B. (2004) When sugars guide axons: insights from heparan sulphate proteoglycan mutants. *Nat Rev Genet,* 5**,** 923-35.

LESLEY, J., GAL, I., MAHONEY, D. J., CORDELL, M. R., RUGG, M. S., HYMAN, R., DAY, A. J. & MIKECZ, K. (2004) TSG-6 modulates the interaction between hyaluronan and cell surface CD44. *J Biol Chem,* 279**,** 25745-54.

LI, J., HAGNER-MCWHIRTER, A., KJELLEN, L., PALGI, J., JALKANEN, M. & LINDAHL, U. (1997) Biosynthesis of heparin/heparan sulfate. cDNA cloning and expression of D-glucuronyl C5-epimerase from bovine lung. *J Biol Chem,* 272**,** 28158-63.

LIBEU, C. P., LUND-KATZ, S., PHILLIPS, M. C., WEHRLI, S., HERNAIZ, M. J., CAPILA, I., LINHARDT, R. J., RAFFAI, R. L., NEWHOUSE, Y. M., ZHOU, F. & WEISGRABER, K. H. (2001) New insights into the heparan sulfate proteoglycan-binding activity of apolipoprotein E. *J Biol Chem,* 276**,** 39138-44.

LIDHOLT, K. & LINDAHL, U. (1992) Biosynthesis of heparin. The D-glucuronosyl- and N-acetyl-D-glucosaminyltransferase reactions and their relation to polymer modification. *Biochem J,* 287 (Pt 1) **,** 21-9.

LINDAHL, U., KUSCHE-GULLBERG, M. & KJELLEN, L. (1998) Regulated diversity of heparan sulfate. *J Biol Chem,* 273**,** 24979-82.

LINDAHL, U., KUSCHE, M., LIDHOLT, K. & OSCARSSON, L. G. (1989) Biosynthesis of heparin and heparan sulfate. *Ann N Y Acad Sci,* 556**,** 36-50.

LINDAHL, U., THUNBERG, L., BACKSTROM, G., RIESENFELD, J., NORDLING, K. & BJORK, I. (1984) Extension and structural variability of the antithrombin-binding sequence in heparin. *J Biol Chem,* 259**,** 12368-76.

LINDBLOM, P., GERHARDT, H., LIEBNER, S., ABRAMSSON, A., ENGE, M., HELLSTROM, M., BACKSTROM, G., FREDRIKSSON, S., LANDEGREN, U., NYSTROM, H. C., BERGSTROM, G., DEJANA, E., OSTMAN, A., LINDAHL, P. & BETSHOLTZ, C. (2003) Endothelial PDGF-B retention is required for proper investment of pericytes in the microvessel wall. *Genes Dev,* 17**,** 1835-40.

LINDEMANN, D. & SCHNITTLER, H. (2009) Genetic manipulation of endothelial cells by viral vectors. *Thromb Haemost,* 102**,** 1135-43.

LINFERT, D., CHOWDHRY, T. & RABB, H. (2009) Lymphocytes and ischemia-reperfusion injury. *Transplant Rev (Orlando) ,* 23**,** 1-10.

LIU, C. J., LEE, P. H., LIN, D. Y., WU, C. C., JENG, L. B., LIN, P. W., MOK, K. T., LEE, W. C., YEH, H. Z., HO, M. C., YANG, S. S., LEE, C. C., YU, M. C., HU, R. H., PENG, C. Y., LAI, K. L., CHANG, S. S. & CHEN, P. J. (2009) Heparanase inhibitor PI-88 as adjuvant therapy for hepatocellular carcinoma after curative resection: a randomized phase II trial for safety and optimal dosage. *J Hepatol,* 50**,** 958-68.

LIU, X., HU, H. & YIN, J. Q. (2006) Therapeutic strategies against TGF-beta signaling pathway in hepatic fibrosis. *Liver Int,* 26**,** 8-22.

LIU, Y. (2002) Hepatocyte growth factor and the kidney. *Curr Opin Nephrol Hypertens,* 11**,** 23-30.

LIU, Y. (2004) Epithelial to mesenchymal transition in renal fibrogenesis: pathologic significance, molecular mechanism, and therapeutic intervention. *J Am Soc Nephrol,* 15**,** 1-12.

LIU, Y. (2006) Renal fibrosis: new insights into the pathogenesis and therapeutics. *Kidney Int,* 69**,** 213-7.

LIVAK, K. J. & SCHMITTGEN, T. D. (2001) Analysis of relative gene expression data using real-time quantitative PCR and the 2(-Delta Delta C(T)) Method. *Methods,* 25**,** 402-8.

LORTAT-JACOB, H. (2006) Interferon and heparan sulphate. *Biochem Soc Trans,* 34**,** 461-4.

LORTAT-JACOB, H. (2009) The molecular basis and functional implications of chemokine interactions with heparan sulphate. *Curr Opin Struct Biol,* 19**,** 543-8.

LORTAT-JACOB, H., BALTZER, F. & GRIMAUD, J. A. (1996) Heparin decreases the blood clearance of interferon-gamma and increases its activity by limiting the processing of its carboxyl-terminal sequence. *J Biol Chem,* 271**,** 16139-43.

LORTAT-JACOB, H., KLEINMAN, H. & GRIMAUD, J. A. (1990) [Connective matrix and localization of a biological signal: demonstration of a matrix receptor for interferon-gamma in basement membranes]. *C R Acad Sci III,* 311**,** 143-7.

LORTAT-JACOB, H., TURNBULL, J. E. & GRIMAUD, J. A. (1995) Molecular organization of the interferon gamma-binding domain in heparan sulphate. *Biochem J,* 310 (Pt 2) **,** 497-505.

LOTERSZTAJN, S., JULIEN, B., TEIXEIRA-CLERC, F., GRENARD, P. & MALLAT, A. (2005) Hepatic fibrosis: molecular mechanisms and drug targets. *Annu Rev Pharmacol Toxicol,* 45**,** 605-28.

LUCIGNANI, G. (2007) Rubor, calor, tumor, dolor, functio laesa... or molecular imaging. *Eur J Nucl Med Mol Imaging,* 34**,** 2135-41.

LUDWIG, J. (1989) Classification and terminology of hepatic allograft rejection: whither bound? *Mayo Clin Proc,* 64**,** 676-9.

LYON, M., DEAKIN, J. A. & GALLAGHER, J. T. (1994a) Liver heparan sulfate structure. A novel molecular design. *J Biol Chem,* 269**,** 11208-15.

LYON, M., DEAKIN, J. A., MIZUNO, K., NAKAMURA, T. & GALLAGHER, J. T. (1994b) Interaction of hepatocyte growth factor with heparan sulfate. Elucidation of the major heparan sulfate structural determinants. *J Biol Chem,* 269**,** 11216-23.

LYON, M., RUSHTON, G. & GALLAGHER, J. T. (1997) The interaction of the transforming growth factor-betas with heparin/heparan sulfate is isoform-specific. *J Biol Chem,* 272**,** 18000-6.

MACARTHUR, J. M., BISHOP, J. R., STANFORD, K. I., WANG, L., BENSADOUN, A., WITZTUM, J. L. & ESKO, J. D. (2007) Liver heparan sulfate proteoglycans mediate clearance of triglyceride-rich lipoproteins independently of LDL receptor family members. *J Clin Invest,* 117**,** 153-64.

MACCARANA, M., SAKURA, Y., TAWADA, A., YOSHIDA, K. & LINDAHL, U. (1996) Domain structure of heparan sulfates from bovine organs. *J Biol Chem,* 271**,** 17804-10.

MADRI, J. A. & GRAESSER, D. (2000) Cell migration in the immune system: the evolving inter-related roles of adhesion molecules and proteinases. *Dev Immunol,* 7**,** 103-16.

MAHONEY, D. J., MULLOY, B., FORSTER, M. J., BLUNDELL, C. D., FRIES, E., MILNER, C. M. & DAY, A. J. (2005) Characterization of the interaction between tumor necrosis factor-stimulated gene-6 and heparin: implications for the inhibition of plasmin in extracellular matrix microenvironments. *J Biol Chem,* 280**,** 27044-55.

MARNEROS, A. G. & OLSEN, B. R. (2005) Physiological role of collagen XVIII and endostatin. *Faseb J,* 19**,** 716-28.

MEISSEN, J. K., SWEENEY, M. D., GIRARDI, M., LAWRENCE, R., ESKO, J. D. & LEARY, J. A. (2009) Differentiation of 3-O-sulfated heparin disaccharide isomers: identification of structural aspects of the heparin CCL2 binding motif. *J Am Soc Mass Spectrom,* 20**,** 652-7.

MELROSE, J., SMITH, S., GHOSH, P. & WHITELOCK, J. (2003) Perlecan, the multidomain heparan sulfate proteoglycan of basement membranes, is also a prominent component of the cartilaginous primordia in the developing human fetal spine. *J Histochem Cytochem,* 51**,** 1331-41.

MIDDLETON, J., PATTERSON, A. M., GARDNER, L., SCHMUTZ, C. & ASHTON, B. A. (2002) Leukocyte extravasation: chemokine transport and presentation by the endothelium. *Blood,* 100**,** 3853-60.

MIYAZAKI, M., NISHINO, T., ABE, K., FURUSU, A., KOJI, T. & KOHNO, S. (2003) Regulation of renal extracellular matrix metabolism. *Contrib Nephrol,* 139**,** 141-55.

MONTECLARO, F. S. & CHARO, I. F. (1996) The amino-terminal extracellular domain of the MCP-1 receptor, but not the RANTES/MIP-1alpha receptor, confers chemokine selectivity. Evidence for a two-step mechanism for MCP-1 receptor activation. *J Biol Chem,* 271**,** 19084-92.

MORII, T., FUJITA, H., NARITA, T., KOSHIMURA, J., SHIMOTOMAI, T., FUJISHIMA, H., YOSHIOKA, N., IMAI, H., KAKEI, M. & ITO, S. (2003a) Increased urinary excretion of monocyte chemoattractant protein-1 in proteinuric renal diseases. *Ren Fail,* 25**,** 439-44.

MORII, T., FUJITA, H., NARITA, T., SHIMOTOMAI, T., FUJISHIMA, H., YOSHIOKA, N., IMAI, H., KAKEI, M. & ITO, S. (2003b) Association of monocyte chemoattractant protein-1 with renal tubular damage in diabetic nephropathy. *J Diabetes Complications,* 17**,** 11-5.

MUL, F. P., ZUURBIER, A. E., JANSSEN, H., CALAFAT, J., VAN WETERING, S., HIEMSTRA, P. S., ROOS, D. & HORDIJK, P. L. (2000) Sequential migration of neutrophils across monolayers of endothelial and epithelial cells. *J Leukoc Biol,* 68**,** 529-37.

MULLOY, B. & RIDER, C. C. (2006) Cytokines and proteoglycans: an introductory overview. *Biochem Soc Trans,* 34**,** 409-13.

MUNRO, S. (1998) Localization of proteins to the Golgi apparatus. *Trends Cell Biol,* 8**,** 11-5.

MURATA, K., OCHIAI, Y. & AKASHIO, K. (1985) Polydispersity of acidic glycosaminoglycan components in human liver and the changes at different stages in liver cirrhosis. *Gastroenterology,* 89**,** 1248-57.

MURDOCH, C. & FINN, A. (2000) Chemokine receptors and their role in inflammation and infectious diseases. *Blood,* 95**,** 3032-43.

MURPHY, P. M., BAGGIOLINI, M., CHARO, I. F., HEBERT, C. A., HORUK, R., MATSUSHIMA, K., MILLER, L. H., OPPENHEIM, J. J. & POWER, C. A. (2000) International union of pharmacology. XXII. Nomenclature for chemokine receptors. *Pharmacol Rev,* 52**,** 145-76.

MURRAY, J. (2002) Interview with Dr Joseph Murray (by Francis L Delmonico) . *Am J Transplant,* 2**,** 803-6.

NASSER, N. J. (2008) Heparanase involvement in physiology and disease. *Cell Mol Life Sci,* 65**,** 1706-15.

NELSON, P. J. & KRENSKY, A. M. (2001a) Chemokines and allograft rejection: narrowing the list of suspects. *Transplantation,* 72**,** 1195-7.

NELSON, P. J. & KRENSKY, A. M. (2001b) Chemokines, chemokine receptors, and allograft rejection. *Immunity,* 14**,** 377-86.

NEUBERGER, J. & ADAMS, D. H. (1998) What is the significance of acute liver allograft rejection? *J Hepatol,* 29**,** 143-50.

NGUAN, C. Y. & DU, C. (2009) Renal tubular epithelial cells as immunoregulatory cells in renal allograft rejection. *Transplant Rev (Orlando) ,* 23**,** 129-38.

NICOLE, S., DAVOINE, C. S., TOPALOGLU, H., CATTOLICO, L., BARRAL, D., BEIGHTON, P., HAMIDA, C. B., HAMMOUDA, H., CRUAUD, C., WHITE, P. S., SAMSON, D., URTIZBEREA, J. A., LEHMANN-HORN, F., WEISSENBACH, J., HENTATI, F. & FONTAINE, B. (2000) Perlecan, the major proteoglycan of basement membranes, is altered in patients with Schwartz-Jampel syndrome (chondrodystrophic myotonia) . *Nat Genet,* 26**,** 480-3.

NILSSON, T., HOE, M. H., SLUSAREWICZ, P., RABOUILLE, C., WATSON, R., HUNTE, F., WATZELE, G., BERGER, E. G. & WARREN, G. (1994) Kin recognition between medial Golgi enzymes in HeLa cells. *Embo J,* 13**,** 562-74.

NOBLE, P. W. (2002) Hyaluronan and its catabolic products in tissue injury and repair. *Matrix Biol,* 21**,** 25-9.

O'DONNELL, C. D., KOVACS, M., AKHTAR, J., VALYI-NAGY, T. & SHUKLA, D. (2010) Expanding the role of 3-O sulfated heparan sulfate in herpes simplex virus type-1 entry. *Virology,* 397**,** 389-98.

O'REILLY, M. S., BOEHM, T., SHING, Y., FUKAI, N., VASIOS, G., LANE, W. S., FLYNN, E., BIRKHEAD, J. R., OLSEN, B. R. & FOLKMAN, J. (1997) Endostatin: an endogenous inhibitor of angiogenesis and tumor growth. *Cell,* 88**,** 277-85.

OKADA-BAN, M., THIERY, J. P. & JOUANNEAU, J. (2000) Fibroblast growth factor-2. *Int J Biochem Cell Biol,* 32**,** 263-7.

OLSSON, U., OSTERGREN-LUNDEN, G. & MOSES, J. (2001) Glycosaminoglycan-lipoprotein interaction. *Glycoconj J,* 18**,** 789-97.

ORNITZ, D. M. (2000) FGFs, heparan sulfate and FGFRs: complex interactions essential for development. *Bioessays,* 22**,** 108-12.

PALLERLA, S. R., LAWRENCE, R., LEWEJOHANN, L., PAN, Y., FISCHER, T., SCHLOMANN, U., ZHANG, X., ESKO, J. D. & GROBE, K. (2008) Altered heparan sulfate structure in mice with deleted NDST3 gene function. *J Biol Chem,* 283**,** 16885-94.

PAN, Y., WOODBURY, A., ESKO, J. D., GROBE, K. & ZHANG, X. (2006) Heparan sulfate biosynthetic gene Ndst1 is required for FGF signaling in early lens development. *Development,* 133**,** 4933-44.

PANKONIN, M. S., GALLAGHER, J. T. & LOEB, J. A. (2005) Specific structural features of heparan sulfate proteoglycans potentiate neuregulin-1 signaling. *J Biol Chem,* 280**,** 383-8.

PAPPIN, D. J., HOJRUP, P. & BLEASBY, A. J. (1993) Rapid identification of proteins by peptide-mass fingerprinting. *Curr Biol,* 3**,** 327-32.

PARISH, C. R. (2006) The role of heparan sulphate in inflammation. *Nat Rev Immunol,* 6**,** 633-43.

PARISH, C. R., HINDMARSH, E. J., BARTLETT, M. R., STAYKOVA, M. A., COWDEN, W. B. & WILLENBORG, D. O. (1998) Treatment of central nervous system inflammation with inhibitors of basement membrane degradation. *Immunol Cell Biol,* 76**,** 104-13.

PEASE, J. E. & WILLIAMS, T. J. (2006) The attraction of chemokines as a target for specific anti-inflammatory therapy. *Br J Pharmacol,* 147 Suppl 1**,** S212-21.

PENKO, M. E. & TIRBASO, D. (1999) An overview of liver transplantation. *AACN Clin Issues,* 10**,** 176-84.

PERKINS, D. N., PAPPIN, D. J., CREASY, D. M. & COTTRELL, J. S. (1999) Probability-based protein identification by searching sequence databases using mass spectrometry data. *Electrophoresis,* 20**,** 3551-67.

PETITOU, M., CASU, B. & LINDAHL, U. (2003) 1976-1983, a critical period in the history of heparin: the discovery of the antithrombin binding site. *Biochimie,* 85**,** 83-9.

PETTERSSON, I., KUSCHE, M., UNGER, E., WLAD, H., NYLUND, L., LINDAHL, U. & KJELLEN, L. (1991) Biosynthesis of heparin. Purification of a 110-kDa mouse mastocytoma protein required for both glucosaminyl N-deacetylation and N-sulfation. *J Biol Chem,* 266**,** 8044-9.

PFAFFL, M. W. (2001) A new mathematical model for relative quantification in real-time RT-PCR. *Nucleic Acids Res,* 29**,** e45.

PIKAS, D. S., ERIKSSON, I. & KJELLEN, L. (2000) Overexpression of different isoforms of glucosaminyl N-deacetylase/N-sulfotransferase results in distinct heparan sulfate N-sulfation patterns. *Biochemistry,* 39**,** 4552-8.

PILIA, G., HUGHES-BENZIE, R. M., MACKENZIE, A., BAYBAYAN, P., CHEN, E. Y., HUBER, R., NERI, G., CAO, A., FORABOSCO, A. & SCHLESSINGER, D. (1996) Mutations in GPC3, a glypican gene, cause the Simpson-Golabi-Behmel overgrowth syndrome. *Nat Genet,* 12**,** 241-7.

PINHAL, M. A., SMITH, B., OLSON, S., AIKAWA, J., KIMATA, K. & ESKO, J. D. (2001) Enzyme interactions in heparan sulfate biosynthesis: uronosyl 5-epimerase and 2-O-sulfotransferase interact in vivo. *Proc Natl Acad Sci U S A,* 98**,** 12984-9.

POTZINGER, H., GERETTI, E., BRANDNER, B., WABITSCH, V., PICCININI, A. M., REK, A. & KUNGL, A. J. (2006) Developing chemokine mutants

with improved proteoglycan affinity and knocked-out GPCR activity as anti-inflammatory recombinant drugs. *Biochem Soc Trans,* 34**,** 435-7.

POWELL, A. K., FERNIG, D. G. & TURNBULL, J. E. (2002) Fibroblast growth factor receptors 1 and 2 interact differently with heparin/heparan sulfate. Implications for dynamic assembly of a ternary signaling complex. *J Biol Chem,* 277**,** 28554-63.

PRESTO, J., THUVESON, M., CARLSSON, P., BUSSE, M., WILEN, M., ERIKSSON, I., KUSCHE-GULLBERG, M. & KJELLEN, L. (2008) Heparan sulfate biosynthesis enzymes EXT1 and EXT2 affect NDST1 expression and heparan sulfate sulfation. *Proc Natl Acad Sci U S A,* 105**,** 4751-6.

PRODJOSUDJADI, W., GERRITSMA, J. S., VAN ES, L. A., DAHA, M. R. & BRUIJN, J. A. (1995) Monocyte chemoattractant protein-1 in normal and diseased human kidneys: an immunohistochemical analysis. *Clin Nephrol,* 44**,** 148-55.

PROUDFOOT, A. E. (2006) The biological relevance of chemokine-proteoglycan interactions. *Biochem Soc Trans,* 34**,** 422-6.

PROUDFOOT, A. E., FRITCHLEY, S., BORLAT, F., SHAW, J. P., VILBOIS, F., ZWAHLEN, C., TRKOLA, A., MARCHANT, D., CLAPHAM, P. R. & WELLS, T. N. (2001) The BBXB motif of RANTES is the principal site for heparin binding and controls receptor selectivity. *J Biol Chem,* 276**,** 10620-6.

PROUDFOOT, A. E., HANDEL, T. M., JOHNSON, Z., LAU, E. K., LIWANG, P., CLARK-LEWIS, I., BORLAT, F., WELLS, T. N. & KOSCO-VILBOIS, M. H. (2003) Glycosaminoglycan binding and oligomerization are essential for the in vivo activity of certain chemokines. *Proc Natl Acad Sci U S A,* 100**,** 1885-90.

PUIG, O., CASPARY, F., RIGAUT, G., RUTZ, B., BOUVERET, E., BRAGADO-NILSSON, E., WILM, M. & SERAPHIN, B. (2001) The tandem affinity purification (TAP) method: a general procedure of protein complex purification. *Methods,* 24**,** 218-29.

QI, W., CHEN, X., PORONNIK, P. & POLLOCK, C. A. (2006) The renal cortical fibroblast in renal tubulointerstitial fibrosis. *Int J Biochem Cell Biol,* 38**,** 1-5.

RAATS, C. J., VAN DEN BORN, J., BAKKER, M. A., OPPERS-WALGREEN, B., PISA, B. J., DIJKMAN, H. B., ASSMANN, K. J. & BERDEN, J. H. (2000) Expression of agrin, dystroglycan, and utrophin in normal renal tissue and in experimental glomerulopathies. *Am J Pathol,* 156**,** 1749-65.

RACUSEN, L. C. & HAAS, M. (2006) Antibody-mediated rejection in renal allografts: lessons from pathology. *Clin J Am Soc Nephrol,* 1**,** 415-20.

RACUSEN, L. C., RAYNER, D. C., TRPKOV, K., OLSEN, S. & SOLEZ, K. (1995) The Banff classification of renal allograft pathology: where do we go from here? *Transplant Proc,* 27**,** 2561-3.

RACUSEN, L. C., SOLEZ, K., COLVIN, R. B., BONSIB, S. M., CASTRO, M. C., CAVALLO, T., CROKER, B. P., DEMETRIS, A. J., DRACHENBERG, C. B., FOGO, A. B., FURNESS, P., GABER, L. W., GIBSON, I. W., GLOTZ, D., GOLDBERG, J. C., GRANDE, J., HALLORAN, P. F., HANSEN, H. E., HARTLEY, B., HAYRY, P. J., HILL, C. M., HOFFMAN, E. O., HUNSICKER, L. G., LINDBLAD, A. S., YAMAGUCHI, Y. & ET AL. (1999) The Banff 97 working classification of renal allograft pathology. *Kidney Int,* 55**,** 713-23.

RANSOHOFF, R. M. (2009) Chemokines and chemokine receptors: standing at the crossroads of immunobiology and neurobiology. *Immunity,* 31**,** 711-21.

RAPRAEGER, A. C., GUIMOND, S., KRUFKA, A. & OLWIN, B. B. (1994) Regulation by heparan sulfate in fibroblast growth factor signaling. *Methods Enzymol,* 245**,** 219-40.

REEVES, W. H., KANWAR, Y. S. & FARQUHAR, M. G. (1980) Assembly of the glomerular filtration surface. Differentiation of anionic sites in glomerular capillaries of newborn rat kidney. *J Cell Biol,* 85**,** 735-53.

REHM, M., BRUEGGER, D., CHRIST, F., CONZEN, P., THIEL, M., JACOB, M., CHAPPELL, D., STOECKELHUBER, M., WELSCH, U., REICHART, B., PETER, K. & BECKER, B. F. (2007) Shedding of the endothelial

glycocalyx in patients undergoing major vascular surgery with global and regional ischemia. *Circulation,* 116**,** 1896-906.

REIZES, O., LINCECUM, J., WANG, Z., GOLDBERGER, O., HUANG, L., KAKSONEN, M., AHIMA, R., HINKES, M. T., BARSH, G. S., RAUVALA, H. & BERNFIELD, M. (2001) Transgenic expression of syndecan-1 uncovers a physiological control of feeding behavior by syndecan-3. *Cell,* 106**,** 105-16.

REK, A., BRANDNER, B., GERETTI, E. & KUNGL, A. J. (2009) A biophysical insight into the RANTES-glycosaminoglycan interaction. *Biochim Biophys Acta,* 1794**,** 577-82.

RICHARDSON, T. P., TRINKAUS-RANDALL, V. & NUGENT, M. A. (2001) Regulation of heparan sulfate proteoglycan nuclear localization by fibronectin. *J Cell Sci,* 114**,** 1613-23.

RIDER, C. C. (2006) Heparin/heparan sulphate binding in the TGF-beta cytokine superfamily. *Biochem Soc Trans,* 34**,** 458-60.

RIENSTRA, H., KATTA, K., CELIE, J. W., VAN GOOR, H., NAVIS, G., VAN DEN BORN, J. & HILLEBRANDS, J. L. (2010) Differential expression of proteoglycans in tissue remodeling and lymphangiogenesis after experimental renal transplantation in rats. *PLoS One,* 5**,** e9095.

RIESENFELD, J., HOOK, M. & LINDAHL, U. (1980) Biosynthesis of heparin. Assay and properties of the microsomal N-acetyl-D-glucosaminyl N-deacetylase. *J Biol Chem,* 255**,** 922-8.

RINGVALL, M., LEDIN, J., HOLMBORN, K., VAN KUPPEVELT, T., ELLIN, F., ERIKSSON, I., OLOFSSON, A. M., KJELLEN, L. & FORSBERG, E. (2000) Defective heparan sulfate biosynthesis and neonatal lethality in mice lacking N-deacetylase/N-sulfotransferase-1. *J Biol Chem,* 275**,** 25926-30.

ROBERTSON, H., ALI, S., MCDONNELL, B. J., BURT, A. D. & KIRBY, J. A. (2004) Chronic renal allograft dysfunction: the role of T cell-mediated tubular epithelial to mesenchymal cell transition. *J Am Soc Nephrol,* 15**,** 390-7.

ROBERTSON, H. & KIRBY, J. A. (2003) Post-transplant renal tubulitis: the recruitment, differentiation and persistence of intra-epithelial T cells. *Am J Transplant,* 3**,** 3-10.

ROBERTSON, H., WHEELER, J., MORLEY, A. R., BOOTH, T. A., TALBOT, D. & KIRBY, J. A. (1998) Beta-chemokine expression and distribution in paraffin-embedded transplant renal biopsy sections: analysis by scanning laser confocal microscopy. *Histochem Cell Biol,* 110**,** 207-13.

RONG, J., HABUCHI, H., KIMATA, K., LINDAHL, U. & KUSCHE-GULLBERG, M. (2001) Substrate specificity of the heparan sulfate hexuronic acid 2-O-sulfotransferase. *Biochemistry,* 40**,** 5548-55.

ROPS, A. L., VAN DEN HOVEN, M. J., BAKKER, M. A., LENSEN, J. F., WIJNHOVEN, T. J., VAN DEN HEUVEL, L. P., VAN KUPPEVELT, T. H., VAN DER VLAG, J. & BERDEN, J. H. (2007) Expression of glomerular heparan sulphate domains in murine and human lupus nephritis. *Nephrol Dial Transplant,* 22**,** 1891-902.

ROPS, A. L., VAN DEN HOVEN, M. J., BASELMANS, M. M., LENSEN, J. F., WIJNHOVEN, T. J., VAN DEN HEUVEL, L. P., VAN KUPPEVELT, T. H., BERDEN, J. H. & VAN DER VLAG, J. (2008) Heparan sulfate domains on cultured activated glomerular endothelial cells mediate leukocyte trafficking. *Kidney Int,* 73**,** 52-62.

ROSEN, S. D. (1999) Endothelial ligands for L-selectin: from lymphocyte recirculation to allograft rejection. *Am J Pathol,* 155**,** 1013-20.

ROSKAMS, T., ROSENBAUM, J., DE VOS, R., DAVID, G. & DESMET, V. (1996) Heparan sulfate proteoglycan expression in chronic cholestatic human liver diseases. *Hepatology,* 24**,** 524-32.

ROT, A. (1996) Inflammatory and Physiological Roles of Chemokines. *Pathol Oncol Res,* 2**,** 16-20.

ROT, A. & VON ANDRIAN, U. H. (2004) Chemokines in innate and adaptive host defense: basic chemokinese grammar for immune cells. *Annu Rev Immunol,* 22**,** 891-928.

RUSTER, M., SPERSCHNEIDER, H., FUNFSTUCK, R., STEIN, G. & GRONE, H. J. (2004) Differential expression of beta-chemokines MCP-1 and RANTES and their receptors CCR1, CCR2, CCR5 in acute rejection and

chronic allograft nephropathy of human renal allografts. *Clin Nephrol,* 61**,** 30-9.

RYGIEL, K. A., ROBERTSON, H., MARSHALL, H. L., PEKALSKI, M., ZHAO, L., BOOTH, T. A., JONES, D. E., BURT, A. D. & KIRBY, J. A. (2008) Epithelial-mesenchymal transition contributes to portal tract fibrogenesis during human chronic liver disease. *Lab Invest,* 88**,** 112-23.

SADIR, R., IMBERTY, A., BALEUX, F. & LORTAT-JACOB, H. (2004) Heparan sulfate/heparin oligosaccharides protect stromal cell-derived factor-1 (SDF-1) /CXCL12 against proteolysis induced by CD26/dipeptidyl peptidase IV. *J Biol Chem,* 279**,** 43854-60.

SALMIVIRTA, M., LIDHOLT, K. & LINDAHL, U. (1996) Heparan sulfate: a piece of information. *Faseb J,* 10**,** 1270-9.

SAPHIRE, A. C., BOBARDT, M. D., ZHANG, Z., DAVID, G. & GALLAY, P. A. (2001) Syndecans serve as attachment receptors for human immunodeficiency virus type 1 on macrophages. *J Virol,* 75**,** 9187-200.

SARIBAS, A. S., MOBASSERI, A., PRISTATSKY, P., CHEN, X., BARTHELSON, R., HAKES, D. & WANG, J. (2004) Production of N-sulfated polysaccharides using yeast-expressed N-deacetylase/N-sulfotransferase-1 (NDST-1) . *Glycobiology,* 14**,** 1217-28.

SAYEGH, M. H. & CARPENTER, C. B. (2004) Transplantation 50 years later--progress, challenges, and promises. *N Engl J Med,* 351**,** 2761-6.

SCHENAUER, M. R., YU, Y., SWEENEY, M. D. & LEARY, J. A. (2007) CCR2 chemokines bind selectively to acetylated heparan sulfate octasaccharides. *J Biol Chem,* 282**,** 25182-8.

SCHENKEL, A. R., MAMDOUH, Z. & MULLER, W. A. (2004) Locomotion of monocytes on endothelium is a critical step during extravasation. *Nat Immunol,* 5**,** 393-400.

SCHNAPER, H. W., HAYASHIDA, T., HUBCHAK, S. C. & PONCELET, A. C. (2003) TGF-beta signal transduction and mesangial cell fibrogenesis. *Am J Physiol Renal Physiol,* 284**,** F243-52.

SCHOLEFIELD, Z., YATES, E. A., WAYNE, G., AMOUR, A., MCDOWELL, W. & TURNBULL, J. E. (2003) Heparan sulfate regulates amyloid

precursor protein processing by BACE1, the Alzheimer's beta-secretase. *J Cell Biol,* 163**,** 97-107.

SCHONHERR, E. & HAUSSER, H. J. (2000) Extracellular matrix and cytokines: a functional unit. *Dev Immunol,* 7**,** 89-101.

SCHUBERT, S. Y., ILAN, N., SHUSHY, M., BEN-IZHAK, O., VLODAVSKY, I. & GOLDSHMIDT, O. (2004) Human heparanase nuclear localization and enzymatic activity. *Lab Invest,* 84**,** 535-44.

SCHULZE, A., GRIPON, P. & URBAN, S. (2007) Hepatitis B virus infection initiates with a large surface protein-dependent binding to heparan sulfate proteoglycans. *Hepatology,* 46**,** 1759-68.

SCHUPPAN, D. (1990) Structure of the extracellular matrix in normal and fibrotic liver: collagens and glycoproteins. *Semin Liver Dis,* 10**,** 1-10.

SCHWARTZ, N. B., RODEN, L. & DORFMAN, A. (1974) Biosynthesis of chondroitin sulfate: interaction between xylosyltransferase and galactosyltransferase. *Biochem Biophys Res Commun,* 56**,** 717-24.

SEGERER, S., DJAFARZADEH, R., GRONE, H. J., WEINGART, C., KERJASCHKI, D., WEBER, C., KUNGL, A. J., REGELE, H., PROUDFOOT, A. E. & NELSON, P. J. (2007) Selective binding and presentation of CCL5 by discrete tissue microenvironments during renal inflammation. *J Am Soc Nephrol,* 18**,** 1835-44.

SEGERER, S., JOHNSON, Z., REK, A., BALTUS, T., VON HUNDELSHAUSEN, P., KUNGL, A. J., PROUDFOOT, A. E., WEBER, C. & NELSON, P. J. (2009) The basic residue cluster (55) KKWVR(59) in CCL5 is required for in vivo biologic function. *Mol Immunol,* 46**,** 2533-8.

SEGERER, S., NELSON, P. J. & SCHLONDORFF, D. (2000) Chemokines, chemokine receptors, and renal disease: from basic science to pathophysiologic and therapeutic studies. *J Am Soc Nephrol,* 11**,** 152-76.

SERTIE, A. L., SOSSI, V., CAMARGO, A. A., ZATZ, M., BRAHE, C. & PASSOS-BUENO, M. R. (2000) Collagen XVIII, containing an endogenous inhibitor of angiogenesis and tumor growth, plays a critical role in the maintenance of retinal structure and in neural tube closure (Knobloch syndrome) . *Hum Mol Genet,* 9**,** 2051-8.

SEVERIN, I. C., GAUDRY, J. P., JOHNSON, Z., KUNGL, A., JANSMA, A., GESSLBAUER, B., MULLOY, B., POWER, C., PROUDFOOT, A. E. & HANDEL, T. (2010) Characterization of the chemokine CXCL11-heparin interaction suggests two different affinities for glycosaminoglycans. *J Biol Chem,* 285**,** 17713-24.

SHAW, J. P., JOHNSON, Z., BORLAT, F., ZWAHLEN, C., KUNGL, A., ROULIN, K., HARRENGA, A., WELLS, T. N. & PROUDFOOT, A. E. (2004) The X-ray structure of RANTES: heparin-derived disaccharides allows the rational design of chemokine inhibitors. *Structure,* 12**,** 2081-93.

SHEK, F. W. & BENYON, R. C. (2004) How can transforming growth factor beta be targeted usefully to combat liver fibrosis? *Eur J Gastroenterol Hepatol,* 16**,** 123-6.

SHEVCHENKO, A., SCHAFT, D., ROGUEV, A., PIJNAPPEL, W. W., STEWART, A. F. & SHEVCHENKO, A. (2002) Deciphering protein complexes and protein interaction networks by tandem affinity purification and mass spectrometry: analytical perspective. *Mol Cell Proteomics,* 1**,** 204-12.

SHIMAOKA, M., TAKAGI, J. & SPRINGER, T. A. (2002) Conformational regulation of integrin structure and function. *Annu Rev Biophys Biomol Struct,* 31**,** 485-516.

SHRIVER, Z., SUNDARAM, M., VENKATARAMAN, G., FAREED, J., LINHARDT, R., BIEMANN, K. & SASISEKHARAN, R. (2000) Cleavage of the antithrombin III binding site in heparin by heparinases and its implication in the generation of low molecular weight heparin. *Proc Natl Acad Sci U S A,* 97**,** 10365-70.

SHWORAK, N. W., HAJMOHAMMADI, S., DE AGOSTINI, A. I. & ROSENBERG, R. D. (2002) Mice deficient in heparan sulfate 3-O-sulfotransferase-1: normal hemostasis with unexpected perinatal phenotypes. *Glycoconj J,* 19**,** 355-61.

SHWORAK, N. W., LIU, J., PETROS, L. M., ZHANG, L., KOBAYASHI, M., COPELAND, N. G., JENKINS, N. A. & ROSENBERG, R. D. (1999) Multiple isoforms of heparan sulfate D-glucosaminyl 3-O-

sulfotransferase. Isolation, characterization, and expression of human cdnas and identification of distinct genomic loci. *J Biol Chem,* 274**,** 5170-84.

SILBERT, J. E. & SUGUMARAN, G. (2002) Biosynthesis of chondroitin/dermatan sulfate. *IUBMB Life,* 54**,** 177-86.

SIS, B., MENGEL, M., HAAS, M., COLVIN, R. B., HALLORAN, P. F., RACUSEN, L. C., SOLEZ, K., BALDWIN, W. M., 3RD, BRACAMONTE, E. R., BROECKER, V., COSIO, F., DEMETRIS, A. J., DRACHENBERG, C., EINECKE, G., GLOOR, J., GLOTZ, D., KRAUS, E., LEGENDRE, C., LIAPIS, H., MANNON, R. B., NANKIVELL, B. J., NICKELEIT, V., PAPADIMITRIOU, J. C., RANDHAWA, P., REGELE, H., RENAUDIN, K., RODRIGUEZ, E. R., SERON, D., SESHAN, S., SUTHANTHIRAN, M., WASOWSKA, B. A., ZACHARY, A. & ZEEVI, A. (2010) Banff '09 meeting report: antibody mediated graft deterioration and implementation of Banff working groups. *Am J Transplant,* 10**,** 464-71.

SMITS, N. C., LENSEN, J. F., WIJNHOVEN, T. J., TEN DAM, G. B., JENNISKENS, G. J. & VAN KUPPEVELT, T. H. (2006) Phage display-derived human antibodies against specific glycosaminoglycan epitopes. *Methods Enzymol,* 416**,** 61-87.

SOLEZ, K., COLVIN, R. B., RACUSEN, L. C., HAAS, M., SIS, B., MENGEL, M., HALLORAN, P. F., BALDWIN, W., BANFI, G., COLLINS, A. B., COSIO, F., DAVID, D. S., DRACHENBERG, C., EINECKE, G., FOGO, A. B., GIBSON, I. W., GLOTZ, D., ISKANDAR, S. S., KRAUS, E., LERUT, E., MANNON, R. B., MIHATSCH, M., NANKIVELL, B. J., NICKELEIT, V., PAPADIMITRIOU, J. C., RANDHAWA, P., REGELE, H., RENAUDIN, K., ROBERTS, I., SERON, D., SMITH, R. N. & VALENTE, M. (2008) Banff 07 classification of renal allograft pathology: updates and future directions. *Am J Transplant,* 8**,** 753-60.

SOLEZ, K., COLVIN, R. B., RACUSEN, L. C., SIS, B., HALLORAN, P. F., BIRK, P. E., CAMPBELL, P. M., CASCALHO, M., COLLINS, A. B., DEMETRIS, A. J., DRACHENBERG, C. B., GIBSON, I. W., GRIMM, P. C., HAAS, M., LERUT, E., LIAPIS, H., MANNON, R. B., MARCUS, P. B., MENGEL, M., MIHATSCH, M. J., NANKIVELL, B. J., NICKELEIT, V.,

PAPADIMITRIOU, J. C., PLATT, J. L., RANDHAWA, P., ROBERTS, I., SALINAS-MADRIGA, L., SALOMON, D. R., SERON, D., SHEAFF, M. & WEENING, J. J. (2007) Banff '05 Meeting Report: differential diagnosis of chronic allograft injury and elimination of chronic allograft nephropathy ('CAN') . *Am J Transplant,* 7**,** 518-26.

SOTNIKOV, I., HERSHKOVIZ, R., GRABOVSKY, V., ILAN, N., CAHALON, L., VLODAVSKY, I., ALON, R. & LIDER, O. (2004) Enzymatically quiescent heparanase augments T cell interactions with VCAM-1 and extracellular matrix components under versatile dynamic contexts. *J Immunol,* 172**,** 5185-93.

STANFORD, K. I., WANG, L., CASTAGNOLA, J., SONG, D., BISHOP, J. R., BROWN, J. R., LAWRENCE, R., BAI, X., HABUCHI, H., TANAKA, M., CARDOSO, W. V., KIMATA, K. & ESKO, J. D. (2010) Heparan sulfate 2-O-sulfotransferase is required for triglyceride-rich lipoprotein clearance. *J Biol Chem,* 285**,** 286-94.

STICKENS, D., ZAK, B. M., ROUGIER, N., ESKO, J. D. & WERB, Z. (2005) Mice deficient in Ext2 lack heparan sulfate and develop exostoses. *Development,* 132**,** 5055-68.

STRADER, A. D., REIZES, O., WOODS, S. C., BENOIT, S. C. & SEELEY, R. J. (2004) Mice lacking the syndecan-3 gene are resistant to diet-induced obesity. *J Clin Invest,* 114**,** 1354-60.

STRUTZ, F., ZEISBERG, M., HEMMERLEIN, B., SATTLER, B., HUMMEL, K., BECKER, V. & MULLER, G. A. (2000) Basic fibroblast growth factor expression is increased in human renal fibrogenesis and may mediate autocrine fibroblast proliferation. *Kidney Int,* 57**,** 1521-38.

SUEYOSHI, T., KAKUTA, Y., PEDERSEN, L. C., WALL, F. E., PEDERSEN, L. G. & NEGISHI, M. (1998) A role of Lys614 in the sulfotransferase activity of human heparan sulfate N-deacetylase/N-sulfotransferase. *FEBS Lett,* 433**,** 211-4.

SUGAHARA, K. & KITAGAWA, H. (2000) Recent advances in the study of the biosynthesis and functions of sulfated glycosaminoglycans. *Curr Opin Struct Biol,* 10**,** 518-27.

SWEENEY, M. D., YU, Y. & LEARY, J. A. (2006) Effects of sulfate position on heparin octasaccharide binding to CCL2 examined by tandem mass spectrometry. *J Am Soc Mass Spectrom,* 17**,** 1114-9.

TAMSMA, J. T., VAN DEN BORN, J., BRUIJN, J. A., ASSMANN, K. J., WEENING, J. J., BERDEN, J. H., WIESLANDER, J., SCHRAMA, E., HERMANS, J., VEERKAMP, J. H. & ET AL. (1994) Expression of glomerular extracellular matrix components in human diabetic nephropathy: decrease of heparan sulphate in the glomerular basement membrane. *Diabetologia,* 37**,** 313-20.

TANAKA, Y., FUJII, K., HUBSCHER, S., ASO, M., TAKAZAWA, A., SAITO, K., OTA, T. & ETO, S. (1998) Heparan sulfate proteoglycan on endothelium efficiently induces integrin-mediated T cell adhesion by immobilizing chemokines in patients with rheumatoid synovitis. *Arthritis Rheum,* 41**,** 1365-77.

TATRAI, P., DUDAS, J., BATMUNKH, E., MATHE, M., ZALATNAI, A., SCHAFF, Z., RAMADORI, G. & KOVALSZKY, I. (2006) Agrin, a novel basement membrane component in human and rat liver, accumulates in cirrhosis and hepatocellular carcinoma. *Lab Invest,* 86**,** 1149-60.

TATRAI, P., EGEDI, K., SOMORACZ, A., VAN KUPPEVELT, T. H., TEN DAM, G., LYON, M., DEAKIN, J. A., KISS, A., SCHAFF, Z. & KOVALSZKY, I. (2010) Quantitative and qualitative alterations of heparan sulfate in fibrogenic liver diseases and hepatocellular cancer. *J Histochem Cytochem,* 58**,** 429-41.

TAYLOR, K. R. & GALLO, R. L. (2006) Glycosaminoglycans and their proteoglycans: host-associated molecular patterns for initiation and modulation of inflammation. *Faseb J,* 20**,** 9-22.

TEN DAM, G. B., KURUP, S., VAN DE WESTERLO, E. M., VERSTEEG, E. M., LINDAHL, U., SPILLMANN, D. & VAN KUPPEVELT, T. H. (2006) 3-O-sulfated oligosaccharide structures are recognized by anti-heparan sulfate antibody HS4C3. *J Biol Chem,* 281**,** 4654-62.

TERASAKI, P. I. (2003) Humoral theory of transplantation. *Am J Transplant,* 3**,** 665-73.

THELEN, M. (2001) Dancing to the tune of chemokines. *Nat Immunol,* 2**,** 129-34.

THOMPSON, S. M., FERNIG, D. G., JESUDASON, E. C., LOSTY, P. D., VAN DE WESTERLO, E. M., VAN KUPPEVELT, T. H. & TURNBULL, J. E. (2009) Heparan sulfate phage display antibodies identify distinct epitopes with complex binding characteristics: insights into protein binding specificities. *J Biol Chem,* 284**,** 35621-31.

THYBERG, J. & MOSKALEWSKI, S. (1999) Role of microtubules in the organization of the Golgi complex. *Exp Cell Res,* 246**,** 263-79.

TIEGS, G. & LOHSE, A. W. (2010) Immune tolerance: what is unique about the liver. *J Autoimmun,* 34**,** 1-6.

TINDALL, K. R. & KUNKEL, T. A. (1988) Fidelity of DNA synthesis by the Thermus aquaticus DNA polymerase. *Biochemistry,* 27**,** 6008-13.

TIPPNER, C., NASHAN, B., HOSHINO, K., SCHMIDT-SANDTE, E., AKIMARU, K., BOKER, K. H. & SCHLITT, H. J. (2001) Clinical and subclinical acute rejection early after liver transplantation: contributing factors and relevance for the long-term course. *Transplantation,* 72**,** 1122-8.

TRAISTER, A., SHI, W. & FILMUS, J. (2007) Mammalian Notum induces the release of glypicans and other GPI-anchored proteins from the cell surface. *Biochem J*.

TRPKOV, K., CAMPBELL, P., PAZDERKA, F., COCKFIELD, S., SOLEZ, K. & HALLORAN, P. F. (1996) Pathologic features of acute renal allograft rejection associated with donor-specific antibody, Analysis using the Banff grading schema. *Transplantation,* 61**,** 1586-92.

TURNBULL, J., POWELL, A. & GUIMOND, S. (2001) Heparan sulfate: decoding a dynamic multifunctional cell regulator. *Trends Cell Biol,* 11**,** 75-82.

UEMURA, T., IKEGAMI, T., SANCHEZ, E. Q., JENNINGS, L. W., NARASIMHAN, G., MCKENNA, G. J., RANDALL, H. B., CHINNAKOTLA, S., LEVY, M. F., GOLDSTEIN, R. M. & KLINTMALM, G. B. (2008) Late acute rejection after liver transplantation impacts patient survival. *Clin Transplant,* 22**,** 316-23.

UENO, M., YAMADA, S., ZAKO, M., BERNFIELD, M. & SUGAHARA, K. (2001) Structural characterization of heparan sulfate and chondroitin sulfate of syndecan-1 purified from normal murine mammary gland epithelial cells. Common phosphorylation of xylose and differential sulfation of galactose in the protein linkage region tetrasaccharide sequence. *J Biol Chem,* 276**,** 29134-40.

UNGER, E., PETTERSSON, I., ERIKSSON, U. J., LINDAHL, U. & KJELLEN, L. (1991) Decreased activity of the heparan sulfate-modifying enzyme glucosaminyl N-deacetylase in hepatocytes from streptozotocin-diabetic rats. *J Biol Chem,* 266**,** 8671-4.

VAN DEN BORN, J., PIKAS, D. S., PISA, B. J., ERIKSSON, I., KJELLEN, L. & BERDEN, J. H. (2003) Antibody-based assay for N-deacetylase activity of heparan sulfate/heparin N-deacetylase/N-sulfotransferase (NDST) : novel characteristics of NDST-1 and -2. *Glycobiology,* 13**,** 1-10.

VAN DEN BORN, J., PISA, B., BAKKER, M. A., CELIE, J. W., STRAATMAN, C., THOMAS, S., VIBERTI, G. C., KJELLEN, L. & BERDEN, J. H. (2006) No change in glomerular heparan sulfate structure in early human and experimental diabetic nephropathy. *J Biol Chem,* 281**,** 29606-13.

VAN DEN BORN, J., VAN DEN HEUVEL, L. P., BAKKER, M. A., VEERKAMP, J. H., ASSMANN, K. J. & BERDEN, J. H. (1992) A monoclonal antibody against GBM heparan sulfate induces an acute selective proteinuria in rats. *Kidney Int,* 41**,** 115-23.

VAN HORSSEN, J., WESSELING, P., VAN DEN HEUVEL, L. P., DE WAAL, R. M. & VERBEEK, M. M. (2003) Heparan sulphate proteoglycans in Alzheimer's disease and amyloid-related disorders. *Lancet Neurol,* 2**,** 482-92.

VAN KUPPEVELT, T. H., DENNISSEN, M. A., VAN VENROOIJ, W. J., HOET, R. M. & VEERKAMP, J. H. (1998) Generation and application of type-specific anti-heparan sulfate antibodies using phage display technology. Further evidence for heparan sulfate heterogeneity in the kidney. *J Biol Chem,* 273**,** 12960-6.

VAN KUPPEVELT, T. H., JENNISKENS, G. J., VEERKAMP, J. H., TEN DAM, G. B. & DENNISSEN, M. A. (2001) Phage display technology to obtain antiheparan sulfate antibodies. *Methods Mol Biol,* 171**,** 519-34.

VASILESCU, J., GUO, X. & KAST, J. (2004) Identification of protein-protein interactions using in vivo cross-linking and mass spectrometry. *Proteomics,* 4**,** 3845-54.

VENKATACHALAM, K. V., AKITA, H. & STROTT, C. A. (1998) Molecular cloning, expression, and characterization of human bifunctional 3'-phosphoadenosine 5'-phosphosulfate synthase and its functional domains. *J Biol Chem,* 273**,** 19311-20.

VESTWEBER, D. & BLANKS, J. E. (1999) Mechanisms that regulate the function of the selectins and their ligands. *Physiol Rev,* 79**,** 181-213.

VIERLING, J. M. & FENNELL, R. H., JR. (1985) Histopathology of early and late human hepatic allograft rejection: evidence of progressive destruction of interlobular bile ducts. *Hepatology,* 5**,** 1076-82.

VLODAVSKY, I. & FRIEDMANN, Y. (2001) Molecular properties and involvement of heparanase in cancer metastasis and angiogenesis. *J Clin Invest,* 108**,** 341-7.

VONGCHAN, P., WARDA, M., TOYODA, H., TOIDA, T., MARKS, R. M. & LINHARDT, R. J. (2005) Structural characterization of human liver heparan sulfate. *Biochim Biophys Acta,* 1721**,** 1-8.

WANG, L., FUSTER, M., SRIRAMARAO, P. & ESKO, J. D. (2005) Endothelial heparan sulfate deficiency impairs L-selectin- and chemokine-mediated neutrophil trafficking during inflammatory responses. *Nat Immunol,* 6**,** 902-10.

WARNER, R. G., HUNDT, C., WEISS, S. & TURNBULL, J. E. (2002) Identification of the heparan sulfate binding sites in the cellular prion protein. *J Biol Chem,* 277**,** 18421-30.

WEBB, L. M., EHRENGRUBER, M. U., CLARK-LEWIS, I., BAGGIOLINI, M. & ROT, A. (1993) Binding to heparan sulfate or heparin enhances neutrophil responses to interleukin 8. *Proc Natl Acad Sci U S A,* 90**,** 7158-62.

WHITELOCK, J. M. & IOZZO, R. V. (2005) Heparan sulfate: a complex polymer charged with biological activity. *Chem Rev,* 105**,** 2745-64.

WIJNHOVEN, T. J., LENSEN, J. F., WISMANS, R. G., LAMRANI, M., MONNENS, L. A., WEVERS, R. A., ROPS, A. L., VAN DER VLAG, J., BERDEN, J. H., VAN DEN HEUVEL, L. P. & VAN KUPPEVELT, T. H. (2007) In vivo degradation of heparan sulfates in the glomerular basement membrane does not result in proteinuria. *J Am Soc Nephrol,* 18**,** 823-32.

WILLIAMS, K. J., LIU, M. L., ZHU, Y., XU, X., DAVIDSON, W. R., MCCUE, P. & SHARMA, K. (2005) Loss of heparan N-sulfotransferase in diabetic liver: role of angiotensin II. *Diabetes,* 54**,** 1116-22.

WILSON, V. A., GALLAGHER, J. T. & MERRY, C. L. (2002) Heparan sulfate 2-O-sulfotransferase (Hs2st) and mouse development. *Glycoconj J,* 19**,** 347-54.

WONG, C. H., HEIT, B. & KUBES, P. (2010) Molecular regulators of leucocyte chemotaxis during inflammation. *Cardiovasc Res,* 86**,** 183-91.

WONG, W. K., ROBERTSON, H., CARROLL, H. P., ALI, S. & KIRBY, J. A. (2003) Tubulitis in renal allograft rejection: role of transforming growth factor-beta and interleukin-15 in development and maintenance of CD103+ intraepithelial T cells. *Transplantation,* 75**,** 505-14.

WOODS, A. (2001) Syndecans: transmembrane modulators of adhesion and matrix assembly. *J Clin Invest,* 107**,** 935-41.

XIA, G., CHEN, J., TIWARI, V., JU, W., LI, J. P., MALMSTROM, A., SHUKLA, D. & LIU, J. (2002) Heparan sulfate 3-O-sulfotransferase isoform 5 generates both an antithrombin-binding site and an entry receptor for herpes simplex virus, type 1. *J Biol Chem,* 277**,** 37912-9.

XIA, J. L., DAI, C., MICHALOPOULOS, G. K. & LIU, Y. (2006) Hepatocyte growth factor attenuates liver fibrosis induced by bile duct ligation. *Am J Pathol,* 168**,** 1500-12.

YAMAGUCHI, N. & FUKUDA, M. N. (1995) Golgi retention mechanism of beta-1,4-galactosyltransferase. Membrane-spanning domain-dependent homodimerization and association with alpha- and beta-tubulins. *J Biol Chem,* 270**,** 12170-6.

YANG, J. & LIU, Y. (2001) Dissection of key events in tubular epithelial to myofibroblast transition and its implications in renal interstitial fibrosis. *Am J Pathol,* 159**,** 1465-75.

YANG, J. & LIU, Y. (2002) Blockage of tubular epithelial to myofibroblast transition by hepatocyte growth factor prevents renal interstitial fibrosis. *J Am Soc Nephrol,* 13**,** 96-107.

YAYON, A., KLAGSBRUN, M., ESKO, J. D., LEDER, P. & ORNITZ, D. M. (1991) Cell surface, heparin-like molecules are required for binding of basic fibroblast growth factor to its high affinity receptor. *Cell,* 64**,** 841-8.

YU, W. H. & WOESSNER, J. F., JR. (2000) Heparan sulfate proteoglycans as extracellular docking molecules for matrilysin (matrix metalloproteinase 7) . *J Biol Chem,* 275**,** 4183-91.

YUAN, Z. & TEASDALE, R. D. (2002) Prediction of Golgi Type II membrane proteins based on their transmembrane domains. *Bioinformatics,* 18**,** 1109-15.

ZARBOCK, A. & LEY, K. (2008) Mechanisms and consequences of neutrophil interaction with the endothelium. *Am J Pathol,* 172**,** 1-7.

ZEISBERG, E. M., POTENTA, S. E., SUGIMOTO, H., ZEISBERG, M. & KALLURI, R. (2008) Fibroblasts in kidney fibrosis emerge via endothelial-to-mesenchymal transition. *J Am Soc Nephrol,* 19**,** 2282-7.

8 Appendix

8.1 Sequence NDST1-pcDNA3

pcDNA3 vector containing human NDST1 cDNA was sent for sequencing. Routine sequencing primers T7 and Sp6 were used for the reaction. Beginning and end of NDST1 sequence are highlighted in yellow (first two and last two triplets of the NDST1 open reading frame).

```
sequence        AGGATGCCTGCCCTGGCATGCCTCCGGAGGCTGTGTCGGCACGTGTCCCCGCAGGCTGTC 124
comparator      AGGATGCCTGCCCTGGCATGCCTCCGGAGGCTGTGTCGGCACGTGTCCCCGCAGGCTGTC 480
                ************************************************************

sequence        CTTTTCCTGCTGTTCATCTTCTGCCTGTTCAGCGTTTTCATCTCGGCCTACTACCTATAT 184
comparator      CTTTTCCTGCTGTTCATCTTCTGCCTGTTCAGCGTTTTCATCTCGGCCTACTACCTATAT 540
                ************************************************************

sequence        GGCTGGAAGCGAGGCCTGGAGCCCTCGGCGGATGCCCCCGAGCCTGACTGCGGGGACCCG 244
comparator      GGCTGGAAGCGAGGCCTGGAGCCCTCGGCGGATGCCCCCGAGCCTGACTGCGGGGACCCG 600
                ************************************************************

sequence        CCGCCTGTGGCCCCCAGTCGCCTGCTGCCACTCAAGCCTGTGCAGGCAGCCACCCCTTCC 304
comparator      CCGCCTGTGGCCCCCAGTCGCCTGCTGCCACTCAAGCCTGTGCAGGCAGCCACCCCTTCC 660
                ************************************************************

sequence        CGCACAGACCCGTTGGTGCTGGTCTTTGTGGAGAGCCTCTACTCGCAACTGGGCCAGGAG 364
comparator      CGCACAGACCCGTTGGTGCTGGTCTTTGTGGAGAGCCTCTACTCGCAACTGGGCCAGGAG 720
                ************************************************************

sequence        GTGGTGGCCATCCTGGAGTCCAGCCGCTTCAAATACCGCACAGAGATTGCGCCGGGCAAG 424
comparator      GTGGTGGCCATCCTGGAGTCCAGCCGCTTCAAATACCGCACAGAGATTGCGCCGGGCAAG 780
                ************************************************************

sequence        GGTGACATGCCCACGCTCACTGACAAGGGCCGTGGCCGCTTCGCCCTCATCATCTATGAG 484
comparator      GGTGACATGCCCACGCTCACTGACAAGGGCCGTGGCCGCTTCGCCCTCATCATCTATGAG 840
                ************************************************************

sequence        AACATCCTCAAGTATGTCAACCTGGACGCCTGGAACCGGGAGCTGCTGGACAAGTACTGT 544
comparator      AACATCCTCAAGTATGTCAACCTGGACGCCTGGAACCGGGAGCTGCTGGACAAGTACTGT 900
                ************************************************************

sequence        GTGGCCTACGGCGTGGGCATCATTGGCTTCTTCAAGGCCAATGAGAACAGCCTGCTGAGT 604
comparator      GTGGCCTACGGCGTGGGCATCATTGGCTTCTTCAAGGCCAATGAGAACAGCCTGCTGAGT 960
                ************************************************************

sequence        GCGCAGCTCAAGGGCTTCCCCCCTGTTCCTGCACTCAAACCTGGGCCTGAAGGACTGCAGC 664
comparator      GCGCAGCTCAAGGGCTTCCCCCCTGTTCCTGCACTCAAACCTGGGCCTGAAGGACTGCAGC 1020
                ************************************************************
```

```
sequence        CGCATCCTCGAAGCTGCGTGCCCTCCAGAACCGCTGCCTGGTCCCTGGCTGGTACGCCAC 1466
comparator      CGCATCCTCGAAGCTGCGTGCCCTCCAGAACCGCTGCCTGGTCCCTGGCTGGTACGCCAC 2699
                ************************************************************

sequence        CCACATCGAGCGCTGGCTCAGTGCCTATCACGCCAACCAGATTCTGGTCTTGGATGGCAA 1526
comparator      CCACATCGAGCGCTGGCTCAGTGCCTATCACGCCAACCAGATTCTGGTCTTGGATGGCAA 2759
                ************************************************************

sequence        ACTGCTTCGCACAGAACCTGCCAAAGTGATGGACATGGTGCAGAAGTTCCTTGGGGTGAC 1586
comparator      ACTGCTTCGCACAGAACCTGCCAAAGTGATGGACATGGTGCAGAAGTTCCTTGGGGTGAC 2819
                ************************************************************

sequence        CAACACCATTGACTACCACAAAACCTTGGCGTTTGATCCAAAGAAAGGATTTTGGTGCCA 1646
comparator      CAACACCATTGACTACCACAAAACCTTGGCGTTTGATCCAAAGAAAGGATTTTGGTGCCA 2879
                ************************************************************

sequence        ACTGCTTGAAGGAGGAAAAACCAAGTGTCTGGGCAAAAGCAAGGGCCGGAAATATCCCGA 1706
comparator      ACTGCTTGAAGGAGGAAAAACCAAGTGTCTGGGCAAAAGCAAGGGCCGGAAATATCCCGA 2939
                ************************************************************

sequence        GATGGACTTGGATTCCCGAGCCTTCCTGAAGGACTATTACCGGGACCACAACATCGAGCT 1766
comparator      GATGGACTTGGATTCCCGAGCCTTCCTGAAGGACTATTACCGGGACCACAACATCGAGCT 2999
                ************************************************************

sequence        CTCCAAGCTGCTGTATAAGATGGGCCAGACACTTCCCACTTGGCTACGAGAGGACCTCCA 1826
comparator      CTCCAAGCTGCTGTATAAGATGGGCCAGACACTTCCCACTTGGCTACGAGAGGACCTCCA 3059
                ************************************************************

sequence        GAACACCAGGTAGCCGTGGCCACCACAGCCAGACTGAACGTTTGTGAAAGCTAGGACATC 1886
comparator      GAACACCAGGTAGCCGTGGCCACCACAGCCAGACTGAACGTTTGTGAAAGCTAGGACATC 3119
                ************************************************************
```

8.2 Sequence NDST1-pCTAP

Sequence of NDST1-pCTAP was verified by sequencing using routine sequencing primers T3 and T7. To ensure correct sequence of the whole insert additional internal sequencing primers were designed (internal primer binding sites underlined). pCTAP DNA shown in blue, NDST1 cDNA shown in black and restriction sites shown in red.

*Eco*RI NDST1cDNA

5‘…GGG CTG CAG *GAA TTC* G GAG GCC AGG ATG CCT GCC

CTG GCA TGC CTC CGG AGG CTG TGT CGG CAC GTG TCC

CCG CAG GCT GTC CTT TTC CTG CTG TTC ATC TTC TGC

CTG TTC AGC GTT TTC ATC TCG GCC TAC TAC CTA TAT

GGC TGG AAG CGA GGC CTG GAG CCC TCG GCG GAT

GCC CCC GAG CCT GAC TGC GGG GAC CCG CCG CCT GTG

GCC CCC AGT CGC CTG CTG CCA CTC AAG CCT GTG CAG

GCA GCC ACC CCT TCC CGC ACA GAC CCG TTG GTG CTG

GTC TTT GTG GAG AGC CTC TAC TCG CAA CTG GGC CAG

GAG GTG GTG GCC ATC CTG GAG TCC AGC CGC TTC AAA

TAC CGC ACA GAG ATT GCG CCG GGC AAG GGT GAC

ATG CCC ACG CTC ACT GAC AAG GGC CGT GGC CGC TTC

GCC CTC ATC ATC TAT GAG AAC ATC CTC AAG TAT GTC

AAC CTG GAC GCC TGG AAC CGG GAG CTG CTG GAC

AAG TAC TGT GTG GCC TAC GGC GTG GGC ATC ATT GGC

TTC TTC AAG GCC AAT GAG AAC AGC CTG CTG AGT GCG

CAG CTC AAG GGC TTC CCC CTG TTC CTG CAC TCA AAC

CTG GGC CTG AAG GAC TGC AGC ATC AAC CCC AAG TCC

CCG CTG CTC TAC GTG ACG CGA CCT AGC GAG GTG GAG

AAA GGT GTG CTC CCC GGC GAG GAC TGG ACG GTT TTC

CAG TCA AAT CAC TCC ACC TAT GAG CCA GTG CTG CTG

GCC AAG ACG CGC TCG TCT GAG TCC ATC CCA CAC CTG

GGC GCA GAC GCC GGC CTG CAT GCT GCA CTG CAC GCC

ACT GTG GTC CAG GAC CTG GGC CTG CAC GAC GGC ATC

CAG CGC GTG CTG TTT GGC AAC AAC CTG AAC TTC TGG

CTG CAC AAG CTT GTC TT C GTG GAT GCC GTG GCC

TTCC TC ACG GGG AAG CGC CTC TCC CTG CCA TTG GAC

CGC TAC ATC CTG GTG GAC ATT GAT GAC ATC TTC GTG

GGC AAG GAG GGC ACA CGC ATG AAG GTG GAG GAC

GTG AAG GCC CTG TTT GAC ACA CAG AAC GAA CTA CGC

GCA CAC ATC CCA AAC TTC ACC TTC AAC CTG GGC TAC

TCA GGG AAA TTC TTC CAC ACA GGT ACC AAT GCT GAG

GAC GCT GGG GAT GAT CTG CTG CTG TCG TAT GTG AAG

GAG TTC TGG TGG TTC CCC CAC ATG TGG AGC CAC ATG

CAG CCC CAC CTT TTC CAC AAC CAG TCC GTG TTG GCC

GAG CAG ATG GCC TTG AAC AAG AAG TTC GCT GTC GAG

CAT GGC ATT CCC ACA GAC ATG GGG TAT GCA GTG GCG

CCC CAC CAC TCG GGC GTG TAC CCC GTG CAC GTG CAG

CTG TAC GAG GCT TGG AAG CAG GTG TGG AGC ATC CGC

GTG ACC AGC ACG GAG GAG TAC CCC CAC CTG AAG

CCA GCC CGC TAC CGC CGT GGC TTC ATC CAC AAT GGC

ATC ATG GTT CTC CCA CGG CAG ACC TGC GGC CTC TTC

ACA CAC ACC ATC TTC TAC AAC GAG TAC CCT GGC GGC

TCC AGT GAG CTG GAC AA A ATC ATC AAC GGG GGC GAG CTC TTC CTC ACC GTG CTC CTC AAT CCT ATC AGC ATC TTC ATG ACG CAC CTG TCC AAC TAT GGG AAT GAC CGC CTG GGC CTG TAC ACC TTC AAG CAC CTG GTG CGC TTC CTG CAC TCC TGG ACG AAC CTC CGG CTG CAG ACA CTG CCC CCT GTG CAG TTG GCG CAG AAG TAC TTC CAG ATC TTC TCC GAG GAG AAG GAC CCG CTC TGG CAG GAC CCC TGC GAG GAC AAA CGT CAC AAA GAC ATC TGG TCC AAG GAG AAG ACG TGT GAC CGC TTC CCA AAG CTC CTC ATC ATC GGC CCC CAG AAA ACA GGC ACC ACT GCC CTC TAC CTG TTC CTG GGC ATG CAC CCT GAC CTA AGC AGC AAC TAC CCC AGC TCT GAG ACC TTT GAG GAG ATC CAG TTT TTT AAT GGC CAC AAC TAT CAC AAA GGC ATC GAC TGG TAC ATG GAG TTC TTC CCC ATC CCT TCC AAC ACC ACC TCC GAC TTC TAC TTT GAG AAA AGC GCC AAC TAC TTT GAT TCA GAA GTG GCG CCC CGG CGG GCA GCA GCC CTC TTG CCC AAA GCC AAG GTC CTG ACC ATC CTC ATC AAC CCC GCG GAC CGG GCC TAT TCC TGG TAC CAG CAC CAG CGA GCC CAT GAC GAC CCA GTG GCC CTA AAG TAC ACC TTC CAT GAG GTG ATT ACC GCC GGC TCT GAC GCA TCC TCG AAG CTG CGT GCC CTC CAG AAC CGC TGC CTG GTC CCT GGC TGG TAC GCC ACC CAC ATC GAG CGC TGG CTC AGT GCC TAT CAC GCC AAC CAG ATT CTG GTC TTG GAT GGC AAA CTG CTT CGC ACA GAA CCT GCC AAA GTG ATG GAC ATG GTG CAG AAG TTC CTT GGG GTG ACC AAC

ACC ATT GAC TAC CAC AAA ACC TTG GCG TTT GAT CCA

AAG AAA GGA TTT TGG TGC CAA CTG CTT GAA GGA

GGA AAA ACC AAG TGT CTG GGC AAA AGC AAG GGC

CGG AAA TAT CCC GAG ATG GAC TTG GAT TCC CGA GCC

TTC CTG AAG GAC TAT TAC CGG GAC CAC AAC ATC GAG

CTC TCC AAG CTG CTG TAT AAG ATG GGC CAG ACA CTT

CCC ACT TGG CTA CGA GAG GAC CTC CAG AAC ACC AGG

CTC GAG GGA AGC GGT AGC GGT ACC **ATG GAC GAG** … 3 ‘

***Xho*I** **pCTAP DNA……..... SBP-tag.....**

8.3 Example of MS analysis

a

A57169 **Mass:** 100804 **Score:** 325 **Expect:** 1e-26 **Queries matched:** 44

[heparan sulfate]-glucosamine N-sulfotransferase (EC 2.8.2.8) - human

Observed	Mr(expt)	Mr(calc)	ppm	Start	End	Miss	Peptide
1075.5623	1074.5550	1074.5498	4.85	846	853	1	R.AFLKDYYR.D
1150.5582	1149.5509	1149.5567	-5.04	144	152	0	K.YVNLDAWNR.E
1173.6124	1172.6051	1172.6091	-3.36	549	557	0	R.FLHSWTNLR.L
1202.6318	1201.6245	1201.6278	-2.69	866	875	0	K.MGQTLPTWLR.E
1206.6073	1205.6000	1205.6040	-3.34	337	346	0	K.ALFDTQNELR.A
1218.6179	1217.6106	1217.6227	-9.90	866	875	0	K.MGQTLPTWLR.E + Oxidation (M)
1224.7315	1223.7242	1223.7238	0.39	699	709	0	K.VLTILINPADR.A
1238.5666	1237.5593	1237.5628	-2.84	710	718	0	R.AYSWYQHQR.A
1294.6176	1293.6104	1293.6176	-5.59	815	825	0	K.GFWCQLLEGGK.T + Carbamidomethyl (C)
1335.7901	1334.7828	1334.7922	-7.04	558	569	0	R.LQTLPPVQLAQK.Y
1336.7779	1335.7706	1335.7802	-7.17	133	143	0	R.FALIIYENILK.Y
1353.7535	1352.7462	1352.7387	5.56	472	483	0	R.GFIHNGIMVLPR.Q
1355.6937	1354.6864	1354.6153	52.5	677	688	0	K.SANYFDSEVAPR.R
1379.7801	1378.7728	1378.7861	-9.61	292	304	0	K.LVFVDAVAFLTGK.R
1422.7046	1421.6974	1421.7126	-10.69	814	825	1	K.KGFWCQLLEGGK.T + Carbamidomethyl (C)
1442.8022	1441.7949	1441.8082	-9.18	184	196	0	K.GFPLFLHSNLGLK.D
1490.9089	1489.9016	1489.8980	2.38	67	80	0	R.LLPLKPVQAATPSR.T
1509.8153	1508.8080	1508.8127	-3.07	313	325	0	R.YILVDIDDIFVGK.E
1535.8970	1534.8897	1534.8872	1.68	292	305	1	K.LVFVDAVAFLTGKR.L
1549.9188	1548.9115	1548.9028	5.67	131	143	1	R.GRFALIIYENILK.Y
1584.7646	1583.7573	1583.7653	-5.10	837	849	1	K.YPEMDLDSRAFLK.D
1600.7644	1599.7571	1599.7603	-1.95	837	849	1	K.YPEMDLDSRAFLK.D + Oxidation (M)
1601.7993	1600.7920	1600.7820	6.21	751	763	0	R.CLVPGWYATHIER.W + Carbamidomethyl (C)
1617.8608	1616.8535	1616.8773	-14.75	204	217	0	K.SPLLYVTRPSEVEK.G
1627.8403	1626.8330	1626.8365	-2.16	455	468	0	R.VTSTEEYPHLKPAR.Y
1689.8847	1688.8774	1688.8291	28.6	113	128	1	R.TEIAPGKGDMPTLTDK.G + Oxidation (M)
1776.9954	1775.9882	1775.9054	46.6	332	346	1	K.VEDVKALFDTQNELR.A
1827.9747	1826.9674	1826.9679	-0.26	764	779	0	R.WLSAYHANQILVLDGK.L

b

```
  1 MPALACLRRL CRHVSPQAVL FLLFIFCLFS VFISAYYLYG WKRGLEPSAD
 51 APEPDCGDPP PVAPSRLLPL KPVQAATPSR TDPLVLVFVE SLYSQLGQEV
101 VAILESSRFK YRTEIAPGKG DMPTLTDKGR GRFALIIYEN ILKYVNLDAW
151 NRELLDKYCV AYGVGIIGFF KANENSLLSA QLKGFPLFLH SNLGLKDCSI
201 NPKSPLLYVT RPSEVEKGVL PGEDWTVFQS NHSTYEPVLL AKTRSSESIP
251 HLGADAGLHA ALHATVVQDL GLHDGIQRVL FGNNLNFWLH KLVFVDAVAF
301 LTGKRLSLPL DRYILVDIDD IFVGKEGTRM KVEDVKALFD TQNELRAHIP
351 NFTFNLGYSG KFFHTGTNAE DAGDDLLLSY VKEFWWFPHM WSHMQPHLFH
401 NQSVLAEQMA LNKKFAVEHG IPTDMGYAVA PHHSGVYPVH VQLYEAWKQV
451 WSIRVTSTEE YPHLKPARYR RGFIHNGIMV LPRQTCGLFT HTIFYNEYPG
501 GSSELDKIIN GGELFLTVLL NPISIFMTHL SNYGNDRLGL YTFKHLVRFL
551 HSWTNLRLQT LPPVQLAQKY FQIFSEEKDP LWQDPCEDKR HKDIWSKEKT
601 CDRFPKLLII GPQKTGTTAL YLFLGMHPDL SSNYPSSETF EEIQFFNGHN
651 YHKGIDWYME FFPIPSNTTS DFYFEKSANY FDSEVAPRRA AALLPKAKVL
701 TILINPADRA YSWYQHQRAH DDPVALKYTF HEVITAGSDA SSKLRALQNR
751 CLVPGWYATH IERWLSAYHA NQILVLDGKL LRTEPAKVMD MVQKFLGVTN
801 TIDYHKTLAF DPKKGFWCQL LEGGKTKCLG KSKGRKYPEM DLDSRAFLKD
851 YYRDHNIELS KLLYKMGQTL PTWLREDLQN TR
```

c

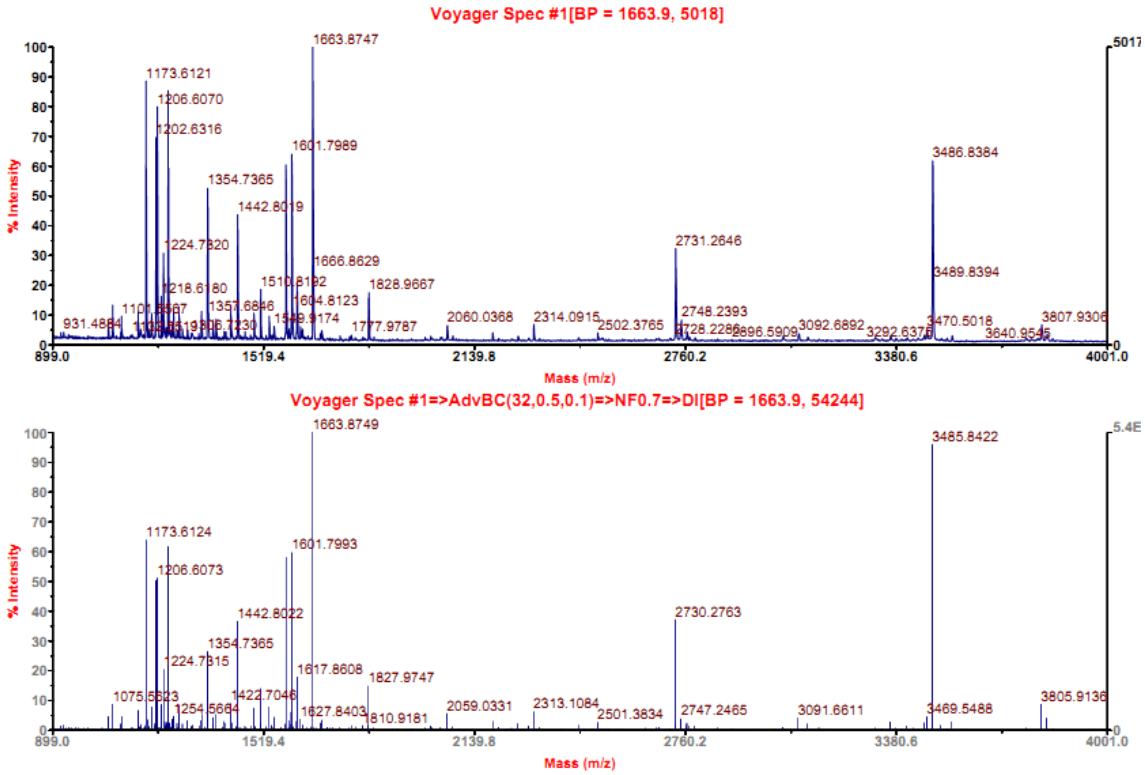

Figure 8-2 Example of MS peptide mass fingerprinting analysis

Mascot analysis: results list of peptide hits (a), matching peptides shown in red (b) and representation of mass spectra aquired (c).

8.4 Presentations arising from this study

NDST1 and Heparan Sulphate in Inflammation
Julia Spielhofer, Graeme O'Boyle, John A Kirby and Simi Ali
Poster presentation, 15th European Carbohydrate Symposium, Vienna, Austria, July 2009

Novel targets in Transplant Biology
Julia Spielhofer
Poster presentation, Marie Curie conference, a satellite meeting of the Euroscience Open Forum, Barcelona, Spain, July 2008

NDST1 in Heparan Sulphate Biosynthesis and Biology
Julia Spielhofer, Kerstin Lehner, Graeme O'Boyle, John A Kirby and Simi Ali
Poster presentation, 4th Glycan Forum, Berlin, Germany, May 2008

Alteration of Heparan Sulphate Composition during Inflammation
Julia Spielhofer, Kerstin Lehner, John A Kirby and Simi Ali
Poster presentation, Biochemical Society Annual Symposium 'Structure and Function in Cell Adhesion', Manchester, UK, May 2007